International Symposium on

**C** e l l u l a r
**A** u t o m a t a
**M** o d e l i n g   f o r
**U** r b a n   a n d
**S** p a t i a l
**S** y s t e m s

Oporto Portugal

November    8-10    2012

Editors: Nuno Norte Pinto, Joana Dourado, and Ana Natálio

The present volume contains the short papers and abstracts reviewed and presented at CAMUSS, the International Symposium on Cellular Automata Modeling for Urban and Saptial Systems, held in Oporto on November 8 to 10, 2012.

Cite as:
In N. N. Pinto, J. Dourado, A. Natálio (Eds), Proceedings of CAMUSS, the International Symposium on Cellular Automata Modeling for Urban and Saptial Systems, Oporto, November 8 to 10, 2012, Coimbra: Department of Civil Engineering of the University of Coimbra

Book cover created by Nuno Norte Pinto and designed by Luís Batista

Printed in Coimbra, Portugal by Pantone-4

# Proceedings of CAMUSS

Edited by

Nuno Norte Pinto

Joana Dourado

Ana Natálio

# Table of Contents

# Organizing Committee

Nuno Norte Pinto, University of Coimbra ......................................... Portugal

Joana Dourado, University of Coimbra ............................................ Portugal

Ana Natálio, University of Porto ....................................................... Portugal

Helena Pina, University of Porto ....................................................... Portugal

# Scientific Committee

Nuno Norte Pinto, University of Coimbra .......................................... Portugal

Michael Batty, CASA University College London............................. UK

Roger White, Memorial University New Foundland .......................... Canada

Helen Couclelis, University of California at Santa Barbara ............... USA

Keith Clarke, University of California at Santa Barbara .................... USA

Geoffrey Caruso, University of Luxembourg .................................... Luxembourg

Denise Pumain, University of Paris.................................................... France

Danielle Marceau, University of Calgary .......................................... Canada

David O'Sullivan, University of Aukland ......................................... New Zealand

Suzana Dragicevic, Simon Frasier University ................................... Canada

Itzhak Benenson, Tel Aviv University................................................ Israel

Yichun Xie, Eastern Michigan University......................................... USA

Juval Portugali, Tel Aviv University ................................................. Israel

Elisabete Silva, University of Cambridge.......................................... UK

Ferdinando Semboloni, University of Firenze ................................... Italy

Daniel Czamanski, Technion Israel Institute of Technology.............. Israel

Yan Liu, University of Queensland .................................................... Australia

Cláudia Almeida, National Institute for Space Research .................... Brazil

Guy Engelen, VITO Flemish Institute for Technological Research ... Belgium

Carlo Lavalle, IES, Joint Research Center......................................... Italy

Paul Torrens, University of Maryland ............................................... USA

Anthony Yeh, Hong Kong University ................................................ PR China

Xia Li, Sun Yat-sen University ......................................................... PR China

José Barredo, IES, Joint Research Center............................................ Italy

Fulong Wu, University College London............................................ UK

# CAMUSS, a Symposium on Cellular Automata in Geography and Urban Studies

**Nuno Norte Pinto**

Cellular Automata (CA) models have been used in Geography and Urban Studies for some decades now, becoming one of the most popular concepts in contemporary spatial modeling.

CA models are today very sophisticated, having evolved significantly both in theoretical and in practical terms, with many models already being used to support policy design in different geographic contexts.

CA have gained a sound scientific presence in the Geography and Urban Studies literature. A quick and non-exhaustive search on the Web of Knowledge gives us more than 1900 papers on "urban" or "spatial" CA published since only 1991.

However, it seems that the discussion over CA mainly happened in the literature. When many colleagues were asked if they could remember of one large, dedicated meeting on CA in Geography and Urban Studies, they always gave the same answer: they remembered none.

Despite some short and usually very local workshops about CA, and many parallel sessions dedicated to CA, usually in the same Geography and Geocomputation conferences, there is no memory of a larger meeting that had focused on the complex scientific structure that CA already has.

Such a meeting is, in my opinion, essential, especially now, when new computation capabilities are available, and when it is easier to handle larger and more disaggregated datasets, increasing the simulation capacities of other modeling concepts such as agent-based simulation.

I wish to welcome you to CAMUSS, the (first) International Symposium on Cellular Automata Modeling for Urban and Spatial Systems.

CAMUSS was launched with a simple program: to bring together researchers who have been and still are working on CA modeling applied to urban and spatial systems.

CAMUSS aims to create the proper forum for a deep reflection on the scientific history of CA in Geography and Urban Studies through the presentation of the state-of-the-art research on CA, and to devise a new research agenda in this field for the next years.

In spite of the very high level of specification that CAMUSS was targeting – only CA-linked submissions were accepted – it was really satisfying to be able to gather such a significant group of contributions from all the corners of the world.

More than fifty contributions were submitted and more than forty were accepted to the program, authored by more than ninety researchers.

The program has fourteen parallel sessions, each one focusing on a main topic related to CA. Parallel sessions were scheduled to provide participants the proper time to present their research and to have a fruitful discussion with an audience of true experts on CA.

The program has three keynote lectures by three of the most influential researchers and authors on CA:

- Professor Michael Batty, Director of CASA and Bartlett Professor of Planning, University College London, United Kingdom;
- Professor Helen Couclelis, Professor at the Department of Geography of the University of California at Santa Barbara, United States of America;
- Professor Roger White, Professor at the Department of Geography of the Memorial University of Newfoundland, Canada.

This is what I believe to be the proper setting for having a deep discussion about the history of CA as a modeling tool in Geography and Urban Studies, and about what will be the future research on CA in the mid- and long-term.

The goal of CAMUSS was already accomplished by the quality of the work presented in these Proceedings.

Bem hajam.[¤]

---

[¤] The traditional way to say "thank you all very much" in Portugal.

# SHORT PAPERS

# Development and applications of urban cellular automata in China

## Xia LI[1]; Yimin CHEN; Bin AI

[1]School of Geography and Planning, Sun Yat-sen
University, Guangzhou, 510275, PR
China;
Email: lixia@mail.sysu.edu.cn; lixia@graduate.hku.hk

**Keywords:** cellular automata, urban development, China

**Abstract[¤]**

China has come to a new era of rapid urbanization and urban expansion. Since the late 1990s, many studies on using cellular automata techniques have been carried out to tackle urban and regional development problems. Cellular automata (CA) have been used as a useful tool to support land use planning and policy analysis as well as to explore scenarios for future development in this fast developing country. There is a growing demand for the application of CA in some planning departments in major Chinese cities. Especially, many applications are found in the coastal cities, such as Guangzhou, Dongguan, Shenzhen, Shanghai and Beijing in China. Significant modifications have been made so that CA can be suited to a lot of urban simulation and planning tasks in this region. Much effort has been made to generate a high degree of reality in urban simulation by using a richer set of GIS data for the calibration. Some classical CA models have been established by Chinese scholars who have used a variety of intelligent methods, such as MCE, ANN, and GA methods, for calibrating these models.

## 1. Rapid urbanization and urban expansion in China

In the 20th century, rapid urbanization has become a typical geographical phenomenon because of economic development and population growth around the world. For example, the urban population increased from 220 million in 1900 to 732 million in 1950 (29% of the world's population), and to 3.3 billion (the first time in history over half of the world's population) in 2007 (Potsiou, 2010). The growth trend continues into the 21th century as 60% of the world's population will be urbanized by 2030 according to the report. This rush to the cities has resulted in unprecedented urban expansion and land use changes in many fast growing regions, associating with severe ecological, economic and social problems.

China's urbanization before 1980s was slow and even stagnated during the Cultural Revolution (1966-1976) (He and Wu 2005). The economic reforms under Deng Xiaoping's leadership broke many bottlenecks and strongly stimulate the

---

[¤] This contribution has its references in an 'Author-Date' format.

urban development. The policy of economic decentralization resulted in the diversification of investment sources (e.g. foreign direct investments); while the land leasing system became an effective way to bring local revenue and also the tactic to attract investors to promote local economy (Wu 1998). In addition, the reforms in household registration (hukou) system smoothed the urban-rural migration that increased urban population and speeded up the urbanization process (Chan and Zhang 1999). In post-reform China, rapid urban expansion was witnessed in the coastal areas. It is reported that urban land increased 40-60% during 1990-1995 in Pearl River Delta (60.11%), Yangtze River Delta (54.29%) and Beijing-Tianjin-Tangshan zone (42.18%) (Tian et al. 2005). However, the fast urbanization paces caused the serious problem of farmland loss in eastern China (Seto et al. 2000). While in the hinterland, the quantity of arable land increased because of the change of production conditions, economic benefits and climatic conditions (Liu et al. 2003).

## 2. Cellular automata for urban simulation and planning in China

A better understanding of these changes is important for tackling various urban planning and environmental management issues in this fast growing country. There is a demand to develop a kind of simulation models which can assist the complex decision-making processes associated with the economic and development transition. The fast emergence of geographical cellular automata (CA) in China has been witnessed since the late 1990s. A number of CA models have been proposed to solve the complex urban and regional development problems in this region. For example, Wu (1998) developed a CA model, SimLand, to simulate rural-urban land conversion by incorporating the multi-criteria evaluation (MCE) method. The logistic regression method was proposed to calibrate CA models by using training data (Wu 2002, Li et al. 2008). Li and Yeh (2002) proposed a neural network-based CA (ANN-CA) model to reduce the influence of spatial autocorrelation in urban and land use simulation. An advantage of this model is that spatial variables are not necessarily required to be independent of each other. Attempts have also been made by using genetic algorithms to calibrate CA models (Li et al. 2008). Recently, A Geographical Simulation and Optimization System (GeoSOS) is proposed by Li et al. (2011). GeoSOS is a computer-based system to simulate, predict, optimize, and display geographical patterns and processes (downloaded at http://www.geosimulation.cn/). As a bottom-up approach, GeoSOS consists of three major integrated components, CA, ABMs, and SIMs. This system is equipped with some common CA algorithms, such as MCE-CA, logistic-CA, PCA-CA, ANN-CA, and Decision-tree-CA. It also provides spatial optimization algorithms (e.g. facility-siting, path-finding, and area optimization) by modifying ant algorithms.

To present a review on applications of urban CA models in China, we used Google Scholar to search international articles with the keyword combinations of "cellular automata + land use change + China" and "cellular automata + urban + China". Thereafter the articles were manually filtered to match the topic. Finally, 44 articles were selected for this review. We have not included Chinese papers or books in the analysis. For example, Zhou et al. (1998) published a Chinese book titled

"Geographical cellular automata" which should have some influences on the study of cellular automata in China.

Table 1 lists these applications with the information of the model and the validation method. Most of the CA applications are within those coastal cities in eastern China. This is not surprised because this part of China is experiencing the fast industrialization and urbanization processes (Seto and Fragkias 2005, Luo and Wei 2009, Deng et al. 2010). However, the rapid urban development also gives rise to a lot of ecological and environmental issues (Li et al. 2007, Deng et al. 2009, Fang et al. 2009). Therefore, these cities in eastern China can be the perfect experiment fields for the implementation of various CA models for the assessment of urban development policies. From the perspective of regional studies using CA models, there are two notable application areas: Pearl River Delta (PRD) and Northern China. The PRD is one of the economically dynamic regions and the world's famous manufacturing base. This region also suffers serious environmental problems caused by fast urbanization, including the loss of farmland (Seto et al. 2002, Li and Yeh 2004a), the degradation of mangrove forest (Liu et al. 2008a), air pollution (Guo et al. 2006), etc. Researchers, such as Wu (1996) and Li and Yeh (2000), brought in the CA models to address the issues of sustainable urban development in PRD during late 1990s. These were also the first CA applications in China. The region of Northern China spans from moist zone, semi-moist, semiarid zone and arid zone with obvious climate transition and regional differences (He et al. 2005). This region contains the agriculture-pasture transition zone, and the environment and eco-system here are relatively vulnerable. Studies conducted by He et al (2005), Li and He (2008), and Chen et al (2008) mainly focus on the assessing the potential impacts of land use/cover change on the local eco-systems.

It can be seen from Table 1 that those widespread models in China are the family of CA models based on multi-criteria evaluation (MCE-CA) (Wu and Webster 1998) or artificial neural network (ANN-CA) (Li and Yeh 2002), and the SLEUTH model (Clarke et al. 1997). This is related to the pros and cons when applying these models to the specific simulation problem. The family of the MCE-CA models calculates the development probability of a cell from the weighted sum or product of a group of factors (Santé et al. 2010). Thus the main issue when using MCE-CA for urban simulation is how to soundly define the weights of the factors. Usually this requires the sophisticated domain knowledge or expertise in the field of urban studies. Lately, researchers developed several approaches to automatically calibrate the model, such as logistic regression (Wu 2002) and Monte-Carlo approach (Chen et al. 2002). More recently, techniques from artificial intelligence are introduced for the calibration of CA models, including genetic algorithms (Li et al. 2008), support vector machines (Yang et al. 2008), swarm intelligence (Liu et al. 2008c, Feng et al. 2011), artificial immune systems (Liu et al. 2010), etc. For a long time, urban simulation using these models has been simplified into the simulation of, for a particular land use type (e.g., built-up area), "changed or not" (developed or undeveloped). This is caused by the difficulty in handling the complex interactions among various land use types. Such problem can be solved by using the ANN-CA. The non-linearity of ANN makes it possible in dealing with the complex relationships of land use conversion. Thus the ANN-CA can fit well the objective of

simulating the change of multiple land use types in a large area, such as northern China (Li and He 2008).

Table 1 Selected studies on using CA for urban simulation in China

| Article | Model | Study area | Validation method |
|---|---|---|---|
| Kuang (2011) | ANN-CA | Beijing, Tianjin and Tangshan | Kappa index and PCM |
| Chen et al (2002) | MCE-CA (Mont-Carlo calibration) | Beijing | Cell-by-Cell comparison |
| Long et al (2009) | Logistic-CA | Beijing | Cell-by-Cell comparison |
| Yang et al (2011) | ANN-CA | Beijing | N/A |
| He et al (2006) | SD-MCE-CA (Mont-Carlo calibration) | Beijing | Kappa index |
| Wang et al (2006) | MCE-CA | Beijing | N/A |
| Pan et al (2010) | CLUE-S | Beijing | Kappa index |
| Li and Yeh (2001) | ANN-CA | Dongguan | Cell-by-Cell comparison |
| Li and Yeh (2000) | Grey-cell CA | Dongguan | N/A |
| Li and Yeh (2004b) | Decision-Tree CA | Dongguan | Cell-by-Cell comparison |
| Huang and Gao (2011) | MCE-CA (GA calibration) | Dongguan | Cell-by-Cell comparison |
| Wu et al (2010) | ANN-CA | Dongying | Fuzzy Kappa index |
| Li et al (2008) | GA-CA | Guangzhou and Dongguan | Cell-by-Cell comparison |
| Liu et al (2008c) | ACO-CA | Guangzhou | Cell-by-Cell comparison and Kappa index |
| Wu (1996) | Fuzzy-CA | Guangzhou | N/A |
| Wu (2002) | Logistic-CA | Guangzhou | Cell-by-Cell comparison and Moran I |
| Liu et al (2008b) | Kernel-based CA | Guangzhou | Cell-by-Cell comparison and Kappa index |
| Wu and Webster (1998) | MCE-CA | Guangzhou | Cell-by-Cell comparison |
| Gong et al | Logistic-CA | Guangzhou | Cell-by-Cell comparison |

Table 1 (cont) Selected studies on using CA for urban simulation in China

| Article | Model | Study area | Validation method |
|---|---|---|---|
| (2009) | | | |
| Liu and Liu (2009) | SLEUTH | Hangzhou | Lee-Sallee statistic |
| Ke (2006) | N/A | Jiangning (Nanjing) | N/A |
| Xu et al (2006) | SLEUTH | Lanzhou | N/A |
| He et al (2005) | SD-CA | Northern China | Cell-by-Cell comparison and Kappa index |
| Li and He (2008) | SD-ANN-CA | Northern China | Cell-by-Cell comparison and Kappa index |
| Chen et al (2008) | iCLUE | Northern China | Cell-by-Cell comparison |
| Li and Liu (2006) | CBR-CA | Pearl River Delta | Cell-by-Cell comparison and Kappa index |
| Liu et al (2010) | AIS-CA | Pearl River Delta | Cell-by-Cell comparison |
| Fan et al (2008) | Markov-CA | Pearl River Delta | N/A |
| Fu et al (2010) | MCE-CA | Qingdao | N/A |
| Wang et al (2009) | Markov-CA | Rizhao | N/A |
| Huang et al (2008) | MCE-CA | Shanghai | Cell-by-Cell comparison |
| Han et al (2009) | SD-CA | Shanghai | Kappa index |
| Feng et al (2011) | PSO-CA | Shanghai | Cell-by-Cell comparison and Kappa index |
| Zhang et al (2011) | MCE-AHP-CA | Shanghai | Assessment of quantity and location disagreement |
| Xi et al (2010) | SLEUTH | Shenyang and Fushun | Kappa index |
| Wu et al (2009) | SLEUTH | Shenyang | ROC curves, multiple-resolution error budget and landscape metrics |
| Yang et al (2008) | SVM-CA | Shenzhen | Cell-by-Cell comparison and Kappa index |
| Sui and Zeng (2001) | MCE-CA | Shenzhen | Cell-by-Cell comparison |
| Wang and Li (2010) | RBFN-based CA | Shenzhen | Figure of merit |

Table 1 (cont) Selected studies on using CA for urban simulation in China

| Article | Model | Study area | Validation method |
|---------|-------|-----------|-------------------|
| Xie et al (2007) | ABM-CA | Suzhou | Cell-by-Cell comparison |
| Cheng and Masser (2002) | MCE-CA | Wuhan | Visual comparison |
| Cheng and Masser (2003) | MCE-CA | Wuhan | N/A |
| Li et al (2003) | Population diffusion model | Xi'an | N/A |
| Liu et al (2011) | ANN-CA | Xiangtan | N/A |

The weakness of this model is its lack of the explanatory power about the geographical process. This is due to the black-box essence of ANN. Compared with the ANN-CA, the SLEUTH model differentiates the growth types into spontaneous growth, new spreading center growth, edge growth and road-influenced growth. Thus the SLEUTH model can help users better understand the urbanization process of the study area. However, because the calibration method is a brute-force method, the time-consuming calibration procedure becomes the major drawback of SLEUTH. Therefore, it can be extremely difficult to apply the SLEUTH in large area with fine resolution data.

In most of the studies shown in Table 1, CA models were used to simulate real urban forms based on the replication of the historical growth process. The success in replicating historical urban growth indicates that the model is able to capture the regularity of the evolution of urban forms. Thereafter the model is used to predict the potential future form by means of scenario simulations. These applications have demonstrated the power of CA models for produce realistic urban forms as a means to find solutions for practical problems. For example, He et al (2006) incorporated system dynamics (SD) with CA to simulate the urban expansion of Beijing during 1994-2001, and predict the development patterns under different policies with respect to the limitation of water resources and environmental deterioration. In addition to the simulation of real urban forms, CA models were also popular in studies on exploring explore and validate hypothetical ideas related to urban dynamics (Santé et al. 2010). The very first example is Wu (1996), in which the author integrated fuzzy set theory and CA to model sustainable urban development. Li and Yeh (2000) used the constrained CA model to assess the benefits of compact development in fast growing city. Recent studies also reveal the utilization of artificial intelligence to produce the hypothetical urban forms, such as genetic algorithms (Li et al. 2008) and artificial immune systems (Liu et al. 2010).

## 3. Conclusion

China has come to a new era of rapid urbanization and urban expansion. Since the late 1990s, many studies on using cellular automata techniques have been carried out to tackle urban and regional development problems. Cellular automata (CA) have been used as a useful tool to support land use planning and policy analysis as well as to explore scenarios for future development in this fast developing country. There is a growing demand for the application of CA in some planning departments in major Chinese cities. Especially, many applications are found in the coastal cities, such as Guangzhou, Dongguan, Shenzhen, Shanghai and Beijing in China.

Significant modifications have been made so that CA can be suited to a lot of urban simulation and planning tasks in this region. Much effort has been made to generate a high degree of reality in urban simulation by using a richer set of GIS data for the calibration. Some classical CA models have been established by Chinese scholars who have used a variety of intelligent methods, such as MCE, ANN, and GA methods, for calibrating these models (Wu 1998, 2002, Li 2000, 2002, 2011).

## References

Chan, K.W. & Zhang, L., 1999. The hukou system and rural-urban migration in China: Processes and changes. The China Quarterly, (160), 818-855.

Chen, J., Gong, P., He, C., Luo, W., Tamura, M. & Shi, P., 2002. Assessment of the urban development plan of Beijing by using a CA-based urban growth model. PE & RS-Photogrammetric Engineering & Remote Sensing, 68 (10), 1063-1071.

Chen, Y., Li, X., Su, W. & Li, Y., 2008. Simulating the optimal land-use pattern in the farming-pastoral transitional zone of Northern China. Computers, Environment and Urban Systems, 32 (5), 407-414.

Cheng, J. & Masser, I., Year. Cellular automata based temporal process understanding of urban growth. In: Bandini, S., Chopard, B. & Tomassini, M., ed. 5th International Conference on Cellular Automata for Research and Industry, Geneva, Switzerland, 325-336.

Cheng, J. & Masser, I., 2003. Urban growth pattern modeling: a case study of Wuhan city, PR China. Landscape and Urban Planning, 62 (4), 199-217.

Chryssy Potsiou, 2010. Rapid Urbanization and Mega Cities: The Need for Spatial Information Management, the International Federation of Surveyors (FIG) report, Kalvebod Brygge 31-33, DK-1780 Copenhagen V, Denmark.

Clarke, K., Hoppen, S. & Gaydos, L., 1997. A self-modifying cellular automaton model of historical urbanization in the San Francisco Bay area. Environment and planning B, 24, 247-262.

Deng, J.S., Wang, K., Hong, Y. & Qi, J.G., 2009. Spatio-temporal dynamics and evolution of land use change and landscape pattern in response to rapid urbanization. Landscape and Urban Planning, 92 (3-4), 187-198.

Deng, X., Huang, J., Rozelle, S. & Uchida, E., 2010. Economic Growth and the Expansion of Urban Land in China. Urban Studies, 47 (4), 813-843.

Fan, F., Wang, Y. & Wang, Z., 2008. Temporal and spatial change detecting (1998–2003) and predicting of land use and land cover in Core corridor of Pearl River Delta (China) by using TM and ETM+ images. Environmental Monitoring and Assessment, 137 (1), 127-147.

Fang, M., Chan, C. & Yao, X., 2009. Managing air quality in a rapidly developing nation: China. Atmospheric environment, 43 (1), 79-86.

Feng, Y., Liu, Y., Tong, X., Liu, M. & Deng, S., 2011. Modeling dynamic urban growth using cellular automata and particle swarm optimization rules. Landscape and Urban Planning, 102 (3), 188-196.

Fu, Q., Song, J., Mao, F. & Zhou, W., Year. Simulation of city development using cellular automata and agent based integrated model: A case study of Qingdao cityed. 18th International Conference on GeoinformaticsIEEE, 1-4.

Gong, J., Liu, Y., Xia, B. & Zhao, G., 2009. Urban ecological security assessment and forecasting, based on a cellular automata model: A case study of Guangzhou, China. Ecological Modelling, 220 (24), 3612-3620.

Guo, H., Wang, T., Blake, D., Simpson, I., Kwok, Y. & Li, Y., 2006. Regional and local contributions to ambient non-methane volatile organic compounds at a polluted rural/coastal site in Pearl River Delta, China. Atmospheric environment, 40 (13), 2345-2359.

Han, J., Hayashi, Y., Cao, X. & Imura, H., 2009. Application of an integrated system dynamics and cellular automata model for urban growth assessment: A case study of Shanghai, China. Landscape and Urban Planning, 91 (3), 133-141.

He, C., Okada, N., Zhang, Q., Shi, P. & Zhang, J., 2006. Modeling urban expansion scenarios by coupling cellular automata model and system dynamic model in Beijing, China. Applied Geography, 26 (3-4), 323-345.

He, C., Shi, P., Chen, J., Li, X., Pan, Y., Li, J. & Li, Y., 2005. Developing land use scenario dynamics model by the integration of system dynamics model and cellular automata model. Science in China Series D: Earth Sciences, 48 (11), 1979-1989.

He, S. & Wu, F., 2005. Property-led redevelopment in post-reform China: a case study of Xintiandi redevelopment project in Shanghai. Journal of Urban Affairs, 27 (1), 1-23.

Huang, G. & Gao, W., 2011. Simulation Study on CA Model Based on Parameter Optimization of Genetic Algorithm and Urban Development. Procedia Engineering, 15, 2175-2179.

Huang, H., Zhang, L., Guan, Y. & Wang, D., 2008. A cellular automata model for population expansion of Spartina alterniflora at Jiuduansha Shoals, Shanghai, China. Estuarine, Coastal and Shelf Science, 77 (1), 47-55.

Ke, C.Q., Year. Urban Growth Modeling of Jiangning Through Cellular Automataed.IEEE, 1489-1492.

Kuang, W., 2011. Simulating dynamic urban expansion at regional scale in Beijing-Tianjin-Tangshan Metropolitan Area. Journal of Geographical Sciences, 21 (2), 317-330.

Li, L., Sato, Y. & Zhu, H., 2003. Simulating spatial urban expansion based on a physical process. Landscape and Urban Planning, 64 (1-2), 67-76.

Li, X. & Liu, X.P., 2006. An extended cellular automation using case-based reasoning form simulating urban development in a large complex region. International Journal of Geographical Information Science, 20 (10), 1109-1136.

Li, X., Yang, Q.S. & Liu, X.P., 2008. Discovering and evaluating urban signatures for simulating compact development using cellular automata. Landscape and Urban Planning, 86 (2), 177-186.

Li, X., Yeh, A., Wang, S., Liu, K., Liu, X., Qian, J. & Chen, X., 2007. Regression and analytical models for estimating mangrove wetland biomass in South China using Radarsat images. International Journal of Remote Sensing, 28 (24), 5567-5582.

Li, X. & Yeh, A.G., 2002. Neural-network-based cellular automata for simulating multiple land use changes using GIS. International Journal of Geographical Information Science, 16 (4), 323-343.

Li, X. & Yeh, A.G.O., 2000. Modelling sustainable urban development by the integration of constrained cellular automata and GIS. International Journal of Geographical Information Science, 14 (2), 131-152.

Li, X. & Yeh, A.G.O., 2001. Calibration of cellular automata by using neural networks for the simulation of complex urban systems. Environment and Planning A, 33 (8), 1445-1462.

Li, X. & Yeh, A.G.O., 2004a. Analyzing spatial restructuring of land use patterns in a fast growing region using remote sensing and GIS. Landscape and Urban Planning, 69 (4), 335-354.

Li, X. & Yeh, A.G.O., 2004b. Data mining of cellular automata's transition rules. International Journal of Geographical Information Science, 18 (8), 723-744.

Li X, Chen Y M, Liu X P, Li D, He J Q., 2011. Concepts, methodologies, and tools of an integrated Geographical Simulation and Optimization System (GeoSOS). International Journal of Geographical Information Science. 25(4), 633–655

Li, Y.C. & He, C.Y., 2008. Scenario simulation and forecast of land use/cover in northern China. Chinese Science Bulletin, 53 (9), 1401-1412.

Liu, F., Zhang, Z., Sun, F., Zuo, L. & Wang, X., Year. Urban Spatial Expansion of Xiangtan City, China. In: Li, X., ed. Geoinformatics 2011: The 19th International Conference on Geoinformatics Shanghai, China, 1-8.

Liu, J., Liu, M., Zhuang, D., Zhang, Z. & Deng, X., 2003. Study on spatial pattern of land-use change in China during 1995–2000. Science in China Series D: Earth Sciences, 46 (4), 373-384.

Liu, K., Li, X., Shi, X. & Wang, S.G., 2008a. Monitoring mangrove forest changes using remote sensing and GIS data with decision-tree learning. Wetlands, 28 (2), 336-346.

Liu, X., Li, X., Shi, X., Wu, S. & Liu, T., 2008b. Simulating complex urban development using kernel-based non-linear cellular automata. Ecological Modelling, 211 (1-2), 169-181.

Liu, X., Li, X., Shi, X., Zhang, X. & Chen, Y., 2010. Simulating land-use dynamics under planning policies by integrating artificial immune systems with cellular automata. International Journal of Geographical Information Science, 24 (5), 783-802.

Liu, X.P., Li, X., Liu, L., He, J. & Ai, B., 2008c. A bottom-up approach to discover transition rules of cellular automata using ant intelligence. International Journal of Geographical Information Science, 22 (11-12), 1247-1269.

Liu, Y. & Liu, X., Year. Applying SLEUTH for simulating urban expansion of Hangzhoued., 747104-1.

Long, Y., Mao, Q. & Dang, A., 2009. Beijing Urban Development Model: Urban Growth Analysis and Simulation. Tsinghua Science & Technology, 14 (6), 782-794.

Luo, J. & Wei, Y., 2009. Modeling spatial variations of urban growth patterns in Chinese cities: The case of Nanjing. Landscape and Urban Planning, 91 (2), 51-64.

Pan, Y., Roth, A., Yu, Z. & Doluschitz, R., 2010. The impact of variation in scale on the behavior of a cellular automata used for land use change modeling. Computers, Environment and Urban Systems, 34 (5), 400-408.

Santé, I., García, A., Miranda, D. & Crecente, R., 2010. Cellular automata models for the simulation of real-world urban processes: A review and analysis. Landscape and Urban Planning, 96 (2), 108-122.

Seto, K. & Fragkias, M., 2005. Quantifying spatiotemporal patterns of urban land-use change in four cities of China with time series landscape metrics. Landscape Ecology, 20 (7), 871-888.

Seto, K., Woodcock, C., Song, C., Huang, X., Lu, J. & Kaufmann, R., 2002. Monitoring land-use change in the Pearl River Delta using Landsat TM. International Journal of Remote Sensing, 23 (10), 1985-2004.

Seto, K.C., Kaufmann, R.K. & Woodcock, C.E., 2000. Landsat reveals China's farmland reserves, but they're vanishing fast. Nature, 406 (6792), 121-121.

Sui, D. & Zeng, H., 2001. Modeling the dynamics of landscape structure in Asia's emerging desakota regions: a case study in Shenzhen. Landscape and Urban Planning, 53 (1-4), 37-52.

Tian, G., Liu, J., Xie, Y., Yang, Z., Zhuang, D. & Niu, Z., 2005. Analysis of spatio-temporal dynamic pattern and driving forces of urban land in China in 1990s using TM images and GIS. Cities, 22 (6), 400-410.

Wang, G., Chen, J., Li, Q. & Ding, H., 2006. Quantitative assessment of land degradation factors based on remotely-sensed data and cellular automata: a case study of Beijing and its neighboring areas. Environmental Sciences, 3 (4), 239-253.

Wang, S., Li, J., Wu, D., Liu, J., Zhang, K. & Wang, R., 2009. The strategic ecological impact assessment of urban development policies: a case study of Rizhao City, China. Stochastic Environmental Research and Risk Assessment, 23 (8), 1169-1180.

Wang, Y. & Li, S., 2010. Simulating multiple class urban land-use/cover changes by RBFN-based CA model. Computers & Geosciences, 37 (2), 111-121.

Wu, D., Liu, J., Wang, S. & Wang, R., 2010. Simulating urban expansion by coupling a stochastic cellular automata model and socioeconomic indicators. Stochastic Environmental Research and Risk Assessment, 24 (2), 235-245.

Wu, F., 1996. A linguistic cellular automata simulation approach for sustainable land development in a fast growing region. Computers, Environment and Urban Systems, 20 (6), 367-387.

Wu, F., 1998. The new structure of building provision and the transformation of the urban landscape in metropolitan Guangzhou, China. Urban Studies, 35 (2), 259.

Wu, F. & Webster, C., 1998. Simulation of land development through the integration of cellular automata and multicriteria evaluation. Environment and planning B, 25, 103-126. [58] Wu, F.L., 2002. Calibration of stochastic cellular automata: the application to rural-urban land conversions. International Journal of Geographical Information Science, 16 (8), 795-818.

Wu, X., Hu, Y., He, H.S., Bu, R., Onsted, J. & Xi, F., 2009. Performance evaluation of the SLEUTH model in the Shenyang metropolitan area of Northeastern China. Environmental Modeling and Assessment, 14 (2), 221-230.

Xi, F., He, H.S., Hu, Y., Bu, R., Chang, Y., Wu, X., Liu, M. & Shi, T., 2010. Simulating the impacts of ecological protection policies on urban land use sustainability in Shenyang-Fushun, China. International Journal of Urban Sustainable Development, 1 (1-2), 111-127.

Xie, Y.C., Batty, M. & Zhao, K., 2007. Simulating emergent urban form using agent-based modeling: Desakota in the suzhou-wuxian region in china. Annals of the Association of American Geographers, 97 (3), 477-495.

Xu, X., Zhang, F. & Zhang, J., Year. Modelling the impacts of different policy scenarios on urban growth in Lanzhou with remote sensing and cellular automataed.IEEE, 1435-1438.

Yang, Q.S., Li, X. & Shi, X., 2008. Cellular automata for simulating land use changes based on support vector machines. Computers & Geosciences, 34 (6), 592-602.

Yang, W., Li, F., Wang, R. & Hu, D., 2011. Ecological benefits assessment and spatial modeling of urban ecosystem for controlling urban sprawl in Eastern Beijing, China. Ecological Complexity, 8 (2), 153-160.

Zhang, Q., Ban, Y., Liu, J. & Hu, Y., 2011. Simulation and analysis of urban growth scenarios for the Greater Shanghai Area, China. Computers, Environment and Urban Systems, 35 (2), 126-139.

Zhou C. H., Sun Z, L., and Xie Y. C. (1999), Geographical cellular automata. Chinese Science Press (in Chinese). pp. 163.

# Calibration of an urban cellular automata model by using statistic techniques and a genetic algorithm

Application to a small urban settlement of NW Spain

## A.M. GARCÍA; I. SANTÉ; R. CRECENTE

Land Laboratory, University of Santiago de Compostela

E.P.S Campus Universitario s/n, Lugo, 27002, Spain

+34.982.82.32.92, andresmanuel.garcia@usc.es

## Abstract

Cellular automata (CA) have been widely used to simulate and analyze urban growth processes due to their simplicity and capability of representing emergent complex dynamics. Nevertheless, CA have not been used too much outside the research realm, due to the lack of flexibility of implemented models or the difficulties for their calibration and validation.

In the present article, the model of White and Engelen is used as a basis, because it is one of the most flexible and widely used in the bibliography, so as to produce a model inspired in it which will offer fewer difficulties by the time of calibrating it. This will be achieved reducing the coefficients to be calibrated so as to be able to automate this task using a genetic algorithm (GA). The obtained model will be tested, simulating urban growth in the municipality of Ribadeo (NW Spain) and analyzing the results.

## Introduction

Cellular Automata (CA) stand out among the most used urban models, due to their capability of reproducing complex dynamics, similar to those found in real cities, from simple rules. There are several examples of the application of urban CA to the simulation of the expansion of big cities [1, 2, 3, 4, 5].

In most of the cases, models were not used outside the scientific community due to, among other factors, the lack of flexibility to accurately simulate different urban dynamics and the lack of validation and calibration methods to make them more user-friendly and ensure accurate simulations [6].

In recent years new calibration techniques are being applied. Mainly heuristic optimization techniques such as simulated annealing and genetic algorithms (GA), which constitute two of the most robust heuristic techniques. GA have been widely used for CA calibration [7, 8, 9, 10, 11,12].

In this paper, a simplification of the calibration process of an urban CA is proposed, using logistic regressions and a GA to improve its flexibility. Most of the existing models were applied in large cities where urban growth is fast and abundant, thus

there is a lot of information that can be used to identify urban dynamics. However, in urban areas with slow and scarce growth, these dynamics are more difficult to identify [13]. This is the case of Ribadeo, a small municipality in NW Spain [14]. Testing the model in such an area with so different characteristics, will allow to better assess its flexibility. The paper starts describing the structure of the model, which is based on the model of White et al. [1]. Then, the calibration process is explained, where two novelties are introduced; the reduction of the number of calibration parameters by using logistic regressions, a representation of the distance decay influence of neighbouring land uses in the central cell using two linear functions and a GA for the calibration of the remaining parameters. Finally, the results of the simulation of urban growth in Ribadeo are analyzed and a series of conclusions are drawn.

## 1. Urban CA model

One of the first widespread empirical applications of urban CA models was developed by White el at. [1]. This model keeps the essence of formal CA rules and hence their simplicity. Furthermore, it simulates several land use dynamics and uses an extended circular neighborhood that accounts for the distance decay influence of several land uses on the central cell state. These characteristics allow a great flexibility by the time of simulating different types of dynamics [6].

This model considers two types of land uses: fixed, which influence the dynamics of other land uses but do not participate in simulated dynamics, and active, which both influence the dynamics of other uses and participate in the simulated dynamics and thus are affected by growth rates. The transition rule of the model is based on equation 1, which provides the transition potential of each cell from land use $h$ to each active land use $j$ ($P_{hj}$):

$$P_{hj} = vs_j\left(1 + N_j\right) + H_j \qquad (1)$$

where $s_j$ is the cell suitability for land use $j$, $N_j$ is the neighborhood effect and $H_j$ is an inertia parameter that models the resistance of land use $h$ to change to land use $j$. $v$ is a stochastic variable which introduces randomness in the model and is determined by equation 2:

$$v = 1 + \left[-\ln(rand)\right]^\alpha \qquad (2)$$

where *rand* is a random number between 0 and 1 and α is a coefficient that controls the degree of randomness introduced in the model. The effect of the neighborhood *(Nj)* is calculated with equation 3:

$$N_j = \sum_d \sum_i m_{kjd} I_{id} \qquad (3)$$

where $I_{id}$ is 1 if cell $i$ at distance $d$ is occupied by land-use $k$ and is 0 if it is not. In White et al. [1] a circular neighborhood with a radius of 6 cells is used, where the influence of each cell is modeled by means of a coefficient $m_{kd}$, which value depends on land-use $k$ in cell $i$ and on the distance $d$ of cell $i$ to the central cell. Cells transition in each interaction of the model to the land use for which they show a higher transition potential until the growth rate for that land use is reached. In the model proposed in this paper, the random variable is scaled using an exponential curve (equation 4) which allows controlling better the degree of randomness introduced in the model [15]. The random parameter in the equation is generated using the algorithm of VB.

$$v = \exp(-\alpha \times (1 - rand)) \qquad (4)$$

Besides, in order to model the relative importance of suitability $s_j$ with respect to neighborhood, this value is scaled with the coefficient $\beta$. This way the suitability factor is scaled in a similar way to that of the stochastic variable with the $\alpha$ coefficient of equation 2.

Finally, a series of restrictions $(R_j)$ are considered that take the value 0 or 1 depending on whether the cell can be developed or not because of some kind of constraint. Once the aforementioned modifications are made, equation 1 remains as follows (equation 5):

$$P_{hj} = R_j * v * s_j^{\beta} * \left(1 + N_j\right)_j + H_j \qquad (5)$$

## 2. Model calibration

The calibration of the proposed model is complex because of the high number of calibration parameters. The model of White is usually calibrated by trial and error or by expert knowledge [1, 3, 4, 16, 17]. Trial and error is very time-consuming [18] and both methods do not assure accurate results since they may introduce a lot of subjectivity [19]. These shortcomings are overcome by reducing the number of calibration parameters so as to be able to automate the calibration process using a GA.

### 2.1 Parameter calculation using statistical methods.

The suitability factor $(s_j)$ was calculated by using a logistic regression, therefore it will be avoided to calibrate as many parameters as the number of variables considered to calculate the suitability. This method has already been used to calibrate an urban CA model in [20].

Another way of reducing the number of parameters is simplifying the calculation of the neighborhood effect. This can be done by using a function of the distance to calculate the influence of the neighbouring land uses on the transition potential of the central cell. This function could have several shapes [21], which can be simplified by using two linear functions (Figure 1):

$$f(x) = a + bx \qquad (6)$$

$$f(x) = c + dx \qquad (7)$$

where x is the distance to the central cell and a, b, c and d are the coefficients of the linear function.

Therefore, it is not necessary to calibrate one $m_{kjd}$ coefficient for each land use $k$ and equidistant cell to the central cell (for a circular neighborhood with a radius of 3 cells 7 coefficients $m_{kjd}$ would have to be calibrated for each couple of land uses, as shown in figure 2), since the four parameters that define the two lines (a, b, c and d) are enough to model the distance decay effect.
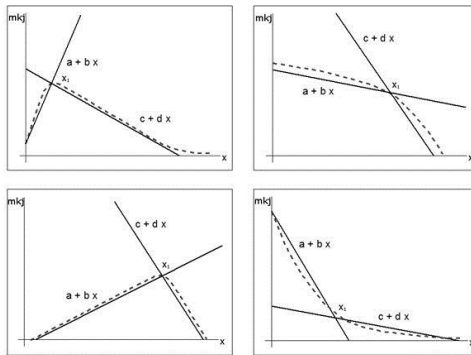


Figure 1: Examples of simplification of distance decay functions by using two linear functions.

|   |   |   | 6 |   |   |   |
|---|---|---|---|---|---|---|
|   | 5 | 4 | 3 | 4 | 5 |   |
|   | 4 | 2 | 1 | 2 | 4 |   |
| 6 | 3 | 1 | 0 | 1 | 3 | 6 |
|   | 4 | 2 | 1 | 2 | 4 |   |
|   | 5 | 4 | 3 | 4 | 5 |   |
|   |   |   | 6 |   |   |   |

Figure 2: Cells numbered considering their equidistance to the central cell in a 3 cell radius neighborhood.

**2.2. Genetic Algorithm**

In spite of having considerably reduced the number of calibration parameters (from 213 to 138), they are still quite a few; therefore the calibration process remains difficult. This is the reason why a GA [22] is used to accomplish this task.

This calibration method is inspired on the genetic evolution of populations and is composed of the following phases: (i) initialization, where an initial population of possible solutions is randomly generated, (ii) evaluation, where the goodness of the solution provided by each individual is calculated using a fitness function, (iii) selection, where the best individuals are selected according to their fitness, (iv) cross-breeding, where selected individuals are cross breeded to create the following population of solutions, and (v) mutation, where random variations are introduced in the values of the obtained population of solutions.

In our case, a first population of 700 possible solutions was randomly generated, so as to have a number of individuals higher than the number of allele and not too high so as to make the algorithm too computationally intensive.This way it is ensured that the initial populatin is diverse enough and the computation time is not too long.The simulations corresponding to those 700 possible solutions were evaluated to select the parents using the tournament method. In the tournament process all individuals where randomly chosen two by two and compared. The best ones in each comparison were selected to cross-breed. Every couple of chosen individuals generated two sons. In the cross-breeding process two recombination points were randomly set, where the information of each parent was interchanged to generate each son. The best individual in each population is selected to survive in the following generation. A mutation rate of 0.008% is applied to all individuals of the population of descendant, except for the surviving one. The mutation rate was determined by trial and error considering that it would produce variability enough so that the algorithm would not get stuck in a local optimum. This was checked comparing the mean and maximum values of the fitness function for each generation, if the maximum value did not vary the mean should compensate this stability producing strong variations of its value in each iteration.

By the time of selecting a fitness function, it was considered that indexes that evaluate cell by cell coincidence do not account for the coincidence of the patterns. That is why the index proposed in [23] in combination with three spatial metrics [24] - the number of patches (NP), the area weighted mean patch area (AREA_AM) and the edge density (ED) – were used. The index proposed in [23] not only accounts for cell by cell coincidence but also measures whether cells were located close to their real position or not, giving thus a better assessment of the accuracy of the model than the kappa index.

The index described in [23] is calculated running all over the real $R$ and simulated maps $S$ windows with several resolutions $g$ (1 cell side, 2, 3, 4, …, n cells side). In each window, the number of cells $n$ occupied by each land-use $j$ in the real $Rn,j$ and simulated maps $Sn,j$ is calculated. The lowest value for each map and land use is chosen and all the values for all land-uses are added. Then each window is weighted by the number of cells that the window covers, $Wn$, all the values from all windows in which the maps are divided at each resolution are added $g(Ng)$ and the resulting value is divided by the number of cells of the map.

Equation 8 is used to calculate indexes for each window resolution $Pg$. Equation 9 is used to calculate a global index for all the window resolutions. In equation 9, b scales the relative importance of each resolution in the final index, in our case b was

given a value of 1.2. *P* will have the value 1 if there is a perfect match and 0 if the cells do not match at all.

$$Pg = \frac{\sum_{n=1}^{Ng}\left[Wn\sum_{j}^{J} MIN(Rn, j, Sn, j)\right]}{\sum_{n=1}^{Ng} Wn} \qquad (8)$$

$$P = \frac{\sum_{g}^{G} \exp^{b \times g} \times Pg}{\sum_{g}^{G} \exp^{b \times g}} \qquad (9)$$

Only active land uses were considered in the fitness function. The values of the spatial metrics for the simulated map where subtracted to the values for the real map. The absolute values of these subtractions and the value of *P* (eq. 9) were used in the fitness function. So that these values varied within the same range, the maximum and minimum values for each index in each interaction of the AG were taken and used to normalize the indexes (eq. 10). Finally, the normalized values where used in equation 11 to calculate the fitness function (*F*). *F* was used to evaluate the individuals of each generation, thus the higher the value, the better the individual will be.

$$Normalized\ value = \frac{Value - \min value}{\max value - \min value} \qquad (10)$$

$$F = \left[\frac{\dfrac{normalized\ NP + normalized\ AREA\_AM + normalized\ ED}{3} + Normalized\ P}{2}\right]^{-1} \qquad (11)$$

## 3. Case study

The study area is located in the municipality of Ribadeo (NW Spain) (map 1). Ribadeo is located at a crossroad of important routes connecting the regions of Asturias and Galicia and concentrates the commercial activities and services of the surrounding areas. Ribadeo has 6000 inhabitants and experienced a growth of 1000 inhabitants in the last 10 years. The study area is formed by the main urban core of Ribadeo and its 4 surrounding parishes (sub-municipal administrative division in the region of Galicia), towards which the urban core is expanding.

Map 1: Location of the study area and land use map of 2007.

The data for the model calibration were obtained by fotointerpetation of aerial images of 1978, 1995 and 2007. A cadastral map of 1995 and a digital terrain model obtained from the Spanish national topographic map were also used. All this information was converted to raster format of 35 x 35 m resolution, and processed to obtain the maps of the input variables.

Land uses where classified as in the model of White et al. [1]:

- Fixed land uses; water surfaces, roads, institutional, parks, rail tracks.
- Active land uses; commercial, industrial and residential.

Agriculture and forest land uses where considered as fixed land uses, yet they could be transformed to urban land-uses.

First, the suitability maps *(sj)* were calculated using the logistic regression technique described in section 2.1 (Map 2).

Map 2: Suitability maps for the active land uses.

The model was calibrated using the land use maps of 1978 and 1995. The AG was run until the best fitness value did not increase during several interactions (this happened from interaction 52 on, when the fitness function increased from an initial value of $3.95 \times 10^{-8}$ to a value of $4.47 \times 10^{-7}$). The coefficients obtained in the calibration (table 2) where used to simulate urban growth between 1995 and 2007. Results were validated comparing them with the land use map of the year 2007. The amount of growth of each active land use in each interaction was determined dividing the real growth in the period to be simulated by the number of interactions of the simulation.

Table 2 Coefficients obtained in the calibration with the GA

| Industrial land-use Potential | | | | |
|---|---|---|---|---|
| Land-uses Neighborhood | a | b | c | d |
| Agriculture | -15.73 | -1.94 | 74.42 | -11.94 |
| Water | 18.35 | 1.42 | -82.68 | 7.03 |
| Commercial | 15.27 | 0.06 | 2.76 | -0.50 |
| Roads | -43.73 | -1.07 | 96.80 | 0.97 |
| Forest | -19.81 | 2.11 | 55.90 | 0.78 |
| Industrial | -69.44 | -0.15 | 1.19 | -0.47 |
| Institutional | 89.94 | -0.14 | 15.98 | 0.00 |
| Parks | 34.18 | 0.34 | -14.99 | -0.51 |
| Residential | -98.98 | 0.74 | -85.63 | -2.51 |
| | | $\alpha$ | | 4.53 |
| | | $\beta$ | | 5.50 |
| | | H | | 33837.97 |
| Commercial land-use potential | | | | |
| Land-uses Neighborhood | a | b | c | d |
| Agriculture | -1.05 | 0.61 | 33.10 | -5.96 |
| Water | -25.26 | -0.57 | -71.82 | 2.14 |
| Commercial | -69.79 | -2.34 | -18.75 | 0.07 |
| Roads | 41.08 | -1.60 | 78.94 | 0.02 |
| Forest | 6.00 | 2.06 | -99.54 | -1.02 |
| Industrial | 82.46 | 0.64 | -11.04 | 0.11 |
| Institutional | -80.02 | 0.00 | 41.64 | -125.34 |
| Parks | -30.96 | 1.96 | -30.85 | 17.19 |
| Residential | 12.17 | -0.49 | 90.18 | -0.65 |
| | | a | | 2.78 |
| | | $\beta$ | | 1.82 |
| | | H | | 265816.4 |

Table 2 (cont) Coefficients obtained in the calibration with the GA

| Residential land-use potential | | | | |
|---|---|---|---|---|
| Land-uses Neighborhood | a | b | c | d |
| Agriculture | -4.58 | -1.64 | 63.85 | 0.95 |
| Water | 89.51 | 2.64 | 32.25 | -2.68 |
| Commercial | -39.35 | -0.93 | -0.55 | 0.86 |
| Roads | 48.06 | 0.21 | -12.97 | 13.97 |
| Forest | -49.20 | 1.80 | -6.74 | 0.20 |
| Industrial | 35.41 | 1.98 | -97.94 | 0.11 |
| Institutional | 92.93 | -0.53 | 89.63 | -1.23 |
| Parks | 86.09 | -0.41 | 61.85 | -5.28 |
| Residential | -67.89 | -1.57 | 69.27 | -4.70 |
| | | a | | 5.93 |
| | | β | | 3.44 |
| | | H | | 113284.80 |

The results of the proposed model were compared with the results obtained using the original model of White. The neighborhood parameters used in the model of White where the same than those used in the application of this model to Cincinnati [1], since according to the authors, these parameters should not vary too much between different cities. The stochastic variable and the accessibility were calibrated by trial and error and the suitability was calibrated using a logistic regression and the same variables as in the proposed model.

The index proposed in [23] (table 4) show that cells simulated with the proposed model were located closer to the real ones than those simulated with the model of White.

Considering the figure of merit (table 4), the results are even better for the proposed model. The figure of merit is calculated subtracting the partial hits (urban land uses simulated as different urban land uses) to the hits and dividing the result between the addition of the misses (urban land uses which are simulated as non urban land uses), false alarms (non urban land uses which are simulated as urban land uses ), hits and partial hits.

The values of the spatial metrics show that the residential land use simulated with the proposed model presents patterns closer to reality (table 3). Commercial and industrial land use patterns were not correctly simulated because the amount of growth in the study period for these uses was low and there was not enough information to calibrate them correctly. The values for the AREA_AM are better in the patterns simulated with the model of White since - as it can be seen in map 2 - this model simulated growth concentrated along the main roads whereas the

proposed model simulated more disperse patters which are in general lines closer to the real ones.
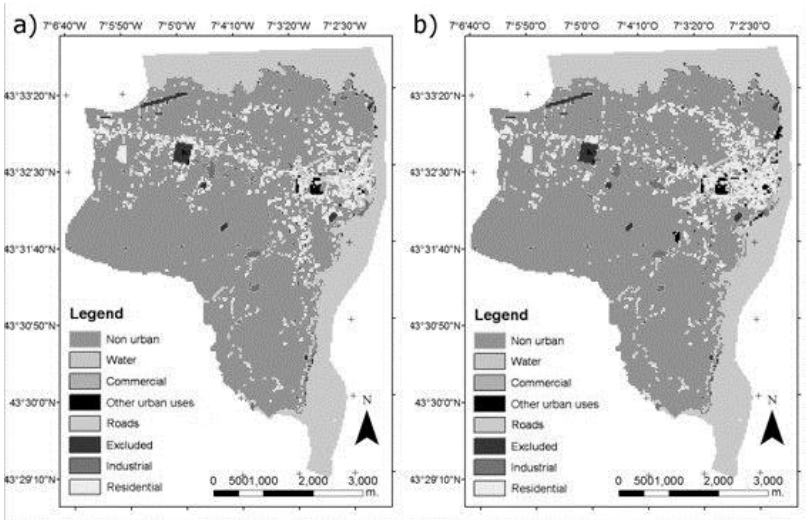


Map 3: a) Map simulated with the proposed model for the year 2007 b) map simulated with the model of white for the year 2007.

Table 3: Results of the evaluation metrics for the proposed and the White models

| Proposed model | | | NP | AREA_AM | ED |
|---|---|---|---|---|---|
| Pontius index | 0.9201 | Residential | 224 | 37.29 | 18.43 |
| | | Industrial | 43 | 1.84 | 2.79 |
| | | Commercial | 23 | 0.55 | 1.13 |
| White et al (1997) | | | NP | AREA_AM | ED |
| Pontius index | 0.9195 | Residential | 234 | 19.52 | 20.46 |
| | | Industrial | 46 | 3.24 | 2.4 |
| | | Commercial | 29 | 1.35 | 1.06 |
| Real data | | | NP | AREA_AM | ED |
| | | Residential | 224 | 18.73 | 18.25 |
| | | Industrial | 45 | 2.07 | 2.66 |
| | | Commercial | 13 | 1.76 | 0.84 |

Table 4 Figure of merit of the results of the proposed model and the model of white.

| | Figure of merit | Hits | Partial hits | Misses | False alarms |
|---|---|---|---|---|---|
| Proposed model | 7.09% | 69 | 5 | 447 | 382 |
| White et al (1997) | 3.3% | 68 | 36 | 417 | 436 |

## Conclusions

The model proposed by White et al. [1] has many advantages for the simulation of small urban areas but its main drawback is the high number of calibration parameters. The modifications proposed in this paper allowed to automate the calibration process, making it simpler without losing the flexibility of the model of White. This was achieved using logistic regressions to calculate the suitability and simplifying the neighborhood coefficients by representing the distance decay effects with two linear functions. The method used to scale the randomness degree was also improved using an exponential function.

The obtained results show that GA are a good tool to calibrate CA models, since better results are yielded than using expert knowledge or trial and error methods. Most of the errors produced in the simulation of the study area are due to the scarcity of data to calibrate the model, caused by the characteristics of the study area which presents a low and slow growth. The mismatches between the real and simulated data are also due to the deficiencies of the validation method, since, even using several indexes that considered both the cell to cell match and the spatial pattern of land uses the complexity of growth patterns could not be accurately captured. Future research should focus on finding validation methods which can better evaluate the complex aspects of urban dynamics.

## References

[1]   White, R., G. Engelen, I. Uljee (1997), The use of constrained cellular automata for high-resolution modeling of urban land-use dynamics. Environment and Planning B: Planning and Design, 24(3), pp. 323-343.

[2]   Clarke, K.C., L.J. Gaydos (1998), Loose-coupling a cellular automaton model and GIS: long-term urban growth prediction for San Francisco and Washington/Baltimore, International Journal of Geographical Information Science, 12(7), pp. 699-714.

[3]   Barredo, J.I.; M. Kasanko, N. McCormick, C. Lavalle (2003), Modeling dynamic spatial processes: simulation of urban future scenarios through cellular automata, Landscape and Urban Planning, 64(3), pp. 145-160.

[4]   Barredo, J.I., L. Demicheli, C. Lavalle, M. Kasanko, N. McCormick (2004), Modeling future urban scenarios in developing countries: an application case study in Lagos, Nigeria, Environment and Planning B: Planning and Design, 31(1), pp. 65-84.

[5]   Arai, T., T. Akiyama (2004), Empirical analysis for estimating land use transition potential functions – case in the Tokyo metropolitan region, Computers, Environment and Urban Systems, 28(1-2), pp. 65-84.

[6]   Santé, I., A.M. García, D. Miranda, R. Crecente (2010) Cellular automata models for the simulation of real-world urban processes: A review and analysis. Landscape and Urban Planning, 96(2), pp. 108-122.

[7]   Jenerette, G.D., J. Wu (2001), Analysis and simulation of land-use change in the central Arizona-Phoenix region, USA. Landscape Ecology, 16, pp. 611-626.

[8]   Goldstein, N.C. (2003), Brains vs. Brawn-Comparative strategies for the calibration of a cellular automata-based urban growth model, 7th International Conference of Geocomputation, University of SouthHampton, UK.

[9]   D'Amborsio, D., W. Spataro, G. Iovine (2006), Parallel genetic algorithms for optimizing cellular automata models of natural complex phenomena: An application to debris flows, Computers & Geosciences, 32(7), pp. 861-875.

[10] Li, X., Q. Yang, X. Liu, (2008), Discovering and evaluating urban signatures for simulating compact development using cellular automata. Landscape and Urban. Planning, 86, pp. 177-186.

[11] Shan, J.; S. Alkheder, J. Wang (2008), Genetic algorithms for the calibration of cellular automata urban growth modeling. Photogrammetric Engineering and Remote Sensing, 74(10), pp. 1267-1277.

[12] Al-Ahmadi, K., L. See, H. Heppenstall, J. Hogg, (2008), Calibration of a fuzzy cellular automata model of urban dynamics in Saudi Arabia, Ecological Complexity, 6(2), pp. 80-101.

[13] García, A.M., I. Santé, M. Boullón, R. Crecente, D. Miranda (2010a), Comparative analysis on cellular automata models for the simulation of small urban cores in Galicia (NW Spain). In Actas VI Congreso Internacional de Ordenación del Territorio, Pamplona (Spain), July 11th, FUNDICOT press, pp. 640-654.

[14] García A.M., I. Santé, R. Crecente, D. Miranda (2011), Land development dynamics by morphological areas: a case study of Ribadeo, NW Spain, Environment and Planning B, in press.

[15] García, A.M., I. Santé, R. Crecente (2010b), An analysis of the effect of the stochastic component of urban cellular automata models. Computers Environment and Urban Systems, 35, pp. 289-296.

[16] Yüzer, M.A. (2004), Growth estimations in settlement planning using a land use cellular automata model (LUCAM). European Planning Studies, 12(4), pp. 551-561.

[17] Kocabas, V., S. Dragicevic (2006), Assessing a cellular automata model behavior using a sensitivity analysis approach. Computers, Environment and Urban Systems, 30(6), pp. 921-953.

[18] Al-Ahmadi, K; See, L; Heppenstall, A; Hogg, J (2009) Calibration of a fuzzy cellular automata model of urban dynamics in Saudi Arabia. Ecological Complexity, 6(2), 80-101.

[19] Yeh, A.G.O; Li, X (2006) Errors and Uncertainties in urban cellular automata. Computers Environment and Urban Systems, 30, pp. 10-28

[20] Wu, F.L. (2002), Calibration of stochastic cellular automata: the application to rural-urban land conversions. International Journal of Geographical Information Science, 16(8), pp. 795-818.

[21] Xie, Y. (1996), A generalized model for cellular urban dynamics. Geographical Analysis, 28, pp. 350-373.

[22] Holland, J.H. (1975), Adaptation in natural and artificial systems. University of Michigan Press, Ann Arbor, vii, 183 pp.

[23] Pontius, R.G. (2002), Statistical methods to partition effects of quantity and location during comparison of categorical maps at multiple resolutions. Photogrammetric Engineering and Remote Sensing, 68(10), pp.1041-1049.

[24] McGarigal, K.; Cushman, S.; Neel, M. e Ene, E. (2002). FRAGSTATS: Spatial Pattern Analysis Program for Categorical Maps. URL www.umass.edu/landeco/research/fragstats/ fragstats.html.

# Hybrid Automata Simulation of Residential Migration in the City of Vancouver

**Piper JACKSON[1]; Valerie SPICER[2]**

[1]Software Technology Lab, School of Computing Science
1.778.782.7007, piper_jackson@sfu.ca
[2]MoCCSy Program – The IRMACS Centre
1.778.782.7064, vspicer@sfu.ca
[1,2]Simon Fraser University
8888 University Drive, Burnaby BC, M5A 1S6, Canada

**Keywords:** Cellular Automata, Agent-Based System, Urban Migration, Complex Systems, Social Simulation

**Abstract**

The process for extending an existing model of residential migration of households within an urban environment is presented. The model employs a hybrid framework consisting of cellular automata to represent the urban landscape, and agent automata to represent the households. The challenges of working with realistic temporal and spatial features are addressed.

**Introduction**

For decades researchers have tried to determine the process through which a household decides where to live [3][7]. Residential movement is the movement of populations on a household scale. It impacts the composition of cities and the character of neighborhoods. Recent advances in computing technology have allowed researchers to start investigating social phenomena using software models which can capture the complexity of social dynamics. Furthermore, researchers have extended these modeling techniques which utilize simulation technology to explore the processes of residential migration [6].

The Modelling of Complex Social Systems (MoCCSy) Urban Migration project is a recent attempt to capture the residential movement problem in a computable form [4]. This is an interdisciplinary project drawing on the expertise of researchers in Computing Science, Criminology, Environmental Science, Geography and Mathematics. This group worked in an iterative, three stage process with the eventual goal of developing a model that correctly represents expert domain knowledge, is mathematically sound, and can be examined through computational means. These criteria correspond to the three stages of the process, illustrated in Figure 1. This process is described in full in [2].

Previous stages of the project focused on the general phenomena of residential movement and neighborhood formation [4]. As such, the environment included in the model was abstract in nature. Here, we present our findings with regard to extending that model to include geographical features based on real data. This paper

begins by outlining the background of the subject matter and modeling process, which is followed by a summary of the model design. The methods used to extend the model by integrating real geographical data to generate the simulation environment are described, and results from test runs on the simulation model are presented. Finally, we discuss issues and challenges encountered during this process and mention techniques used to deal with them.

## Background

Computational modeling is an approach to research that utilizes software representations of phenomena in order to analyse them in a novel manner. A model is a parsimonious version of something in the real world, ostensibly facilitating understanding by only including salient aspects of the subject matter. Models can help to reduce uncertainty about the future, test "what if" scenarios, and have the potential to reveal underlying structural characteristics and relationships. Models also are a formal explanation of understanding, and serve to communicate ideas and share in knowledge discovery [5].
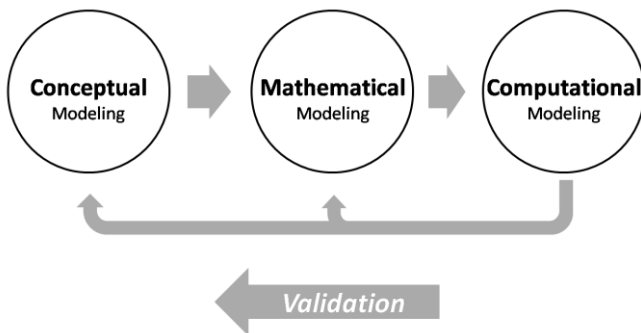


Figure 1: The iterative process for modeling complex phenomena. Adapted from [2].

The decision by a household to stay in their current location or move to a new one is a complex process [12]. In reality, a household will consider myriad social and material factors, weighing the benefits and disadvantages of each option. Access to employment, commuting time, family size, income and personal relationships can all affect the decision to migrate. Sources of stress in the current location may also motivate a change of location [3]. This complexity makes modeling of residential migration difficult to do with traditional linear models, whereas computational modeling can address these issues [11]. Cellular automata (CA) have been used by researchers in similar work because of their capacity for simulating local interactions [9][10]. Likewise, agent automata have been shown to be useful for representing the actions of agents in an urban environment [1]. Hybrid models that use both types of automata have also been developed [8].

Torrens (2007) developed a simulation model of residential mobility which integrates numerous factors involved in this process [6]. Properties are differentiated by tenure (rental versus purchase), size, and monthly cost, among other things. Households have characteristics such as income, age, size and ethnicity. Local housing markets and communities are also considered. A unique aspect of this model is that it represents these entities as geographic automata – a paradigm that includes the capabilities of both cellular and agent automata. One of the limitations of this project is that the representation of space is abstract.

**Existing Simulation Model**

The research presented here extends the urban migration model developed through the MoCCSy research group, which is described in full in [4] (including justification of design choices and theoretical background). In the model, the environment is represented by cellular automata. The individual cells represent residential locations, and can contain one or more households. The households are represented by simple agent automata. The most important characteristic of a household is its *social structure* value. This value is used to capture all features that correspond to social coherence. Thus, a variety of contributing factors, such as household income, education, ethnicity, and so on, are compressed into a single representative variable. This approach avoids the difficulty of operationalizing the individual factors and to instead focus upon their cumulative effect on residence choice.

A positive social structure value indicates adherence to social norms and lawful behavior, while negative values indicate an emphasis on personal freedom and lack of community duty. Extreme negative values can also indicate criminal inclinations. Our fundamental assumption is that households are attracted to neighborhoods with a social structure value similar to their own when selecting a new residence. The social structure of a cell is either the average social structure of all of its residents, in the case of a high density cell (such as an apartment building), or the average of all the cells in a 1-radius Moore neighborhood, in the case of a low density cell (such as a single family home).

The decision of a household to look for a new home is probabilistic, with the actual chance of this being dependent on the difference in value between its social structure and that of the cell it inhabits. If a household does not move, it is subject to social influence from its neighbors, its social structure slowly becoming more similar. Finally, all households are subject to regular random perturbations of varying intensity – this represents the individual factors in life that alter social structure, such as employment, illness and family relations. Thus we consider this model to be a hybrid CA-agent model, since local change (at the neighborhood level) is propagated using cellular automata structures, while household units are represented by agents with the ability to move.

Social attractors are another entity that may be present in a run of the simulation model, depending on the scenario chosen. These are institutions that attract households of similar value. A positive attractor, such as a church or school, attracts households of positive social structure, while a negative attractor, such as a drinking establishment, attracts households of negative social structure.
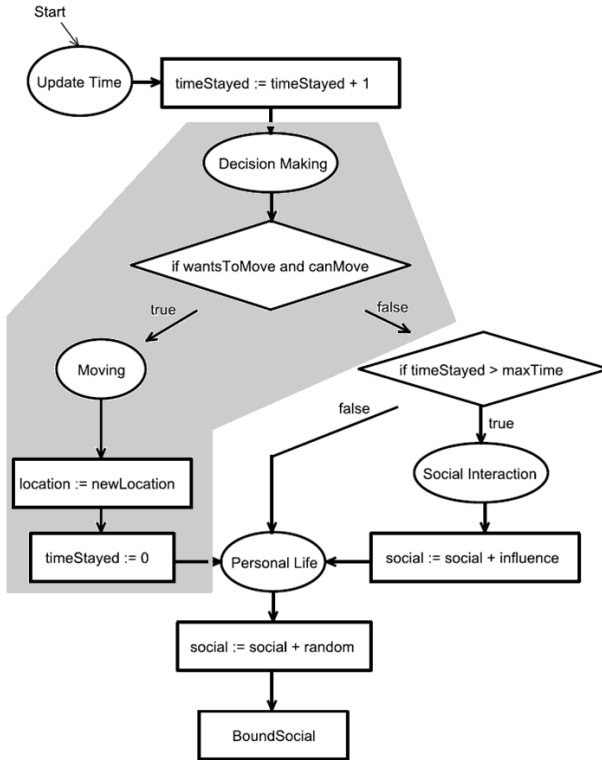
Figure 2: Outline of household behavior. The part related to residence change is highlighted.

## Data

The goal in this stage of the project is to implement a geographic environment that matches the general residential features of a real environment. Vancouver is selected due to its diverse neighborhoods and the availability of data from the City of Vancouver's Open Data Catalogue. A land use map was generated using the City of Vancouver's district zoning data (Map 1). Since the 75 different zoning classifications are too cumbersome to work with, these are aggregated into 9 general classes of zoning types. While the zoning data gives a general idea of where people in the city live, it is not sufficient for generating an environment for the simulation. Some parks are classified as residential area (including the spacious Stanley Park located downtown), despite having no residences. Further, the Comprehensive Development classification is used as a catch-all to mark areas that need special regulation. Both the mixed commercial and condominium high-rises of Yaletown and the luxurious homes of Shaughnessy fit into this classification, despite having

radically different residential densities. Due to these problems, a map of dwelling density is clearly necessary.

The residential density map (Map 2) is prepared by using the *Dwellings Occupied by Usual Residents* data at the dissemination block level from the 2006 Census of Canada. Dissemination blocks vary in size, so some larger blocks have a high number of dwellings while being quite sparse. To adjust for this, the area of each block is calculated using the ArcGIS Spatial Analyst extension. The total dwelling count for each block is then divided by its size to generate a final density value of dwellings per hectare. The resulting map shows Vancouver's concentration of residential density in the downtown core and relative sparseness throughout much of the west side.
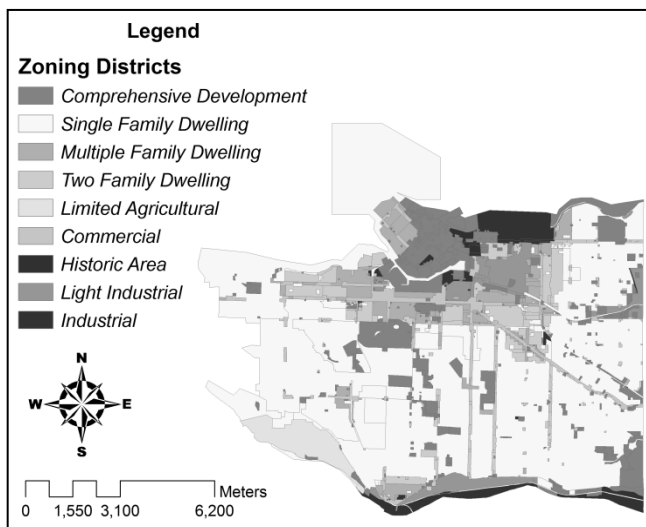


Map 1: Vancouver zoning districts, 2009. Source: City of Vancouver, Open Data Catalogue.

The residential density map (Map 2) is prepared by using the *Dwellings Occupied by Usual Residents* data at the dissemination block level from the 2006 Census of Canada. Dissemination blocks vary in size, so some larger blocks have a high number of dwellings while being quite sparse. To adjust for this, the area of each block is calculated using the ArcGIS Spatial Analyst extension. The total dwelling count for each block is then divided by its size to generate a final density value of dwellings per hectare. The resulting map shows Vancouver's concentration of residential density in the downtown core and relative sparseness throughout much of the west side.

Each of these maps is rasterized and then saved as a text file. The program can then import the values from a matching set of zoning and density text files to construct an urban environment with cell values that match the raster grid. Files with cell sizes of

25, 50 and 100 square meters are prepared in order to test the model at different levels of spatial resolution.

**Extensions to Simulation Model**

The addition of an environment modeled after the real world required changes in other parts of the simulation model. Many of these changes are purely graphical, such as adding functionality to display the zoning district types on the map. Another change is to show dwelling density values using a logarithmic scale, in a similar way to how density levels are classified in Map 2. Other changes are of a structural nature.
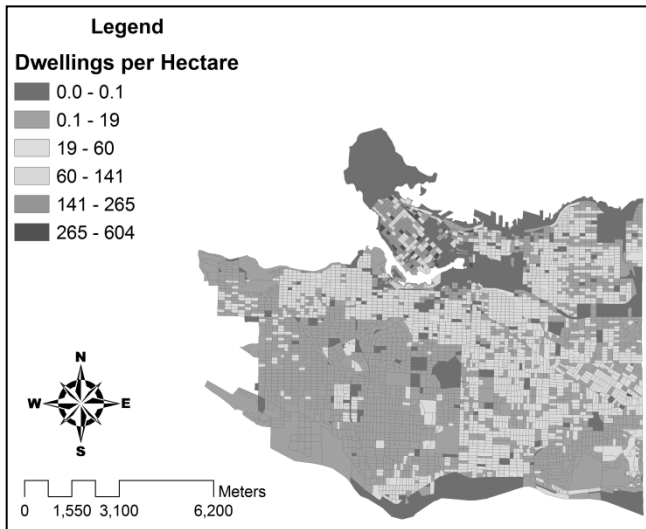


Map 2: Dwellings occupied by usual residents, Vancouver, 2006. *Source*: Census of Canada.

In particular, the effect of the land use types on household behavior needs to be determined. Since the zoning districts show the land use of a cell, they can be used to determine how much the effect the actions and behavior of the residents have on the social structure of the neighborhood. An example of this is in a primarily commercial area where there are many residences above places of business, but the character of the neighborhood is determined more by the businesses than by the residents. The mirror situation is a neighborhood composed primarily of resident homeowners: the behavior of the residents is the main source of neighborhood social structure. In the original model, low density cells used a radius one Moore neighborhood to calculate social structure, while high density cells did not consider any neighboring cells for this calculation. These ideas were composed to come up with a *neighborhood factor* variable, determined by the zoning district type.

The neighborhood factor determines the weighting of neighboring cells in determining the cell social structure. It is noted as $F$, such that $F_{ij}$ is the neighborhood factor for the cell at grid location $(i, j)$. A radius one Moore neighborhood is still used, so the number of neighborhood cells on a square grid is 8. Given that $S_{ij}(t)$ is the average social structure of all residents at cell $(i, j)$ at time step $t$, and with 8 neighboring cells $(i', j')$, the social structure of cell $(i, j)$ at time step $t$ is denoted as $V_{ij}(t)$ such that:

$$V_{ij}(t) = \frac{S_{ij}(t) + F_{ij} \times \sum S_{i'j'}(t)}{1 + F_{ij} \times 8}$$

(1)

Note that for the case $F_{ij} = 0$, $V_{ij}(t) = S_{ij}(t)$. This is identical to the previous version, where high density cells ignore neighboring cells when determining cell social structure. Likewise, for $F_{ij} = 1$, $V_{ij}(t)$ is an average of the $S_{ij}(t)$ for all of the cells in the $3 \times 3$ neighborhood. Thus the options of the original version are still present, but intermediate levels of neighborhood interaction are now possible. One difference from the previous version is that the neighborhood factor is determined only by zoning type, and not the actual density of a cell. While we can expect a high correspondence between density and zoning district type, this model allows for some variance in behavior. For example, it is now possible to model high levels of interaction in a densely populated neighborhood that is primarily residential, as might be seen in the eastern half of Vancouver.

Table 1: Neighborhood factor by zoning district type

| Zoning District Type | Neighborhood Factor |
| --- | --- |
| Single Family Dwelling | 1.0 |
| Limited Agriculture | 1.0 |
| Two Family Dwelling | 0.7 |
| Multiple Family Dwelling | 0.3 |
| Comprehensive Development | 0.0 |
| Commercial | 0.0 |
| Industrial | 0.0 |
| Light Industrial | 0.0 |
| Historical | 0.0 |

The original model was typically run on a $50 \times 100$ grid of cells that contained a total of 9500 households on average. The capacity of the City of Vancouver from the data generated is 253,680 dwellings. Running the simulation model with this massive increase in households resulted in the program grinding to a near standstill. Upon analysis, the part of household behavior that demanded the most processor resources was related to residence change: the decision to move and the process of finding a new home location. The solution to this problem is to change the temporal scale of the model. Previously, time steps corresponded to one month, that being the shortest duration conceivable between typical residence changes. With a time step of that length, all households needed an opportunity to evaluate their satisfaction with

their current location and decide whether or not to move. By changing the duration of a time step to a single day, it became acceptable to only give a small proportion of the total household population the opportunity to consider movement. Social structure changes due to social interaction and personal factors could still occur on a daily basis. This change in scale enabled the program to run at a reasonable speed. However, some adjustments to the model would be required. The implications of changing the temporal scale are discussed in the next section.

## Results

With the change in temporal scale, fewer households are given the opportunity to move during each time step. Since the cells are subject to influence from their neighbors in the steps that they do not change location, it seemed likely that the new model would be sensitive to changes in the social influence factor variable. This variable determines the magnitude of change in social threshold of a household being influenced by its neighbors. In order to test this, the simulation was run for 50 steps using a range of values for the social influence factor, and the standard deviation of the social threshold values of the households was recorded at both the beginning and end of a run. Table II lists the average standard deviations for five runs of each value chosen for the social influence factor. No standard deviation score for any run varied more than 1% from the average.

Table 2: Sensitivity to Social Influence factor

| Social Influence Factor | Initial Social Threshold Standard Deviation | Final Social Threshold Standard Deviation |
|---|---|---|
| 0.1 | 2.020462 | 0.4595 |
| 0.01 | 2.021267 | 1.857773 |
| 0.001 | 2.020333 | 2.111683 |
| 0.0001 | 2.021514 | 2.139422 |

Not surprisingly, the initial standard deviations are almost identical, since they are dependent only upon initialization of the households, prior to any opportunity for social influence. The final standard deviations show the impact of the social influence factor: large values result in small amounts of variance in social threshold. In other words, when the magnitude of social influence is high, the social structure values of the households move closer to each other. This takes place through local interactions, but occurs throughout the system. This results in an averaging effect that causes social threshold values to approach zero over time.

Figures 3 and 4 illustrate the effect of the social influence factor. The non-residential areas are colored black; this includes parks and industrial areas. The remaining areas are residential, colored in a grayscale continuum to denote social structure, where white is positive and black is negative. Gray coloring shows areas where social structure equals or is close to zero, and these clearly dominate in Figure 3, a high social influence factor scenario. In Figure 4, there is more variation in social structure values, as shown by speckling cell coloring in the residential areas.

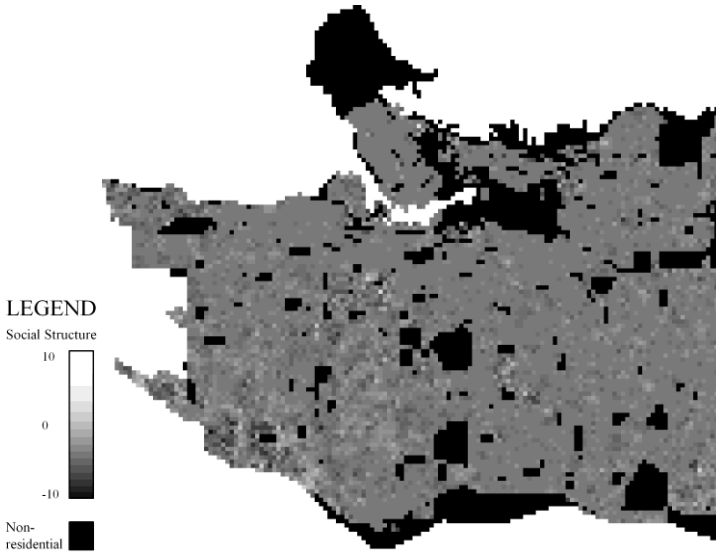Figure 3: The simulation run with social influence factor set at 0.1.



Figure 4: The simulation run with social influence factor set at 0.001.

**Discussion**

One issue that turned out to be very important when bringing real data into a simulation model is scale. The effect of changing the temporal scale has already been discussed, but the choice of spatial scale was also critical. Although it was relatively easy to prepare the data at a variety of resolutions, actually getting each of those data sets to run was more of a challenge. Table III summarizes the time it took the program to initialize the model entities (cells and agents) and also the time to run the simulation for 50 time steps. This was done for each resolution available, and also performed both with and without attractors present in the environment. A dual core 2.0 Ghz AMD CPU system with 2 gigabytes of memory and running Windows 7 was used to test the program.

Table 3: Program Execution Time

| Cell Size (m$^2$) | Initialization Time (seconds) | | Run Time (seconds) | |
|---|---|---|---|---|
| | No Attractors | Attractors | No Attractors | Attractors |
| 100 | 0.45 | 18.03 | 10.83 | 11.44 |
| 50 | 1.5 | 333.01 | 165.25 | 170.62 |
| 25 | ——————— | insufficient memory | | ——————— |

In the case of the highest resolution, 25 m$^2$ cells, the program was unable to run at all due to insufficient memory. With the cells at 50 m$^2$ in size, the program was able to run successfully, but the times are an order of magnitude slower than at the lowest resolution (100 m$^2$). Initially, households searching for a new location would compare each potential location with all of the appropriate attractors in the entire environment. This resulted in the run time for scenarios with attractors taking roughly twice as much time as they currently do. However, since attractors do not move in the model, a preprocessing stage was added in which the relative locations of attractors to each cell are calculated. This has dramatically reduced the run time for scenarios with attractors in them, in exchange for a longer initialization time. This trade-off is particularly worth it for long runs of a thousand time steps or more. Eliminating redundant work and improving efficiency can often be ignored in research software development when working on abstract models due to the processing power of modern CPUs. Using large data sets from real sources changes this: it is possible for the CPU, memory or both to be insufficient to run the program at a satisfying pace.

This version of the program did not include a legend explaining the meaning of the colors shown in the display. This was an oversight due to the simplicity of the base model, where screen elements could be easily explained verbally. However the added complexity of the extended model makes verbal explanation inefficient and is intimidating for people new to the program. Of course, having a legend is one of the cornerstones of cartography, being a key by which the information contained in a map can be interpreted by a reader. By extending the project to make it clearly geographical in nature, the importance of a legend was made apparent. A legend implemented in software can be very flexible, adjusting its contents dynamically to the factors currently on display and their associated levels.

However, there is also a more fundamental issue at work here: research is only valuable if it can be communicated to others. This is even truer of research that is intended to be used by others in the manner of a tool, like with a software model. It is easy when working on a program by oneself to forget about all of this, since the intimacy engendered by the familiarity of the inner workings of the system allows immediate comprehension of the program's behavior. Research software must prioritize explanation and communication in order to reach out to colleagues and peers.

## Conclusion

While still in its early stages, this project illustrates several considerations that can arise when enabling a simulation model to utilize real data. For applications that involve geography, determining the appropriate temporal and spatial scales is of particular importance. A successful strategy employed here is that of simplifying the problem first, either by using coarse data or reducing the number of operations, before attempting to adjust the model in terms of behavior or efficiency. The advantage of this strategy is that a working model can be achieved more quickly, which can in turn be used to facilitate further improvements.

## Acknowledgments

## References

[1]   Batty, M., Y. Xie (2005), Urban Growth Using Cellular Automata Models. In D. Maguire, M. Batty, M. Goodchild (Eds.), GIS, Spatial Analysis and Modeling, ESRI Press, Redlands

[2]   Brantingham, P., U. Glässer, P. Jackson, M. Vajihollahi (2009), Modeling Criminal Activity in Urban Landscapes. In N. Memon, J. D. Farley, D. L. Hicks, T. Rosenorn (Eds.), Mathematical Methods in Counterterrorism, Springer, Berlin

[3]   Brown, L. A., E. G. Moore (1970), The Intra-Urban Migration Process: A Perspective. Geografiska Annaler. Series B, Human Geography, 52(1), pp. 1-13

[4]   Dabbaghian, V., P. Jackson, V. Spicer, K. Wuschke (2010), A cellular automata model on residential migration in response to neighborhood social dynamics. Mathematical and Computer Modelling, 52, pp. 1752-1762

[5]   Goodchild, M. F. (2005), GIS and Modeling Overview. In D. Maguire, M. Batty, M. Goodchild, (Eds.), GIS, Spatial Analysis and Modeling, ESRI Press, Redlands

[6]   Torrens, P. M. (2007), A geographic automata model of residential mobility. Environment and Planning B: Planning and Design, 34(2), pp. 200-222

[7]   Wolpert, J. (1965), Behavioral aspects of the decision to migrate. Paper in Regional Science, 15(1), pp. 159-169

[8]   Xie, Y., M. Batty K. Zhao (2007), Simulating Emergent Urban Form Using Agent-Based Modeling: Desakota in the Suzhou-Wuxian Region in China. Annals of the Association of the American Geographers, 97(3), pp. 477-495

[9] Li, X. (2008), Simulating urban dynamics using cellular automata. In L. Liu, J. Eck (Eds.), Artificial Crime Analysis Systems: Using Computer Simulations and Geographic Information Systems, pp. 125-139, Idea Press, Hershey

[10] Schelling, T. (1971), Dynamic models of segregation. The Journal of Mathematical Sociology, 1(2), pp. 143-186.

[11] Hegselmann, R., A. Flache (1998), Understanding complex social dynamics: a plea for cellular automata based modelling. Journal of Artificial Societies and Social Simulation, 1(3).

[12] Clark, W.A.V., M.C. Deurloo, F.M. Dieleman (2006), Residential mobility and neighbourhood outcomes. Housing Studies, 21(3), pp. 323-342

# Geospatial Cellular Automata Programmed in Python for Social Sciences

## Igor LUGO[1]; Marcos VALDIVIA[1]

[1]Research Professor
Centro Regional de Investigaciones Multidisciplinarias
Universidad Nacional Autónoma de México
Av. Universidad s/n, Cto. 2, Col. Chamilpa, CP 62210, Cuernavaca, Morelos, Mexico
Tel.: +52 (777) 317 50 11 and +52 (777) 317 52 99, ext. 109; fax: + 52 (777) 317 58 81; Email
address: igorlugo@correo.crim.unam.mx (Igor Lugo)

## Abstract

Using standard and third-party libraries of Python, we generate a cellular automaton with geospatial information to study spatial externalities. Cells correspond to polygon geometries to define the shape, size, and neighborhood configuration, and the transitional rule consists of a simple spatial autoregressive model. To illustrate the construction and performance of this model, we use data of the Mexico City Metropolitan Area for studying production spillovers. The results suggest a simple method of building a cellular automaton using Python's libraries that process efficiently geospatial data and produce effective spatial simulations for the social sciences.

## Introduction

The increasing capability to collect, compute, and visualize geographic information is one of the most challenging and novel tasks for fields related to spatial analysis. Although the existence and development of the Geographic Information Systems (GIS) and computational platforms, the integration of cellular automata (CA) to the GIS technology is not trivial [1, 2, 3, 4, 5]. In particular, a dynamic programming language applied to social sciences is required to process, analyze, and develop geospatial information.

Python (http://www.python.org/) represents one of the best-developed programming languages used for a variety of GIS domains. Its relevance consists in versatile applications that combine standard and third-party libraries covering and supporting many programming needs, for example to write simple functions or to design complex modules.

The purpose of this work is to show the application of such libraries for generating a CA that uses geospatial information, specifically vector geometries, to define the shape, size, and neighborhood configuration of cells, and that applies a

simple spatial autoregressive model (SAR) as a transitional rule to analyze the effect of spatial externalities in urban areas.

We exemplify the construction and performance of such CA with data of the Mexico City Metropolitan Area (MCMA) to explore production spillovers. The data is based on a vector layer that contains polygon geometries related to census tracts (CT). Each of them includes industrial census data in the year of 2004.

The rest of the document consists of four sections. The second section presents a summary of computer developments, including Python libraries, for spatial simulations. The third section explains the construction of the CA. The fourth section illustrates the usage of it, analyzing spatial externalities in the MCMA. Finally, we conclude with a section of closing remarks.

## Computer Developments for Spatial Simulations

Nowadays, computer developments related to geospatial information are based on the GIS technology in which simulation platforms have integrated it into their environment for analyzing complex spatial phenomena.

Some of the most important simulation platforms with such a characteristic are Swarm, NetLogo, Cormas, and Repast. They use geospatial vector data (points, lines, and polygons) to provide a more realistic representation of the spatial organization, but in practice they are limited to geoprocessing, manipulation, and store methods [6]. From the point of view of the modeler, although these platforms offer a simple and powerful programming language, a graphical interface, and a comprehensive documentation, they exhibit higher costs of learning [6, 7, 8].

Dealing with such restrictions, we use Python as our computing framework that not only presents a collection of features covered and supported much programming needs and showed a very simple and consistent syntax, but also provides a wide range of libraries making possible to process and develop geospatial data for social simulations [9, 10, 11, 12]. Such libraries are *OGR* (http://www.gdal.org/ogr/) to manipulate geospatial vector information, *NumPy* (http://numpy.scipy.org/) to handle computation of large and multidimensional numeric data, *Matplotlib* (http://matplotlib.sourceforge.net/) to compute and plot 2D data, and *Pygame* (http://pygame.org/) to create video games. These and other libraries, for example *PySAL* (http://pysal.org/) and *Rpy* (http://rpy.sourceforge.net/), have increased in the last years, showing an important growth in the programming contributions compared to other languages. Some benefits of these libraries are to process efficiently geospatial information and develop methods for advance spatial operations, for example storing environment results and speeding up the simulation performance.

## Geospatial Cellular Automata

The first component for modeling a CA with geospatial information is the neighborhood configuration that represents different levels of connectivity, contiguity, and distance between localized objects [13, 14, 15]. Following the work of Moreno et al. [5, 16] who proposed a model called vector-base geographic cellular automaton (VecGCA), we define a CA with such a neighborhood as geospatial cellular automata

(GCA). Two differences exist between Moreno's et al. and our model: the name and application. We are interested in simplifying the model identification and generalizing the applicability for social simulations.

The second component ofthe GCA, which differentiates the social science application from others, is the transitional rule. In this case, we use a SAR process for studying the neighboring effects of productivity.

The following subsections present the construction of the GCA by showing the application of Python's libraries for generating the neighborhood configuration and by explaining the derivation of the transitional rule from the unconstrained spatial Durbin model.

### Neighborhood configuration

Based on the object-oriented paradigm, we mix the *OGR*, *NumPy*, *Matplotlib*, and *Pygame* libraries to show the construction of a set of functions and a class object that produces a GCA (Figure 1).
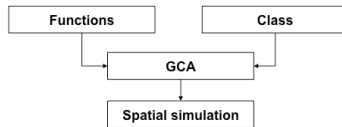
Figure 1: Integration of libraries

Functions manipulate geospatial data in order to extract, save, and retrieve the geometry of each vector layer feature, using a binary format. The class object defines each cell and visualizes it in a surface object. After building the spatial configuration, we define the transitional rule to perform the spatial simulation.

The set of functions processes geospatial information by using the *OGR* library.

Modules of such library help us to create functions related to read, save, and retrieve data (Figure 2).
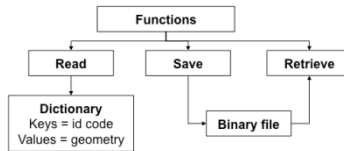
Figure 2: Basic functions

The first function reads the geometry of each feature and returns a dictionary (associative array) indexed by keys (id codes) and values (geometries). This dictionary is an efficient Python object to store and extract geospatial data, and it depends on the size of information. Then, using the *NumPy* library and the created dictionary, we save and retrieve information as a binary format.[1] In sum, these functions help to collect fundamental geospatial data for generating the structure of the GCA.

Next, using the Python's class object, we create the neighborhood structure of the GCA. Each cell corresponds to specific feature in the vector layer, showing unique location, shape, size, and neighborhood configuration. Two types of information define this class: attributes and methods (Figure 3).

Attributes characterizes the object, for example the id code of the feature, and methods modifies, computes, or extracts such attributes using functions, for example returning the id code of the first feature of the layer. Three basic attributes define a cell in the model: id code, geometry, and neighbors. On the other hand, the essential method is a function that draws the geometry of a cell in a surface object. Applying the instantiation operation, which creates a new instance of the class, we assign a cell to every feature in the vector layer. Finally, cells are collected in a list object, container of items.
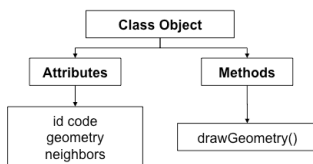


Figure 3: Python class object

To conclude the construction of the GCA, we use the *Pygame* library for displaying the geometry of cells into an alternative GIS environment, a window in the desktop. We use the list object of cells and the *drawGeometry()* function to reproduce the geospatial information of the original vector data. In addition, the *Matplotlib* library is applied for generating simple statistical measures and graph visualizations.

**Transitional rule**

The transitional rule is related to the analysis of spatial externalities. Economists and geographers have studied them for many years, where the former have contributed importantly in the theoretical and empirical analysis of them [8], and the latter have proposed significant cellular automata models as a tool for analyzing spatial dynamics [17, 18]. In this case, the unconstrained form of the spatial Durbin model applied in spatial econometrics provides the general framework to define a transitional rule [19, 20]. The unconstrained model in matrix notation is specified as follows:

$$y = \lambda\, Wy + X\, \beta + WX\, \gamma + u \qquad (1)$$

where *y* is *n* by 1 vector of a dependent variable, $\lambda$ is the spatial autoregressive coefficient, *Wy* is the spatially lagged dependent variable, *X* is a set of explanatory variables, *WX* is a set of spatially lagged exogenous variables, $\gamma$ is the coefficient associated to *WX*, and *u* is a vector of error terms [20].

Based on equation (1), we define the transitional rule as the following SAR model:

$$y = \lambda\, Wy + u \qquad (2)$$

Equation (2) suggests a diffusion process depended on the scale effect in the neighborhood of each cell and randomness.

**Production Spillovers in the Mexico City Metropolitan Area**

In this section, we illustrate the application of the proposed GCA, presenting the case of the MCMA to analyze the spatial diffusion of productivity. The geospatial information of the area corresponds to a set of CTs (5004 polygons), which the Mexican Statistics Office (INEGI in Spanish acronym) defines as small urban-area units confined by physical and natural limits, for example streets, avenues, and rivers [21]. They define the scale and structure of the analysis and exhibit data of labor productivity in the manufacturing sector (Map 1).
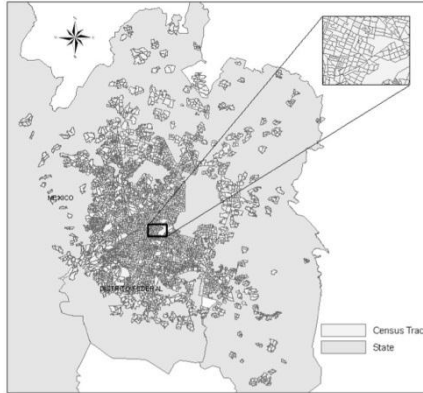


Map 1: Spatial structure of the MCMA.

Applying the read and store functions explained in the past section to the geospatial data of Map 1, we obtain a dictionary formed by id codes as keys and geometries, neighbors, and productivity data as values of each feature. Then, we create each cell of the GCA, using the class object (Figure 4).
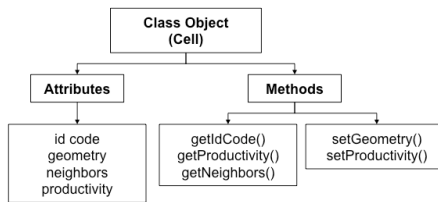


Figure 4: Cell class object

Each cell has four attributes: *id code, geometry, neighbors, and productivity*. The id code is a classification number associated with every CT, geometry contains coordinates that defines the urban polygon, neighbors refer to CTs vicinities (contiguous and noncontiguous), and productivity corresponds to a statistical value of the manufacture sector.

Two sets of functions define the class method. The first returns the value of attributes, and the second displays and modifies the geometry and productivity data respectively.

Using the cell class, we generate an instance object that is collected in a list object.

Then, we reproduce the spatial structure of the MCMA, using the *setGeometry()* function (Figure 5).
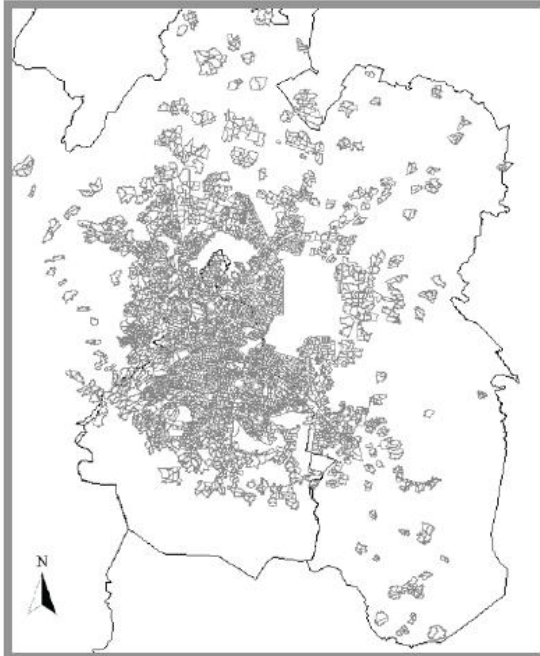


Figure 5: Visualization of the GCA

Next, we specify the transitional rule followed the equation (2), specifically a SAR time lag-process [19, 20, 22]. This process provides the local and simplest mechanism to produces a change in the level of productivity per cell in the GCA. We define it as follows:

$$P_{i,t+1} = \rho W \, P_{i,t} + \varepsilon_{i,t} \qquad (3)$$

where $P_{i,t}$ and $P_{i,t+1}$ are the productivity of cell $i$ at time $t$ and $t+1$ respectively; $\rho$ is the spatial autoregressive parameter; $W$ is the spatial weight matrix, which depends on the productivity value of $k$ cells associated with an $i$ neighborhood at time $t$, $\Omega_{i,t}$;[3] and $\varepsilon_{i,t}$ is the independent disturbance term normally-distributed. Therefore, $WP_{i,t}$ is row standardized as follows:

$$\text{WP}_{i,t} = 1 / n \sum_{k \in \Omega_{i,t}}^{n} P_{k,t} \tag{4}$$

Equation (3) and (4) describe a scale averaging model that spreads the productivity throughout the system based on local conditions [22, 23, 24, 25].

In addition, equation (3) only operates when the CT has at least one adjacent neighbor, otherwise the rule follows the next specification:

$$P_{i,t+1} = \rho \, P_{j,t} + \varepsilon_{j,t} \tag{5}$$

where $P_{j,t}$ corresponds to the productivity value of the CT with the shortest distance from *i* to *j*.

**Overview of the process**

To explain the dynamics of the GCA, we present a flowchart to display how every cell interacts to each other and changes its value of productivity according to its neighborhood configuration (Figure 6).
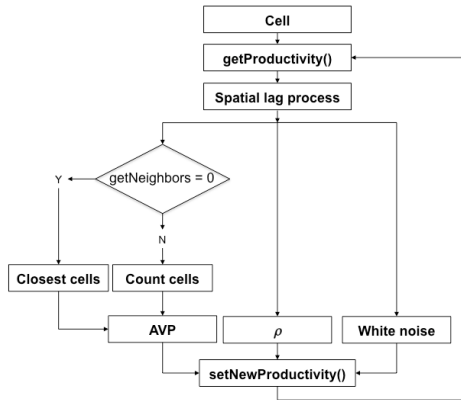


Figure 6: Programming routine

Once cells are collected in the list object, the simulation process starts defining the transitional rule of each of them. The productivity value is retrieved from the vector data (*getProductivity()*), and each cell inspects its neighbors (*spatial lag-process*). If the cell has not neighbors, it will compute the shortest distance to the closest neighbor. This measure is based on the geometric centroid of polygonal cells, and it quantifies a maximum number of neighbors equal to one. On the other hand, if the number of neighbors is different to zero, each cell will apply the SAR (1) process, which we rename as the average value of productivity (AVP). Neighbors of each cell are row standardized, and the cell is synchronously updated.

We consider the scaling parameter $\rho$ for regulating the intensity of the contagion among cells [26, 27, 28, 29]. Essentially, from an economic perspective, three equilibria outcomes are possible when $\rho$ is equal to one: 1) all CTs have zero productivity, 2) everyone has the same average productivity value equal to the initial condition, and 3) each CT increases its value until reaching an exogenous upper bound. Finally, we

introduce in the spatial lag-process a white noise with the form of a random variable *iid (0,1)* representing external shocks in the system.

The core of the programming routine is a loop that updates the productivity attribute of each cell in every time step under the conditions just mentioned. That is, at each time step the productivity value is stored in a new list object.

**Neighborhood and productivity characteristics**

Two important characteristics of the GCA applied to the MCMA are studied before we present simulation experiments: neighborhood structure and productivity value. The neighborhood structure is analyzed by a histogram (Figure 7), where the x-axis represents the number of neighbors around a cell, and the y-axis corresponds to the probability of a cell related to the number of neighbors.
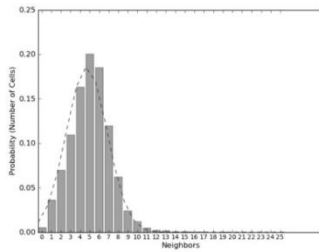


Figure 7: Neighborhood configuration: $\mu = 5$, $\sigma = 2$

The histogram show an asymmetrical distribution with a positive skew meaning that few cases of cells have more than 10 neighbors, and most of them have a neighborhood formed by 10 or less cells. In particular, around 70% of cells have four to six neighbors, the mean of the distribution is equal to five with a standard deviation of two, and the first bin exhibits few cells with zero neighbors or isolated cells. In brief, the neighborhood configuration presents a high level of connectivity and contiguity, exhibiting a heterogeneous structure that affects the dynamics and interactions across the area [30].

In addition, Figure 8 displays a distribution that exhibits the productivity value in natural logarithms.[4]

This figure shows a normal distribution with a mean of 3.97 and standard deviation of 0.8. More than 70% of cells have a productivity value between 2.94 and 3.97 representing 1.27 and 3.71 thousands dollars/employee respectively.[5]

Figure 8: Distribution of productivity: $\mu = 3.97$, $\sigma = 0.8$

**Deterministic model**

The first case of the spatial experiments is a deterministic model. It displays a graphical interface and exhibits one scenario of spatial interaction, which represents the simplest case of analysis [31]. The transitional rule of the model is as follows:

$$P_{i,t+1} = \rho W \, P_{i,t} \qquad (6)$$

where the productivity of each cell at time $t+1$, $P_{i,t+1}$, depends on $\rho$ and the AVP of its neighborhood at time $t$, $WP_{i,t}$.

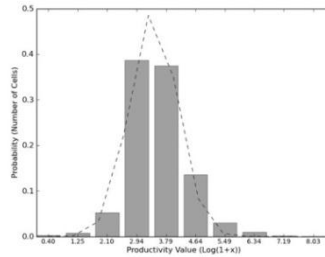The initial condition of the experiment is based on the productivity value of each CT, and no additional inputs are added to the spatial interaction. To simplify the analysis, we set $\rho$ equal to one. Under these conditions, we expect that the system produces contagion in the long run, where all CTs will converge to the average initial value. Nevertheless the dynamics of contagion is uneven along the time, the model presents important implications in terms of spatial inequality. Figure 9 displays the sequence of the simulation in six different time steps, where the run time is equal to 100, and each time step corresponds to a year.

Figure 9 shows the spread of productivity in the MCMA based on three levels: low, medium, and high.[6] In time $= 0$ (initial conditions), we see a large number of cells with low productivity values. On the other hand, only few cells have medium and high values. In the following time periods, cells with medium and high values extend their productivity to close areas. For example, in time $= 20$ and time $= 40$, there is a localized and well-defined area of medium and high values. The last three spatial visualizations show a reinforcement of increasing productivity values. In essence, medium and high values are more probable to spread their level of productivity to contiguous cells and produce a localized area of intense spatial interaction.
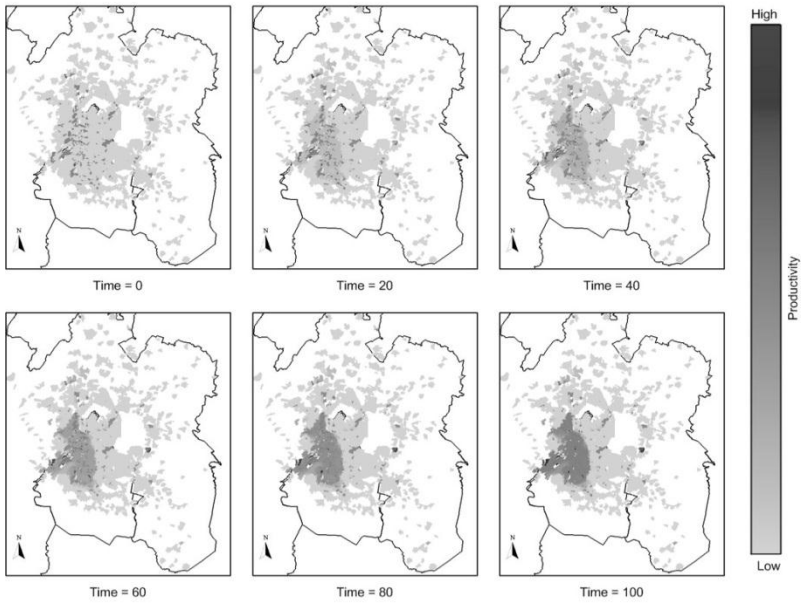
Figure 9: Deterministic model

In addition, the dynamics of the productivity based on AVP values and the initial and final distribution of them are displayed in Figure 10 and 11.
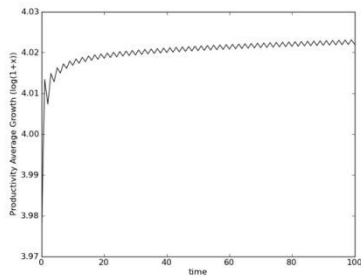


Figure 10: Dynamics of productivity
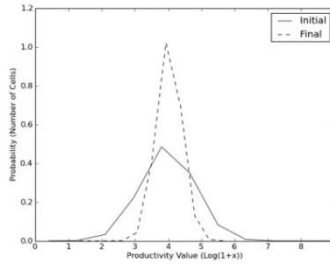
Figure 11: Initial and final productivity distribution

Figure 10 shows only a small increased and stable pattern in the AVP value. From an initial value of 3.97, the AVP increases and remains stable around the value of 4.02, and its dispersion decreases from 0.8 to 0.3 (Figure 11).[7] This result suggests that, around the time step equal to 20, the area of medium and high levels of productivity persists until the last time step, that is, the spatial interaction increases and intensifies the productivity.

**Random Model**

Under this experiment, we consider equation (3) as the transitional rule. The use of the random variable *iid (0, 1)* produces a stochastic spatial lag-process and simulates external shocks in the system. Applying a batch processing, we run each simulation 1000 times with a total number of time steps equal to 100.

After running the model, we obtain the following results: a mean value of 4.021 (3.9 thousands dollars/employee), a variance equals to 0.011, and a standard deviation of 0.113 (8.04 dollars/employee). Compared this mean value with the initial condition of productivity in the deterministic model (3.7 thousands dollars/employee), we see an increasing value of the AVP, approximately 5%. In addition, Figure 12 shows an increasing dispersion of the average productivity in three different time steps, meaning heterogeneity in every simulation. These results confirm an incremental productivity with high dispersion in its values throughout cells.
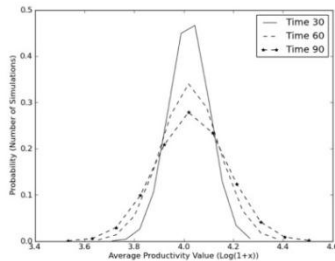


Figure 12: Average productivity distribution in three different time steps

Finally, Figure 13 presents 10 simulations to exemplify the effect of including the random component in the deterministic model. Figure 13 shows a wide variety of dynamics in productivity, which fluctuates around the long-run equilibrium presented in the deterministic model.
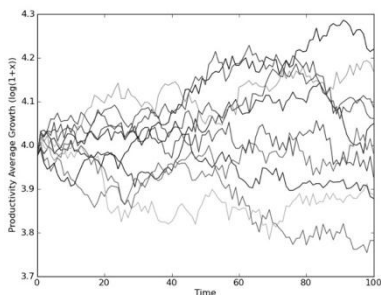


Figure 13: Teen simulations of productivity average growth

## Conclusion

The integration of standard and third-party libraries into a programming routine in Python makes the proces of building a GCA easy, if we compare it to other computer platforms. Python's libraries provide a set of powerful tools to analyze spatial phenomena, generate spatial simulations, and extend the range of application in social sciences. This integration offers the advantages to study large and complex data and to add other libraries that cover different types of analysis and that develop specific geospatial applications.

The proposed GCA model incorporates efficiently the heterogeneous neighborhood structures and transitional rules related to spatial externalities. In the case of production spillovers in the MCMA, we can extend the model to add more variables, for example the human capital (number of years a person attends school) and its neighborhood average value. They can complement the traditional spillover analysis and give new insights into the mechanism of spatial interactions in metropolitan areas.

## Acknowledgment

## Footnotes

1. Another option to save and retrieve this information is the pickle module (http://docs.python.org/library/pickle.html).

2. Options of Python's libraries for drawing objects are the following: Pyglet (http://www.pyglet.org/) and PyGTK (http://www.pygtk.org/).

3. In this case, the type of neighborhood induces heteroskedasticity (the number of neighbors is different in each cell).

4. In order to avoid negative values of productivity, we use the logarithm function: log (1 + x), where x = productivity.

5. The inverse of the logarithmic value is computed as following: exp (z) – 1, where z = log (1+ x). In addition, the exchange rate applied is 1 USD = 14.05 MXP.

6. The color diffusion is based on a frequency distribution of productivity per time steps, wherethe total number of bins is 10. Low values are related to the first bins between one to seven, medium values are between seven and nine, and high values correspond to nine and ten.

7. The small oscillation between every time step is related to the synchronous update.

## References

[1]    Gimblett, R. H. (2002), Integrating Geographic Information Systems and Agent-based Modeling Techniques, A Volume in the Santa Fe Studies in the Sciences of Complexity, Oxford University Press

[2]    Torrens P.M., I. Benenson (2005), Geographic Automata System, International Journal of Geographical Information Science, 19(4), pp. 385-412

[3]    Axelrod, R. (2007), Simulation in the social sciences, In J.-P. Reynard (Eds.), Handbook of research on nature inspired computing for economy and management, pp. 90-100, Hershey, CA: Idea Group

[4]    Crooks, A., C. Castle, M. Batty (2008), Key challenges in agent-based modeling for geo-spatial simulation. Computers, Environment and Urban Systems, 32, pp. 417-430

[5]    Moreno N., F. Wang, D.J. Marceau (2009), Implementation of a dynamic neighborhood in a land-use vector-based cellular automata, Computer, Environments, and Urban Systems, 33, pp. 44-54

[6]    Railsback, S.F., S.L. Lytinen, S.K. Jackson (2006), Agent-based Simulation Platforms: Review and Development Recommendations, Simulation, 82 (9), pp. 609-623

[7]    Irwin, E.G. (2010), New Directions for Urban Economic Models of Land Use Change: Incorporating Spatial Dynamics and Heterogeneity (2009-10), Journal of Regional Science, 50 (1), pp. 65-91

[8]    Desmet, K., E. Rossi-Hansberg (2010), On Spatial Dynamics, Journal of Regional Science, 50 (1), pp. 43-63

[9]    Goldwasser, M.H., D. Letscher (2008), Object-Oriented Programming in Python, Pearson Prentice Hall.

[10]  Rey, S.J. (2009), Show Me the Code: Spatial Analysis and Open Source, Journal of Geographical Systems, 11, pp. 191-207

[11]  Rey, S.J. L. Anselin (2010), PySAL: A Python Library of Spatial Analytical Methods, In M. Fischer and A. Getis (Eds.), Handbook of Applied Spatial Analysis: Software Tools, Methods and Applications, Springer, Berlin

[12]  Westra, E. (2010), Python Geospatial Development, Packt Publishing

[13]  Janerette, G.D., J. Wu (2001), Analysis and simulation of land-use change in the central Arizona-Phoenix region, USA, Landscape Ecology, 16, pp. 611-629

Chen Q., A.E. Mynett (2003), Effects of cells size and configuration in cellular automata based prey-predator modeling, Simulation Modelling Practice and Theory, 11(7-8), pp. 609-625

[14] Ménard, A., D.J. Marceau (2005), Simulating the impact of forest management scenarios in an agricultural landscape of southern Quebec, Canada, using a geographic cellular automata, Landscape and Urban Planning, 79(3-4), pp. 253-265

[15] Moreno N., A. Ménard, D.J. Marceau (2008), VecGCA: A vector-based geographic cellular automata model allowing geometrical transformations of objects, Environmental and Planning B: Planning and Design, 35, pp. 647-665

[16] Wagner, D.F. (1997), Cellular automata and geographic information systems, Environment and Planning B: Planning and Design, 24, pp. 219-234

[17] Batty, M., Y. Xie (1994), From cells to cities, Environment and Planning B, 21, pp. 531-548

[18] Anselin, L. (1980), Estimation methods for spatial autoregressive structures, Regional Science Dissertation and Monograph Series 8, Field of Regional Science, Cornell University, Ithaca, N.Y.

[19] Anselin, L. (2006), Spatial Econometrics, In T.C. Mills and K. Patterson (Eds.), Palgrave Handbook of Econometrics, pp. 901-969, Volume 1, Econometric Theory, Basingstoke, Palgrave Macmillan

[20] Instituto Nacional de Geografia y Estadistica (INEGI) (2011), Marco Geoestadístico Nacional. Accessed January 25, 2011 http://www.inegi.org.mx/geo/contenidos/geoestadistica/catorcen.aspx.

[21] Anselin, L. (1988a), Spatial Econometrics: Methods and Models, Dord-drecht: Kluwer Academic Publishers

[22] Vicsek, T., A.S. Szalay (1987), Fractal Distribution of Galaxies Modeled by a Cellular Automaton-Type Stochastic Process, Physical Review Letters, 38, pp. 2818-2821

[23] Batty, M. (2005), Cities and Complexity, Understanding Cities with Cellular Automata, Agent-Based Models, and Fractals, MIT Press, Cambridge, Massachusetts

[24] Smith, M.J., M.F. Goodchild, P.A. Longley (2007), Geospatial Analysis: A Comprehensive Guide to Principles, Techniques, and Software Tools, Troubador Publishing Ltd, 2nd edition

[25] Anselin, L., (1988b), Lagrange multiplier test diagnostics for spatial dependence and heterogeneity, Geographical Analysis, 20, pp. 1–17

[26] Anselin, L. (1990), Spatial dependence and spatial structural instability in applied regression analysis, Journal of Regional Science, 30, pp. 185-207

[27] Fotheringham, A.S., M.E. Charlton, C. Brunsdon (1998), Geographical weighted regression: a natural evolution of the expansion method for spatial data analysis, Environment and Planning A, 30, pp. 1905-1927

[28] Gao, X., Y. Asami, C.F. Chung (2006), An empirical evaluation of spatial regression models, Computers and Geosciences, 32, pp. 1040-1051

[29] Irwin, E.G. (2010), New Directions for Urban Economic Models of Land Use Change: Incorporating Spatial Dynamics and Heterogeneity (2009-10), Journal of Regional Science, 50 (1), pp. 65-91

[30] Grimm, V., S.F. Railsback (2005), Individual-based Modeling and Ecology, Princeton, NJ: Princeton University Press

# Cells but not cities: building a cellular automata land use model for the Doñana natural area, SW Spain.

## Richard HEWITT[1]

[1]University of Alcalá C/. Colegios, 2
28801, Alcalá de Henares
Madrid, Spain
Tel.: (+34) 91 885 44 29 , richard.hewitt@uah.es

**Keywords:** Doñana, cellular automata model, calibration, intensive cultivation, natural protected area

## Abstract

Results are presented from the application of a Cellular Automata (CA) model, built using the Metronamica® software application, to the Doñana Natural Area, a series of interconnected ecosystems of outstanding importance for biodiversity at the mouth of the River Guadalquivir in the Spanish Autonomous community of Andalucía, South West Spain. A National Park since 1969 and recognized by UNESCO as a world heritage natural property since 1994, Doñana has nevertheless suffered serious degradation and loss of large areas of marshland, dune and coastal habitat since 1950, through tourism development, intensive agriculture and afforestation of fast growing non-native tree species (e.g. Eucalyptus), and corresponding contamination and over-exploitation its aquifer. The paper discusses the development of a pilot model for Doñana, from analysis of land use dynamics, through technical calibration procedure and assessment of calibration gioodness of fit to cross tabulation and map comparison.
A trial simulation is presented. The paper concludes with a brief discussion of the potential of the model for simulation of future scenarios, and the improvements that will be made in the construction of the full model.

## Introduction

The Doñana Natural Area (hereafter Doñana) is a series of interconnected ecosystems of outstanding importance for biodiversity at the mouth of the River Guadalquivir in the Spanish Autonomous community of Andalucía, South West Spain. A National Park since 1969 and recognized by UNESCO as a world heritage natural property since 1994, Doñana has nevertheless suffered serious degradation and loss of large areas of marshland, dune and coastal habitat since 1950, through tourism development, intensive agriculture and afforestation of fast growing non-native tree species (e.g. Eucalyptus), and corresponding contamination and over-exploitation of its aquifer. Despite a series of measures aimed a promoting sustainable development, this important natural area remains highly threatened by the

modern development paradigm of growth without limits [1]. In the following communication, results are presented from the application of a Cellular Automata (CA) model, built using the Metronamica® software application, developed by the Research Institute for Knowledge Systems (RIKS), of Maastricht, Netherlands, to Doñana. The research was carried out under the remit of the DUSPANAC research project (funded by the Autonomous Body for National Parks (OAPN) on behalf of the Spanish Environment Ministry). The project is ongoing, but nevertheless, three important objectives have been already achieved: Preliminary land use change analysis [2]; Stakeholder engagement for determination of model parameters [3] and construction of a pilot model, subject of the present communication.

**Aims of the paper:**

1. to provide a brief background to the application of CA-type models to modelling of natural areas.
2. To explain the modelling procedure employed, which may serve as a prototype for future land use modelling of natural areas.
3. To review the lessons learnt from the pilot model, and the steps which will need to be taken in future to improve the model and its applicability to decision support in the Doñana natural area.

**The contribution of CA to land use modeling**
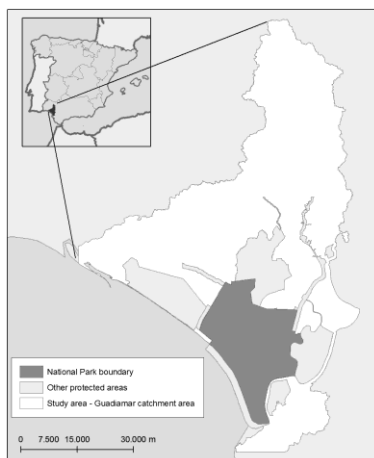


Map 1: Doñana study area

Most modern-day applications of CA are based on the work of von Neumann in the late 1940's, posthumously published as *The Theory of Self-Reproducing Automata* [4]. The application of CA to land use is usually attributed to the geographer Waldo Tobler, who developed the foundations for a raster-based "cellular geography" [5]

Early CA land use models were aimed principally at modeling urban growth (e.g. [6]), but the discipline has since expanded its scope to take in non-urban applications (e.g. [7]), and has increasingly moved beyond pure description and explanation of patterns of land use growth and change into, for example, policy recommendations for greener growth and sustainable development (e.g. [8]), integrated decision support and participatory approaches [9] and natural hazard assessment [10]. While CA techniques have been applied to the study of a wide range of natural and ecological phenomena [11], studies of land use change in natural areas using CA-type models are less common, principally because the pattern of cellular evolution exhibited in a typical CA land use model is particularly appropriate for modelling urban land use change. However, some notable examples do exist. White *et al* [12] constructed an integrated CA model for the Caribbean island of St Lucia, designed as a decision support tool to explore possible environmental, social, and economic consequences of hypothesized climate change. In this work (SimLucia), evolution of natural vegetation, forest and agriculture was actively modelled [12]. In a more recent study, Moreno e*t al* [13] incorporated a CA known as SpaSim to model the dynamic evolution of a forest preserve in Venezuela using land cover classes such as forest, forest plantation and agriculture. The work aimed to understand the land cover dynamics that have occurred in the reserve, simulate the effect of land use policies on the reserve, and evaluate their effect on sustainability of the forest reserve.

**CA modeling and Doñana**

In Doñana, the researcher is confronted with two worlds, two opposing poles, of conservation versus development. The development boom, principally based on tourism and intensive agriculture, has transformed the region over the last 60 years, from one of the most impoverished in Spain to the point where per capita income is above the national average [1]. Conversely, there has also been increasing recognition of the importance of Doñana and ever greater efforts made to protect it. Unfortunately, over the same time period, areas outside the limits of the protected space have become increasingly degraded and are clearly affecting the protected area itself (e.g. [14]. The conservation versus development model has thus entered a crisis phase. However, though it is quite easy to see what the problem might be (development that favors the regional economy in the short term but destroys an important natural area), it is not at all easy to bring about a solution. CA land use models are powerful tools for understanding this type of complexity, as they allow actor decisions to be represented as land use consequences in the territory. The CA neighborhood rules of attraction and repulsion are ideal for representing the competition and pressure for the same land use location that is so acute in, and so characteristic of, the Doñana natural area.

**Methods**

Drawing on historical patterns of land use change since 1990 detected by cross tabulation analysis of corine land cover maps [2], together with information gathered in participatory workshops, an initial, or 'pilot' CA model was developed. The pilot

model was an essential precursor to the main modeling phase and development of future scenarios as it allowed for the testing of software, data and methodology prior to commitment of extensive resources.

The modeling software that we used in this project is part of a suite of software, a tool kit called Geonamica®. Metronamica®, the land use modeling component of Geonamica®, is a *geographical* land use model (*sensu* Tobler [5]), operating in a graphical application environment for the windows platform. At the core of the model is the transition potential (TP) computation which determines the future state of the cells (change or no change). TP is calculated as a function where a set of endogenous factors interact to update the state of the cell in every time step (oneyear). These factors are *neighborhood rules*, which determine the relationship between different land use classes in terms of attraction and repulsion; *accessibility* to facilitate or constrain land use conversions depending on the distance from the cells to the network; *zoning*, that is, extant land planning regulations; a set of biophysical *suitability* parameters; and a *stochasticity* variable in order to avoid over-determinism in the model. This TP function determines the likelihood of each cell in the model to change from one use to another.
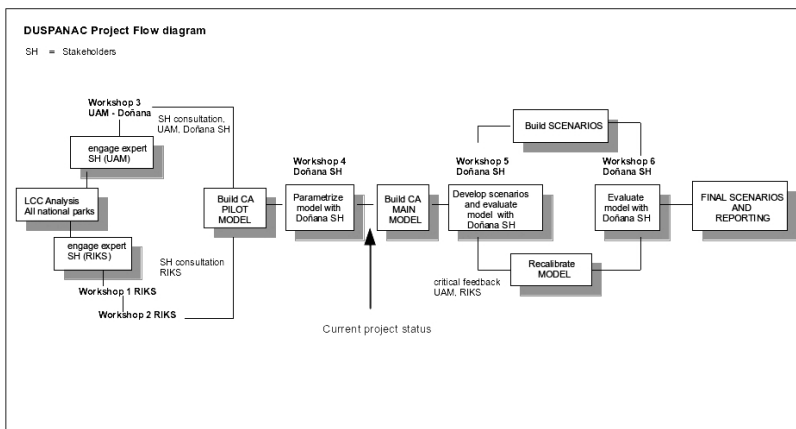


Figure 1: the Modeling chain

Construction of the model followed the procedure defined by RIKS [15], this can be briefly summarized as follows:

1. Analysis of dynamics of land use/cover change (LUCC) in the territory to be modeled.

2. Definition of activity types according to LUCC dynamics observed: land use classes must be divided into three groups, vacant (passive, does not grow but is occupied by other land uses - e.g. non-irrigated crops) function (active, dynamic, will grow and occupy other land uses, e.g. urban residential) and feature (static, restrictive, will not change and cannot be occupied by other land uses - e.g. water)

3. Introduction of initial land use map M1 (corine 1990), classified according to activity types.

4. Introduction of second land use map M2 (corine 2000), for model calibration.

5. Introduction of land use demand for function land use classes for calibration, taken from M2

6. Establishment of parameters (neighborhood rules, accessibility, suitability, zoning)

7. Simulated map MS2 for technical calibration

8. Other simulations, scenarios etc.

After all parameters have been set (steps 1-6), transition potential is calculated for all of the maps in the model, and then applied to M1 to produce a simulation of change over the period between M1 and M2, expressed as a new map, MS2 (step 7). In this way, the first part of the model calibration begins, which we refer to here as *technical calibration*. Once technical and empirical calibration (see final section) have been completed satisfactorily, land use simulations based on future scenarios can be developed.

**Technical calibration procedure**

Technical calibration of the model is defined here as the process of obtaining an acceptable degree of fit between the simulated map, MS2 and the real map, M2 of the territory at the second date (in our case, the year 2000). The degree of fit gives us a guide to the reliability (confidence level) of the model with respect to the land use change trends observed in the territory.



Figure 2: land use changes in Doñana, 1990-2006,

Land use change dynamics and activity types:

With reference to figure 2, the principal LUCC in the territory observed from map comparison between 1990, 2000 and 2006 can be summarized as follows:

1. Significant expansion of fruit and berry plantations (F) between 1990 and 2000 (Intensive cultivation of citrus and strawberry). Principal contributing land uses (in order of greatest to least contribution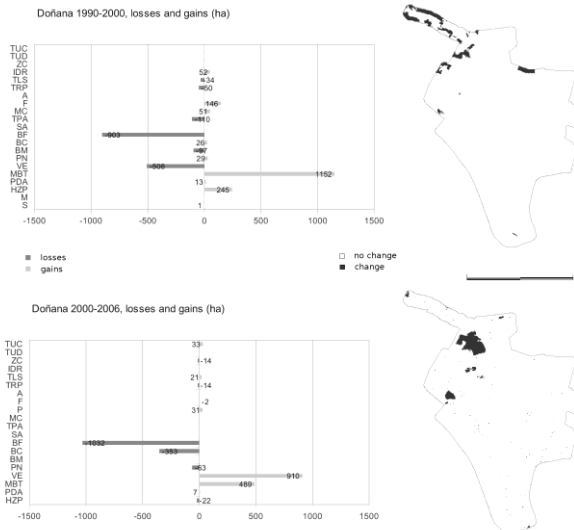) were grassland (PN) (55 ha), other irrigated crops (TRP) (44 ha), non-irrigated crops (TLS) (30 ha) and sclerophyllus vegetation (VE) (15 ha). Other irrigated crops have also increased, taking 29 hectares and 12 hectares from VE and shrubland (MBT) respectively.

It is clear that these changes represent agricultural intensification; they have all occurred outside the national park, just inside the area which is also excluded from the zone of lesser protection comprising the natural park. A 50 ha area of formerly irrigated land (TRP) in 1990 had become crop mosaic (MC) by 2000. Thus, in terms of *land use dynamics* (neighborhood rules), we see that TRP, PN, TLS and MBT are likely to be sensitive to occupation by F, and that MBT and VE are sensitive to occupation by TRP. Clearly, given the location of the new intensive cultivation, *zoning* will be very important in the model. F and TRP, and probably MC as well, need to be designated as function activity types in the model to reflect their susceptibility to increase, taking over other land use types.

2. Important increase in MBT between 1990 and 2000, taking 912 hectares from broad-leaved forest (BF), and 96 hectares from mixed forest (BM). This increase has occurred principally in the north-west extension to the natural park (Figure 4). As MBT has continued to increase in the second period (2000-2006), this time from conifer forest (BC) (648 ha) and BM (137 ha), expansion of shrubland should be considered an important dynamic and also will be assigned to activity type function.

3. The vulnerability of this location to development of tourist infrastructure is evidenced by the construction of a 52 hectare camp site (IDR) between 1990 and 2000 in a zone previously given over to natural vegetation (VE) on the shoreline just to the north west of the national park (in a small pocket of land lacking natural protection related to the tourist resort of Matalascañas). A 53 hectare construction site is also in evidence. In the second period (2000-2006), 15 hectares of which had become urban fabric by 2006. It is clear that all types of urban fabric (TUC and TUD) as well as construction sites (ZC) and sports and leisure facilities (IDR) must be assigned to function activity types.

*Land use demand:*

Table 1: Land use demand for the 8 function activity types

| Description | Spanish acronym | ha 1990 | ha 2000 | ha 2006 |
|---|---|---|---|---|
| Continuous urban Fabric | TUC | 407 | 407 | 451 |
| Discontinuous urban fabric | TUD | 6 | 6 | 6 |
| Construction areas | ZC | 53 | 53 | 38 |
| Sports and leisure facilites | IDR | 13 | 65 | 65 |
| Permanently Irrigated land | TRP | 419 | 369 | 351 |
| Fruit and berry plantations | F | 100 | 241 | 241 |
| Crop Mosaic | MC | 0 | 50 | 50 |
| Shrubland | MBT | 3307 | 4464 | 4939 |

On the basis of the observed LUCC dynamics (Table 1), land use demand was set for the 8 function classes.

*Neighborhood rules:*

The neighborhood rules (methods, step 6) are key to the transition potential computation which comprises the core of the CA model. To determine the neighborhood rules, relative values representing *persistence, attraction* and *repulsion* are applied to all land use categories with respect to the function categories in the model (Figure 3). These parameters are then applied by the model to each cell with respect to all other cells in its neighborhood, a total of 197 cells including the cell itself (up to 8 cells in any direction). As only the cells belonging to the function categories are have the ability to relocate within the model, neighborhood parameters must be set to establish their behavior, with respect to themselves (*persistence*) and other functions or non-functions (*attraction and repulsion*). The most intuitive way to explain this concept is in terms of a graph for each land use, having x representing distance in any direction away from a cell containing that land use and y representing *relative force of attraction* (RFA).

*Other parameters, accessibility, suitability and zoning:*

Three network layers were included in the pilot model, roads, irrigation channels and rivers. In the initial calibration, accessibility was applied only to the irrigated crops (TRP) and fruit and berry plantations (F) land uses, principally because these were the most important dynamics likely to be affected by accessibility conditions. Zoning parameters were established on the basis of the land use restrictions of the use and management master plan (PRUG), with highest and second highest level protected areas (reserve and restricted use) being designated strictly restricted (no occupation permitted by new land use), protected areas outside of these zones weakly restricted, and other areas, such as the buffer corridor, unrestricted for all anthropogenic land use functions. Non-anthropogenic land use functions (shrubland) were allowed everywhere.

**Technical calibration goodness of fit:**

The goodness of fit of the technical calibration depends on two key parameters, *quantity* and *location*. As we have seen previously, quantity is determined initially by the input demand for each land use, but ultimately by the amount of available land on the map relative to the ranking for that land use in the transition potential table; that is, even if all demand for one particular land use is not completely allocated, the model run may terminate anyway because all available locations have been filled with other land uses that scored more highly in the TP ranking. Although not all demand will necessarily be allocated, this is quite a satisfactory way to deal with real world pressure, competition and uncertainty. This makes it difficult to estimate the success of the technical calibration exercise solely in terms of *quantity*. A good basic starting point is to compare the cross tabulation for M1 and M2 with its counterpart for the simulated map (M1 and MS2); Table 2 (below).

It can be seen that there are some early successes, and quite a few areas where the model has not performed well. For example, the expansion of the shrubland category (MBT) over this time period has been adequately represented in terms of gains from

the relevant categories in approximately correct proportions. Though there is clearly room for improvement, the model seems to be beginning to reflect the LUCC observed in reality. Turning to the expansion of fruit and berry cultivation (F), we can see, from the diagonal, that the inertia of this category (the RFA with respect to itself; Figure 3) is successfully preventing migration or occupation of existing F. The 141 new hectares required have been drawn from grassland (PN) and (TRP), again reflecting the real situation. However, while in the model the major part of the gain to this category has come from PN, in reality we can see that vegetation (VE) and non-irrigated land (TLS) have also contributed, something the model has been unable to reflect.
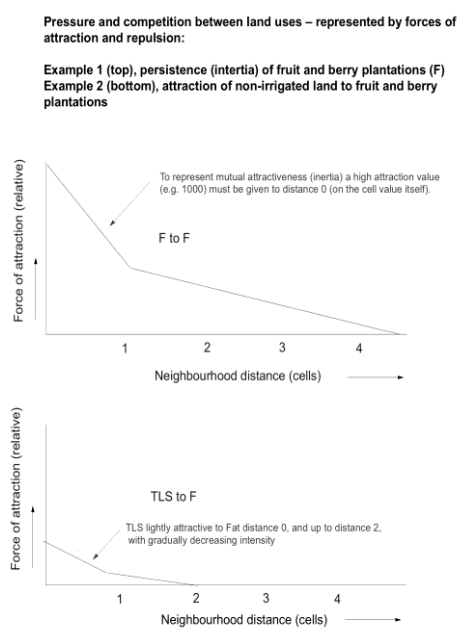


Figure 3: Examples of neighborhood rules

In this case the adequate response would be to return to the neighborhood rules and try to establish a greater attractiveness for F at distance 0 for the VE and TLS columns. The loss of 50 ha of other irrigated land (TRP) has been correctly modeled with respect to F, which has gained 35 ha in the model against 44 in reality. But again, something is not quite right, as in the model it can be seen that TRP has not passed 50 ha to crop mosaic (MC), as happened in reality (MC has instead gained from PN) and has lost 19 ha to TLS, a vacant land category which should not have gained. This behavior, gain to a non-function category, is probably caused by the model seeking to obtain the correct demand for TRP (which has decreased over the modeled period) and allocating excess cells to the first available category (i.e.

category 0, TLS). It needs to be remembered in these cases that the demand for vacant categories is invisible to the model. In this case, it is very likely that this unwanted behavior can be compensated for by making TLS more attractive to F, thus solving two problems at once. MC needs also to be made more attractive to TRP so that the model does not find itself with surplus demand at the end of the run. On this basis, further adjustments were made to the neighborhood rules, resulting in some improvements (Table 3).

Table 2: comparison of cross tabulation results. Corine 1990 (M1) occupied the columns in both cases. M1 has been crossed with the first simulation attempt (MS2) at top, and with the real corine map for 2000, below.

| | TLS | A | P | TPA | SA | BF | BC | BM | PN | VE | PDA | HZP | M | S | TUC | TUD | ZC | IDR | TRP | F | MC | MBT | LA | E | M | Total |
|---|---|---|---|---|---|---|---|---|---|---|---|---|---|---|---|---|---|---|---|---|---|---|---|---|---|---|
| TLS | 3010 | | | | | | | | | | | | | | | | | | 19 | | | | | | | 3029 |
| A | | 152 | | | | | | | | | | | | | | | | | | | | | | | | 152 |
| P | | | | | | | | | | | | | | | | | | | | | | | | | | 0 |
| TPA | | | | 414 | | | | | | | | | | | | | | | | | | | | | | 414 |
| SA | | | | | 78 | | | | | | | | | | | | | | | | | | | | | 78 |
| BF | | | | | | 1630 | | | | | | | | | | | | | | | | | | | | 1630 |
| BC | | | | | | | 6510 | | | | | | | | | | | | | | | | | | | 6510 |
| BM | | | | | | | | 857 | | | | | | | | | | | | | | | | | | 857 |
| PN | | | | | | | | | 1378 | | | | | | | | | | | | | | | | | 1378 |
| VE | | | | | | | | | | 9364 | | | | | | | | | | | | | | | | 9364 |
| PDA | | | | | | | | | | | 3879 | | | | | | | | | | | | | | | 3879 |
| HZP | | | | | | | | | | | | 22994 | | | | | | | | | | | | | | 22994 |
| M | | | | | | | | | | | | | 937 | | | | | | | | | | | | | 937 |
| S | | | | | | | | | | | | | | 304 | | | | | | | | | | | | 304 |
| TUC | | | | | | | | | | | | | | | 407 | | | | | | | | | | | 407 |
| TUD | | | | | | | | | | | | | | | | 6 | | | | | | | | | | 6 |
| ZC | | | | | | | | | | | | | | | | | 53 | | | | | | | | | 53 |
| IDR | | | | | | | 54 | | | | | | | | | | | 13 | | | | | | | | 67 |
| TRP | | | | | | | | | | | | | | | | | | | 365 | | | | | | | 365 |
| F | 1 | | | | | 1 | | | 104 | | | | | | | | | | | 35 | 100 | | | | | 241 |
| MC | | | | | | | | | 50 | | | | | | | | | | | | | | | | | 50 |
| MBT | 4 | | | | | 1001 | 24 | 21 | 3 | 90 | 13 | 1 | | | | | | | | | | 3307 | | | | 4464 |
| LA | | | | | | | | | | | | | | | | | | | | | | | 6647 | | | 6647 |
| E | | | | | | | | | | | | | | | | | | | | | | | | 1369 | | 1369 |
| M | | | | | | | | | | | | | | | | | | | | | | | | | 7682 | 7682 |
| Total | 3015 | 152 | 0 | 414 | 78 | 2632 | 6588 | 878 | 1535 | 9454 | 3892 | 22995 | 937 | 304 | 407 | 6 | 53 | 13 | 419 | 100 | 0 | 3307 | 6647 | 1369 | 7682 | 72877 |

| | TLS | A | P | TPA | SA | BF | BC | BM | PN | VE | PDA | HZP | M | S | TUC | TUD | ZC | IDR | TRP | F | MC | MBT | LA | E | M | Total |
|---|---|---|---|---|---|---|---|---|---|---|---|---|---|---|---|---|---|---|---|---|---|---|---|---|---|---|
| TLS | 2985 | | | | | | | | | | | | | | | | | | | | | | | | | 2985 |
| A | | 152 | | | | | | | | | | | | | | | | | | | | | | | | 152 |
| P | | | | | | | | | | | | | | | | | | | | | | | | | | 0 |
| TPA | | | | 159 | | | | | | 48 | 73 | | | | | | | | | | | 17 | | | | 297 |
| SA | | | | | 78 | | | | | | | | | | | | | | | | | | | | | 78 |
| BF | | | | | | 1720 | | | | | | | | | | | | | | | | | | | | 1720 |
| BC | | | | | | | 6581 | | | | | | | | | | | | | | | 33 | | | | 6614 |
| BM | | | | | | | | 782 | | | | | | | | | | | | | | | | | | 782 |
| PN | | | | | | | | | 1432 | 131 | | | | | | | | | | | | | | | | 1563 |
| VE | | | | | | | | | | 8950 | | | | | | | | | | | | | | | | 8950 |
| PDA | | | | | | | | | | | 3892 | | | | | | | | | | | | | | 14 | 3906 |
| HZP | | | | 255 | | | | | | | | 22995 | | | | | | | | | | | | | | 23250 |
| M | | | | | | | | | | | | | 937 | | | | | | | | | | | | | 937 |
| S | | | | | | | | | | | | | | 304 | | | | | | | | | | | | 304 |
| TUC | | | | | | | | | | | | | | | 407 | | | | | | | | | | | 407 |
| TUD | | | | | | | | | | | | | | | | 6 | | | | | | | | | | 6 |
| ZC | | | | | | | | | | | | | | | | | 53 | | | | | | | | | 53 |
| IDR | | | | | | | 52 | | | | | | | | | | | 13 | | | | | | | | 65 |
| TRP | | | | | | | | | | 29 | | | | | | | | | 325 | 3 | | 12 | | | | 369 |
| F | 30 | | | | | | | | | 55 | 15 | | | | | | | | | 44 | 97 | | | | | 241 |
| MC | | | | | | | | | 50 | | | | | | | | | | | | | | | | | 50 |
| MBT | | | | | | 912 | 7 | | 96 | 204 | | | | | | | | | | | | 3245 | | | | 4464 |
| LA | | | | | | | | | | | | | | | | | | | | | | | 6647 | | | 6647 |
| E | | | | | | | | | | | | | | | | | | | | | | | | 1369 | | 1369 |
| M | | | | | | | | | | | | | | | | | | | | | | | | | 7668 | 7668 |
| Total | 3015 | 152 | 0 | 414 | 78 | 2632 | 6588 | 878 | 1535 | 9454 | 3892 | 22995 | 937 | 304 | 407 | 6 | 53 | 13 | 419 | 100 | 0 | 3307 | 6647 | 1369 | 7682 | 72877 |

Table 3: second comparison of cross tabulation results after adjustment of neighborhood rules.

| | TLS | A | P | TPA | SA | BF | BC | BM | PN | VE | PDA | HZP | M | S | TUC | TUD | ZC | IDR | TRP | F | MC | MBT | LA | E | M | Total |
|---|---|---|---|---|---|---|---|---|---|---|---|---|---|---|---|---|---|---|---|---|---|---|---|---|---|---|
| TLS | 2973 | | | | | | | | | | | | | | | | | | | | | | | | | 2973 |
| A | | 152 | | | | | | | | | | | | | | | | | | | | | | | | 152 |
| P | | | | | | | | | | | | | | | | | | | | | | | | | | 0 |
| TPA | | | | 414 | | | | | | | | | | | | | | | | | | | | | | 414 |
| SA | | | | | 78 | | | | | | | | | | | | | | | | | | | | | 78 |
| BF | | | | | | 1634 | | | | | | | | | | | | | | | | | | | | 1634 |
| BC | | | | | | | 6512 | | | | | | | | | | | | | | | | | | | 6512 |
| BM | | | | | | | | 857 | | | | | | | | | | | | | | | | | | 857 |
| PN | | | | | | | | | 1446 | | | | | | | | | | | | | | | | | 1446 |
| VE | | | | | | | | | | 9357 | | | | | | | | | | | | | | | | 9357 |
| PDA | | | | | | | | | | | 3874 | | | | | | | | | | | | | | | 3874 |
| HZP | | | | | | | | | | | | 22988 | | | | | | | | | | | | | | 22988 |
| M | | | | | | | | | | | | | 937 | | | | | | | | | | | | | 937 |
| S | | | | | | | | | | | | | | 304 | | | | | | | | | | | | 304 |
| TUC | | | | | | | | | | | | | | | 407 | | | | | | | | | | | 407 |
| TUD | | | | | | | | | | | | | | | | 6 | | | | | | | | | | 6 |
| ZC | | | | | | | | | | | | | | | | | 53 | | | | | | | | | 53 |
| IDR | | | | | | | 54 | | | | | | | | | | | 13 | | | | | | | | 67 |
| TRP | | | | | | | | | | 1 | 1 | | | | | | | | 363 | | | | | | | 365 |
| F | 34 | | | | | | | | 85 | | 2 | | | | | | | | | 20 | 100 | | | | | 241 |
| MC | 4 | | | | | 1 | | | | 3 | 0 | 6 | | | | | | | | 36 | | | | | | 50 |
| MBT | 4 | | | | | 997 | 22 | 21 | 4 | 91 | 17 | 1 | | | | | | | | | | 3307 | | | | 4464 |
| LA | | | | | | | | | | | | | | | | | | | | | | | 6647 | | | 6647 |
| E | | | | | | | | | | | | | | | | | | | | | | | | 1369 | | 1369 |
| M | | | | | | | | | | | | | | | | | | | | | | | | | 7682 | 7682 |
| Total | 3015 | 152 | 0 | 414 | 78 | 2632 | 6588 | 878 | 1535 | 9454 | 3892 | 22995 | 937 | 304 | 407 | 6 | 53 | 13 | 419 | 100 | 0 | 3307 | 6647 | 1369 | 7682 | 72877 |

With respect to *location*, once the quantity has been approximately correctly located by the iterative process described above (set neighborhood rules, output cross tabulations, adjust neighborhood rules, return to cross tabulations etc), the more

intractable problem of *location* can be considered. The key to a workable *useful* model (see [16]) lies in the production of a visually acceptable simulation, where land use changes can be seen by model end users and stakeholders to have occurred in locations where available empirical knowledge suggests it is likely to occur.
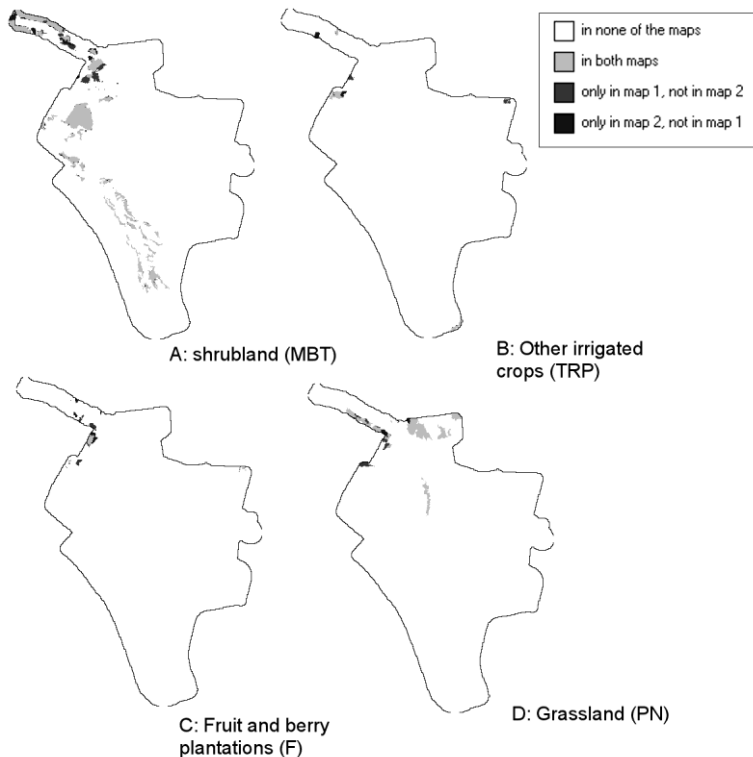


Map 2: Map Comparison results for 4 key land use categories. In the legend, map 1 refers to the real map for the year 2000, while map 2 is MS2, the calibration simulation for the same date.

The results of the model for MS2 (the year 2000) are shown above. Simple visual inspections were carried out in the Map Comparison Kit, a software application provided by RIKS for free download at http://www.riks.nl/mck/. Though the software does offer a range of techniques for statistical comparison of maps, in this case, the simplest, visual comparison method (per category comparison for each land use class) was used in this case to assess whether the simulation performance was broadly acceptable. The model shows success in some areas, for example (compare with Figure 2) in the area of extension to the park proper in the northwest corner the growth of new shrubland following loss of eucalyptus plantation has been simulated with a fairly high degree of success (MBT, map 2A). It can also be seen that the claims of success in terms of *quantity* (above) are not borne out with respect to

*location*. Though new hectares of fruit and berry cultivation (F; map 2C) were simulated in terms of changes to and from the appropriate categories, the simulation did not choose the correct locations. This is probably because there were a large number of possible locations given neighborhood, accessibility and zoning rules relative to a small quantity of new F to be allocated.

## Pilot simulation: massive expansion of citrus and strawberry

The final part of the *technical* modeling process consists in the application of the calibrated model to future scenarios. For this purpose a simple simulation was built on the basis of empirical knowledge of the evolution of the Doñana natural area and the results of cross tabulation analysis of land use changes. This scenario postulates an explosive growth of citrus and strawberry cultivation to a total demand of 2000 ha in the currently available locations by 2030 (Map 3). The simulation, which we have called *massive expansion of citrus and strawberry,* is extreme. However, although continued expansion of intensive cultivation in the zone immediately adjacent to the protected natural area is highly undesirable from the point of view of conservation, the historical tendency does indicate that further expansion is possible. It is very unlikely indeed that an expansion of intensive citrus and strawberry cultivation as great as that postulated in this scenario would or could take place, but sometimes *what if...* type scenarios may be important in communicating future threats or risks to stakeholders or testing resilience of zoning measures against hypothetical worst-case scenarios.
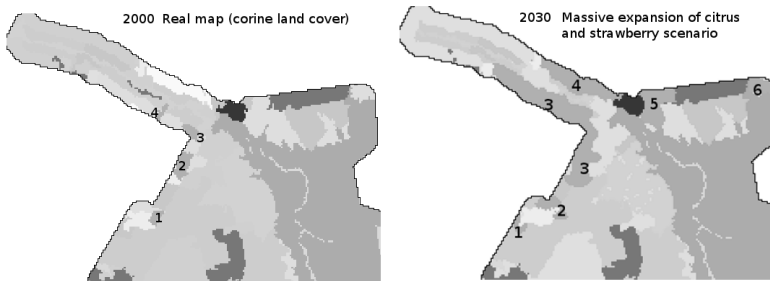


Map 3: Results of the massive expansion of citrus and strawberry scenario for the year 2030. Areas of fruit and berry cultivation are numbered. This highly unrealistic test scenario nevertheless illustrates the potential of the model to address real world questions of interest to natural resource managers, such as: what areas are most vulnerable to expansion of intensive cultivation?

## Conclusions and future work to improve the model

At present, the work presented here has not attempted to integrate knowledge outside the realm of the technical accuracy parameters presented here by involving the stakeholder community in the model building process. It is generally accepted that decisions are likely to be implemented with less conflict and more success when

they are driven by those who are likely to bear their consequences [17]. Though participatory work is ongoing, some stakeholder feedback has already been obtained [3]; in summary, stakeholders and researchers are in agreement that the model could be improved in the following ways:

1. Improved land use mapping. The corine land cover data used in the pilot study is too simplistic, future modelling work will employ larger scale land use/cover maps [3].

2. Accessibility maps were not included for all land cover types in the pilot model. Accessibility to infrastructures is likely to inhibit or stimulate LUCC, so including accessibility for a wider range of land use classes is likely to improve the model.

3, Suitability maps were not included in the pilot model. Physical suitability is important to avoid allocation of particular land use types in areas where they are not normally suitable (e.g. irrigated crops in mountain areas).

4. Study area does not take into account a large enough area to reflect all possible implications in the territory; the study area will accordingly be extended to include the whole of the hydrological catchment of the river Guadiamar (Map 1).

5. At present, the scenarios discussed are very simple, and currently not aligned with those developed for Doñana through participatory workshops by Palomo *et al* [18].

## Acknowledgments

## References

[1]    Montes, C. (2007) Construir Resiliencia para Doñana en un mundo cambiante. *Revista Sostenible* 35:14-15, 2007.

[2]    Hewitt, R. and F. Escobar, (In prep.) Los cambios recientes en la ocupación del suelo de los parques nacionales españoles, una aproximación general de la base de datos de corine land cover 1990-2000-2006.

[3]    Hewitt, R., Hernández-Jiménez, V., Encinas, M.A. and F. Escobar, (2012) Land use modelling and the role of stakeholders in natural protected areas: the case of Doñana, Spain. International congress on environmental modeling and software 2012.

[4]    von Neumann, J. (1966) and A. W. Burks,(ed). Theory of Self-Reproducing Automata.Urbana    and    London:    Univ.    of    Illinois    Press.

[5]    Tobler, W. (1979), Cellular Geography, S. Gale & G. Olsson, eds., Philosophy in Geography, Reidel, Dortrecht; pp 379-386.

[6]    White, R., & Engelen, G. (1993) Cellular automata and fractal urban form: a cellular modelling approach to the evolution of urban land-use patterns. *Environment and Planning A,* 25(8), 1175–1199

[7]    Wickramasuriya, R. C., Bregt, A. K., van Delden, H., & Hagen-Zanker, A. (2009) The dynamics of shifting cultivation captured in an extended Constrained Cellular Automata land use model. *Ecological Modelling*, 220(18), 2302–2309.

[8]    Hernandez Jimenez, V., N. Winder, (2006). Running experiments with the Madrid Simulation Model. Workpackage 5, TiGrESS Final Report. Newcastle upon Tyne, UK.: Newcastle University.

[9]    Kok, K., H. van Delden, (2009). Combining two approaches of integrated scenario development to combat desertification in the Guadalentín watershed, Spain. *Environment and Planning B: Planning and Design*, 36(1), pp.49-66.

[10]   Barredo, J., G. Engelen, (2010). Land Use Scenario Modeling for Flood Risk Mitigation. *Sustainability* 2, no. 5: 1327-1344.

[11]   Parker, D.C., Manson, S.M., Janssen, M.A., Hoffmann, M.J. and Deadman, P. (2003) Multi-Agent Systems for the Simulation of Land-Use and Land-Cover Change: A Review. Annals of the Association of American Geographers, Vol. 93, No. 2, p. 314-337

[12]   White, R., Engelen, G., and Uljee, I., (2000). Modeling land use change with linked Cellular Automata and socio-economic models: a tool for exploring the impact of climate change on the island of st. Lucia . Book Chapter outline, available online at: http://terra-geog.lemig2.umontreal.ca/donnees/geo3532/CA_integrated_model_ex.pdf. August 2012.

[13]   Moreno, N., Quintero, R., Ablan, M., Barros, R., Dávila, J., Ramírez, H., G. Tonella, et al. (2007). Biocomplexity of deforestation in the Caparo tropical forest reserve in Venezuela: An integrated multi-agent and cellular automata model. *Environmental Modelling & Software*, 22(5), 664–673

[14]   Munoz-Reinoso, J.C., (2001) Vegetation changes and groundwater abstraction in SW Donana, Spain, Journal of Hydrology, Elsevier

[15]   RIKS B.V. , (2011). Metronamica Documentation. Retrieved from: http://www.riks.nl/resources/documentation/Metronamica%20documentation.pdf, March 2012

[16]   Box, G.E.P. (1979) Some Problems of Statistics and Everyday Life. Journal of the American Statistical Association, Vol. 74, No. 365, p. 1-4. Retrieved from: http://www.jstor.org/stable/2286713. February 2012

[17]   Voinov,A. and F. Bousquet. Modelling with stakeholders. *Environmental Modelling & Software* 25: 1268, 2010.

[18]   Palomo, I., Martín-López, B. , López-Santiago C. and C. Montes. Participatory Scenario Planning for Natural Protected Areas management under ecosystem services framework: the Doñana social-ecological system, SW, Spain. *Ecology&Society,* 16:23, 2011

# Detecting surface flow concentrations using a cellular automaton metric: a new way of detecting potential impacts of flash floods in dry valleys

## J. DOUVINET[1]; D. DELAHAYE[2]; P. LANGLOIS[3]

[1]University of Avignon / UMR ESPACE 7300 CNRS
74 rue Louis Pasteur, Case 17, F-84000 AVIGNON, France
(+33) 4 90 16 25 16 ; johnny.douvinet@univ-avignon.fr (correspondent author)
[2] LETG-Géophen / University of Caen Basse-Normandie / UMR 6554 CNRS
Esplanade de la Paix, F-14035 CAEN Cedex 2, France
(+33) 2 31 56 65 94, daniel.delahaye@unicaen.fr
[3]Univeristy of Rouen / MTG - UMR IDEES 8586 CNRS
27 rue Thomas Becket, F-76821 MONT-SAINT-AIGNAN Cedex
(+33) 2 35 14 60 00 ; patrice.langlois@univ-rouen.fr

## Abstract

This paper aims to investigate a new way of locating potential impacts of flash floods. Mapping surface flow concentrations, using a new metric based on a cellular automaton RuiCells, is shown to qualitative align with observed and known instances of damage caused by flash floods in 4 small 'dry valleys' located in northern France (Parisian Basin). Numerical simulations enable the assessment of the relations between the organisation of thalwegs networks and surfaces for a given basin form. An index of concentration (IC) allows detecting the confluences in upstream of which networks and surfaces are spatially well organised. A strong correlation between observed damage, field experiments, local knowledge and maps of IC index exists as simulations underline many places where flash floods induce important material or human damage and where further surface flow concentration results in highly-incised gullies. In rare cases, no validation is possible because nobody can confirm the degradations.

## Introduction

The origin and the prediction of flash floods in small and ungauged basins is getting increasing attention [1, 2] and the last decades have seen an increase in forecasting of such events in numerous countries [3, 4,]. Such type of natural hazards threatens people, causes increasing losses of buildings and infrastructures and occurs in a short time-duration. Generated shortly following high rainfall intensities, flash flood are characterized by sudden onset or rapid rising time. A surge may rush down the main valley just a few minutes after rainfall has peaked [5, 6]. To better address the lack of available information, various models and approaches have been carried out. By necessity, the investigations on recent

flash floods generally are event-based and opportunistic as they enhance the information content [2, 7]. While meteorological observations provide relevant details on the timing and location of convection in the storm environment [8], hydrological and physical processes remain still difficult to assess because: i) flow measurements and classical field-based experimentations (as the reconstitution of maximum peak discharges thanks to slack water deposits) are rarely collected in basins of small-size; ii) these flood are insufficiently documented and are difficult to monitor in real time because they produce destructive effects to measuring devices; iii) the infrequency of these events makes the statistical analysis and calibration of models delicate.

In this study, our objectives are to use a cellular automaton approach (the CA known as *RuiCells* – 9, 10, 11] in order to: i) promote further understanding of the effects of runoff concentrations which are influenced by basin form, slope and the drainage network during flash floods and ii) to measure the potentials of concentration since local to global scales. The framework used is common to other cellular automata and respect two main properties: a CA is a model simplifying the reality to a group of automates dealing with information and inducing cellular actions; CA use precise and finite state, as homogeneous and interconnected cells. The guiding principle of *RuiCells* follows the idea that mechanical rules of flow based on topography can be combined with a cellular automata representation of spatial processes to better assess the complex relations between basin structures and surface flow pathways. While numerous distributed hydrological models have been realized with Digital Elevation Maps, none of them allow for the estimation of potential surface flow concentration in all parts within a basin. Numerous studies have typically focused on the relation between the global catchment morphology and its hydrological response measured at the final outlet. These studies underlined difficulties encountered when linking local responses (sub-basins or hillslopes) to this global behaviour and this aim has been one of the main issues for geomorphologists since the 1970's [12, 13]. A few studies have successfully shown that the drainage network organisation plays a key role on hydrological functionality. Others recently defined the global response as the result of linear system (with a linear relation between mean discharges and the basin sizes) and show that global catchment response can be summarized by an IUH, Instantaneous Unit Hydrograph [14], evolving in a Geomorphologic Instantaneous Unit Hydrograph [15]. However, in this study we use a cellular automaton approach to better link the local hydrological rules to the emergence of global hydrological responses. Our main goal is to identify all sub-basins in which high surface flow concentrations can be hidden at larger scales and this approach is applied on small- size basins where floods occurred in order to create prevention maps. Assuming that this tool is relevant to the planning of and protection from such types of events, it could be useful for the understanding of floods in valleys which remain ungauged. Moreover, definition of flood potential in temporary streams is required to assess the extent of probable flooding in the future.

## Framework and structure of the specific French CA model *RuiCells*

Previous experimentations in CA modelling for surface water flow provide several advices and recommendations. The main difficulty in these models is generally to establish all the links between topographic variables, such as the elevation and its derivative, and hydraulic variables as water fluxes. Furthermore, from a numerical perspective, square lattices induce problems for simulating the runoff routing [16], as surface flows do not follow the real drainage. Different studies also highlighted the critical influence of the DEMs cells size on the accuracy of extracted networks [17, 18]. Consequently, in the CA model *RuiCells*, we choose to use a lattice based on triangular, regular and interconnected cells based on a Digital Elevation Model (DEM) and we define simple rules to simulate the interactions between basin form, slope and the drainage network.

The structure of *RuiCells* is basically summarized as follows. The first step permits to create a topological mesh in triangular finite elements. In this, the direction of the steepest slope gives the downstream direction of flow and this information available in each cell is draped over the DEM (figure 1). The lowest diagonal was chosen to obtain more realistic flows. Each cell contains the pointer to its lowest downstream neighbour. The s e c o n d step a s s i g n s one hydrological rule for each cell: the triangular facets represent elementary cells on hill-slopes; the linear portions the thalwegs; and several nodes the local closed depressions. Combining these rules in the third step, we aim to simulate the interactions between these various surface water flows [18, 19]. Each cell is linked to upstream / downstream cell(s) by a flow graph to form a cellular unit.

The connectivity between those cells is directed predominantly b y the morphological link structured by the mesh (or lattice) as well as the neighbourhood topology of cells. There, contrary t other CA classical models, flow pathways are not only guided by the neighbourhood or vicinity conditions. This approach assumes that linear r u n o f f s and s p a t i a l r u n o f f s are dependent and a synchronous advection operator also avoids the problem of order in calculi. Indeed, process is iterative in *RuiCells*. It means that surface, flows or other values used during the simulation flow at the same moment. Consequently, *RuiCells* is based on a generalized cellular automaton model, in which cells have different facets and in which flow pathways represent real effects of the morphological structure and not only its topology. The structure of the CA used here is different from classical cellular automata models: we respect formal guidelines (a spatial lattice, a small number of states, one iterative process) but we adapt them to answer to one hydrological problem (hence, important changes appear for transition or neighbouring rules). So it can be considered as a GCA – Geographical Cellular Automata [20].
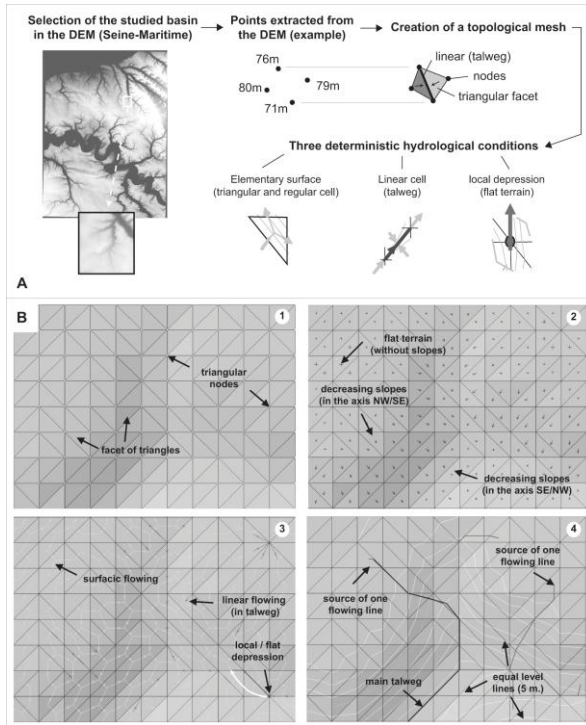
Figure 1: Construction of the cellular unit based on a Digital Elevation Map in *RuiCells*

## The Cellular Routing Scheme (CRS)

At the beginning of the simulations, cells are initialized with their own surface and the automaton handles the advection operator moving each surface between each cell simultaneously. We conserve the main property defined as *locality* in classical Cellular Automata [10]: the transition rules operate on cells directly based on local neighbourhood. But in this case, we do not use the Moore (4) or Von Neumann (8) neighbourhood (for example) because the surface flow follows the downstream direction as defined previously. Here, the Cellular Routing Scheme (CRS) depends on the surface flow from each cell and on the updating of the values of all the sub- states. Surface flow is routed downstream via each row of cells until the downstream boundary is reached. The main difficulty rises when two neighbouring cells exist. A previous study has shown that a flow partitioning in various directions is better [17] The flow dispersion is classically deduced by dividing the flow between a maximum of two neighbouring downstream grid cells [21]. However, the routing scheme used here is proportionally partitioned according to the slope angle and such a procedure

improves the diffusion of surfaces on each cell (figure 1). The triangular mesh gives satisfactory results, particularly in floodplains and thalwegs.

## Simulation outputs

Graphs obtained at the end of the simulation process show the sum of surfaces at interaction and not only the number of cells as a function of distance *n* from the outlet. Steps are not time but rather length-steps because the surface flow diffusion depends on the spatial lattice size. So, these graphs give a picture of the theoretical spatial behaviour of a given basin in two dimensions and improve previous methods. The width-function defined by Shreve (1969) informed on the number of links in the network at a flow distance x to the outlet but the graphs obtained with *RuiCells* are not only based on the distance along networks. The Link Frequency Distribution or the area-distance-function proposed by Kirkby (1976) also not gave the same results because the distribution of pixels covering the drainage area was always used [13], while the surface flowing in *RuiCells* follows three deterministic rules (differences between surface, linear or node transition) and is based on a triangular lattice. For the same reasons, this modelling approach offers more realistic results than those obtained with the area-distance-function and differs from those using a surface flow travel time probability distribution through networks [13] as time is not integrated during the CA iterative process.

## A specific index to measure surface flow concentrations

To quantify the surface flow concentrations at local scales, we propose to divide the highest peak of surfaces (*Smax*) observed on the surface flow graphs by the square root of the basin area (*A'*) located upstream (figure 2). *Smax* is equal to the highest line of cells located at a distance from the outlet and is measured at a given iteration (*ItMax*). We also divide *Smax* by the square root of upstream in following the well- shown relation between discharges and square root of basin areas. We multiply the ratio by 100 to render the analysis easier: the value obtained for *Smax* corresponds to a percentage of the average diameter of the basin. This index of concentration – IC – enables us to survey the increase of basin width with the cumulative distance of surfaces from the outlet and it offers a new metric to encapsulate the intensity of flows (figure 2). Values automatically calculated during the simulation process are available in each cell and have same significance regardless of the basin area if the numerical model never changes. The results should be interpreted differently if the resolution evolves. Even if indexes do not have a scalar dependence, a numerical model with higher resolution naturally gives lower values for the peak of surfaces (*Smax*) and consequently for the IC index. In this study, we always use a DEM of 50 meters long. When IC indexes are equal to 50, it indicates a medium surface flow concentration; *i.e* the peak of surfaces equals to the half of the average diameter. When IC indexes exceed the value 55 (this arbitrary threshold was validated during our first field investigations), networks and surfaces appear

really well-structured. Points or linear with IC up to 55 are potential points of important concentration of surface flows on a short distance. Next, we investigate whether these simulations capture what is occurring in reality and whether they should be linked to instances of damage after previous flash flood events on the five studied basins.
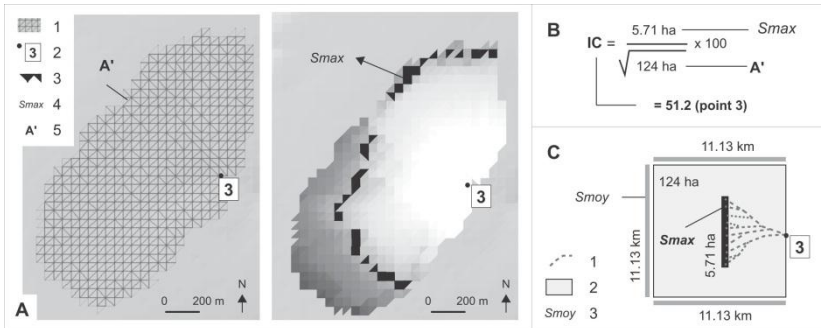


Figure 2: Calculation of the specific Index of Concentration, uniquely on the point 3 here.

## A case study: potentials of concentration in four basins of small size (<25km²)

Maximum surface flow concentrations emerge mapping the index of concentration (IC) in five studied basins. The basin of St-Martin presents high value (IC = 56.3) at point 2 as networks and surfaces are well-organized in upstream (figure 3). Values greatly increase from points 3 to 2 but gradually decrease downstream from point 2: the maximum peak of surfaces never changes while upstream area increases. In the basins of Warnette, the same patterns are observed (high values and compact forms) but the IC index is not so important because areas present a gentle compactness.

In L'Eaunette, the flow concentration suddenly increases in the main channel due to cumulative and constant contributions of the sub-basins into point 2. The basin of Aunette presents internal homothetic behaviour [13] due to several concentrations measured at the outlet of upstream sub-basins. Values decrease between confluences but the flow concentration increases again at points 2 and 3 and at the final outlet. In these basins, the IC index remains high when the peak of surfaces and the average diameter proportionally increase. Concentric organization of surfaces in compact form, regular contributions of sub-basins and self-organized networks explain high values. On the other hand, elongated shapes, spatial shifted contributions of sub-basins and non-hierarchical networks flatten this IC index. This result explains why indexes are unrelated to the basin scale and confirms that a basin area is convenient for investigating the spatial behaviour of a basin in self-similar basins but not in non-self similar areas [22].
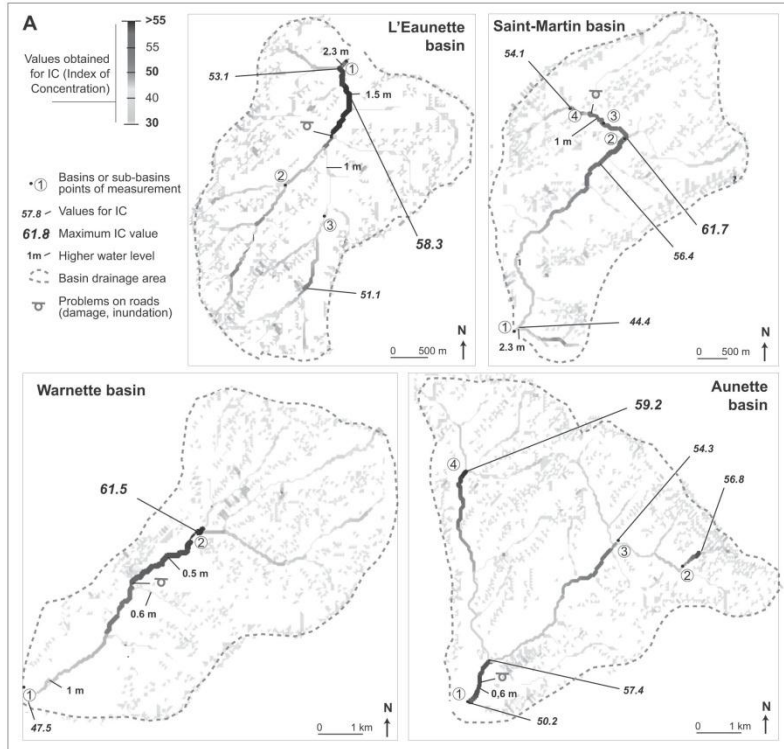
Figure 3: Maps of IC obtained on four studied basins in Northern-France.

## Links with instances of damage observed after flash flood events

Field observations were conducted in the five basins just a few days after flash flood events (figure 4). In the basin of Saint-Martin, high IC matched exactly the sections where most of the damages were registered after the event of June 16th, 1997. The section with IC up to 50 [between points 3 to 2, going upstream to downstream] presented erosions in the road along a distance of 500 m with an average depth ranging from 1 to 2 m. Several cars were dragged resulting in the death of 3 people. In this section, high concentrations induced high level of risk for urbanized areas: the sudden rising peak occurred in less than 15 minutes, taking people outside by surprise. Sediments, stones and roundballers were transported up to the final outlet located 2.1 km full downstream. Extensive financial costs (3 M €) and losses in human life were finally linked in this section to high surface flow concentration which were aggravated by farming upstream areas [11]. Other damage was located at the overall outlet, where urbanization faced to flood. In the basin of L'Eaunette, inundated areas and damage were also

correlated to the simulations. Inhabitants, field measurements and videos confirm that the water levels reached 1 m to 2.3 m in the center of Villers-Plouich, where gravels, sediments (clay, limestones) and straw deposits in several houses exceed 50cm. Collective water networks were saturated in the western part of Gouzeaucourt, but the sudden peak wave appeared clearly along the road D917 from the sub-basin Bois Gaucher just after the confluence identified as the first upstream point with IC up to 55.
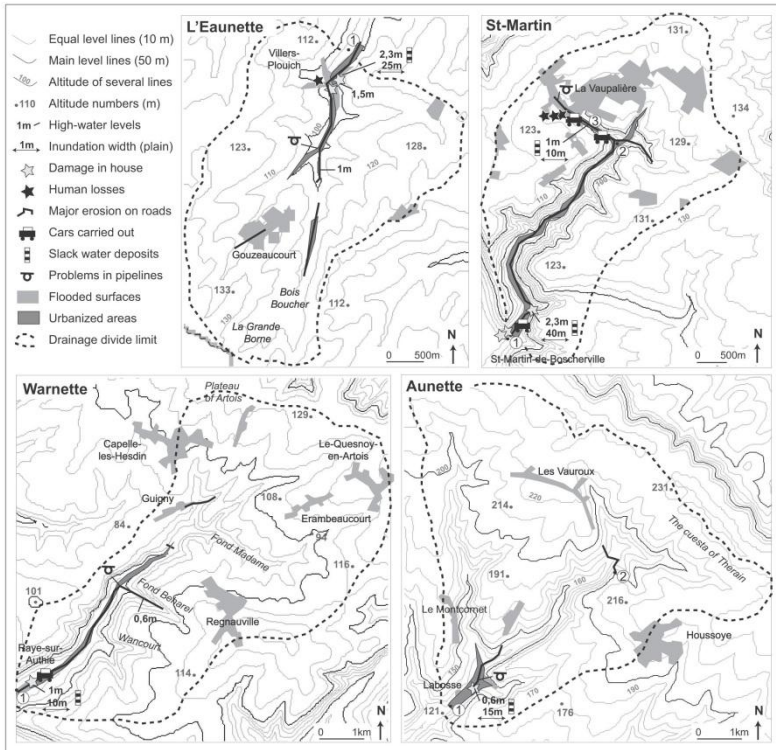


Figure 4: Links with instances of damage on the four studied basins (related to the figure 3).

The water-treatment plant located near the D917 was also affected, resulting in water pollution. Forests downstream tried to reduce the effects of flow accumulation, thus flooding decreased where the river joined the town of Marcoing (located 3.1 km in the north). The other points with high IC on the basin of Aunette sustained less damage. In rare case, as in the basin of L'Eaunette (figure 4), high IC exists in grasslands and in uninhabited areas. As nobody lives near these sites, correlation between simulation and material losses is difficult to evaluate. But in each case study, hydrological problems have been observed due to surface flow concentration, particularly along roads which

enhance flow velocity. Thus mapping the IC values appears to be a good indicator of what is taking place on the ground. Intersecting morphological process, numerical simulations and damage due to flash flood offers promising prospects.

## Discussion

Previous reviews have focused on the effects and impacts of morphological features on hydrological responses over the past forty years [13, 22, 23]. But well-assessing the dynamics and potentials of spatial behaviours remains challenge. Traditionally, the width-function or the distance-area function provided methods to characterise the catchment response as a function of its geomorphologic properties. But these methods present important drawbacks [11]: they describe morphological features in a planar dimension and they never consider the dynamical impacts of topography on surface flow concentration. Some reviews indicated other limitations such as scale dependency [24] or fractal properties which can falsify the results of compactness or circulatory indexes [25]. In this case, with a CA approach, we propose a new metric to account for the interactions between networks, forms and surfaces. Hortonian systems present a regular increase of the spatial behaviour and of the surface flow concentration due to regular contributions from the tributaries. It clearlyconveys internal homothetic behaviours when several high surface concentrations are observed at several outlets. In addition, simulations show original patterns such as a decrease of surface concentration due to non-hierarchical organisation of networks, or various internal efficiencies. Mapping the IC (Index of Concentration) permits to calculate and quantify this concentration in all parts of a given basin. In summary, this study confirms that more than the basin size, the morphological structure and that the spatial organisation of networks determine the distribution of surface flow concentration and the potential accuracy of runoff processes.

## Conclusion

The understanding of flash floods in small and ungauged dry valleys is hampered by a lack of hydrological and geomorphological data. The rareness and violence of such events do not render the measurement of the role played by the topography easy. In this study, we propose to use numerical simulations based on the cellular automaton *RuiCells* as a new metric of measuring dynamics of spatial behaviours across scales.

The Index of Concentration allows measurement and quantification of the dynamic effects of morphological components from local (cellular) to global (outlet) scales on surface-flow concentrations. Morphological systems defined by the relationship between the basin form, network, surface and its distance to the outlet, appear of paramount importance compared to basin size. This information has been suggested theoretically for a long time but this cellular application can confirm such evidence. Some basins such as L'Aunette basin present internal homothetic behaviour but others present local concentration which remains hidden if we stay at the global scale (Saint-

Martin). Using the IC, we detect where the surface flow concentrations can suddenly appear and induce damage on houses and/or roads. Validation with real losses, local knowledge and field measurements in these five study basins gives satisfying results even if damage in some places remain unknown due to the lack of people to confirm such observations. In addition, the strong interaction between land-use cover and topography requires important attention at local scale: high percentage of cultivated areas upstream points of concentrations in the Saint-Martin and L'Eaunette basins explain violent onsets despite these areas representing a small part at the global scale. This work is in progress to identify other basins in which cultivated areas are dominant upstream concentration. This work is being carried out in 60 basins in the Nord-Pas-de-Calais and 180 basins in Seine-Maritime. Our hope is to be able to help risk managers to locate areas with high exposure to flash floods to plan structural measures to reduce such sensibility to violent hazards.

## Acknowledgments

## References

[1]   Borga M., Gaume E., Creutin J.D., Marchi L. (2008), Surveying flash floods: gauging the ungauged extremes. Hydrological processes 22, pp. 3883-3885.

[2]   Gaume E., Bain V., Bernardara P., Newinger O., Barbuc M., Bateman A., Blaskovicova L., Bloschl G., Borga M. Dumitrescu A., Daliakopoulos I, Garcia J., Irismescu A., Kohnova S., Koutroulis A. Marchi L., Matreat S., Medina V., Preciso E., Sempre-Torres D., Strancalie G., Szolgay J., Tsnais I., Velasco D., Viglione A. (2009), A compilation of data on European flash floods. Journal of Hydrology, 367, pp. 70-78.

[3]   Montz B.E., Grunfest R. (2002), Flash flood mitigation: recommendations for research and applications. Environment Hazards, 4, pp. 1-15.

[4]   Balmforth D.J., Dibben P. (2006), A Modelling Tool for Assessing Flood Risk. Water Practice and Technology, IWA Proceedings on Urban Damage, 1, pp. 345-356.

[5]   Schmitz G.H., Cullmann J, (2008), PAI-OFF: a new proposal for online flood forecasting in flash flood prone catchments. Journal of hydrology, 360, pp. 1-14.

[6]   Ortega J.E., Heydt G.G. (2009), Geomorphological and sedimentological analysis of flash floods deposits. The case of the 1997 Rivillas flood (Spain). Geomorphology, 112 (1-2), pp. 1-14.

[7]   Douvinet J., Delahaye D. (2010), Caractéristiques des « crues rapides » du nord de la France (Bassin parisien) et risques associés. Géomorphologie : relief, environnement, processus, 1, pp. 73-90.

[8]   Hazenberg P., Yu N., Boudevillain B., Delrieu G., Uijlenhoet R. (2011), Scaling of raindrop size distributions and classification of radar reflectivity–rain rate relations in intense Mediterranean precipitation. Journal of Hydrology, 402, pp. 179-192.

[9]   Langlois P., Delahaye D. (2002), Ruicells, un automate cellulaire pour la simulation du ruissellement de surface. Revue Internationale de Géomatique, 12, pp. 461-487.

[10] Delahaye D., Guermond Y., Langlois P. (2001), Spatial interaction in the runoff process. Proc. of the 12th European Colloquium on Theoretical and Quantitative Geography, St-Valéry-en-Caux, France, 2001, http://www.cybergeo.eu/index3795.html.

[11] Douvinet J., Delahaye D., Langlois P. (2008), Modélisation de la dynamique potentielle d'un bassin versant et mesure de son efficacité structurelle. Cybergéo, Revue européenne de géographie, 412, 18 p. http://www.cybergeo.revues.org/16103.

[12] Veltri M., Veltri P., Maiolo M. (1996), On the fractal dimension of natural channel network. Journal of Hydrology, 187, pp. 137-144.

[13] Rodriguez-Iturbe I., Rinaldo A. (1997), Fractal river basins, chance and self-organization. Cambridge University Press, Cambridge, 547 p.

[14] Lopez J.J., Gimena F.N., Goni M., Agirre U. (2005) Analysis of a unit hydrograph model based on watershed geomorphology represented as a cascade of reservoirs. Agricultural Water Management, 77, pp. 128-143.

[15] Cudennec C., Gogien F., Bourges J., Duchesne J., Kallel R. (2002), Relative roles of geomorphology and water input distribution in an extreme flood structure. Publication IAHS, 271, pp. 187-192.

[16] Mita D., Catsaros W., Gouranis N. (2001), Runoff cascades, channel network and computation hierarchy determination on a structured semi-irregular triangular grid. Journal of Hydrology, 244, pp. 105-118.

[17] Palacios-Vélez O.L., Gandoy-Bernasconi W., Cuevas-Renaud B. (1998), Geometric analysis of surface runoff and the computation order of unit elements in distributed hydrological models. Journal of hydrology, 211, pp. 266-274.

[18] Vogt J.V., Colombo R., Bertolo F. (2003), Deriving drainage network and catchments boundaries as a new methodology combining digital elevation data and environmental characteristics. Geomorphology, 53, pp. 281-298.

[19] Murray A.B., Paola C. (1994), A cellular model of braided rivers. Nature 371, pp. 54-57

[20] Ménard A., Marceau D.J. (2006), Simulating the impact of forest management scenarios in an agricultural landscape of southern Quebec, Canada, using a geographic cellular automata. Landscape and Urban Planning 16, 99-110.

[21] Tarboton D.G., Bras R.L., Rodriguez-Iturbe I. (1991), On the extraction of channel networks from Digital Elevation Data. Hydrological Processes 5, pp. 81-100.

[22] Mantilla R., Gupta V.K., Mesa O.J. (2006), Role of coupled dynamics and real network structures on Hortonian scaling of peak flows. Journal of Hydrology, 75, pp. 1-13.

[23] Luo W., Harlin J.M. (2003), A Theoretical Travel Time Based on Watershed Hypsometry, Journal of the American Water Resources Association, 39, pp. 785-792.

[24] Bardossy A., Schmidt F. (2002), GIS approach to scale issues of perimeter-based shape indices for drainage basins. Hydrological Sciences, 47, pp. 931-942.

[25] Bendjoudi H., Hubert P. (2002), Le coefficient de compacité de Gravelius : analyse critique d'un indice de forme des bassins versants. Revue des sciences hydrologiques – Hydrological sciences, 47, pp. 921-930.

# Mining cellular automata rules

The use of a Naïve Bayes classifier to provide transition rules in Phragmites simulation

## Anas ALTARTOURI[1]; Ari JOLMA[1]

[1]Department of Civil and Environmental Engineering, School of Engineering, Aalto University
Niemenkatu 73, 15140 LAHTI, Finland
+358505122710, anas.altartouri@aalto.fi

**Keywords:** Cellular automata, environmental modeling, naïve Bayes, Phragmites, spatial data mining

## Abstract

Transition rules form the main and most important component of the cellular automata (CA) as they control to a great extent the model behavior and output. Contributing to the ongoing effort in the literature, we present in this paper a data mining based approach to empirical derivation of CA transition rules. The methodology employs the Naïve Bayes (NB) classification to predict future generations of the automata and an extended spatial representation of the NB nomogram to visualize the classifier and examine intraregional pattern differences. The methodology is implemented using free and open source software and libraries, and is illustrated in the case of modeling dynamics of an invasive species, namely Phragmites australis. The results suggest that the proposed methodology has high potential to provide transition rules and capture intraregional differences of the process modeled. The extended spatial representation of the classifier nomograms gives insight into the classifier and reveals varying patterns of neighborhood influence among subareas within the studied site.

## Introduction

The cellular automata (CA) paradigm has attracted much attention in modeling spatial processes in both natural and urban environments [1, 2]. Its clear definition of space and time, flexibility for relaxations over the original form, and compatibility with the GIS raster format increase its potential and applicability to a number of domains.

Amongst the CA components, the transition rules have a direct and large influence on the model behavior [3]. In the original form of CA, transition rules are deterministic and based on the states of the cell and its strictly defined neighbors. In order to cope with needs of the environmental and urban systems, certain relaxations of this form are needed [2] as purely deterministic models may yield inaccurate results. These relaxations are needed due to (i) randomness, which is inherent in processes in the natural and, to some degree, the urban environments, and (ii) uncertainty, which is embedded in our knowledge of those processes. Also, transition rules are primarily a function of the neighborhood composition, and for

many applications the shape and size of the "influential" neighborhood may vary [3]. Finally, in environmental and urban systems, there usually are a number of external significant variables that need to be incorporated in the transition rules along with the neighborhood composition [4].

CA transition rules control to a great extent the outcomes of the model. Successful modeling depends on the transition rules capturing the essentials of the modeled process [3]. This requires understanding of the causalities and mechanisms of the process in question. While causal relationships between the process and the external factors might be indicated in the literature, the quantification of those relationships is not always available [4]. Especially the composition and configuration of the neighborhood has to be derived empirically.

Methods that have been applied to derivation of CA transition rules include multi criteria analysis [5], principle component analysis [6], genetic algorithm [7], and neural networks [8]. In this paper, we aim to contribute to this effort by examining the potential of a data mining method, namely the Naïve Bayes (NB) classification, for providing CA transition rules. NB is a widely used classification technique due to its simplicity and good performance on a wide range of problems [9]. The classification is based on Bayes Theorem and the assumption that input variables are conditionally independent given the class variable.

We present a CA modeling methodology that is based on data mining elicited rules and test it on a case study of modeling an invasive species. The main characteristics of the developed methodology are the use of NB classification for providing CA transition rules, and the visualization method, based on using a nomogram, to give insight into the classifier and detect intraregional pattern differences. The methodology aims at a generic tool that is applicable in different fields and capable of revealing hidden patterns through the strength of spatial data mining techniques [10]. The methodology is illustrated in the case study. Finally, we discuss the use of free and open source software (FOSS) in the methodology and CA modeling in general.


## The methodology

The methodology employs a NB classifier to mine CA transition rules and predict the next generation of the automata. A simple NB classifier is presented in Figure 1; the probabilities of an object to belong to each of the possible classes are computed by Bayes Theorem given a number of attributes, then the object is assigned to the class with the maximum probability.

The exercise of determining the next generation of CA can be depicted as a NB problem; for each run of the CA, we attempt to predict the state (class) of each cell (instance) in the next time step ($t+1$) given the composition and configuration of its neighbors as well as a number of auxiliary variables, if any. If we let the cell state in the next time step ($S_{t+1}$) be the response or class variable, and the states of its neighbors in the current time step and, if applicable, the auxiliary variables be the independent variables (or attributes), then we can compose a spatiotemporal NB network as shown in Figure 2. In this case, the "class" and "instance" in the data

mining jargon are, respectively, equivalent to the "state" and "cell" in the CA, and they are used interchangeably throughout this paper.
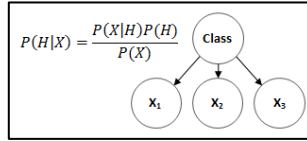


Figure 1: Naïve Bayes classifier, the simplest form of Bayesian networks

The spatiotemporal NB network in Figure 2 is an example of a case where a 5x5 extended Moore neighborhood is adopted. The principle can be applied to any neighborhood size, *i.e.*, 3x3, 7x7, 9x9, etc. It is worth noting that cells within the neighborhood in Figure 2 are labeled to indicate the ring to which they belong. That is, the cell in question is labeled 0, cells adjacent to it (the original eight Moore neighbors) are labeled 100 through 107, cells in the one-step outer ring are denoted 200 through 215, and so forth. This is important for exploring the effect of spatial configuration (or allocation) and we use it later to examine and visualize the influence (weight) of different cells, within the analyzed neighborhood, on predicting the future of the cell in question. This approach allows accounting for the configuration of possible states around the cell in question, rather than merely the composition, in predicting its state in the next generation.

A sample set of instances is needed to build a NB classifier. The quality of the classifier depends on the representativeness of the sample set. As the classifier deals with spatial data, the sample should be spatially stratified, *i.e.* samples should be well spread over the geographic space of the region. The sample should also be stratified with respect to the class variable in order to obtain as good priors as possible for the NB classification. Finally, should auxiliary variables be incorporated, a sample is drawn from their multivariate distribution such that, for each variable, the sample is marginally maximally stratified. Minasny and McBratney [11] introduced a conditional LHS algorithm (cLHS) that samples variables from their multivariate distributions as above mentioned and, in the same time, ensures the occurrence of the value combinations in the real world. Their Matlab code was ported to Octave for this study. The cLHS function receives a table of all instances within the region and returns 10% as a sample.

Classifiers can be visualized using nomograms to provide a summary of the influence of different variables on the classification [12]. Mozina *et al.* [12] introduced a NB nomogram where the variables' domains are measured upon a scale that indicates their contribution to the prediction, with regard to a certain class, as point scores. The prediction is then made by summing the scores and finding the corresponding probability and, thus, class. For the spatial case of this study, we further map the scores of different attributes (states of cells in the neighborhood) back to the neighborhood window. That is, for each cell within the neighborhood window, the method illustrates the effect of that cell being "live" at time *t* on the probability of the cell in question to be "live" at time *t+1*.
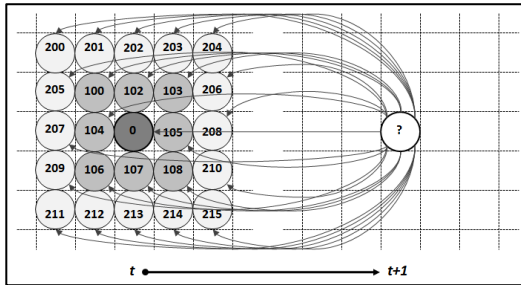
Figure 2: Spatiotemporal NB network; states of cells within the neighborhood window as well as the state of the cell in question in the initial time step form the attributes of the classifier that aims to predict the class of the cell in question in the next time step (*i.e.* assign it to one of the possible states)

## Implementation of the method

The algorithm implementing the methodology is presented in Figure 3. First input grids and parameters are read in and checked. The potential of the NB classification for the problem at hand is tested next. The potential is tested using a 10-fold cross-validation procedure, where data is split into 10 equally sized subsets each of which is used for testing a classifier trained on the remaining subsets. The evaluation result (averaged over the ten runs) is reported to the user, who may choose to halt the execution of the algorithm if low accuracy is reported. A sample is then drawn from the data to build a NB classifier. The algorithm then continues to run the required CA generations.

The model can run in both probabilistic and stochastic modes. In case the probabilistic mode is chosen, the classification is obtained directly from the NB classifier which assigns an instance to the class that maximizes the posterior probability. For the stochastic model, Monte Carlo simulation is run in which the next generation is determined by obtaining the probability of each instance to belong to class "1" (denoting a live cell) from the classifier, drawing a random number, assigning a state according to the drawn number, and moving to the next generation. This is done repeatedly for a number of iterations.

Free and open source software was used in the model development. The model itself was written in Python and Numpy was used for numerical computations. Geospatial Data Abstraction Library (GDAL) and its Python bindings were used for handling input and output of raster grids. Orange Data Mining and Machine Learning Suite was used for the data mining part. Orange provides a range of data mining techniques, including the Naïve Bayes classification and classifier visualization through nomograms [12]. Training samples were obtained by conditional Latin Hypercube Sampling implemented in Matlab [11] and ported to Octave.
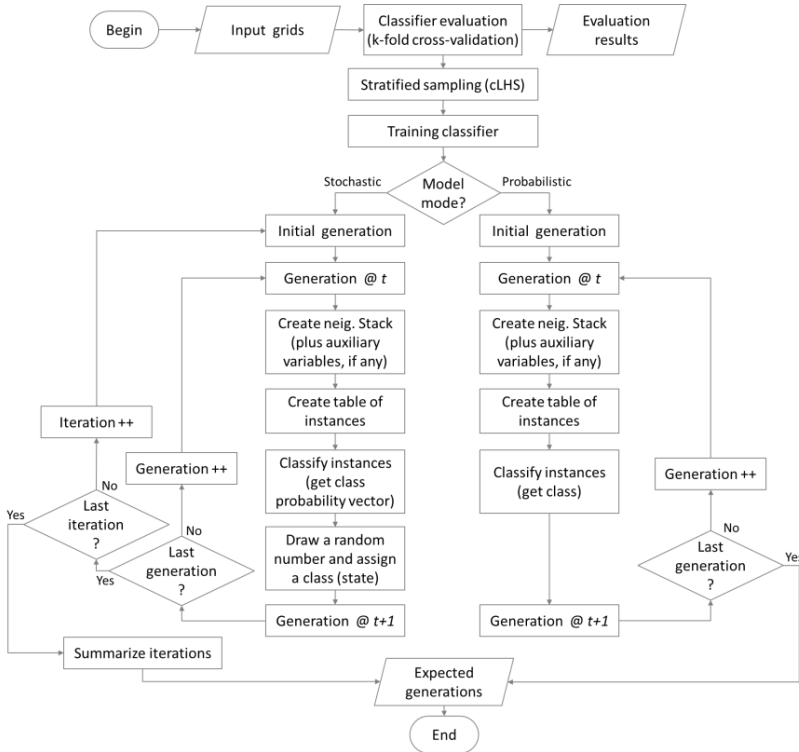
Figure 3: Model flowchart

**Case study and data set**

The developed model is applied on the case of the common reed (*Phragmites australis*) expansion on the Finnish shores. The common reed has taken the Finnish shores in many places in the last decades causing habitat changes, influencing a number of species, and lowering the value of the impacted coastal and archipelago properties [13, 14]. A model capable of predicting future distributions of the reed beds is needed for the planning and management of the area.

Reed coverage maps from Svartbäck (Purola), an approximately 50 km$^2$ site near the outlet of River Kymijoki at Ruotsinpyhtää, were available from years 2003 and 2006 (Figure 4). The area is shallow inner archipelago, with average water depth of 7.5 m. The area represents well the Finnish coast with parts of it influenced by a river and others far away from any river mouths. The openness of the shores within the area varies considerably.

The model spatial resolution was set to 4 m, which is one-third of the mean diameter of the maximum circles inscribed in patches that changed in a three-year-period

(2003-2006). The model was initialized with the coverage of 2003 and run for three generations (years) to predict the cover of 2006. The model was run stochastically for 1000 iterations to simulate the reed dynamics in the study area.

The study area was divided into three subareas (Figure 5) in order to examine the potential of the NB classifier and its nomogram to capture particularities of different subareas. The model was run for the area as a whole using a classifier trained on samples from all parts of it. In order to make comparisons, the model was then run separately for each subarea using a classifier trained on a sample from that area.

Classifiers from the whole area and each subarea were evaluated using 10-fold cross-validation. Model outputs using different classifiers were compared by the accuracy of the predicted reed map of 2006. The accuracy is given by the proportion of cells correctly classified. For our case, the output of the classifier falls within one of four groups as shown in Table 1. Denoting reed-occupied cells by "1" and reed-free cells by "0", the fraction of cells correctly classified as "1" (*i.e. P(Class = 1) >= 50%*) and the fraction of cells correctly classified as "0" (*i.e. P(Class = 1) < 50%*) are, respectively, referred to as the "true positive" and the "true negative" rates. The other two proportions in Table 1 are the error rates referring to cells assigned to one of the classes while observed otherwise.
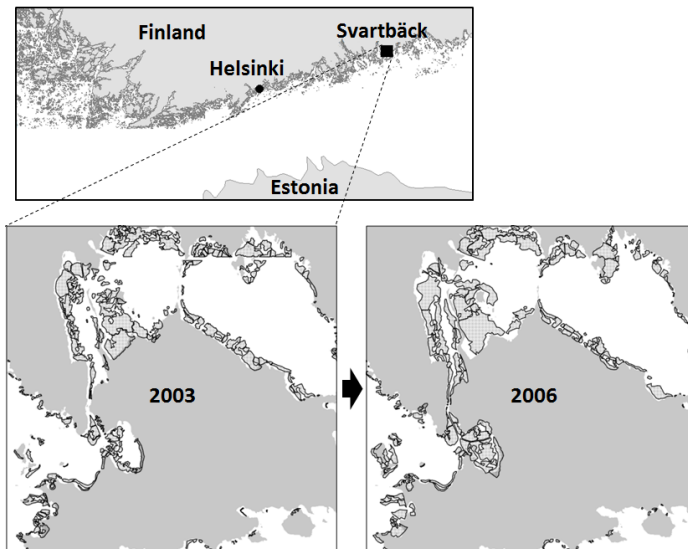


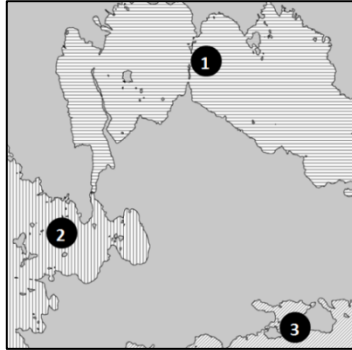Figure 4: Location of study area and its reed coverage in 2003 and 2006

Figure 5: Subareas within the study area for which intraregional pattern differences are examined

## Results

The NB classifiers for different subareas are visualized in Figure 6. Figure 6 (a) shows the nomograms of each classifier. We can observe different patterns of how each attribute influences the probability of the cell in question to be "live" in the next time step. Figure 6 (b) presents the relative importance of the attribute mapped back to its corresponding location in the neighborhood window. The latter figure conveys spatial patterns in the influence. For subarea 1, the influence is as expected, that is, the closer the cell the more influential. In the other subareas the effect is skewed toward the west and north (subarea 2) and the south and east (subarea 3).

Table 2 lists the results of the 10-fold cross-validation for the NB classifiers obtained for different regions (subareas). The table presents the accuracy of each classifier, averaged over the 10 folds. The overall accuracy is above 80%. Classifiers are recording higher accuracies when they are region-specific.

The actual and predicted reed maps of 2006 are shown in Figure 7. The accuracies and errors of the predicted map are presented in Table 1. The accuracy was further investigated for the two possibilities of state change, *i.e.* the accuracy of predicting cells having the state "1" after being "0" (denoted by "0➔1"), and vice versa (denoted by "1➔0"). The model failed to predict any of the "1➔0" cases. For the case of "0➔1" the accuracies are listed in Table 3. It can be noticed that, for subarea 2 and 3, the accuracy is enhanced by applying models with region-specific classifiers.

A stochastic model with 1000 iterations elapsed 9h25m. With a 4 m cell, the raster grid of the area consists of 1407 columns and 1390 rows. The neighborhood window chosen was 9x9. This results in a table of instance with 81 attributes (plus the class attribute) and approximately 2 million instances. The model run time depends greatly on the number of cells within the area and, to a lesser degree, the number of attributes. The model was run under Ubuntu 11.10 OS in a machine with 16 GB RAM and 4 processors at 3.2 GHz each.
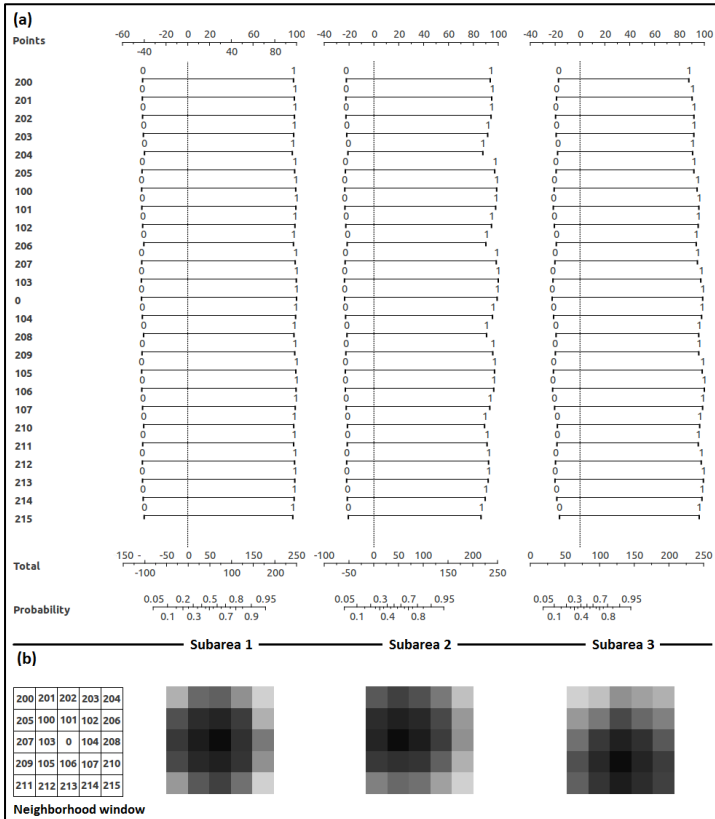
Figure 6: Visualization of classifiers for each subarea; (a) nomograms reflecting the influence of each attribute (cell) on the probability of the class variable (cell state in the next time step) to be classified as "1"; and (b) relative influence of the attributes mapped to their spatial positions in the neighborhood window, with darker cells being more influential

Table 1: Classifier accuracy and error rates

|  | Observed class: "**1**" | Observed class: "**0**" |
|---|---|---|
| Predicted class: "**1**" | True positive **[0.779]** | False positive (error 1) **[0.063]** |
| Predicted class: "**0**" | False negative (error 2) **[0.221]** | True negative **[0.937]** |

Table 2: Average accuracies of classifiers from different geographic areas

| Area | 10-fold cross-validation (averaged) |
|---|---|
| Whole study area | 0.823 |
| Subarea 1 | 0.865 |
| Subarea 2 | 0.871 |
| Subarea 3 | 0.983 |

Table 3: The accuracy of predicting the "0→1" case using generic versus region-specific classifiers for each subarea

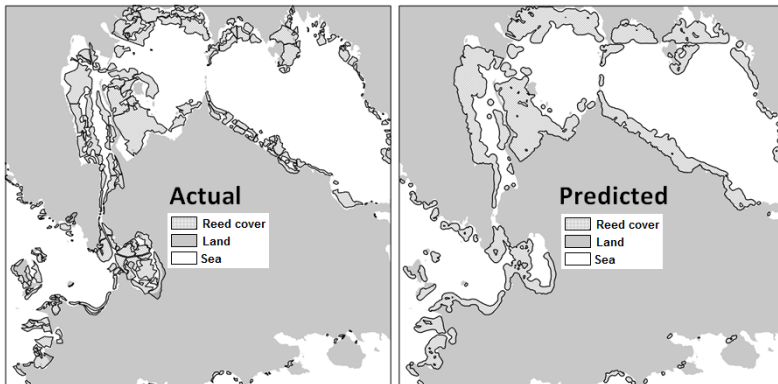| Area | Model applying generic classifier | Model applying site-specific classifier |
|---|---|---|
| Subarea 1 | 0.572 | 0.529 |
| Subarea 2 | 0.459 | 0.528 |
| Subarea 3 | 0.392 | 0.454 |



Figure 7: Actual versus predicted reed coverage of 2006

## Discussion

The method shows high potential of detecting intraregional differences within the study area. The nomograms and their extended spatial representation reveal hidden patterns of the process manifestation in different locations. This can enhance our knowledge of the phenomenon in question. For our case, the unexpected patterns of neighborhood influence in subarea 2 and 3 might be due to region-specific currents, sources of nutrients, or other external factors. With further investigation, the causes can be verified and incorporated in the model to enhance its predictability. Adopting locally trained classifiers yielded higher model accuracy as listed in Table 3. The presented method can help overcome the concern of a single set of rules for large areas [4] by capturing intraregional pattern differences and adopting region-specific rules. The method exploits the available data maximally by analyzing not only the

effect of the composition (quantity) of various categories within the neighborhood, but also the effect of their configuration (allocation).

While the overall accuracy of the NB classifiers and the CA model is good, the ability of the model to precisely predict the state change cases, namely "0→1" and "1→0", is still low. For the case of "0→1", the prediction capability of the model, which was initially low, was enhanced by adopting region-specific classifiers for subareas 2 and 3. This is due to the particularities of those sites revealed by the nomogram and the extended spatial representation of the neighborhood influence (Figure 6). For region 1, however, the predictability of the generic classifier was higher. This might be due to the large area of region 1 which accounts for 70% of the whole study area. Although specific for their own regions, instances from region 2 and 3 are generally in line with those from region 1, and therefore incorporating them in building the classifier increases the training sample size and, consequently, enhances the classifier's performance.

The model failed to detect the "1→0" case altogether. The reason can be the fact that the expansion of reeds, rather than disappearance, was the dominant trend between 2003 and 2006, accounting for two-thirds of the state change cases. This can be solved by training separate classifiers for the expansion (*i.e.* "0→1") and disappearance (*i.e.* "1→0") cases. Another cause can be that the disappearance of reeds is mainly occurring next to the shoreline and is probably due to manual removal. While the CA neighborhood effect reflects on the reed expansion mechanism (which proliferate mainly by rhizomes), it cannot predict results of human intervention such as the manual removal.

The performance of the model can be considerably enhanced by incorporating auxiliary variables, explanatory to the phenomenon, in the classifier or in posterior steps. For the case of reed expansion, those might include the water depth, the sediment type, the nutrient load, and the relative sea openness. The neighborhood influence in many spatial processes, although highly influential, cannot solely explain the process. However, auxiliary variables were not incorporated since the purpose of this work was to examine the potential of data mining techniques to provide CA transition rules, with no emphases on the case study. From this perspective, having reached accuracy over 50% by analyzing merely two maps of reed coverage from different years suggests that the proposed methodology is capable of capturing patterns of the process modeled and providing CA rules that are, when necessary, region-specific.

Both probabilistic and stochastic modes are implemented in the algorithm. The NB classifier is acknowledged for its high performance in predicting the class of an instance [15, 16]. Running the model in a probabilistic mode, thus, exploits the strong feature of the NB classifier, while running a stochastic model allows indicating the uncertainty of the prediction by the probability distributions from different iterations.

Running a stochastic model with 1000 iterations elapsed about 10 hours. A probabilistic model elapses less than 10 minutes. Taking into account the heavy computational load, the model execution is rather fast. For each iteration, arrays of cells' and their neighbors' states are stacked. The number of arrays stacked grows exponentially as the neighborhood size grows; choosing a 9x9 neighborhood

window, for instance, results in a stack of 81 arrays. These arrays are then transposed and flattened to obtain a table of instances readable by the classifier. The effective masking and indexing functions of Numpy help optimizing the model by keeping track of unmasked cells, often faced when modeling natural and urban processes. This makes it possible to avoid classifying irrelevant instances and, in the same time, maintain the spatial position of instances, thus increasing the model efficiency.

The use of FOSS and libraries allows the code modification and reuse by other researchers for other applications. The ability to set different sizes of cells and neighborhood windows and the ability to incorporate any number or combination of variables gives flexibility to the model. Combined with the algorithm efficiency, this helps initializing multiple models with different settings and variables for the purpose of finding the appropriate choice of parameters for the process being modeled.

Further elaboration on a number of aspects would enhance the methodology and the algorithm. This includes testing the methodology for multi categorical applications, building classifiers for each transition case, adding posterior refinement steps (application dependent), and implementing automatic detection and handling of intraregional differences in the process patterns.

## Acknowledgments

## References

[1]    Molofsky, J. & Bever, J. (2004), A new kind of ecology? Bioscience, 54(5), pp. 440-446.

[2]    Pinto, N. & Antunes, A. (2007), Cellular automata and urban studies: A literature survey. Architecture, City, and Environment 1(3), pp. 368-399

[3]    White, R., & Engelen, G. (2000), High-resolution integrated modeling of the spatial dynamics of urban and regional systems. Computers, Environment and Urban Systems, 24, pp. 383-400

[4]    Geertman, S., Hagoort, M., & Ottens, H. (2007), Spatial–temporal specific neighbourhood rules for cellular automata land-use modeling. International Journal of Geographical Information Science, 21 (5), pp. 547-568

[5]    Wu, F., & Webster, C. J. (1998), Simulation of land development through the integration of cellular automata and multicriteria evaluation. Environment and Planning B-Planning and Design, 25, pp. 103-126

[6]    Li, X., & Yeh, A. G. O. (2002), Urban simulation using principal components analysis and cellular automata for land-use planning. Photogrammetric Engineering and Remote Sensing, 68, pp. 341-351

[7]    Jenerette, G. D., & Wu, J. (2001), Analysis and simulation of land-use change in the central Arizona–Phoenix region, USA. Landscape Ecology, 16, pp. 611-626

[8]   Yeh, A. G. O., & Li, X. (2003), Simulation of development alternatives using neural networks, cellular automata, and GIS for urban planning. Photogrammetric Engineering and Remote Sensing, 69, pp. 1043-1052.

[9]   Kuncheva, L. I. (2006), On the optimality of Naïve Bayes with dependent binary features. Pattern Recognition Letters, 27(7), pp. 830-837

[10]  Guo, D. & Mennis, J. (2009), Spatial data mining and geographic knowledge discovery - An introduction. Computers, Environment and Urban Systems, 33, pp. 403-408.

[11]  Minasny, B., & McBratney, A. B. (2006), A conditioned Latin hypercube method for sampling in the presence of ancillary information. Computers and Geosciences, 32 (9), pp. 1378-1388

[12]  Možina, M., Demšar, J., Kattan, M.K. & Zupan, B. (2004), Nomograms for Visualization of Naive Bayesian Classifier. In: European Conference on Principles and Practice of Knowledge Discovery in Databases (PKDD), September 20-24, 2004, Pisa. Available at: http://eprints.fri.uni-lj.si/154/1/PKDD_camera_mozina.pdf

[13]  Ikonen, I., & Hagelberg, E. (eds.) (2007), Read Up on Reed! End report of the Reed Strategy -project (Interreg IIIA –programme). Southwest Finland Regional Environment Centre

[14]  Able, K., & Hagan, S. (2003), Impact of Common Reed, Phragmites australis, on Essential Fish Habitat: Influence on Reproduction, Embryological Development, and Larval Abundance of Mummichog (Fundulus heteroclitus). Estuaries, 26(1), pp. 40-50.

[15]  Larsen, K. (2005), Generalized naive Bayes classifiers. SIGKDD Explorations Newlsetter, 7, pp. 76-81

[16]  Youn, E. and Jeong, M.K. (2009), Class dependent feature scaling method using naive Bayes classifier for text datamining. Pattern Recognition Letters, 30(5), pp. 477-485

# The definition of functional urban regions

Validation of a set of spatial models with recent census data and analysis of an additional model specification

## Rodrigo AJAUSKAS[1]; Gustavo Garcia MANZATO[2]; Antônio Nélson RODRIGUES DA SILVA[3]

### UNIVERSITY OF SÃO PAULO

São Carlos School of Engineering, Department of Transportation Engineering Av. Trabalhador São-carlense 400, CEP 13560-590, São Carlos, SP, Brazil Phone: +55 16 3373 9595
[1] E-mail: rodrigo_ajauskas@hotmail.com
[2] E-mail: gusmanzato@gmail.com
[3] E-mail: anelson@sc.usp.br (corresponding author)

## Abstract

This paper has two objectives. The first one is to examine the performance of a set of spatial models built to define functional urban regions. More specifically, the models are tested using recent census data. In the second objective, an extension of the modeling approach is tested. Instead of predicting density values to later classify them in quadrants of the Moran's scatterplot, the new models directly predict the quadrants. This new approach seems to perform better. In summary, the findings obtained with this study suggest or even confirm the value of spatial analysis techniques as a promising approach to define and monitor FURs. This comes along especially as an alternative approach where more specific data is not available, but usually easily accessible census data may be used for that end.

## Introduction

Large urbanized areas formed by several municipalities bring particular challenges to urban managers and planners. On the one hand, the administrative limits of those conurbations go well beyond the limits of the individual cities that form them. On the other hand, they are often not large enough to match the boundaries of the superior administrative subdivisions, i.e., states or provinces. Therefore, one of the alternatives to deal with that administrative problem is the definition of the so-called Metropolitan Regions (MRs), or Functional Urban Regions (FURs). Several methods have been developed to define FURs. But given the inherent complexity of the concept, it is not always an easy task (for a recent literature review on this topic, see [1] and [2]).
In short, one of the methods for defining FURs is based on commuting flows between regions, as observed in Europe [3] and in the United States [4]. Some authors, however, argue that the commuting intensity itself is not able to show the

degree of economic integration between a metropolitan center and its hinterland (e.g., [5] to [9]).

The lack of proper data is an issue regarding the application of commuting flows-based methods. Some alternative approaches have been presented for proxying commuting data, as suggested by Coombes [10], but they still rely on data that are usually unavailable in developing countries, such as the distribution of jobs. However, the author also lists feasible alternatives, such as using roads or service networks like bus services as a proxy for data on actual patterns of interaction.

In any case, these approaches may still not be viable regarding the need for specific data. Therefore, the authors of the Office of Management and Budget [11] defended another alternative for defining metropolitan areas based on population density values, since it is expected to be available in most census datasets. The authors stated that "residential population density can serve as a surrogate for other measures of activity in the absence of nationally consistent and reliable datasets describing all daily and weekly movements of individuals".

The use of population density for defining FURs can be analyzed in many different ways, though. This was shown by Ramos and Rodrigues da Silva [12] and [13], Ramos *et al.* [14] and Manzato *et al.* [15], who have explored the use of the attribute with spatial analyses tools, such as spatial statistics and spatial modeling. More specifically, the spatial statistics concepts used Exploratory Spatial Data Analysis (ESDA) techniques [16], and the spatial modeling was based on principles of Cellular Automata - CA (e.g., [17] to [22]). Also, Pereira and Rodrigues da Silva [23] investigated another technique based on cluster analysis.

While those applications of spatial analyses using population density led to interesting and promising results for the definition of FURs, Manzato and Rodrigues da Silva [1] extended the approach with the inclusion of an infrastructure supply index. Their assumption claimed that in the absence of traffic flow data as one of the possible methods to define FURs, a proxy measure that quantifies the level of transportation infrastructure supply might relatively well replicate the actual traffic flows. Thus, the definition of FURs could eventually rely on the level of transportation infrastructure supply or, alternatively, on indexes that represent the supply level in each municipality. The findings obtained by these authors and later on by Rodrigues da Silva *et al.* [2] suggested that the use of a transportation infrastructure supply index combined with population density within a spatial analysis-based approach is a promising alternative to define FURs.

Given the above, the objective of this study is twofold. First, with the recent availability of the demographic census carried out in 2010, we tested the models developed by Manzato and Rodrigues da Silva [1] in the sense of validating them with new data. Second, we also explore an extension of their models, considering a simpler model specification. It consists of using essentially the same model structures proposed before by these authors, but taking into account as model attributes only the quadrants of the Moran's scatterplot obtained for both population density and the index of infrastructure supply.

This paper is structured as follows. Next section presents the methodology proposed, followed by the results obtained. At the end, some concluding remarks are drawn and the bibliographic references are listed.

## Methodology

The present study followed the methodology proposed by Manzato and Rodrigues da Silva [1]. They built spatial models to define FURs using ESDA techniques along with principles of CA. In the case of ESDA, zones are classified regarding a given attribute value in relation to the overall average value and also in relation to the average value of the adjacent zones. The results, which can be represented in four quadrants of the Moran's scatterplot and also in maps (the so-called *Box Maps*), can be classified as follows:

1. High-High (HH): in that quadrant are represented the zones with positive value for the zone and positive average value for contiguous neighbors. Positive values are always above the overall average value.
2. Low-Low (LL): in that quadrant are represented the zones with negative value for the zone and negative average value for contiguous neighbors. Negative values are always below the overall average value.
3. Low-High (LH): in that quadrant are represented the zones with negative value for the zone and positive average value for contiguous neighbors.
4. High-Low (HL): in that quadrant are represented the zones with positive value for the zone and negative average value for contiguous neighbors.

Two basic attributes were used: population density and an index of infrastructure supply, as shown in Equation 1. This index refers to an area under the influence of a particular transportation system (in this case, the highway network) and it is composed by weighted buffers around that system.

$$IC_x = \frac{\sum_1^n \gamma(i) A_i}{A_x}$$

(1)

where:

$IC_x$     index of infrastructure supply coverage for zone $x$

$\gamma(i)$     function that determines the weight of each buffer, such as $\gamma(i) \in [0,1]$

$A_i$     area of each buffer comprised in a zone $x$

$A_x$     area of zone $x$

$n$     number of buffers.

Zone $x$ mentioned here is related to the municipality's official administrative boundaries, which comprise our units of observation and where such attributes were calculated at. The quadrants of Moran's scatterplot were also obtained for both population density ($PD_x$) and the index of infrastructure supply ($IC_x$), respectively referred to as $QPD_x$ and $QIC_x$. Along with these four attributes, given this CA-based spatial modeling approach, additional attributes were included. They comprised the average value of the population density in adjacent municipalities ($PD_j$) and the

number of adjacent municipalities in each quadrant of the Moran's scatterplot obtained for $PD_x$ (e.g., $nHH_{x,PD}$, $nLL_{x,PD}$, $nLH_{x,PD}$, and $nHL_{x,PD}$). We have adopted a binary measure of adjacency (neighbor / not neighbor). In sum, nine attributes are defined for such spatial models.

Following Manzato and Rodrigues da Silva [1], two basic model structures were applied. The first is called "3 IN 1 OUT", where input data reflect three periods of time, apart "$x$" years from one another, and the output data is one time-step later. For example, if the output data is "$t$", and "$x$" is equal to ten years, the input data must be "$t - 30$", "$t - 20$" and "$t - 10$" years. The second model structure is called "T, T + 10". Although it apparently has only one period of time for the input data and another one for the output, this structure was constructed in such a way that the information about two or more periods of time is also considered in the model. The data from distinct periods of time are placed on the top of each other, as if they were in the same column of a spreadsheet. Thus, if the first model structure has "$w$" entries (or municipalities, in our case), the second model structure has "3 x $w$" entries. In other words, the second kind of model has more cases in the dataset. On the other hand, it ignores long-term effects that can only be captured if the same entry is seen in several time steps at once, as it is the case of the first structure. Figure 1 exemplifies the model structures described above.
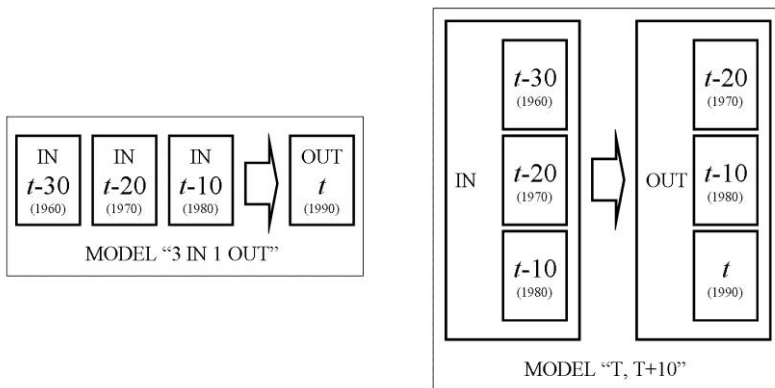


Figure 1: Overview of the proposed model structures

Considering both model structures along with the attributes defined, Manzato and Rodrigues da Silva [1] built a set of four models divided into two groups. We can observe that population density is the basic element among the several attributes used to represent land-use. Therefore, a first group of models only took into account these attributes. Table 1 specifies the model structure and the attributes included in this group. As the interest was also in the influence of the transport infrastructure supply on such modeling phenomenon, a second group of models included the index of infrastructure supply ($IC_x$), as a way to capture some effects of the transportation-land use relationship on the occupation of the territory along time. The index was not, however, included using the respective values across the years analyzed.

Instead, a variation across time steps was considered. For example, in the model structure "3 IN 1 OUT", a difference between periods "$t - 10$" and "$t - 30$" was calculated. For the model structure "T, T + 10" on the other hand, the difference regarded two consecutive years across the respective pairs of periods analyzed. In any case, that variation of the index was normalized between 0.1 and 0.9 to avoid null or extremely high values, what could produce some inconsistencies during the simulations. A summary of the proposed models, with the distinct structures and attributes, is presented in Table 1.

Table 1: Structures and variables used in the distinct models proposed

| Model | Structure | Basic attributes | Input attributes | Output attribute |
|-------|-----------|------------------|------------------|------------------|
| 1 | 3 IN 1 OUT | Population density | $PD_x$; $QPD_x$; $PD_j$; $nHH_{x,PD}$; $nLL_{x,PD}$; $nLH_{x,PD}$; $nHL_{x,PD}$ | $PD_x$ |
| 2 | T, T+10 | | | |
| 3 | 3 IN 1 OUT | Population density + Infrastructure supply | $PD_x$; $QPD_x$; $PD_j$; $nHH_{x,PD}$; $nLL_{x,PD}$; $nLH_{x,PD}$; $nHL_{x,PD}$; $IC_x$ | $PD_x$ |
| 4 | T, T+10 | | | |

The data used to calculate those attributes were obtained essentially from two sources: the demographic censuses carried out by the Brazilian Institute of Geography and Statistics, and the State Highway Department. The former provided initially the population data in the years 1960, 1970, 1980, 1991 (here considered as 1990), and 2000. This same source also provided a vector geographic database with the municipalities' boundaries. The latter provided maps of the state highway network for the years 1960, 1970, 1980, 1990, and 2000.

Given the data available when Manzato and Rodrigues da Silva [1] carried out their study, the spatial modeling process comprised three phases: calibration, validation and forecasting. First, in the calibration phase, they used the 1960, 1970, 1980, and 1990 datasets. In doing so, they obtained the weights and the mathematical functions of the artificial neural networks used to compose the spatial models. In the second phase, they applied the 1970, 1980, 1990, and 2000 datasets for the validation of these models, comparing the predicted results with the real values. These two phases are essential in the modeling process. It is also important to pay attention to the periods taken into account in both phases, as the year 2000 is not considered in the calibration phase because it will be used in the validation phase to test the models. Conversely, producing estimates for periods before the year 1990 would not produce significant results, because such periods were used as outputs for calibrating the models.

The results of the third phase, when the authors forecasted values for a future time step, are of specific interest in this study. In that stage, Manzato and Rodrigues da Silva [1] extended their analyses for estimating values for the year 2010, using the 1980, 1990, and 2000 datasets as input data. Recently, the results of the 2010 demographic census became available [24]. Therefore, using essentially the same models developed before, the estimates of the forecasting phase for 2010 could now be tested with the observed data for the same year. This allowed another evaluation of the set of models proposed.

Notwithstanding this model validation, an extension in the set of models was also tested. These additional models follow the same structures described before (i.e., "3 IN 1 OUT" and "T, T + 10"), but the difference regards the attributes considered as inputs and the output. More specifically, these models are built only using the quadrants of the Moran's scatterplot obtained for both population density and the index of infrastructure supply as inputs, e.g., respectively, $QPD_x$ and $QIC_x$. The output is the quadrants of the Moran's scatterplot for population density ($QPD_x$). Table 2 summarizes the specification of these additional models.

Table 2: Specification of the additional models proposed

| Model | Structure | Basic attribute | Input attributes | Output attribute |
|-------|-----------|-----------------|------------------|------------------|
| 5 | 3 IN 1 OUT | QUADRANTS Population density + Infrastructure supply | $QPD_x; QIC_x$ | $QPD_x$ |
| 6 | T, T+10 | | | |

## Results

The results of models 1 to 6 are presented in Table 3, which shows the partial and total percentages of correct quadrant estimations. This measure is given by the comparison of the observed values in 2010 with the values estimated by the models in the same year. It is important to emphasize that models 1 to 4 estimate population densities and models 5 and 6 directly estimate the quadrants. Therefore, the population densities estimated with models 1 to 4 were subsequently classified in quadrants so that the results became comparable.

Considering models 1 and 2, which have earlier population density values as the basic input attribute, the performance of model 2 appears to be better than model 1. This can be observed by the total percentage of correct quadrant estimations, which is equal to 93 %. The partial results are also higher for model 2, except in quadrant LH. However, given the significant difference in quadrants LL and HL, and in the totals, model 2 performs better.

Analyzing models 3 and 4, which include the index of transportation infrastructure supply, their performances seem to be better than models 1 and 2. The additional attribute indeed contributes to the improvement of the models and this is in line with the original findings obtained by Manzato and Rodrigues da Silva [1]. In a direct comparison of models 3 and 4, although the totals are the same, model 4 has a higher percentage of partial correct estimations in quadrants HH, LH and HL. Therefore, this model seems to be better than model 3.

Looking at the results for models 5 and 6, which are the additional models proposed here, their performances were even better than the previous models. This is especially the case of model 6, which results in the highest percentages of correct quadrant estimations.

Despite the above, it is important to evaluate these findings in terms of the distribution of the errors produced by such model estimations. To this end, we selected the models that performed better within their specifications. That is, the best models between 1 and 2, 3 and 4, and 5 and 6, respectively. From the above, models

2, 4, and 6 had the best performances. Noticeably, they all follow a "T, T + 10" structure.

Considering the models that estimate population density (i.e., models 2 and 4), Map 1 shows the representation of the population density over the territory for observed and estimated values. It is important to emphasize that Map 1 presents the actual values of population density (both observed and estimated) and not the quadrants. Model 2 is able to provide good estimates within the official metropolitan regions (shown by the areas delimited by a white line), but produces errors outside those regions. On the other hand, model 4 provides good estimates outside the official metropolitan regions, but does not perform well within those regions.

Table 3: Partial and total results of the percentages of
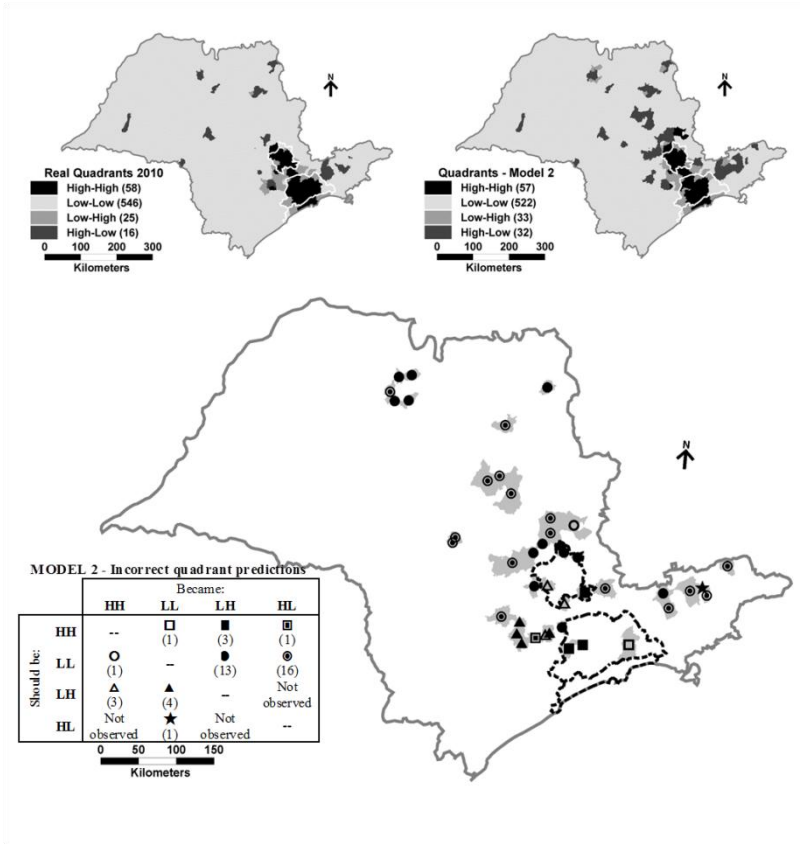correct quadrant estimations in 2010 for models 1 to 6

| Model | HH | LL | LH | HL | Total |
|-------|------|------|------|------|-------|
| 1 | 91 % | 86 % | 88 % | 75% | 87 % |
| 2 | 91 % | 95 % | 71 % | 94 % | 93 % |
| 3 | 85 % | 99 % | 71 % | 69 % | 96 % |
| 4 | 91 % | 97 % | 92 % | 75 % | 96 % |
| 5 | 90 % | 99 % | 79 % | 88 % | 97 % |
| 6 | 91 % | 99 % | 96 % | 88 % | 98 % |

Also, the results of these models can be represented in terms of the quadrants, as shown in Maps 2 and 3. A visual and direct comparison can be made by looking at the two smaller figures on the top of Maps 2 and 3. However, most importantly, we are interested in the distribution of the errors. To this end, we classified the municipalities whose resulting quadrants obtained from the estimated population density deviated from the quadrants obtained from the observed population density values. The legends elaborated for Maps 2, 3 and 4 show the observed occurrences "should be" in contrast with what the estimated occurrences "became". When we analyze the distribution of such occurrences over the territory, it became evident that model 4 produces fewer errors in comparison to model 2.

Finally, Map 4 presents the distribution of the errors produced by model 6. It was argued before that the results of this model were the best, given by the comparison of the percentages of correct quadrant estimations. When looking at the distribution of the errors over the territory, this model produces even fewer incorrect estimates in comparison to both models 2 and 4.
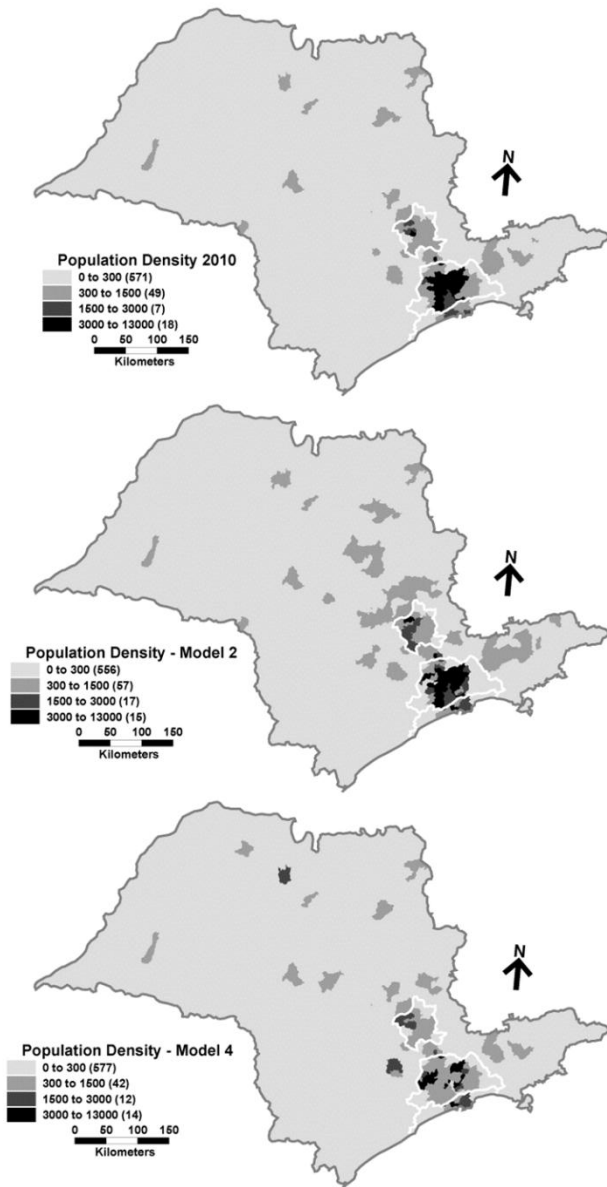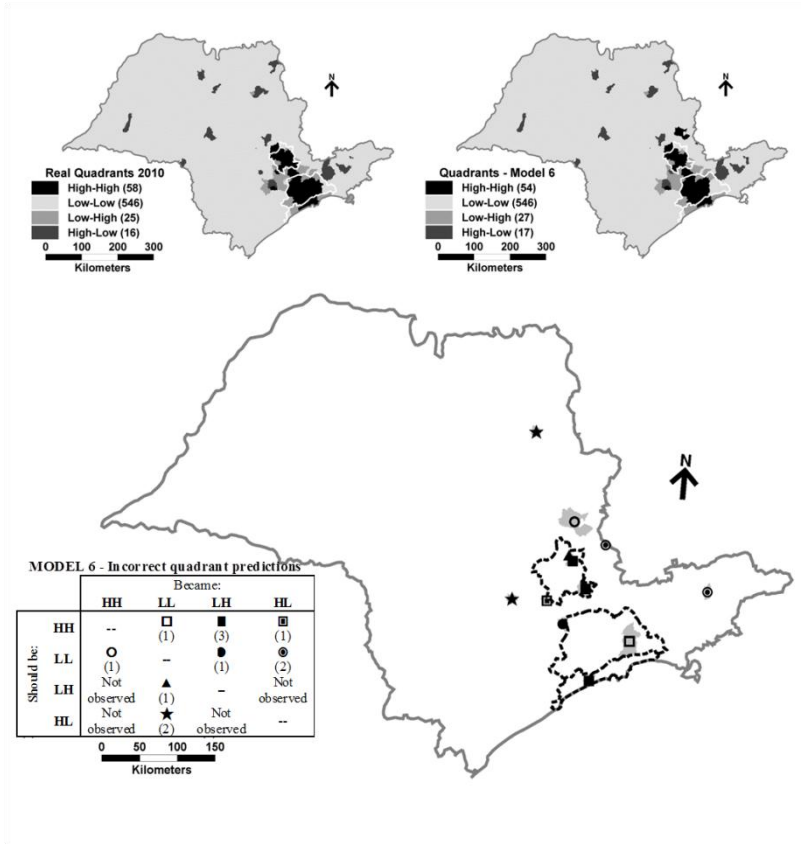
Map 1: Observed and estimated values of population density in 2010

Map 2: Quadrants of observed and estimated values of population density in 2010 and distribution of incorrect quadrant predictions resulting from the application of model 2
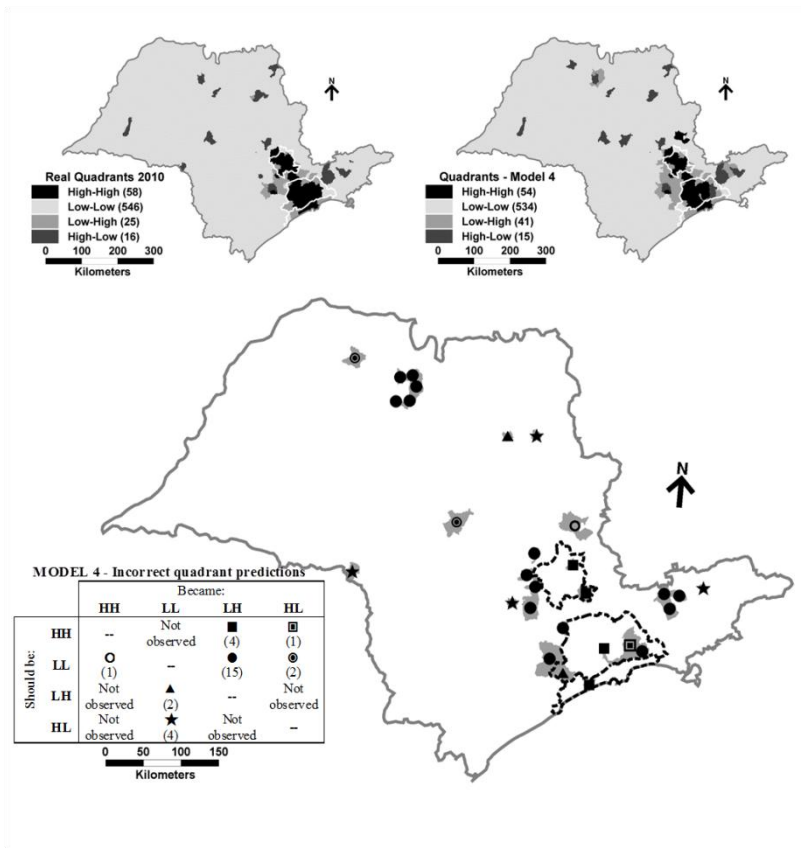
Map 3: Quadrants of observed and estimated values of population density in 2010 and distribution of incorrect quadrant predictions resulting from the application of model 4

Map 4: Quadrants of observed and estimated values of population density in 2010 and distribution of incorrect quadrant predictions resulting from the application of model 6

## Conclusions

This paper had two objectives. The first one was to examine the performance of a set of spatial models built to define functional urban regions. More specifically, the models developed by Manzato and Rodrigues da Silva [1] were tested using recent census data. In the second objective, an extension of the modeling approach was tested. Instead of predicting density values to later classify them in quadrants of the Moran's scatterplot, the new models directly predict the quadrants. The main findings of this study are summarized hereafter.

First, considering a model structure where the population density is estimated, the analysis suggests that models 2 and 4 have the best performances, although they provide different results. Model 2 has similar density distributions when compared

to the actual data (i.e., in 2010) in the official metropolitan regions. However, outside those regions, several density values are not correctly classified using model 2. On the other hand, the predictions of model 4 are not good within and close to the official metropolitan regions, but the model performs better than model 2 in the rest of the state.

Second, when looking at the results provided by the original models in terms of quadrants of the Moran's scatterplot, the performances of models 2 and 4 are significantly improved (Maps 2 and 3). In this particular case, model 4 performs better than model 2. In both cases, however, most incorrect predictions are located around the official metropolitan regions.

Finally, when analyzing the performance of the additional models that were based only on the quadrants of the Moran's scatterplot, the findings suggest that these models (5 and 6) perform better than the previous ones (models 1 to 4). This was shown in the example of model 6 (see Map 4 and Table 3). While model 4 provides correct estimates for 96 % of the cases (municipalities), model 6 predicts 98 % of the total number of cases as correct. In addition, model 6 provides much more uniform predictions within the quadrants. Remarkably, all those advantages come along with a simpler model structure.

In summary, the findings obtained with this study suggest or even may confirm the value of spatial analysis techniques as a promising approach to define and monitor FURs. This comes along especially as an alternative approach where more specific data is not available, but usually easily accessible census data may be used for that end.

## Acknowledgments

## References

[1]   Manzato, G. G., A. N. Rodrigues da Silva (2010), Spatial-temporal combination of variables for monitoring changes in metropolitan areas. Applied Spatial Analysis and Policy, 3(1), pp. 25-44
[2]   Rodrigues da Silva, A. N., H. T. S. Pereira, G. G. Manzato (2011), Spatial analysis methods and variables applied for the definition of Functional Urban Regions - A comparative study in Brazil. In Proceedings of the 12th International Conference on Computers in Urban Planning and Urban Management, Lake Louise, Canada
[3]   Cheshire, P. C., D. G. Hay (1989), Urban Problems in Western Europe: an Economic Analysis, Unwin Hyman, London
[4]   Office of Management and Budget (2000), Standards for defining metropolitan and micropolitan statistical areas, Federal Register, 65(249), December 27
[5]   Coombes, P. P., H. G. Overman (2004), The spatial distribution of economic activities in the European Union. In J. V. Henderson, J. F. Thisse (Eds.), Handbook of Urban and

Regional Economics, 4, Cities and Geography, North Holland, Amsterdam, pp. 2845-2909

[6]   Duranton, G., D. Puga (2004), Micro-foundations of agglomeration economies. In J. V. Henderson, J. F. Thisse (Eds.), Handbook of Urban and Regional Economics, 4, Cities and Geography, North Holland, Amsterdam, pp. 2063-2117

[7]   Rosenthal, S. S., W. C. Strange (2004), Evidence on the nature and sources of agglomeration economies. In J. V. Henderson, J. F. Thisse (Eds.), Handbook of Urban and Regional Economics, 4, Cities and Geography, North Holland, Amsterdam, pp. 2119-2171

[8]   Duranton, G. (2006), Human capital externalities in cities: identification and policy issues. In R. J. Arnott, D. P. McMillen (Eds.), A Companion to Urban Economics, pp. 24-39, Blackwell, Oxford

[9]   Bode, E. (2008), Delineating metropolitan areas using land prices. Journal of Regional Science, 48(1), pp. 131-163

[10]  Coombes, M. (2004), Multiple dimensions of settlement systems: coping with complexity. In T. Champion, G. Hugo (Eds.), New Forms of Urbanization: Beyond the Urban-Rural Dichotomy, pp. 307-324, Ashgate, Aldershot, UK

[11]  Office of Management and Budget (1998), Alternative approaches to defining metropolitan and non-metropolitan areas, Federal Register, 63(244), December 21

[12]  Ramos, R. A. R., A. N. Rodrigues da Silva (2003), A data-driven approach for the definition of metropolitan regions. In Proceedings of the 8th International Conference on Computers in Urban Planning and Urban Management, Sendai, Japan

[13]  Ramos, R. A. R., A. N. Rodrigues da Silva (2007), A spatial analysis approach for the definition of metropolitan regions - the case of Portugal, Environment and Planning B: Planning and Design, 34(1), pp. 171-185

[14]  Ramos, R. A. R., A. N. Rodrigues da Silva, V. P. Miranda (2004), A comparison of two methods for the definition of regional metropolitan areas through an application in the north of Portugal. In Proceedings of the 44th European Congress of the European Regional Science Association, Porto, Portugal

[15]  Manzato, G. G., I. Baria, A. N. Rodrigues da Silva (2007), A GIS-based comparison of methodologies for the definition of metropolitan areas in a developing country. In Proceedings of the 10th International Conference on Computers in Urban Planning and Urban Management, Iguassu Falls, Brazil

[16]  Anselin, L. (1995), Local indicators of spatial association - LISA. Geographical Analysis, 27(2), pp. 93-115

[17]  White, R., G. Engelen (1993), Cellular automata and fractal urban form: a cellular modelling approach to the evolution of urban land-use patterns. Environment and Planning A, 25, pp. 1175–1199

[18]  White, R., G. Engelen (1993), Cellular dynamics and GIS: modelling spatial complexity. Geographical Systems, 1, pp. 237–253

[19]  Batty, M., Y. Xie (1994), From cells to cities. Environment and Planning B: Planning and Design, 21, pp. s31–s48

[20]  Cecchini, A. (1996), Urban modelling by means of cellular automata: generalised urban automata with the help on-line (AUGH) model. Environment and Planning B: Planning and Design, 23, pp. 721–732

[21]  Batty, M., H. Couclelis, M. Eichen (1997), Urban systems as cellular automata. Environment and Planning B: Planning and Design, 24, pp. 159–164

[22]  Clarke, K. C., S. Hoppen, L. Gaydos (1997), A self-modifying cellular automaton model of historical urbanization in the San Francisco Bay area. Environment and Planning B: Planning and Design, 24, pp. 247–261

[23]  Pereira, H. T. S., A. N. Rodrigues da Silva (2010), Comparing spatial analysis methods for the definition of Functional Urban Regions - The case of Bahia, Brazil. In

Proceedings of the 10th International Conference on Design and Decision Support Systems in Architecture and Urban Planning, Eindhoven, The Netherlands

[24] IBGE - Instituto Brasileiro de Geografia e Estatística, População 2010, 2010. Available in http://www.censo2010.ibge.gov.br/resultados_do_censo2010.php. Accessed in Feb 28, 2012

# Identifying transition rules in a cellular automaton by sequential assimilation of observations

## Judith A. VERSTEGEN[1]; Derek KARSSENBERG[2]

[1]Copernicus Institute for Sustainable Development and Innovation, Faculty of Geosciences, Utrecht University, Budapestlaan 6, 3584 CD Utrecht, The Netherlands
+31 30 253 5513, j.a.verstegen@uu.nl

[2]Department of Physical Geography, Faculty of Geosciences, Utrecht University, Heidelberglaan 2, PO Box 80115, 3508 TC Utrecht, The Netherlands
+31 30 253 2768, d.karssenberg@uu.nl

## Abstract

The model structure of a land use change Cellular Automaton (CA), i.e. its set of transition rules, is often identified rather arbitrarily. We propose a more objective approach that selects the model structure from a set of candidate structures using observational data of land use. This is done in a Bayesian framework that sequentially assimilates observational data into the CA, where the model structure is defined as a probability distribution of transition rules. The advantage of the approach is that it combines expert knowledge and observational data in identifying the transition rules, taking into account the uncertainty in the observational data. The approach is evaluated in a case study of a land use change model simulating bioenergy cropland expansion in Brazil.

## Introduction

Land use change models simulate dynamic processes and interactions that are complex and are rarely fully understood [1]. Most land use change models, apart from agent based models, are grounded on some form of constrained Cellular Automaton (CA). A constrained CA can be defined as a discrete cell space with a set of potential cell states and a set of transition rules that control the state of each cell constrained by the number of cells required for each land use type (the demand) [2]. A wide range of individual theories exists to describe the land use system, which gives rise to a variety of transition rules being used [3].

The model structure of a land use change CA, i.e. the set of transition rules, is often identified somewhat arbitrarily, mainly using expert knowledge [4, 5]. In other cases, extensions of standard statistical methods are used, usually some type of regression on a land use map for a single time step, separate from the model itself [6-8]. This comes with the perils of finding rules valid for only a particular point in time, missing feedback effects, or detecting only a single effective combination of rules, while various ones exist. Therefore, such methods are not

oriented towards complexity [9]. Some use more complexity-oriented methods to identify model structure, like neural networks [10, 11], Bayesian networks [12], and particle swarm optimization [13]. A problem with all these approaches is, however, that they do not take into account observation uncertainty [14].

In addition to model structure identification, i.e. defining which processes should be included, model calibration, i.e. parameterization of these processes, is required. Yet, calibration could be considered pointless if the model structure is incorrect. To overcome this problem, we propose a method to simultaneously identify model structure and calibrate parameters of a land use change model using observational data.

Key requirements are to: 1) include prior knowledge about the model structure and parameters; 2) use a sound statistical framework that is capable of reconciling model uncertainty and observation uncertainty; 3) be able to utilize observations not only of the cell state (land use), but also of other variables or derived spatial pattern characteristics, e.g. patch size, zonal summary statistics, or connectivity, because these help to identify the underlying processes [15]; and 4) integrate model running and model structure identification to take into account temporal effects.

Data assimilation techniques have the potential to fulfil these requirements, because they sequentially update the model rules and parameters at time steps when observations are available. Most of these techniques rely on Bayes' theorem and thus have a sound statistical basis. They are increasingly being used to calibrate spatio-temporal models in a wide range of different fields in the environmental sciences, such as oceanography [16], hydrology [17], and atmospheric transport [18], but have, to our knowledge, not yet been applied for model structure identification and are new in the land use change field [19, 20]. Here, the potential of data assimilation for model structure identification and calibration of a land use change CA is evaluated by means of a case study of modelling the expansion of sugar cane fields in the São Paulo state in Brazil. This is relevant in view of the current debate on the sustainability of bioenergy from dedicated crops when land usechange is taken into account [21, 22].

A brief explanation of data assimilation is provided in the next section. The subsequent section outlines the case study setting, model set up with potential structures (prior information) and the observational data. This is followed by preliminary results and a discussion and conclusion section.

## General framework

A CA, with the state variable(s) $z_t$ and initial state $z_0$, can be defined as:

$$\mathbf{z}_t = \mathbf{f}_t(\mathbf{z}_{t-1}, \mathbf{i}_t, \mathbf{p}_t), \text{ for each } t = 1, 2, \ldots, T \qquad (1)$$

In equation 1, $\mathbf{f}_t$ is the set of transition rules at time step $t$ that simulates the system of, in this case, land use change. The vector $\mathbf{i}_t$ represents all inputs and boundary conditions and $\mathbf{p}_t$ contains the parameters. In a stochastic model, the uncertain parts of the system are described stochastically. So, ft is a probability distribution of possible transition rules and it and pt the probability distributions of

the inputs, boundary conditions and parameters. Together, they determine shape of the resulting probability distribution of the state variable, referred to as $\mathbf{p}(zt)$.

Bayes' rule to updates a probability distribution of a variable, when evidence, i.e. an observation, of this variable arrives. So, for the time steps at which observational data are available the following equation is evaluated.

$$p(\mathbf{z}_t|\mathbf{o}_t) = \frac{p(\mathbf{o}_t|\mathbf{z}_t) * p(\mathbf{z}_t)}{p(\mathbf{o}_t)}, \text{ for each } t \tag{2}$$

In equation 2, $p(\mathbf{o}_t)$ is the probability distribution of the observations, accordingly taking into account the uncertainty in these observations. $p(\mathbf{o}_t|\mathbf{z}_t)$ is the joint probability density of the observations at $t$ given the model state, which can be seen as the likelihood that the observations occur given the model. The posterior probability $p(\mathbf{z}_t|\mathbf{o}_t)$ is the probability distribution of the state variable $\mathbf{z}_t$ adjusted to the obseravtions.

Numerically, equation 1 is often solved using Monte Carlo analysis, which represents probability distributions by a number of realizations. A numerical solution of equation 2 is the particle filter, a data assimilation technique that filters these realizations, also called particles, sequentially. At each time step for which observational data are available it uses Bayes' theorem to assess the probability that a certain particle and the observed data can be considered equal [23]. Herein, the following steps are taken:

1. A number of $N$ realizations are drawn from the initial probability distributions of transition rules, inputs, boundary conditions and parameters, resulting in a total number of $N$ particles.

2. For all $N$ particles the land use change model is run up to the next observation moment, i.e. the next moment for which observational data are available.

3. The posterior probability, also called weight, that the modelled state at that moment is correct, given the observations with their uncertainty, is calculated for each of the particles.

4. Using these weights, $N$ particles are drawn to be progressed to the next observation moment. This procedure causes particles with a high weight to be copied (drawn several times) and particles with a low weight to be removed (never drawn).

5. Steps 2 to 4 are repeated until all filter moments are completed and the model has reached the final time step.

Steps 1 and 2 involve the Monte Carlo simulation, step 3 is achieved by solving Bayes' theorem sequentially:

$$p(\mathbf{z}_t^i|\mathbf{o}_t) = \frac{p(\mathbf{o}_t|\mathbf{z}_t^i) * p(\mathbf{z}_t^i)}{\sum_{j=1}^{N} p(\mathbf{o}_t|\mathbf{z}_t^j) * p(\mathbf{z}_t^j)}, \text{ for each } i = 1, 2, \ldots, N \tag{3}$$

In equation 3, $p(z_t^i)$ is the prior probability of model realization $i$, which is alwaysequal to $1/N$ because the same number of particles is drawn after each filter moment (step 4). If the observations are not of the state variable, but of a derived

summary statistic, for example relative proportions of land use in a subarea like sometimes found in census data, the model state has to be converted to that measure before filtering. In equation 3, $p(\mathbf{z}_t^i|\mathbf{o}_t)$ is the posterior probability or weight of particle $i$ and $p(\mathbf{o}_t|\mathbf{z}_t^i)$ is the probability of the observations given particle $i$. Under the assumption that the observation error has a Gaussian distribution, the latter can be defined as:

$$p(\mathbf{o}_t|\mathbf{z}_t^i) = e^{-1/2[\mathbf{o}_t - \mathbf{z}_t^i]^T \mathbf{R}_t^{-1}[\mathbf{o}_t - \mathbf{z}_t^i]}, \text{ for each } t \tag{4}$$

In equation 4, $\mathbf{R}_t$ is the covariance matrix of the observation error and T indicates matrix transposition.

Going through steps 1 to 5 the procedure 'filters' because many particles do not match the observations, receive low weights, and are thus not drawn and not progressed to the next observation moment. So, although the number of particles remains the same, the variation in the particles in terms of their uniqueness in the transition rules and values for inputs, boundary conditions and parameters diminishes. This means that the initial probability distributions of these model components are narrowed. Hence, the particle filter has identified which transition rules are most likely to be valid (model structure), in what ranges the inputs, boundary conditions and parameters are most likely to fall and the model has thereby been calibrated automatically.

**Case study**

A simple case study is defined to test the usability of the particle filter for model structure identification and calibration of a land use change CA. An important current debate in the land use change domain is whether bioenergy from dedicated crops is still sustainable when land use change is taken into account, in view of e.g., carbon emissions [21, 24, 25], rising food prices [26], and biodiversity [27]. For all these aspects it is important to know where bioenergy crops have expanded and will expand in the future. Such forecasts can be made with a land use change CA.

A key player in the bioenergy market is Brazil, mainly with the production of ethanol from sugar cane. Within Brazil, the state of São Paulo has the longest history as well as the largest share (about 60% of the national production in recent years) and still a significant growth in sugar cane production [28, 29]. The actuality of the debate, together with availability of an annual spatial dataset of sugarcane distribution from the National Institute for Space Research in Brazil (INPE) [30] as observational data, makes sugar cane cropland expansion in the São Paulo state a suitable case for testing the usability of the particle filter for model structure identification and calibration.

Model components from the PCRaster Land Use Change model (PLUC) [5, 31] are used to create the set of candidate transition rules (probability distribution of in equation 1). The land use change is steered by the demand for products associated with the land use types, in this case sugar cane. The two most important components of the transition rules are the suitability factors, which determine preferred location of the expansion or contraction, and the allocation mechanism, which determines the

degree of competition between land use types. The allocation mechanism is less important when considering only one land use type, because no competition is involved. So only the suitability factors and their parameters are sampled from a probability distribution. Total suitability for a land use type at time step $t$ can be defined as:

$$\mathbf{s}_t = \sum_{k=1}^{K}(w_k * \mathbf{u}_{k,t}), \text{ for each } t \qquad (5)$$
$$\text{with } \sum_{k=1}^{K}(w_k) = 1$$

In equation 5, $\mathbf{u}_{k,t} \in [0,1]$ is the suitability considering factor $k$, with $k = 1, 2, …, K$ and $w_k \in [0,1]$ is the weight of factor $k$. In the data assimilation, the model structure is defined by updating the distributions of $w_k$ for all suitability factors. Some weights will converge to zero, indicating that the processes, which the associated suitability factors embody, are irrelevant in the observed system. The candidate factors and a short explanation of the processes they represent are listed in Table 1.

Table 1: Candidate suitability factors for sugar cane in São Paulo

| *Suitability factor* | *Process represented* |
|---|---|
| Sugar cane in neighbourhood | Economies of scale |
| Distance to water | Water availability for growth |
| Distance to São Paulo over roads | Transportation costs to the main market |
| Potential yield | Profits |
| Slope | Mechanization potential, erosion |
| Distance to sugar cane mills | Transportation costs to processing unit |

For the Monte Carlo simulation and particle filtering the PCRaster Pyhton framework [32] is connected to the PLUC components. The observational data are 6 annual maps of sugar cane occurrence, classified from Landsat images by INPE for the Canasat project [30], with a resolution of 30 meters and a temporal extent from 2003 to 2010 (a period of strong growth [33], stimulated by the introduction of the flex-fuel vehicles). The data are resampled to a 1 kilometre resolution to align with input data and projected to the Albers Equal Area projection to preserve correctness of area, an important metric property in the model. In order to reduce run time and to show that not only observations of state variables can be used as observational data, but also derived summary statistics, the percentage of sugar cane coverage in 100 x 100 km blocks is used as observational data.

**Preliminary results**

The model is run for 50 realizations, once without and once with particle filtering in time steps 2 to 7 (2004 to 2009) using the percentage of sugar cane coverage in 100 x 100 km blocks as observational data. The evolution of the model structure can be illustrated by the evolution of the weights of the six candidate suitability factors over time (Figure 1). All factors start with a weight distribution that comprises all values between zero and one. Over time, some particles are filtered out and others are copied. Therefore the distributions converge, e.g., distance to sugar cane mills seems

to be important as it's weight converges to 0.7. Some factors' weights converge to zero, which means the processes are irrelevant, at least with their drawn parameterizations, and therefore excluded from the model structure. But, 50 realizations are insufficient to search the complete rule and parameter space. A run with more particles will probably yield different results.
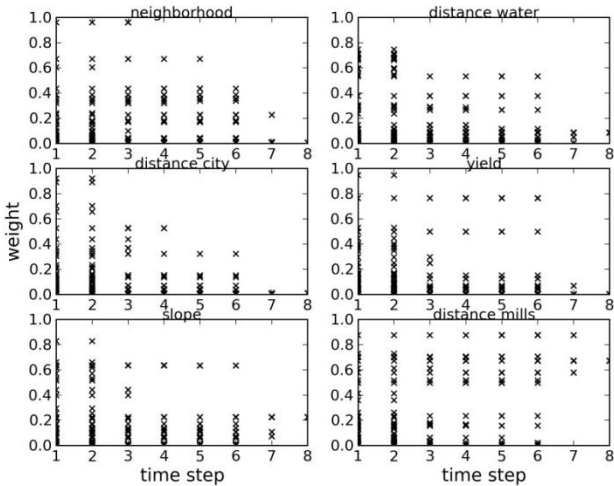


Figure 1: Evolution of the weights of the candidate suitability factors over time in the ensemble of 50 particles. Time step 1 is 2003 and the increment is annual.

To illustrate the effect on the state variable, the resulting probability that sugar cane is present in a cell in a certain year is shown in Figure 2. A value 1 indicates that a cell is certainly occupied by sugar cane, i.e. it was sugar cane in all realizations, a value 0 that it is certainly unoccupied, i.e. it was sugar cane in none of the realizations, and any value in between indicates uncertainty in presence. In 2005, the third time step, the model results with filtering and without filtering (Monte Carlo only) show little difference, as only one filter moment has passed. In 2009, however, the maps with filtering exhibit much less uncertainty, i.e. more cells that have either the value 0 or the value 1. This is because particles in which sugar cane was allocated in wrong locations have been filtered out. As a result, the large areas that remain free of sugar cane coverage, for example in the South-eastern corner and the circular patch in the centre, are predicted much better by the particle filter than by the model without filtering, in which almost all cells in São Paulo have an equal probability to be covered by sugar cane in 2009.

Nonetheless, the 2009 map with filtering still does not match the observations fully. This can have several reasons. An important one is that the percentage of sugar cane coverage in 100 x 100 km blocks was used as observational data, meaning that the model is only required to match the *amount* of sugar cane in a block, independent of

the *arrangement* within this block. The sugar cane is now clustered too much by the model. Including for example average patch size as an observation might solve this. Secondly, as stated before, not enough realizations were used to search the complete parameter space. Furthermore, it is possible that not all relevant processes were included in the set of candidate rules, so that the model will never be able to replicate the observations.
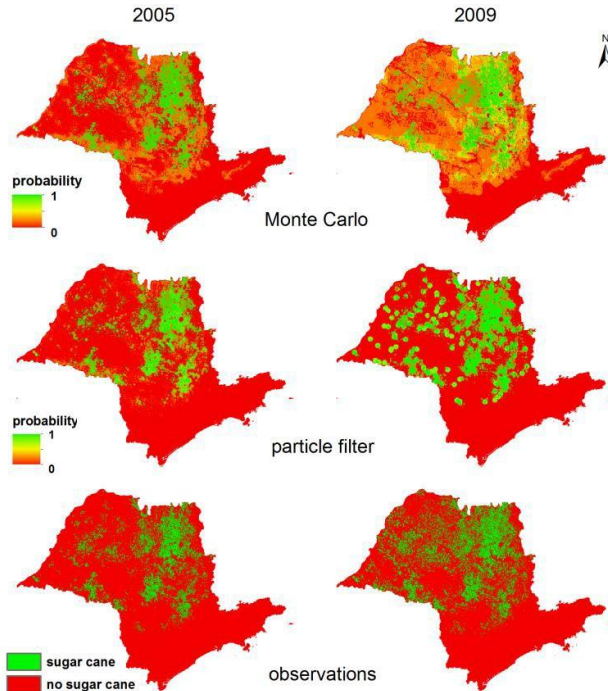


Figure 2: The probability that sugar cane is cultivated in the Monte Carlo run without (top) and with (middle) filtering, and the observations (without uncertainty) (bottom), for 2005 (left) and2009 (right).

**Discussion and conclusion**

The particle filter has the potential to simultaneously identify model structure and calibrate parameters of a land use change CA. We have shown how it can combine prior information and observations, taking into account uncertainty in these observations. The observations can correspond to the state variable or a derived pattern characteristic, so that the absence of good quality land use maps is less of a problem. The approach of integrated model structure identification and model running allows to account for temporal patterns, such as feedback effects, important in complex systems [9].

Further research should be done using more particles to be able to represent the full range of possible transition rule and parameter combinations. In addition, more spatial pattern characteristics should be exploited in the filter, to better capture the underlying processes [15] and thus improve the forecasting capabilities of the model. Validation is needed to proof whether the proposed method results in improved land use change predictions.

## Acknowledgements

## References

[1]    Manson SM. (2006), Land use in the southern Yucatán peninsular region of Mexico: Scenarios of population and institutional change. Computers, Environment and Urban Systems;30(3):230-53.

[2]    White R. (1998), Cities and Cellular Automata. Discrete Dynamics in Nature and Society;2:111,111-125.

[3]    Santé I, García AM, Miranda D, Crecente R. (2010), Cellular automata models for the simulation of real-world urban processes: A review and analysis. Landscape and Urban Planning;96(2):108-22.

[4]    Yu J, Chen Y, Wu J, Khan S. (2011), Cellular automata-based spatial multi-criteria land suitability simulation for irrigated agriculture. International Journal of Geographical Information Science;25(1):131-48.

[5]    van der Hilst F, Verstegen JA, Karssenberg D, Faaij APC. (in press), Spatio-temporal land use modelling to assess land availability for energy crops - illustrated for Mozambique. Global Change Biology Bioenergy;2011.

[6]    Verburg PH, De Koning GHJ, Kok K, Veldkamp A, Bouma J. (1999), A spatial explicit allocation procedure for modelling the pattern of land use change based upon actual land use. Ecological Modelling;116(1):45-61.

[7]    Verburg PH, Soepboer W, Veldkamp A, Limpiada R, Espaldon V, Mastura SSA. (2002), Modeling the spatial dynamics of regional land use: The CLUE-S model. Environmental Management;30(3):391-405.

[8]    Aguiar APD, Câmara G, Escada MIS. (2007), Spatial statistical analysis of land-use determinants in the Brazilian Amazonia: Exploring intra-regional heterogeneity. Ecological Modelling;209(2-4):169-88.

[9]    Manson SM. (2007), Challenges in evaluating models of geographic complexity. Environment and Planning B: Planning and Design;34:245-60.

[10]   Dai E, Wu S, Shi W, Cheung C-, Shaker A. (2005), Modeling Change-Pattern-Value dynamics on land use: An integrated GIS and Artificial Neural Networks approach. Environmental Management;36(4):576-91.

[11]   Li X, Yeh AG-. (2002), Neural-network-based cellular automata for simulating multiple land use changes using GIS. International Journal of Geographical Information Science;16(4):323-43.

[12]   Kocabas V, Dragićević S. (2007), Enhancing a GIS cellular automata model of land use change: Bayesian networks, influence diagrams and causality. Transactions in GIS;11(5):681-702.

[13] Feng Y, Liu Y, Tong X, Liu M, Deng S. (2011), Modeling dynamic urban growth using cellular automata and particle swarm optimization rules. Landscape and Urban Planning;102(3):188-96.

[14] Straatman B, White R, Engelen G. (2004), Towards an automatic calibration procedure for constrained cellular automata. Computers, Environment and Urban Systems;28(1-2):149-70.

[15] Grimm V, Railsback SF. (2012), Pattern-oriented modelling: A 'multi-scope' for predictive systems ecology. Philosophical Transactions of the Royal Society B: Biological Sciences;367(1586):298-310.

[16] Van Leeuwen PJ. (2003), A variance-minimizing filter for large-scale applications. Monthly Weather Review;131(9):2071-84.

[17] Salamon P, Feyen L. (2009), Assessing parameter, precipitation, and predictive uncertainty in a distributed hydrological model using sequential data assimilation with the particle filter. Journal of Hydrology;376(3-4):428-42.

[18] Hiemstra PH, Karssenberg D, van Dijk A. (2011), Assimilation of observations of radiation level into an atmospheric transport model: A case study with the particle filter and the ETEX tracer dataset. Atmospheric Environment;45(34):6149-57.

[19] Remote sensing data assimilation in modeling urban dynamics: Objectives and methodology. Procedia Environmental Sciences; 2011. .

[20] Zhang Y, Li X, Liu X, Qiao J. (2011), The CA model based on data assimilation. Yaogan Xuebao - Journal of Remote Sensing;15(3):475,475-482.

[21] Lapola DM, Schaldach R, Alcamo J, Bondeau A, Koch J, Koelking C, Priess JA. (2010), Indirect land-use changes can overcome carbon savings from biofuels in Brazil. Proceedings of the National Academy of Sciences of the United States of America;107(8):3388-93.

[22] Hellmann F, Verburg PH. (2011), Spatially explicit modelling of biofuel crops in Europe. Biomass and Bioenergy;35(6):2411-24.

[23] Hartig F, Calabrese JM, Reineking B, Wiegand T, Huth A. (2011), Statistical inference for stochastic simulation models - theory and application. Ecology Letters;14(8):816-27.

[24] Fargione J, Hill J, Tilman D, Polasky S, Hawthorne P. (2008), Land clearing and the biofuel carbon debt. Science;319(5867):1235-8.

[25] Searchinger TD, Heimlich R, Houghton RA, Dong F, Elobeid A, Fabiosa J, Tokgoz S, Hayes D, Yu T-. (2008), Use of U.S. croplands for biofuels increases greenhouse gases through emissions from land-use change. Science;319(5867):1238-40.

[26] von Braun J. (2008), Rising food prices: What should be done? EuroChoices;7(2):30-5.

[27] Hellmann F, Verburg PH. (2010), Impact assessment of the European biofuel directive on land use and biodiversity. Journal of Environmental Management;91(6):1389-96.

[28] Sparovek G, Barretto AGdOP, Berndes G, Martins S, Maule R. (2009), Environmental, land-use and economic implications of Brazilian sugarcane expansion 1996-2006. Mitigation and Adaptation Strategies for Global Change;14(3):285-98.

[29] Walter A, Dolzan P, Quilodrán O, De Oliveira JG, Da Silva C, Piacente F, Segerstedt A. (2011), Sustainability assessment of bio-ethanol production in Brazil considering land use change, GHG emissions and socio-economic aspects. Energy Policy;39(10):5703-16.

[30] Rudorff BFT, Aguiar DA, Silva WF, Sugawara LM, Adami M, Moreira MA. (2010), Studies on the Rapid Expansion of Sugarcane for Ethanol Production in São Paulo State (Brazil) Using Landsat Data. Remote Sensing;2(4):1057-1076.

[31] Verstegen JA, Karssenberg D, van der Hilst F, Faaij APC. (2012), Spatio-Temporal Uncertainty in Spatial Decision Support Systems: a Case Study of Changing Land Availability for Bioenergy Crops in Mozambique. Computers, Environment and Urban Systems;36:30-42.

[32] Karssenberg D, Schmitz O, Salamon P, de Jong K, Bierkens MFP. (2010), A software framework for construction of process-based stochastic spatio-temporal models and data assimilation. Environmental Modelling and Software;25:489-502.

[33] Macedo IC, Seabra JEA. (2008). Chapter 4: Mitigation of GHG emissions using sugarcane bioethanol. In: P. Zuurbier, J. van de Vooren, editors. Sugarcane ethanol: Contributions to climate change mitigation and the environment. Wageningen, The Netherlands: Wageningen Academic Publishers.

# Urban Conventions and Residential Location Choice

Exploring a Heterodox Perspective of Urban Economics with a Spatially-Explicit Simulation Model

## Flávia F. FEITOSA[1]; Antônio Miguel V. MONTEIRO[2]

Earth System Science Center (CCST), National Institute for Space Research (INPE), Av. dos Astronautas 1758, 12227-010, São José dos Campos (SP), Brazil.
[1] Phone: +55 (12) 3208-7130, E-mail: flavia@dpi.inpe.br (corresponding author)
[2] Phone: +55 (12) 3208-6513, E-mail: miguel@dpi.inpe.br

**Keywords:** urban simulation model, residential location choice, heterodox urban economics

## Abstract

Since the 1960s, an increasing number of studies have focused on investigating the determinants of urban residential location choices. Despite the valuable contribution of these pioneer studies to the development of urban and spatial economics, many researchers have doubted its applicability to the real world, criticizing some of its simplified assumptions and, most important, the underlying idea that the spontaneous action of market forces promotes higher levels of consumer satisfaction and efficiency of resource use.

Contributing to this debate, this paper presents a spatially-explicit simulation model built to explore an alternative perspective to the one provided by neoclassical models of urban economics. This perspective is based on the theoretical framework proposed by the economist Pedro Abramo in his book "The Kaleidoscopic City", which relies on the heterodox economic literature to develop a new interpretation of how residential choices are made. In this paper, we present simulation experiments that explore the role of entrepreneurs' actions in influencing the residential location choice of families and the emergence of different global and local residential patterns in the city.

## Introduction

Since the 1960s, an increasing number of studies have focused on investigating the determinants of urban residential location choices and their influence on the emergence of spatial patterns that are able to affect the daily life of urban inhabitants. The theoretical basis of the current mainstream approach to urban residential location has its roots in models developed in the beginning of this period by Alonso [1], Muth [2] and others. Following the principles advocated by these neoclassical models, a unique and efficient order is achieved through residential choices that balance a trade-off between housing consumption and commuting costs to work.

Despite the valuable contribution of these pioneer studies to the development of urban and spatial economics, many researchers have doubted its applicability to the real world, criticizing some of its simplified assumptions (e.g., lack of interdependence of location choices) and, most important, the underlying idea that the spontaneous action of market forces promotes higher levels of consumer satisfaction and efficiency of resource use [3,4,5].

Contributing to this debate, this paper presents a spatially-explicit simulation model built to explore an alternative perspective to the one provided by neoclassical models of urban economics. This perspective is based on the theoretical framework proposed by the economist Pedro Abramo in his book "The Kaleidoscopic City" (*La Ville Kaléidoscopique*), first published in French in 1998. Considering the city as a setting for disputes between heterogeneous agents with asymmetric power over the market, the author builds on the heterodox economic literature to develop a new interpretation of how residential choices are made. In this paper, we present simulation experiments that explore the role of entrepreneurs' actions in influencing the residential location choice of families and the emergence of different global and local residential patterns in the city.

Following this introduction, the paper is organized as follows: First, we provide an overview of the theoretical framework that underlies our model of residential location. Second, we introduce the goal and specification of the model, which is called *Kaleidoscopic-City* as a reference to the title of Abramo's book. Then, a series of experiments that explore the relations between entities described in the theoretical framework is presented. Finally, we conclude with some final remarks.

## Crucial Decisions and Urban Conventions: An Alternative Perspective to Urban Residential Location

Instead of considering the trade-off between space and accessibility, Abramo assumes that families choose their location based on *neighborhood externalities*, i.e., they prefer places where lower-income families are not present. According to his approach, the residential location choice represents an investment choice, where, for instance, parents can invest in the family's human capital by offering good neighborhood relations and educational opportunities to their children [3].

While making their decisions, families perceive the urban space as a mosaic of neighborhood externalities and, consequently, evaluate locations that are being constantly modified by their own actions. However, because families' decisions are simultaneous and decentralized, no one can know in advance where each family will decide to live. This uncertainty about the future can become particularly critical when a family decide to make an *opportunistic decision* of investment and move to a location with richer neighbors. This sort of decision may trigger a process that Schelling [6] described as "tipping model": it may disturb some wealthier residents already established in the location, motivate them to move out, and initiate a transformation in the social composition of the neighborhood [3, p.57]. Therefore, an opportunistic decision, seen as "non-rational" by the orthodox theory, has the potential of becoming a *crucial decision*, able to lead the future residential order to

an unexpected configuration and, therefore, establish a context of *radical urban uncertainty* [3, p.58-59].

The state of radical urban uncertainty can be also (and especially) promoted by another type of agent whose actions are essential to configure the urban order: the capitalist-entrepreneur. Based on the Schumpeterian view of entrepreneurship, Abramo emphasizes how entrepreneurs are able to make profits through the *practice of innovation*. By building dwellings that are more innovative and attractive than the existing ones, entrepreneurs avoid competition with old housing stocks and redirect the demand to the locations where their newly built properties are offered. Thus, entrepreneurs are able to modify the urban order by promoting a *fictitious depreciation* of old housing stocks [3, p.71], which does not represent a physical depreciation of properties, but a depreciation in the social status of residents living in the location. This sort of decision made by innovative Schumpeterian entrepreneurs becomes, therefore, a crucial decision that is able to lead to a context of radical urban uncertainty.

Even in this context of uncertainty, market participants need to make their decisions based on a game of cross-anticipation, where each agent must anticipate the location choices of other agents and the neighborhood externalities emerging from them. To address this decision-making problem, Abramo relies on techniques suggested by Keynes [7], which indicate that, more than considering their own preferences, agents try to guess and imitate the choice of other decision-makers [3, p.112]. This mimetic behavior can converge to an *urban convention*, which is a collective conviction regarding the type of family that is going to live in a particular location (neighborhood externality) [3, p.287].

By adopting a mimetic behavior, agents need to identify who is better informed and should be imitated. In this context arises the figure of the Keynesian speculator, whose task is to predict the psychology of the market [3, p.137]. Abramo argues that, in the residential market, the Keynesian speculator and the Schumpeterian entrepreneur are merged into a single figure. Since Schumpeterian entrepreneurs are the only able to promote innovations that depreciate existing residential areas, they seek to assign themselves the role of emitting signals that announce changes in the residential market [3, p.139-140]. Considering the entrepreneurs as better-informed agents, families take these signals into consideration while making their residential location choice. Thus, the urban convention becomes an element of spatial coordination that results from a mimetic speculative process where families elect the entrepreneurs' actions as source of information.

However, if on one hand the entrepreneur sends signals that lead to a spatial order (urban convention), on the other hand they introduce innovations that lead to a fictitious depreciation of housing stocks and the end of the convention. There is, therefore, a tension between the order promoted by urban conventions and the disorder introduced by crucial decisions. According to Abramo, this order-disorder tension is what reveals the context of radical urban uncertainty and kaleidoscopic spatial order that characterizes the market coordination of the urban space [3, p. 143].

## The Kaleidoscopic-City Model

The ordered-disordered dynamic described above, which is quite different from the stable and efficient process advocated by the neoclassical approach, is explored in this paper through the Kaleidoscopic-City model. By simulating the interdependence between the decisions of heterogeneous agents (families and entrepreneurs) and the neighborhood externalities emerging from these decisions, the model seeks to investigate how crucial decisions made by entrepreneurs (innovation) contribute to change the urban spatial order and the lifecycle of different regions in a city.

### Agents and Environment

The model presents two types of agents: families (consumers) and entrepreneurs (producers).

*Families* are spatially explicit agents hierarchized by their *income level*. They are constantly evaluating urban locations and deciding whether to move to a different place. In this evaluation, they take two aspects into consideration: the income level of neighbors (neighborhood externality) and the innovation degree of dwellings.

*Entrepreneurs* are agents responsible for producing dwellings. They are not spatially situated, although their actions are constantly affecting the urban space. They are characterized by a *producer profile*, which can be innovative or imitative.

*Innovative entrepreneurs* produce dwellings with the highest degree of innovation and always in the region recognized by the current urban convention as the one where the richest families are going to live. If convenient, they can establish a new convention by introducing innovations in a different region of the city. *Imitative entrepreneurs*, on the other hand, do not have the ability of establishing new conventions, since the innovation degree of the dwellings they produce simply follows standards already set. Also, they may build in any region of the city, although they have a higher probability of choosing the region that represents the current urban convention.

The *urban environment* that is constantly being perceived and modified by both types of agents is represented by a grid of cells and subdivided in different regions. Each *region* is composed by a set of cells and can, temporarily, be recognized by the urban convention as the region where the richest families are going to live. For simplification, we call this region as "urban-convention region", since this paper only addresses explicitly the anticipation regarding the location of the wealthiest families.

The *cells* can be urbanized or not. Once urbanized, they can accommodate one or more dwellings, depending on the maximum density allowed in the region where they are situated. The dwellings located in a cell are characterized by a certain degree of innovation and can be occupied by family agents.

### Process Overview

The Kaleidoscopic-City model was implemented in Netlogo 5.0 [8] and its simulation schedule is summarized in Figure 1.
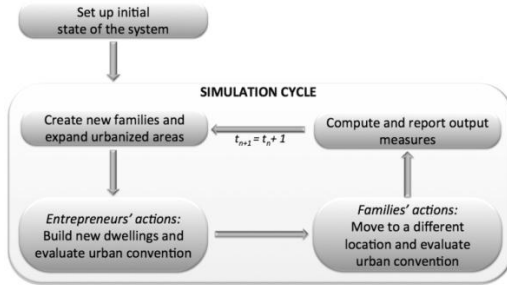
Figure 1: Simulation schedule

**Initial state of the system**

The environment is composed by a finite number of cells ($N = 1254$) and subdivided in 12 different regions. A small number of cells, located within a radius $r$ ($r_0 = 5$ units/cells) from the center of the grid, are already urbanized before the beginning of the simulation. Figure 2 represents the 12 regions in different shades of gray and the central urbanized area in a lighter shade.

An initial number of dwellings ($d_0 = 20$) with equal degree of innovation are randomly located within the urbanized area. Each dwelling is occupied by a family agent (Figure 2). Families have their income level defined according to a power law distribution.

Entrepreneur agents are also created in the initialization phase. Their producer profile (innovative or imitative) is defined according to a user-defined probability.
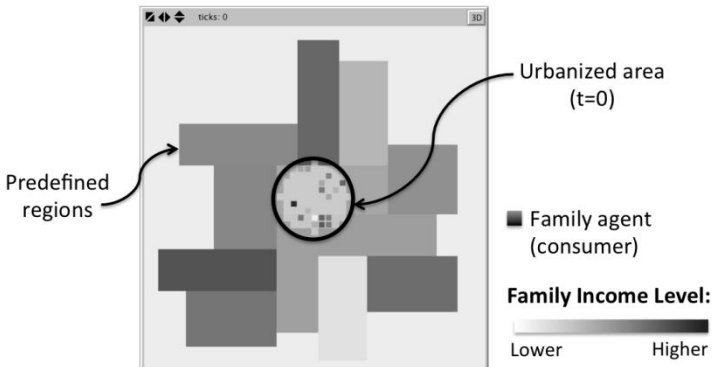


Figure 2: Configuration of regions and family agents' distribution within the initial urbanized area

**Create new families and expand urban areas**

In the first phase of the simulation cycle (Figure 1), *n* new family agents are created ($n=15$). These new families, which are not yet assigned to any location of the

environment, represent a new demand for dwellings and urbanized areas during the current time step. Addressing this demand, an expansion of the urbanized radius will occur in case the total number of families exceeds a predefined threshold.

**Entrepreneurs' actions**

In this second phase of the simulation cycle, the model simulates the entrepreneurs' actions, which are responsible for supplying the demand for new dwellings. For that, it executes the procedures summarized in Figure 3.

The first procedure consists on selecting one of the existing entrepreneurs, which can be an innovator or imitator. Afterwards, the entrepreneur will choose a region to build the new dwellings. An imitative entrepreneur can select any region of the city, with a higher probability (50%) of choosing that region that represents the current urban convention. An innovative entrepreneur, on the other hand, will always build at the urban-convention region. Nevertheless, innovative entrepreneurs can evaluate whether it is convenient to maintain the current convention or not. According to Abramo [3], as the housing density of a region increases and approaches the desired density for the place, the greater the chances that an innovative entrepreneur will attempt to establish a new urban convention (greater uncertainty). In the model, the maximum density allowed for a region is set as the "desired density".
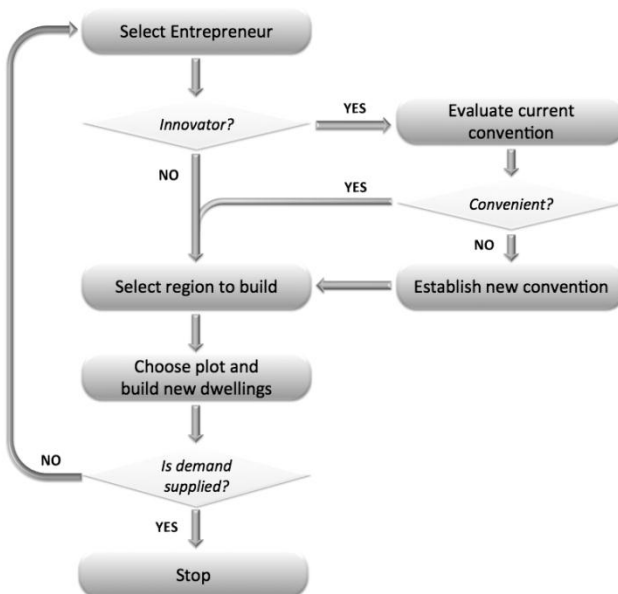


Figure 3: Entrepreneurs' actions

Once the innovative entrepreneur decides to establish a new convention, the region chosen to become the new destination of wealthy families starts a new phase of

development: its maximum density allowed increases by 1, all of its cells are urbanized (in case they were not already) and, most important, the innovation level of the new dwellings built in the region will be the highest of the city.

After selecting a region, the entrepreneur agent will choose a plot and build new dwellings. This process, which starts from the selection of an entrepreneur and finishes with the construction of new dwellings, is repeated until the total number of dwellings meets the demand.

**Families' actions**

In this phase, family agents decide whether to move to a different residential location or not (Figure 4). Families that are already living in the city may want/need to move for different reasons:

- They are unhappy about their neighborhood externality (neighbors' income is lower than desired);
- They are attracted to dwellings with a higher degree of innovation;
- The region where they live received investments that promoted the arrival of new and wealthier residents. Consequently, the region's price is no longer compatible with the family income level (gentrification).
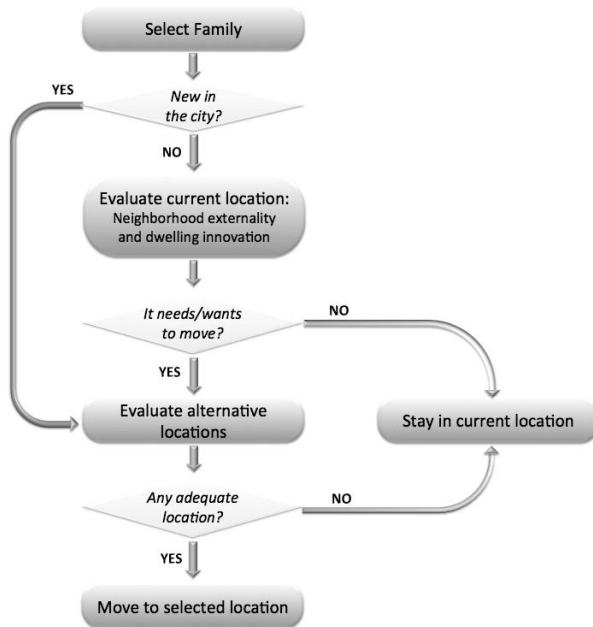


Figure 4: Families' decision-making process

Families who need/want to move will evaluate up to *n* alternative locations (*n*=20). In this evaluation, families search for an available dwelling that meets the following requirements:

▪ Those who are dissatisfied with the innovation degree of their dwellings will look for dwellings whose innovation degree is *within a range* that is compatible with their income.

▪ Those who are already satisfied with the innovation degree of their dwellings, but dissatisfied with the neighborhood externality of their current location, will look for a place where the average neighborhood income is *higher than the average income* of their social group.

Families who find a dwelling that meets the pursued requirements, will then move into the chosen location. Otherwise, they stay in their current dwelling.

Unlike innovative entrepreneurs, families are not able to intentionally destroy or establish an urban convention. Nevertheless, events that are able to disturb rich residents who are living at the urban-convention region may motivate them to move out and initiate a process that encourages innovative entrepreneurs to establish a new urban convention. At the end of a simulation cycle, the model represents this process by measuring how satisfied the urban-convention region's residents are regarding their neighborhood externality. The lower the satisfaction is, the higher is the chance that an innovative entrepreneur will decide to establish a new urban convention.

**Output measures**

At the end of each cycle, two different output measures are computed to monitor the dynamics of urban regions: (a) density of dwellings in each region, and (b) average income of the residents in each region (proxy of land value).

In addition, the spatial distribution of wealthy families is monitored through an urban segregation index that measures the spatial isolation of this income group [9].

**Simulation Experiments and Discussion**

This paper presents experiments that explore the *role of crucial decisions made by innovative entrepreneurs* in shaping the residential order of cities. It investigates how the *practice of innovation* and its ability to establish new urban conventions can affect the residential location choice of families and the configuration of different global and local residential patterns in a city.

To test the impact of innovation and urban conventions, we simulated and compared the emergence of residential patterns under two different conditions: one *without* and the other *with* innovative entrepreneurs.

In the first scenario, without innovation, entrepreneurs are not able to interfere on the establishment of urban conventions, as there is no differentiation among the dwellings they produce and offer to the families. In this case, the only aspect considered by the families while choosing a residential location is the income composition of families living in the neighborhood (neighborhood externality).

In the second scenario, 10% of entrepreneurs have an innovative profile. These entrepreneurs can, therefore, assume an active role on establishing (and destroying) urban conventions. By building innovative dwellings in a certain region of the city, entrepreneurs avoid the concurrency with old housing stocks and can emit signals about the future residential order in the city.

Figures 5 and 6 show the *location of families with different income levels* and the *local isolation index of wealthy families* along the simulation of both scenarios (t=0, t=50, t=100 and t=150). Through the comparison of these two figures, it is possible to observe the *aggregate outcome of the practice of innovation*.

The scenario *without* innovation (Figure 5), where families' residential decisions are only influenced by the social composition of the neighborhoods, the residential dynamics are characterized by a higher degree of inertia, which results in an *increased stability of neighborhood externalities*. As the population of the city increases, families tend to occupy the urban space in a uniform manner and progressively define the regions characterized by the presence of each social group.

The scenario *with* innovation (Figure 6), on the other hand, reveals a situation with a much higher level of uneasiness and uncertainty, characterized by a greater mobility of families in terms of residential location, which is exactly what ensures higher profits for developers.
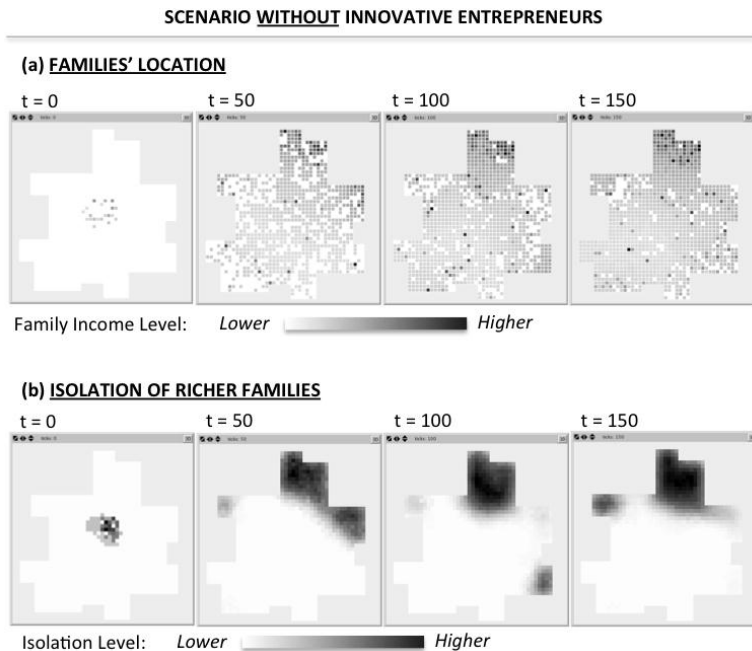


Figure 5: Simulation **without** innovation: (a) families' location and (b) isolation of richer families

The maps showing the isolation of richer families exemplify this difference between both scenarios: while in the first scenario, the wealthiest neighborhood was mainly kept at the same place during the simulation (Figure 5b), the introduction of innovations in the second scenario was constantly modifying the urban conventions and, therefore, promoting a frequent change in the places where the richest families live (Figure 6b).

It is also important to remind that the practice of innovation simulated in this experiment, which aims at moving the wealthiest families to new locations, promotes a fictitious depreciation of older housing stocks. In turn, this depreciation intensifies the urban uncertainty by subverting the conventions that prevailed for other social groups and giving rise to a chain of displacements of families with different income levels.

This process results in what Abramo [3] described as the image of a mosaic of neighborhood externalities in constant mutation or, in other words, the *image of a kaleidoscopic residential order*.
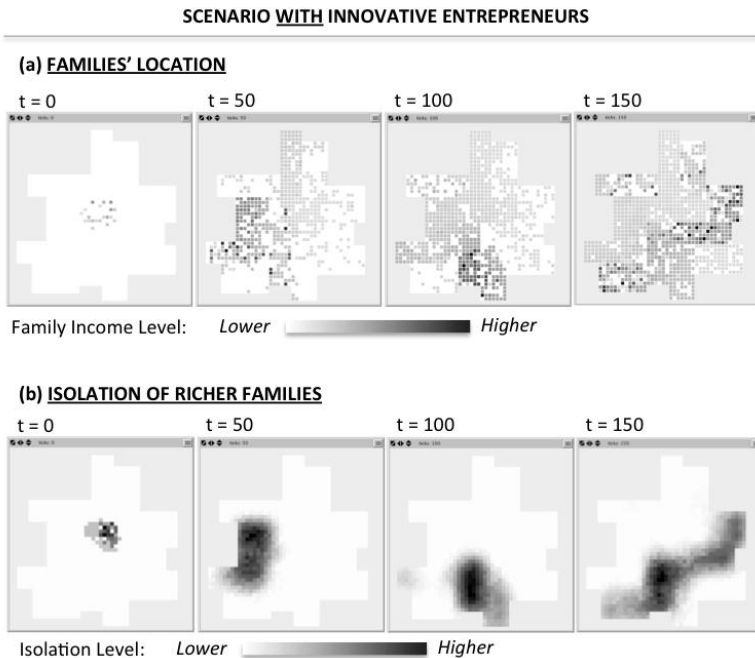


Figure 6: Simulation **with** innovation: (a) families' location and (b) isolation of richer families

The graphs presented in Figures 7 and 8 illustrate these considerations by comparing the evolution of local residential patterns in both scenarios. In these graphs, each line represents the trajectory of an urban region. Two output measures are used to monitor these trajectories:

- density of dwellings, which illustrates how intensive are the investments in a region (Figure 7);
- mean income of families, which is here considered as a proxy of the land price in a region (Figure 8).

In the first simulation experiment (without innovations), the density of dwellings increases uniformly in all regions of the city (Figure 7a). This pattern is very different from the one obtained in the experiment with innovations (Figure 7b), where most regions have periods of accelerated increase in density (when set as the convention region), alternating with periods of stagnation.
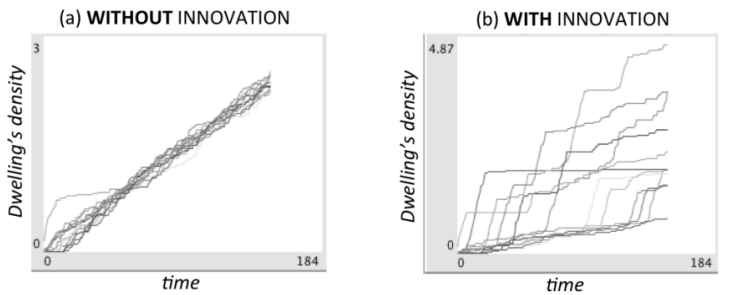


Figure 7: Density of dwellings in the urban regions: scenarios without and with innovation. Each line describes the density of a region.
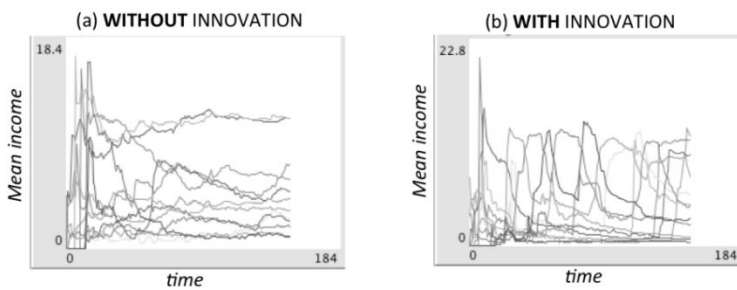


Figure 8: Mean income of families in the urban regions (proxy of land price): scenarios **without** and **with** innovation. Each line describes the average income of families living in a region.

Regarding the mean income of families (Figure 8), it is possible to observe how the variation of this attribute is much smaller in the first scenario (without innovations). The graph in Figure 8a shows that, after an initial instability associated to small population sizes, regions tend to present a relatively stable neighborhood externality (and, therefore, land price). On the other hand, because the innovations introduced in

the second scenario promote a constant restructuration of the existing neighborhood externalities, Figure 8b shows patterns characterized by "peaks and valleys".

The local outcomes of the practice of innovation can be seen in more detail in Figure 9, which shows the trajectory of urban conventions (Figure 9c) and its impact on the development of urban regions (Figure 9a and 9b). In Figure 9a, each line describes the dwelling's density of a region, while in Figure 9b each line describes the average income of families living in a region.



Figure 9: Urban conventions and regions' life cycles.

Taking the example of Region 1 (R1), which is represented by the black line, we can see that in periods when this region is the current urban convention (highlighted with a gray shadow in Figure 9), the place enters a transition period, characterized by intensive investments and a sudden increase in dwellings' density (Figure 9a). At the same time, the region becomes more attractive to richer families and a strong increase in prices takes place (Figure 9b). This transition period ends with the

emergence of a new urban convention. Then, the investments in region 1 cease and the density of dwellings is kept almost constant (phases 1, 2, 3). With the most innovative dwellings of the city being now located in a different region (new urban convention) richer families feel motivated to move out from region 1 and are substituted by families with lower income. This process causes a fictitious depreciation in region 1 (Figure 9b): the housing dwellings remain the same, but the social status of families living in the region (neighborhood externality) decays.

By observing and comparing the different sort of information provided in Figure 9, it is possible, therefore, to see how the succession of urban conventions traces the life cycles of urban regions, including their history of housing stocks and neighborhood externalities. In these life cycles, *transition periods* characterized by the construction of innovative dwellings and increase in prices are separated by *in-between phases* where the housing stock is preserved, but different configurations of neighborhood externalities take place (fictitious depreciation). These dynamic processes, here demonstrated through simulation experiments, are theoretically described in Abramo's book [3].

## Final Remarks

This work presents a spatially-explicit simulation model that explores the heterodox perspective of urban economics proposed by Abramo [3]. Unlike the orthodox school, Abramo's approach assumes that the residential location is not an individual and independent process. Instead, it emphasizes the interdependence between agent's decisions and the spatial externalities emerging from them.

In this paper, we particularly focused on the impacts of entrepreneurs' decisions. While in the neoclassical view entrepreneurs assume the neutral position of price-takers, the Kaleidoscopic-City model emphasizes their active role as price-makers. In the pursuit of higher profits, they can try to manipulate the sovereignty of consumers through the practice of innovation.

This alternative way to envision the residential market has implications for the future urban order and, consequently, for the development of urban policies. The approach explored in the Kaleidoscopic-City model is built on the Keynesian speculative-financial paradigm, and not on the neoclassical exchange paradigm. Studies and policies developed under this perspective should, therefore, do not rely on economic predictions, but on the historical process of urban development and the possibility of having economic agents making crucial decisions that redefine the course of history.

## Acknowledgments

## Reference

[1]  Alonso, W. (1964), Location and land use, Harvard University Press, Boston

[2]  Muth, R. (1969), Cities and housing, University of Chicago Press, Chicago

[3]  Abramo, P. (2007), A cidade caleidoscópica: coordenação espacial e convenção urbana, Bertrand Brasil, Rio de Janeiro

[4]  Edel, M. (2001), Urban and regional economics - Marxist perspectives, Routledge, London

[5]  González, S.J. (2010), Hacia una teoría de la renta del suelo urbano, Ediciones Uniandes, Bogotá

[6]  Schelling, T.C. (1978), Micromotives and macrobehavior, W.W. Norton & Company, London/New York

[7]  Keynes, J.M. (1936), General theory of employment, interest and money, Macmillan Press/St. Martin's Press, London/New York

[8]  Wilensky, U. (1999), NetLogo, Northwestern University, Evanston

[9]  Feitosa, F.F. et al (2007), Global and local spatial indices of urban segregation. International Journal of Geographical Information Science, 21(3), pp.299-323

# From cellular automata to land use models

**Jakub VOREL**

Faculty of architecture, Czech Technical University in Prague
Thakurova 9, 166 34, Czech Republic
+420 777 560 039, kubavorel@gmail.com

**Keywords:** cellular automata, land use, structural validity, agent-based models

## Abstract

Cellular automata that originated from the field of computer science and complexity theory soon found their way into various disciplines. There are several good reasons for the implementation of cellular automata in urban growth and land use change studies, mainly the bottom-up generation of land use change or the availability of raster data on land use and land cover. On the other hand, cellular automata do not explicitly represent the land use change factors and other land use change factors are completely ignored. To overcome the deficiencies of cellular automata for land use modelling, significant modifications to the original concept of cellular automata were adopted. This paper will present the improvements in structured form based on examples of several existing simulation models.

## Introduction

Cellular automata emerged in the field of computer science to be used mainly by proponents of complexity theory to demonstrate the relation between the micro and macro behaviour of complex systems. The cellular automata are based on rather strong assumptions of the autonomy of individual automata behaviour, homogeneity of their characteristics and transition rules. This paper claims that those features make cellular automata suitable for the study of general processes of urban growth, spread of diseases or propagation of innovations, but less for study of land use change processes in general. The main reason is the artificiality of cellular automata that makes them ignore many aspect of the physical, economic and legal reality causing the important drivers and agents of land use change being improperly represented.

Several decades of effort to implement cellular automata for land use simulation have brought many interesting innovations that made the usability of cellular automata for land use studies much more acceptable. The most significant adaptations of cellular automata are described in the background of several existing, well known simulation models.

## Disaggregated description of land uses

The disaggregation of land use to multiple categories is necessary to distinguish the qualitative differences between particular land uses. The examples of land use

categories typically used by models are: housing, industry, service-retail, streets and routes and in the case of the DUEM model [1] or gardens, field crops, pastures, vineyards, riparian, native vegetation, water, urban, barren and feedlots in the case of the SLEUTH model application in San Joaquin County in California, USA [2, 3]. The increase of the number of cellular automata states implies the higher complexity of transition rules. The calibration of complex transition rules is not an easy task as a sufficiently high number of observations of land use transactions between each land use category are required. In reality, land use change is a rather slow process usually offering an insufficient number of observations, especially in some land use categories.

To reconcile the complexity of transition rules with the available data on land use changes usually the number of land use categories is decreased by aggregating the land use categories of rare occurrence or land use categories that rarely undergo transformation. Another solution to the problem is to decrease the size of cells to obtain more observation of land use changes. *A priori* constraining selected land use transitions is yet another strategy how to reduce the transition rules complexity. For example, the CUF II model uses specific land use sequences that are assumed to be significantly more probable than others [4]. The restriction of selected land use transitions responds to the observed irreversibility of some land uses, such as urban land uses that can hardly be transformed to agriculture land use.


**Relaxing the cellular automata shape**

The homogeneity and regularity of cell shape does not conform to the complex morphology of physical structures, administrative and property borders observed in reality. This hinders the acceptance of cellular automata as practical tools for policy impact assessment. Some land use models, e.g. the one developed by Ferdinando Semboloni [5], relax the regular and homogeneous shape of cellular automata to adapt to irregular morphology and enable the representation of the parcel division and merger processes. The uneven spatial distribution of characteristics led, in the case of CUF I model, to individually adapting each cell shape to get cellular automata with homogeneous land use, regulations, ownership or physical characteristics [4, 6].


**Including distant interaction**

Each cellular automaton has a static set of finite neighbours to interact with. The influences from a broader context are gradually propagated through the neighbouring cellular automata by changing their states. This is appropriate for the study of diffusion processes such as processes of succession, spread of infections or dissemination of innovations. In reality, many drivers of land use change are not mediated through neighbouring cellular automata. Many land use change drivers are active in different temporal and spatial scales from the one, in which cellular automata act. For example many types of flows, i.e. flow of products, investment or population are at best ony implicit to the cellular automata transition rules.

The inclusion of distant interaction into cellular automata transition rules is in many cases realized by the extension of the cellular automata neighbourhood. For example, the Metronamica model extends the size of the neighbourhood from the traditional nine cell neighbourhood to one with hundreds of cells [7, 8]. The DUEM model expands the size of the neighbourhood in a similar way.

An extended neighbourhood enables the inclusion of distance as a factor influencing the strength of the interaction between pairs of cellular automata. In this respect, cellular automata get closer to the principle of space-interaction models that utilize some form of distance decay function. The inclusion of the distance decay function into cellular automata interaction further increases the complexity of simulation models and makes the models difficult to calibrate using the available data on land use change. When considering the necessity of evaluating the interaction between each pair of land use categories, the automatic calibration of the distance decay function based on available data as in space-interaction models is not feasible and some simplification of the calibration process is necessary. The Metronamica model reduces the definition of the distance decay function to four representative points, where each point has a special meaning in the neighbourhood. DUEM model implements only two discrete spheres of influence [8].

The inclusion of distant factors of land use change increases the ability of cellular automata to reflect important drivers of land use change. On the other hand it does not change the fact that the cellular automata immobility prevents from meaningful representation of real agents' decision making as the mobile agent can realize its preferences either by exploiting the characteristics of the locality, in which it resides or to move to a new location, from its preferences point of view more suitable. The agent-based models are therefore closer to the decision making processes of real agents such as households and firms and enable the study of the migration processes, residential choice and resulting processes of spatial concentration of agents and resources.

**Making cellular automata size and transition rules mutable**

The cellular automata behaviour is dependent on the size of cells, definition of their states (land use categories) and transition rules. As those characteristics are defined *a priori* and not easily modifiable in the course of simulation, it is impossible to explicitly represent the changing nature of land use transformations. There are several attempts to circumvent the immutable size and behaviour of cellular automata. For example, the SLEUTH model proposes behaviour aggregation by the concept of Deltatron, which is an agent that modifies the behaviour of individual cellular automata in such a way that the coordinated behaviour of a group of cellular automata emerges [2, 3]. A similar concept is used in the OBEUS model, in which the behaviour of unitary urban entities can be aggregated in the form of ensembles called domains. The opposite process of cellular automata division is presented in the model designed by Semboloni that employ the Voronoi partitions to cellular automata [9].

**Reflecting different temporal and spatial dynamics of land use change**

The land use change results from the immediate interaction among cellular automata in their neighbourhood. The transition rules do not reflect the past, land use changes or the potential of land use changes in the future. The autonomous behaviour of individual cellular automata represents the land use change only on the level of individual cells and the larger clusters of identical land uses are only product of their spontaneous behaviour. Therefore, the land use clusters are not regarded as qualitatively different, autonomous entities that would influence the behaviour of individual cellular automata by any means, i.e. by (dis)economies of scale. However, in reality observed land use changes demonstrate the autonomous dynamics that transcend the spatial scale of the automaton neighbourhood and the temporal scale of a single cellular automata cycle.

The land use models based on the principle of cellular automata adopt various strategies to cope with the problem of temporal and spatial dynamics of land use change. One approach, aiming at temporal dynamics of land use changes, is that of the land use life cycle. Each land use, once initiated, must pass through all of the prescribed life stages: initial stage, when it has a potential to initiate the land use changes in neighbouring cells, the maturity stage, when the ability to initiate land use change in its surrounding disappear, the stage of decline, when the land use disappears leaving space for another land use initiation. This principle is applied in the DUEM model [1].

An alternative approach considers land use change to be the result of a gradual accumulation of a particular land use potential over a certain time period. The cumulative potential equals the sum of past potentials in a certain time period that are discounted by the time decay [9].

Yet another approach does not derive the probability of land use changes exclusively from the influences of neighbouring cellular automata, but from past trends describing the overall land use changes. This approach is close to the Markov chain models and is employed by the SLEUTH model [2, 3].

The spatial continuity of land uses that is experienced in the real world as continuous fields of identical land uses had been introduced into the cellular automata by the concept of Deltatron [2, 3] and ensembles of land uses called domains in the OBEUS framework [10]. Deltatron is an agent of land use change residing in delta 2D space that is parallel to the cellular automata 2D space. Deltatron is initiated at the moment when an automaton spontaneously changes its land use. The initiated Deltatron than modifies the behaviour of single cellular automata in the neighbourhood in such a way that the bigger clusters of land uses gradually emerge. When Deltatron cease to be active, the cluster of spontaneously created identical land uses slowly disintegrates [2, 3].

**Economy of land use resources**

Land use changes are generated exclusively by autonomous decisions of cellular automata with regards to their neighbourhood composition ignoring the constraints to global availability of land use resource. The simple solution of the limited

resources allocation problem is to impose exogenous constraints on land use demand. The supply of the land use then does not result from the autonomous cellular automata behaviour anymore, but from the suitability of their characteristics for specific land use. A typical example of this approach is the Metronamica model [7].

Other approaches incorporate the demand and supply factors directly into the individual cellular automata decision making mechanism. This approach is adopted by the CUF II model [4], in which the decision making mechanism of cellular automata has the form of a multi-nominal regression model that evaluates the probability of each land use transition based on demand factors: percentage of employment change, percentage of household change, number of households, number of jobs, job/household ratio and supply factors of land suitability and accessibility. The demand and supply sides are balanced *a priori* and exogenously by calibrating the supply and demand parameters of multi-nominal regression model on the bases of historical land use changes [4].

In both of the cases presented, demand and supply are not adjusted endogenously. To establish the balance between the supply and demand endogenously, the explicit representation of the market mechanism would be necessary. The SLUDGE model created by Dawn Parker demonstrates such a mechanism [11]. The cellular automata in the SLUDGE model represent the landlords who decide between agriculture and industry land uses based on the profit that each land use offers. The profit is determined by two factors: the cost of production that is affected by negative externalities caused by pollution from the industry and the cost of transportation of products to the market place. Agriculture land use is the recipient of the negative externalities produced by a neighbouring industry. Price is established based on the shortage or surplus of products on the market, and the decision making of landlords is influenced exclusively by the price of the products on the market and the cost of production and transportation. During the simulation model run, each landlord tries to find the best use for its land given the neighbouring land uses, distance to market and price of products on the market. The model demonstrates that equilibrium can be attained by different land use configurations with different Pareto efficiency [11]. But even the SLUDGE model is still based on unrealistic assumptions: there is neither communication nor bargaining between individual landlords and the landlords are expected to have homogeneous preferences and willingness to pay. This may be true for many markets with ordinary goods but not for markets that most significantly influence land use: the housing and land markets. Houses and land as traded goods are heterogeneous in their characteristics. Furthermore, the preferences and constraints of individual buyers differ substantially with respect to houses and land.

To overcome the deficiencies the heterogeneous demand, individual characteristics of traded goods and process of individual transactions will need to be explicitly represented [12].

## Inclusion of exogenous factors of land use change

Often the impact of various regulatory and development policies on the behaviour of individual subjects need to be assessed. For those purposes each cellular automaton can be regarded as a landlord autonomously deciding on best use of its cell. Its decision that is based on its ideal preferences can be then externally constrained. In this way the land use simulation models, such as the Metronamica or the SLEUTH, can serve as the experimental environments that enable the impact of policy prescriptions in the form of spatial limits or the impact of various infrastructure projects to be tested.

There are several alternative approaches to the incorporation of external constraints to cellular automata decision making. In the SLEUTH model the autonomous behaviour of cellular automata is constrained ex-post [3]. However, in the Metronamica model, the exogenous factors of suitability, global accessibility and zoning enter directly into the transition function alongside traditional neighbourhood effects [7].

To evaluate the impact of external constraints on the behaviour of individual cellular automata, the unconstrained behaviour of cellular automata has to be considered first on the bases of their ideal preferences. But the inference of cellular automata transition rules only from the observed behaviour of real subjects does not enable the ideal preference structure of the subject to be distilled as a derivation of the subjects' preference structure exclusively from the observed behaviour can lead to the unrealistic behaviour of automaton mainly when there is a significant change in external constraints to their behaviour [14].

To simulate the unconstrained behaviour of cellular automata, the simulation models have to be based on an ideal preference structure that is declared by the decision making entities themselves and not derived from their observed behaviour. Various methods such as the conjoint analysis can be applied for the analysis of the ideal preference structure [15].

## The limits to cellular automata based land use models

The response to the oversimplification of the cellular automata models was the relaxation of the original cellular automata assumptions. The modifications of the original, oversimplified assumptions generally led to the improved predictive validity of land use cellular automata models such as the SLEUTH and the Metronamica [14, 3]. On the other hand, some limits for the representation of real land use change processes are inherent in the cellular automata principles. The cellular automata, while being supportive in illustration of complex system behaviour in general, offer only excessively oversimplified representation of real urban processes. The cellular automata do not reflect the real specificity of particular urban systems behaviour and does not make use of practical and scientific knowledge of them.

The effort to explicitly represent the driving processes of real land use transitions logically leads to more general agent-based models that are better suited to represent diverse subjects and entities participating in land use change, but the lack of suitable

data on the behaviour of individual subjects and data on the specific processes that prevent more widespread use of agent-based models. The cellular automata therefore remain very attractive due to their simplicity and abundance of land use and land cover data.

## Acknowledgments

## References

[1]   Y. Xie and M. Batty (2003), Exploring Cities Using Agent-Based Models and GIS, CASA UCL Working Series Papers 68, [Online]. Available: http://www.bartlett.ucl.ac.uk/casa/pdf/paper68.pdf. [Accessed 2012].

[2]   C. Dietzel and K. C. Clarke (2004), Replication of spatio-temporal land use patterns at three levels of aggregation by an urban cellular automata, Lecture Notes in Computer Science, 3304, 523–532, in Lecture Notes in Computer Science 3305, Springler-Verlag Berlin Heidelberg, pp. 523–532.

[3]   C. Dietzel and K. Clarke (2006), The effect of disaggregating land use categories in cellular automata during model calibration and forecasting, Computers, Environment and Urban Systems, vol. 30, pp. 78-101

[4]   F. Semboloni (2000), The growth of an urban cluster into a dynamic self-modifying spatial pattern, Environment and Planning B - Planning & Design, vol. 27.

[5]   J. Landis (1994), California Urban Futures Model: A New Generation of Metropolitan Simulation Models, Environment and Planning B, vol. 4, no. 21, pp. 399 – 420

[6]   J. Landis (2001), CUF, CUF II, and CURBA: A Family of Spatially Explicit Urban Growth and Land-Use Policy Simulation Models, in Planning Support Systems: Integrating Geographic Information Systems, Models, and Visualization Tools, Redlands, ESRI Press

[7]   RIKS BV (2012), Metronamica documentation, Research Institute for Knowledge Systems (RIKS BV), Maastricht, The Netherlands

[8]   B. Straatman, R. White and G. Engelen (2004), Towards an automatic calibration procedure for constrained cellular automata, Environment and Urban Systems,, vol. 28, no. 1-2, pp. 149-170

[9]   I. Benenson and P. M. Torrens (2004), Geosimulation: Automata-based modeling of urban phenomena, West Sussex: John Wiley & Sons Ltd.

[10] I. Benenson, S. Aronovich and S. Noam (2005), Let's talk objects: generic methodology for urban high-resolution, Computers, Environment and Urban Systems, vol. 29, no. 4, pp. 425-453

[11] D. C. Parker, Landscape Outcomes in a Model of Edge-Effect Externalities: A Computational Economics Approach., University of California at Davis, 1999.

[12] C. D. Parker and T. Filatova (2008), A conceptual design for a bilateral agent-based land market with heterogeneous economic agents, Computers, Environment and Urban Systems, vol. 32, no. 6, pp. 454-463

[13] P. Waddell (2002), UrbanSim: Modeling Urban Development for Land Use, Transportation and Environmental Planning

[14] D. Kim and M. Batty (2011), Calibrating Cellular Automata Models for Simulating Urban Growth: Comparative analysis of SLEUTH and Metronamica: CASA UCL

Working Series Papers 176, [Online]. Available: http://www.bartlett.ucl.ac.uk/casa/pdf/paper176.pdf.

[15] J. Vorel and K. Maier (2007), Learning the public preferences for living environment characteristics: the experimental approach. In PAPERS OF REAL CORP 007. Vienna, Austria, [Online]. Available: http://programm.corp.at/cdrom2007/archiv/papers2007/corp2007_VOREL.pdf.

# Comparing interacting particles systems to cellular automata traffic flow models

## Sylvain LASSARRE[1]; Antoine TORDEUX[2]

[1]Génie des Réseaux de Transports Terrestres et Informatique Avancée — IFSTTAR
Descartes II, 2 rue de la Butte Verte, 93166 Noisy le Grand, France
Tel.: + 33 145 925 764 – E-mail: sylvain.lassarre@ifsttar.fr
[2]Laboratoire Ville Mobilité Transport— Université Paris-Est
19 rue Alfred Nobel, 77455 Marne-la-Vallée, France
Tel.: + 33 164 152 139 – E-mail: antoine.tordeux@enpc.fr

## Abstract

Some interacting particles systems, describing the stochastic evolution of particles jumping on a lattice, are since recently used to model traffic flow. The approach is close to cellular automata. Yet, the time is continuous with particles models while the evolution is discrete with cellular automata. We propose to compare and connect the two modelling approaches. The comparison is illustrated through the basic uni-dimensional totally asymmetric simple exclusion process.

## Introduction

Microscopic traffic flow models by cellular automata have been developed since the 1990's, and based on discrete synchronous time and discrete space. They are used for theoretical purposes as well as simulation tools [1,2,3,4].
Interacting particles systems, proceeding from the fields of probability and statistical physics, are also applied to model traffic flow [5]. The evolution of particles jumping on a lattice by means of Markov jump processes in continuous time and on a discrete space, such as for instance an asymmetric exclusion process [6], is used to model multi-lane traffic flow [7]. The zero-range process [6,8] is fitted to model the evolution of vehicle distance gaps [9] and the evolution of vehicles platoons [10], as well as the misanthrope process [11,12].
One proposes to compare continuous-time interacting particles systems to stochastic discrete-time cellular automata. We try to show how interacting particles systems may be seen as an extension in continuous time of cellular automata in section 2. The main properties of interacting particles processes and cellular automata are introduced. The two modelling approaches are illustrated through the totally asymmetric simple exclusion process in section 3.

## Comparing particles systems to cellular automata

The interacting particles systems are composed of particles and sites, but different interpretations of particles and sites lead to different traffic flow models. For the basic exclusion process, a particle is a vehicle and a site is a cell that may contain at most one vehicle [7]. With the misanthrope process, a site is portion of a lane that may contain several vehicles [12]. The zero-range model is convenient to describe the evolution of the distance gaps in car-following [9]. Then, a site is a vehicle and a particle an unit of distance gap. When a vehicle jump to the next site, a unit of the distance gap is given to the following vehicle. The model is an exact mapping of an exclusion process for which the jump of a vehicle depends solely on the distance gap. The zero-range model is also used to model the evolution of vehicles platoons [10]. A site becomes an empty cell and a particle a vehicle following directly the cell.

Let $S$ be a finite set of sites. $\eta_t(x)$ is the number of particles at site $x \in S$ at time $t$. Then $\eta_t = \{\eta_t(x), x \in S\} \in E$ is the state of the process, with $E = \mathrm{N}^S$ or $E = \{1,\dots,K\}^S$ if the number of particles by site is limited to $K$. In this last bounded case, the interacting particles process is close to a cellular automaton. But the evolution schemes diverge. The former evolves in continuous time while the latter's evolutions is discrete.

### Particles system in continuous time

In continuous time, the process $\eta_t$ is a Markov jump process specified by a rate function at which transitions occur. If $S$ is finite, a transition from $\eta$ to $\xi$ (with $\eta \neq \xi$) occuring at rate $b(\eta, \xi)$ means that:

$$P_\eta(\eta_t = \xi) = b(\eta, \xi)t + o(t) \tag{1}$$

For the totally asymmetric exclusion process, the jump rate is the function:

$$b(\eta, \eta_x) = \lambda(\eta)1_{\eta(x)=1}1_{\eta(x+1)=0} \tag{2}$$

with $\lambda : E \to \Re^+$ the jump rate that may depend on the system state, $x$ a site and

$$\eta_x(x) = \begin{cases} \eta(z) & \text{if } z \neq x, x+1 \\ \eta(x)-1 & \text{if } z = x \\ \eta(x+1)+1 & \text{if } z = x+1 \end{cases}$$

In the simple case considered below, the jump rate is constant $\lambda(\eta) = \lambda$. For the zero-range process, the jump rate depends only on the number of particles on the

departure site, while for the misanthrope process it depends on the numbers of particles at the departure and arrival sites.

The process defined by jump rate function $b$ and space state $E$ is characterised by an operator $\Gamma$, denoted as the generator:

$$\Gamma f(\eta) = \sum b(\eta, \xi) \left[ f(\xi) - f(\eta) \right] \tag{3}$$

where $f$ belongs to $D(E, \Re)$, the set of functions from $E$ to $\Re$ depending on a finite number of coordinates.

The process is usually described by its performances in stationary state. The stationary distribution of the process $\pi : E \to [0,1]$ is such that:

$$\left\{ \forall \eta \in E, \, \mathrm{P}(\eta_t = \eta) = \pi(\eta) \right\} \Rightarrow \left\{ \forall \eta \in E, \, \mathrm{P}(\eta_{t+\delta} = \eta) = \pi(\eta) \right\}$$

For all $\delta > 0$. The stationary distribution is given by the generator. A probability measure $\pi$ on $E$ is stationary for the process $\eta_t$ if and only if the measure is not nil everywhere and if:

$$\sum_{\eta \in E} \pi(\eta) \Gamma f(\eta) = 0, \quad \forall f \in D(E, \Re) \tag{4}$$

Note that the sum is finite since $f$ only depends on a finite number of coordinates.

The set of the stationary distributions is always nonempty for finite $E$. Yet, explicit forms for the stationary distributions exist mainly in basic cases.

A reversible measure $\pi$ such that:

$$\pi(\eta) b(\eta, \xi) = \pi(\xi) b(\xi, \eta), \quad \forall \eta, \xi \in E \tag{5}$$

is stationary. It is easier to solve (5) than (4). Reversibility is a sufficient but not necessary condition for a measure to be stationary. For instance, totally asymmetric process may have a stationary distribution which is clearly not reversible.

The zero-range process admits a unique stationary distribution with a product form for spatial invariant initial configurations. The product form of a stationary distribution means that the number of particles by site are statistically independent in stationary state. This property generally simplifies the calculus. The misanthrope process has this property only in a particular case.

**Discrete time case towards cellular automata**

In a discrete time case, the process is defined at times $\{n\delta, n \in \mathrm{N}\}$ for a given time step $\delta > 0$. The discrete time process $\eta_n$ is yet indexed by $n$. In this case, the process is described by a Markov chain with transition matrix $P$ such that:

$$\mathrm{P}\big(\{\eta_{n+1}=\xi\}/\{\eta_n=\eta\}\big)=\mathrm{P}_\eta(\eta_1=\xi)=P(\eta,\xi)\quad\forall\eta,\xi\in E$$

(6)

$P$ is a probability matrix in the sense that $P(\eta,\xi)\geq 0$ for all $\eta,\xi\in E$ and $\sum_\xi P(\eta,\xi)=1$ for all $\eta\in E$.

For instance, assume that the process represents the evolution of the distance gap of a line of vehicles. A site $x$ is a vehicle and $\eta_n(x)$ is the distance gap of the vehicle $x$ at time $n$. For the basic symmetric model [1], vehicles jump with a speed that is the minimum beetwen the distance gap and the unit. The maximum vehicles' speed is the space step divided by the time step. For this deterministic model:

$$P(\eta_n,\eta_{n+1})=1$$

for

$$\eta_{n+1}(x)=\eta_n(x)+v_{n+1}(x+1)-v_{n+1}(x)$$

with $v_{n+1}(x)=\min\{\eta_n(x),1\}$.

The Markov chains are usually described in stationary state with the invariant distributions $\pi$ of the process $\eta_n$, satisfying:

$$\{\forall\eta\in E,\mathrm{P}(\eta_t=\eta)=\pi(\eta)\}\Rightarrow\{\forall\eta\in E,\mathrm{P}(\eta_{t+1}=\eta)=\pi(\eta)\}$$

and such that:

$$\sum_{\eta\in E}\pi(\eta)P(\eta,\xi)=\pi(\xi),\quad\forall\xi\in E$$

(7)

(this equation is usually related as the master equation in statistic physics). A reversible measure $\pi$ such that:

$$\pi(\eta)P(\eta,\xi)=\pi(\xi)P(\xi,\eta),\quad\forall\eta,\xi\in E$$

is stationary.

As for the continuous time case, the set of stationary distributions is not nil for the discrete time process when $E$ is finite. Explicit formula exist in basic cases. Note that the discrete time approach may lead to complexity due to potential deterministic periodicities that the continuous time case has not.

**Simulation of the processes**

In the continuous time case, each site with at least one particle has an exponential clock giving the jump time of one of its particles. The evolution is event driven and does not require to be specified. At each event (at each jump), one has to : select the site with the minimum next jump time, update the time, realise the jump and

calculate the new jump times of sites where the jump rates have been modified. Note that, from a practical view, the continuous time model avoids the problem of priority between two particles coveting simultaneously the same site, since particles jump successively.

In the discrete time case, the discretisation scheme and the value of the time step must be defined. For cellular automata, the update is synchronous. Yet, as we will show in a particular case in the next section, the choice of a synchronous or a sequential updates leads to different discrete processes.

The process can be simulated too by event as in the continuous time process by substituting the continuous exponential distribution with a discrete geometric distribution. The simulation can also be iterative, by updating all the sites at each time step.

**Connecting the approaches**

We aim now to connect the continuous and discrete time approaches. In the continuous time case, the time $T$ between a transition from $\eta$ to $\xi$ follows a continuous exponential distribution with parameter $b(\eta, \xi)$. In the discrete time case, this time, yet denoted $T_\delta$ is $\delta$ times a discrete geometric distribution with parameter $P(\eta, \xi)$. By choosing:

$$P(\eta, \xi) = \delta \times b(\eta, \xi) \quad \forall \eta, \xi \in E$$

one can explicitly demonstrate that the time for a transition in the discrete case converges in distribution towards the transition time in the continuous case:

$$P(T_\delta \leq t) = 1 - (1 - tb)^{t/\delta} = 1 - e^{-tb + 0(\delta)/\delta} \xrightarrow[\delta \to 0]{} 1 - e^{-tb} = P(T \leq t)$$

for all $t \geq 0$. This mapping allows to compare continuous and discrete time approaches through the value of the time step. Note that $\delta \leq 1/b$ is required so that the time discretisation has a meaning. The performances of the discrete process depend on the value of the time step.

**Totally asymmetric simple exclusion process**

The exclusion process [6] is an interacting particles system for which the number of particle by cell is limited to 1. In the discrete time case, the model corresponds to the NS traffic flow model [2] with a maximal speed value of 1. In the totally asymmetric case, the particles jump only to the next cell with a rate of $\lambda > 0$ if the cell is empty (see jump rate function (2)).

The process is one of the simpler conservative and uni-directional flow models. In the continuous time case, particles jump to next sites if empty, according to independent exponential clocks of parameter $\lambda$. In discrete time case with time step

$\delta > 0$, particles jump to next sites if empty, according to a probability $P$. To connect the models, let us assume that $P = \lambda \delta$. One has $\delta \leq 1/\lambda$ so that $P$ is a probability. The discrete process is deterministic if $\delta = 1/\lambda$ and random for $\delta < 1/\lambda$.

**Stationary distribution of the process**

The stationary distribution of the exclusion process is not known for any rate function. Yet, the simple process where the jump rate is constant is well-known. For an infinite lane and invariant in space initial configurations, if $\eta$ describes the distance gap of the vehicles, the unique stationary distribution $\pi$ of the totally asymmetric simple exclusion process is the product form:

$$\pi_v(\eta) = \prod_{x \in E} \tilde{\pi}_v(\eta(x))$$

[13] with the marginal geometric stationary distribution for the distance gap:

$$\tilde{\pi}_v(n) = (v/\lambda)^n (1 - v/\lambda)$$

For an infinite lane, the distribution depends on a velocity parameter $v$ usually called fugacity. For a bounded case, the invaraint distribution depends on the boudary conditions for an open system, or on the density level for a close system. The fundamental diagram of mean speed or flow volume as a function of density can be considered as a global indicator of the model performances studied in the traffic community. Using the stationary distribution of the distance gap, the mean value is:

$$D(v) = (1 - v/\lambda) \sum_{n=0}^{\infty} n(v/\lambda)^n = \frac{v}{\lambda - v}$$

while the fundamental diagram of flow volume $Q$ as a function of density $\rho$ is:

$$Q(\rho) = \lambda \rho (1 - \rho)$$

In the discrete time, the flow $Q_\delta$ as a function of density is:

$$Q_\delta(\rho) = \frac{1}{2\delta} \left(1 - \sqrt{1 - 4\delta \lambda \rho (1 - \rho)}\right)$$

if the update is synchronous [14], while the performance is the same as in the continuous time case for a random sequential update [15]. As expected, one has:

$$Q_\delta(\rho) \xrightarrow[\delta \to 0]{} Q(\rho)$$

The fundamental diagrams of mean speed and flow volume as a function of density are plotted for the continuous and discrete time cases in figure 1. For this model, the continuous time smooths the performances in stationary state.

**Trajectories obtained**

Some trajectories starting from an initial jam configuration are plotted in figure 2 to compare the approaches. In the deterministic discrete case where $\delta = 1$ the initial jam propagates indefinitely. It is not the case for the stochastic models where $\delta = 0.9$ or $0.5$ or when the time is continuous. In theses cases, the traffic seems to converge towards stationary states that do not explicitly depend on the initial configuration. This is clearly not the case for the deterministic model where the stationary state is a periodic limit state depending on the initial configuration. This observation suggests that the calculus of the stationary state may be easier with the stochastic models.
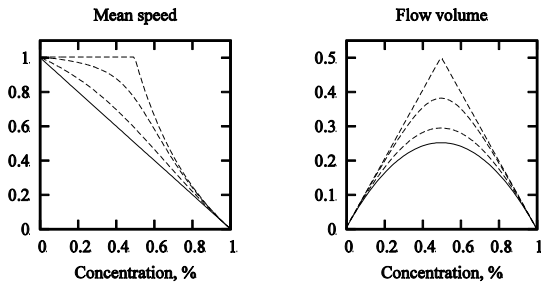


Figure 1: Fundamental diagrams in stationary state for the TASEP in discrete synchronous (with $\delta = 0.5$, $0.9$ and $1$, dotted lines) and continuous time cases $\lambda = 1$.

**Conclusion**

Homogeneous interacting particles systems differ from cellular automata through evolution schemes. The cellular automata models are defined in synchronous discrete time, while the particles systems are continuous in time. In both case, the simulation is easy.

The discrete time approach can lead to additional settings and parameters regarding to the continuous time approach. Yet, time discretisation can have a physical sense such as a reaction time, and allow to control the stochasticity. Notice that there is no periodic stationary state with continuous time models. This aspect may simplify analytical investigation as well as avoid unexpected periodic phenomena (sometimes related as ping-pong effect with cellular automata). Moreover, due to the sequential evolution of the particles, there cannot have conflict where two particles covet the same site simultanously with the continuous time. This aspect concerns notably multi-directional flow models by cellular automata and intersection traffic models. Lastly, the vehicles' maximum speed is bounded to a space step by a time step with

cellular automata (condition similar to CFL one). It is not the case with particles systems since the time is not discretised.
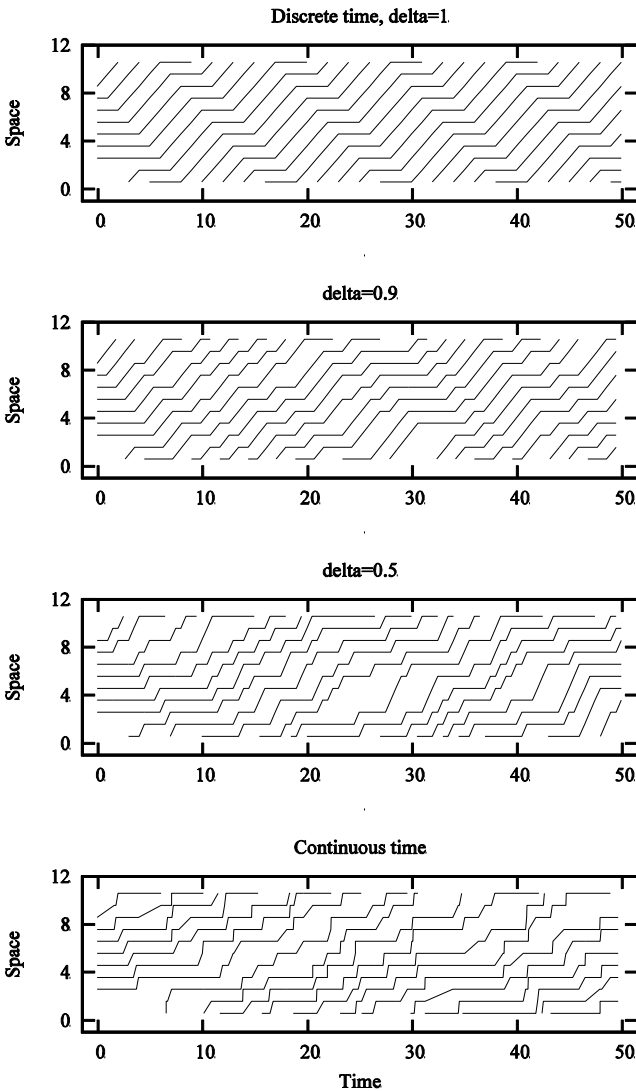


Figure 2: Trajectories of 7 particles since an initial jam configuration with the exclusion process where $\lambda = 1$ for different evolution schemes.

## References

[1]    W. Stephen. A New Kind of Science. Wolfram Media, Champaign, 2002.

[2]   K. Nagel and M. Schreckenberg. A cellular automaton model for freeway traffic. J. Phys. I, 2(12):2221–2229, 1992.

[3]   A. Schadschneider and M. Schreckenberg. Traffic flow models with «slow-to-start» rules. J. Phys. A Math. Gen., 509(7):541–551, 1997.

[4]   R. Barlovic, L. Santen, A. Schadschneider, and M. Schreckenberg. Metastable state in cellular automata for traffic flow. Eur. Phys. J. B, 5(3):793–800, 1998.

[5]   D. Helbing. Traffic and related self-driven many-particle systems. Rev. Mod. Phys., 73(4):1067–1141, 2001.

[6]   F. Spitzer. Interaction of markov processes. Adv. Math., 5:246–290, 1970.

[7]   A. Sopasakis and M. Katsoulakis. Stochastic modeling and simulation of traffic flow : asymetric single exclusion process with Arrhenius look-ahead dynamics. SIAM, 66(3):921–944, 2006.

[8]   E. Andjel. Invariant measures for the zero-range process. Ann. Prob., 10(3):525–547, 1982.

[9]   M. R. Evans. Phase transitions in stochastic models of flow. In A. Schadschneider, T. Pöschel, R. Kühne, M. Schreckenberg, and D. E.Wolf, editors, Traffic and Granular Flow'05, pages 447–459. Springer Berlin Heidelberg, 2007.

[10]  J. Kaupuzs, R. Mahnke, and R. J. Harris. Zero-range model of traffic flow. Phys. Rev. E, 2(72):056125.1–056125.9, 2005.

[11]  C. Cocozza-Thivent. Processus des misanthropes. Z. Wahr. Verw. Geb., 70:509–523, 1985.

[12]  M. Kanai. Two-lane traffic-flow model with an exact steady-state solution. Phys. Rev. E, 6(82):066107, 2010.

[13]  T.M. Liggett. Interacting particle systems. Springer, New-York, 1985.

[14]  A. Schadschneider and M. Schreckenberg. Cellular automation models and traffic flow. J. Phys. A Math. Gen., 26(15):679–683, 1993.

[15]  M. Kanai. Exact solution of the zero-range process: fundamental diagram of the corresponding exclusion process. J. Phys. A, 40(26):7127–7138, 2007.

# Drinking with friends

A cellular automata approach to modeling peer influence on binge drinking behavior

**Piper JACKSON[1]; Andrew REID[2]; Niki HUITSON[2];**
**Kathryn WUSCHKE[2]; Vahid DABBAGHIAN[3]**

[1] Software Technology Lab, School of Computing Science
1.778.782.7007, piper_jackson@sfu.ca (correspondent author)
[2] Institute for Canadian Urban Research Studies (ICURS), School of Criminology
1.778.782.3892, aar@sfu.ca / nrh@sfu.ca / wuschke@sfu.ca
[3] Modelling of Complex Social Systems, The IRMACS Centre
1.778.782.7854, vdabbagh@sfu.ca
[1,2,3]Simon Fraser University
8888 University Drive, Burnaby BC, V5A 1S6, Canada

## Abstract

Abuse of alcohol among post-secondary students is considered a serious health issue and a body of academic literature has developed around its study. Binge drinking, the consumption of five or more drinks in a single setting, is common, and clearly has strong social aspects. The influence of social interaction among peers on binge drinking has been noted but is not yet well understood. A cellular automata simulation of these phenomena is presented here. Model design, methodology, and experimental results are discussed. This project illustrates the role simulation modeling can take during exploratory phases of research.

## Introduction

The heavy consumption and abuse of alcohol among post-secondary students has gained considerable attention in recent decades, influencing a significant body of academic research [2][7][9][15]. Heavy episodic alcohol consumption, known as binge drinking, continues to be a popular social activity among post-secondary students, with a larger proportion of this population engaging in binge drinking than non-students of the same age [7][13].

Binge drinking is defined as the consumption of five or more drinks in a single session[1] (see [3][12]) and has been associated with a number of negative effects, including many with health, behavioral and social consequences [1][5]. Alcohol-related health and wellness concerns are particularly well-documented in recent

---

[1] There is significant variation and debate in the definition of binge drinking among academic literature. Some researchers include gender-specific definitions, such as five drinks per sitting for males, and four for females [6][7] [14]. Others add time constraints to further define a drinking session [5].

research. Long-term alcohol abuse is commonly associated with direct toxic effects such as liver and kidney damage [24]. Various health risks impact the post-secondary population in particular, including illness, injury, risky sexual behavior, alcohol dependence, and death [7][22]. Wechsler and Nelson [14] report than an estimated 1700 college-aged students die from alcohol-related injuries every year, a large proportion of which are associated with motor vehicle accidents. Heavy alcohol consumption has also been linked to poor academic attendance and performance, as well as criminal and deviant behavior, including physical and sexual assaults, vandalism, weapon use, drug use and arrest [2][5][7][10][23]. Second-hand impacts of heavy alcohol consumption have also been documented among non-bingers and abstainers within the post-secondary environment, including personal and property victimization, and interrupted study and sleep patterns [9][22].

Although its consequences are well documented, binge drinking is a complex behavior associated with and influenced by a variety of environmental, biological and social factors. Within the post-secondary setting, age, gender, family history and ease of accessibility to alcohol, among other factors, have been found to be related to the prevalence of binge drinking [13][15]. In addition, recent research has further stressed the importance of social influences on post-secondary student binge drinking. Such behavior is more prevalent among students involved in athletics and social organizations including fraternities and sororities [14][15][22]. The (actual or perceived) drinking patterns of peers and the approval of friends may also influence one's alcohol consumption [8][9][14]. These findings support the theoretical contributions of social learning theory, which proposes that human behavior, including binge drinking, is learned from interactions through peer groups and exposure to alternate values and norms [22]. With this in mind, investigating the effects of peer influences on binge drinking behavior may provide a better understanding of alcohol consumption in post-secondary students.

## Research through simulation modeling

While conventional statistical techniques are able to effectively demonstrate the importance of peer influence on binge drinking, they are limited in their ability to answer more complex questions about such behavior. For example, one may be interested in understanding how different types of social interactions effect the development of binge drinking among groups of college and university students. Similarly, one may be interested in understanding the effect of environmental factors on binge drinking behavior. Through the use of non-linear mathematical modeling techniques, these areas of interest may be explored.

In addition, such techniques may be employed in simulation models to test a variety of scenarios where "what if?" questions may be posed. For example, one may want to know if binge drinking behavior develops differently among populations that have different proportions of drinker types. Alternatively, one may be interested in knowing if populations of binge drinkers change over time when various social and environmental influences change. Through the use of non-linear mathematical modeling, it is possible to capture these complex dynamics and answer research questions that could influence public policy.

With respect to peer influences on drinking behavior, several non-linear mathematical models have been proposed. For example, Gorman, et al developed an agent-based model to examine social dynamics and environmental influences on agents' drinking behaviors [4]. Through a variety of simulations they were able to demonstrate that contacts between agents were important factors in the social dynamics that influenced drinking. Similarly, Ormerod and Wiltshire developed an agent-based model to analyze the growth of binge drinking in the United Kingdom [11]. Through development of a theoretical model and calibration with survey-based data, the authors were able to show that the imitative behavior spreading across social networks is a reasonable hypothesis to account for the patterns of binge drinking that had been observed in recent years.

Agent-based models, however, have some limitations. Applications of agent-based models in the social sciences often involve human agents with complex behavior and psychology that are difficult to quantify and calibrate. As a result, caution must be taken when interpreting the quantitative outcome of such models when the accuracy of the inputs is questionable [25]. In addition, agent-based models require the description of individual units which can be computationally intensive and time consuming [25], limiting the number of agents included in a simulation, as well as their detail and level of interaction.

In this project, we adopt Cellular Automata (CA) modeling as a means to focus solely on the elements of concern: individual state (binging) and local interactions (peer pressure). CA models are well suited for exploring the dynamics that occur within a population, and are useful for visualizing the clustering behaviour of communities. With this more abstract approach, it is possible to simulate large populations with reasonable computational requirements.

**Cellular automata modeling**

In a CA model, a population can be represented in a two dimensional square grid where each cell represents an individual in the population [17]. The state of each cell can vary depending on pre-determined rules. These rules are derived from an existing theoretical framework describing a particular phenomenon and are used to model what is happening in the real world. A CA model can effectively capture social interactions that happen over time [16][19]. Since each cell has the capability of holding the information pertaining to that cell, changes can be recorded. In general, CA models measure time discretely, in other words, progress through time is represented as a series of time steps. The cells capture the information at each time step and their states can alter through successive time steps [20].

In order to simplify the complexity of human behavior, CA modeling must make assumptions which are supported by research. While each cell in a CA model can potentially be influenced by surrounding cells, this model accounts for only four neighbors: north, south, east and west. The assumption here is that individuals are not impacted by everyone that physically surrounds them, but only those people they have social contact with. This type of neighborhood is called the von Neumann neighborhood.

In this CA model the social interactions progress through time steps. The cells capture the information at each time step and alter their state through successive steps. These updates happen simultaneously following the pre-determined transition rules. We assume this model to have a constant population even though there are processes of births, deaths, immigrations and emigrations in any population.

## The model

This model represents a social community of individuals with a high-risk of binging behavior that extends beyond the physical boundaries of a specific geographical area. Specifically, we consider a community of post-secondary students and their direct social acquaintances. This community consists of three types of individuals.

- Non-Binger (NB)
- Occasionally Binger (OB)
- Frequently Binger (FB)

An individual can only play a single role at a time. Over time individuals can transition from one state to the next based on predetermined rules. For example, an OB can become a FB due to social interaction, and later become a NB following a health problem. The purpose of this study is to analyze the evolution of a fixed population in a community of such individuals.

## Model design

This CA model integrates social influences and transition rules. The cells in the grid interact as individuals would in a social community. The cells change over time as they receive and give social influence to their neighbors. After each iteration, the grid is updated to reflect the modifications. Since this is a scenario-based model, the variables can be set according to input data and adjusted to reflect possible changes in the community. Although the cells are stationary, the state of the cell can vary. This reflects the change in social state individuals may experience during their life course. These changes occur as a result of social influences and experiences. We selected the von Neumann neighborhood and use the average of the surrounding cells to describe these social interactions. Further, at any given time only a random subset (i.e., one to four) of the neighbors exert social influence on a cell.

## Modeling Process

The process of developing this model was similar to that described in [18]. We began by surveying existing literature in order to generate a conceptual model of the phenomena under study. We found that for binge drinking, while its characteristics and effects have been well studied, the role of peer pressure is less well understood. Clearly it is important: within the post-secondary setting, direct peer influences may include pressure to consume alcohol by offering a drink, buying a round, or

encouraging drinking games [21]. Social influences may also be indirect or passive in nature, associated with perceived norms of heavy drinking among peer groups, and general accessibility to alcohol within the post-secondary education setting [9][15]. Ambiguity can be discouraging for a modeling project, but it is precisely due to the difficulty of performing real-world experimentation and study on this topic that makes this kind of attempt useful.

We proceeded to develop a mathematical model describing the various categories of binge drinkers, and how change in category occurs. A computational model was built, and preliminary experimentation showed the behavior resulting from the proposed model. From this evidence, we returned to the conceptual and mathematical models, and revised them. This process continued iteratively, noting new behavior, and making changes as our understanding improved or as new questions were raised. We retained intermediate models so that variations in modeling binge drinking can be compared. Through this exploration of the theoretical space associated with modeling binge drinking, we were able to identify some model characteristics that matched our understanding of the phenomena, and some that did not.

This approach is well suited to problems like this where the existing research does not yet fully explain how a process takes place. Combining mathematical modeling with computational simulation allows researchers to develop a possible model of the target phenomena and then test it in action to see if its behavior matches real data and experience, and is also consistent in a logical sense, i.e., the entities and mechanics in the model behave as expected. If the design results in behavior that runs contrary to the intention of the model, such as static behavior when dynamic phenomena are being modeled, or if there is a lack of expected interaction between entities, these are problems with the model itself. With complex phenomena, such problems may only become obvious through experimentation of the model in various scenarios, thus this is not a trivial step in this kind of research.
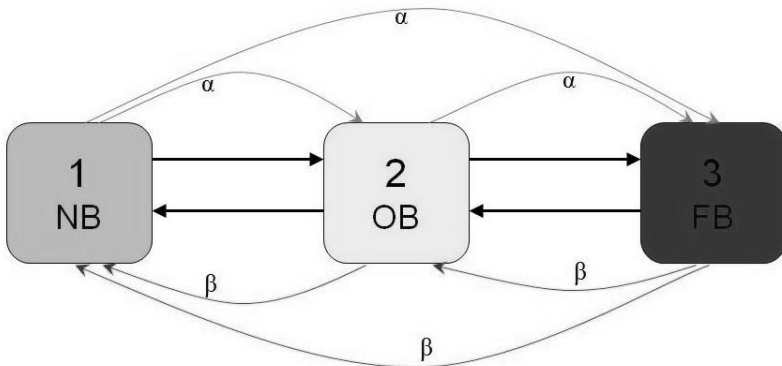


Figure 1: Model of drinking transitions

## A deterministic model for binging

Let $k \in \{1,2,3\}$ denote the state of each individual, where 1 is for NB, 2 is for OB and 3 is for FB. Let the location of each individual $s$ in the grid be denoted by $(i,j)$ and $N_s = N_{ij}$ show the neighborhood of $(i,j)$. We assume $1 \leq N_s \leq 4$. For each individual $(i,j)$ in the grid we define $C_{ij}(t)$ as the social counter of the individual $(i,j)$ at time $t$. Suppose $s$ is of type $k'$ for $k' \in \{1,2,3\}$ and $v_{kk'}$ denotes the values of the social influence of an individual of type $k$ on $s$ in the neighborhood $N_s$. Then we define

$$C_{ij}(t) = C_{ij}(t-1) + \varepsilon + \sum_{k \in N_{ij}} v_{kk'} \tag{1}$$

The parameter $\varepsilon$ is a randomly determined value with a normal distribution centered on zero. Using Figure 1 values of $v_{kk'}$ are $\alpha > 0$ or $\beta < 0$ based on the type of surrounding neighbors.

## Rules:

We assume that at the initial state $C_s(t) = 0$ for each cell $s$ in the grid.

**Case I:** $s$ is a NB ($s=1$)

- if $C_s(t) < -1$ for $T$ time steps then $s$ becomes an OB ($s=2$)
- if $C_s(t) < -10$ then $s$ becomes a FB ($s=3$) in the next time step

**Case II:** $s$ is a OB ($s=2$)

- if $C_s(t) < -1$ for $T$ time steps then $s$ becomes a FB ($s=3$)
- if $C_s(t) < -10$ then $s$ becomes a FB ($s=3$) in the next time step
- if $C_s(t) > 1$ for $T$ time steps then $s$ becomes a NB ($s=1$)
- if $C_s(t) > 10$ then $s$ becomes a NB ($s=1$) in the next time step

**Case III:** $s$ is a FB ($s=3$)

- if $C_s(t) > 1$ for $T$ time steps then $s$ becomes an OB ($s=2$)
- if $C_s(t) > 10$ then $s$ becomes an OB ($s=1$) in the next time step

Here $T$ is the number of time steps needed to effect change in individuals, and 1 and -1 are considered as threshold values for gradually changing the states of individuals. The thresholds 10 and -10 are considered for major circumstances that force individuals to change their states to 1 or 3, respectively.

## Simulation Details

The binge drinking cellular automata application was developed in Java, and as such can run on any common operating system. Many parameters can be altered,

including the dimensions of the grid and length of the simulation. Currently, grids of roughly 10,000 cells or less are supported. Execution time for an experiment can vary between a fraction of a second up to one minute for large grids and/or long simulations (2000 or more steps). Short execution times for experiments are a priority since it allows for more responsive and interactive exploration of the configurations of the simulation. The program features tabbed output allowing visualization of the cellular automata itself, as shown in Figure 2, as well as plots of interesting metrics, including population distributions and average cell value. Plot functionality is supported by the versatile JFreeChart library.



(a) Initial conditions

(b) After 100 steps

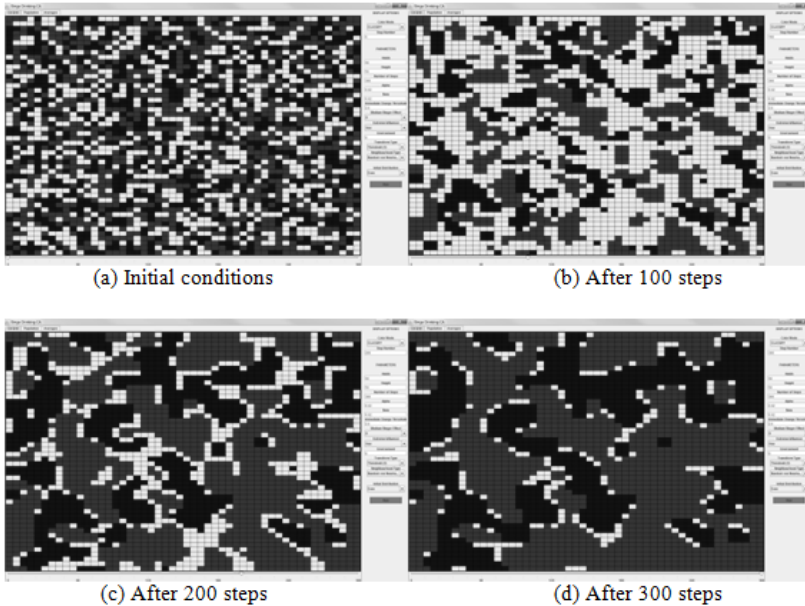(c) After 200 steps

(d) After 300 steps

Figure 2: Binge drinking cellular automata

## Experimental Results

Due to the exploratory nature of the development of this model, many possible configurations of parameter values and options were available for running experiments. The experiments described here used a 50 cell by 50 cell grid, and were run for 600 steps. Various options were tested on our threshold model using the base parameter values. Plots of the distributions of the populations of cell classes can be seen in Figure 3. The options tested were

- Whether or not cells in the extreme binging categories (NB and FB) can change

- • Whether initial cell values are distributed evenly across categories, or are distributed based on relationships found in a survey.

Testing whether or not cells in the most extreme categories could change was investigated since it seemed conceivable that people entrenched in a given behavior would not be susceptible to peer influence. After all four possible combinations of the options were run, some patterns emerged. If the cells in extreme categories do not change, then the CA as a whole quickly becomes dominated by the extreme categories. Any OB cells are eventually influenced by neighbors of one extreme or the other, until no mid-value cells remain. If cells of the extreme values can change, a short initial period is characterized by a flourishing of mid-values, but these are soon after absorbed into large, distinct clusters of extreme value. The use of the survey relationships for setting up experiments had a clear effect, since NB make up more than half of the total population. In this case, NB eventually dominated all the cells if extreme values were capable of changing; if extremes could not change, the OB cells still overwhelmingly changed state to NB. Notably, in all of these experiments the extreme classes end up dominating the cell grid.



(a) Even distribution, extremes do not change

(b) Even distribution, extremes can change

(c) Survey distribution, extremes do not change

(d) Survey distribution, extremes can change

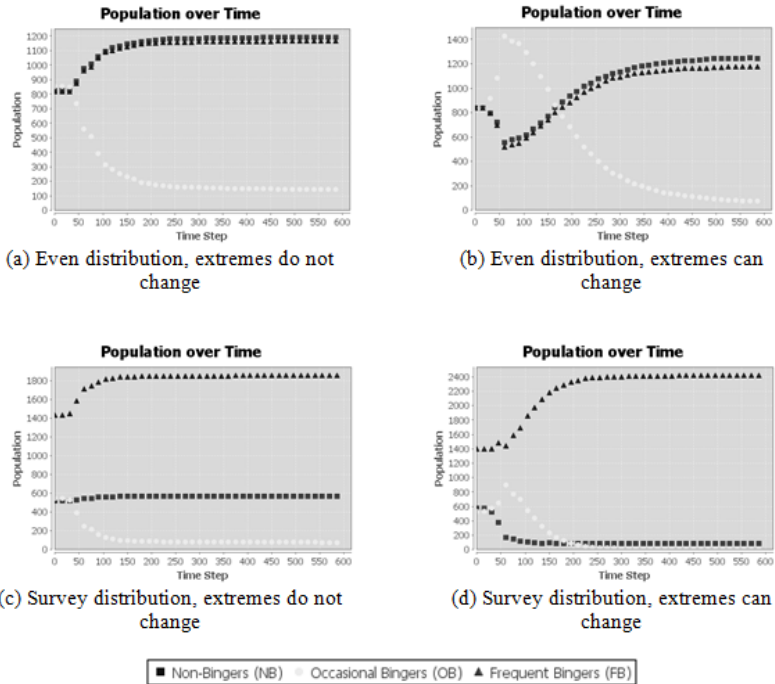■ Non-Bingers (NB)   ○ Occasional Bingers (OB)   ▲ Frequent Bingers (FB)

Figure 3: Experiments on population distributions

Experiments varying the strength of influence were also performed. The strength of positive influences (i.e., against binge drinking) is determined by $\alpha$; the strength of negative influences by $\beta$. They are usually set at 0.02, which allows for gradual but noticeable change over the lifetime of an experiment. If these values are equal, changing them simply alters the rate of change in the model. However, the model behaves differently if $\alpha$ and $\beta$ are not equal. With $\alpha$ set to less than $\beta$, if extremes cannot be influenced, the stronger force initially converts more OB cells, but once there are primarily only extremes left, the effect is minimal, since the remaining cells are entrenched in their behavior. If extremes can be influenced, the stronger force wins out eventually, dominating all cells. However, converting FB to NB, or vice-versa, is still a slow process. Figure 4 shows two runs of the model with $\beta$ (negative influence) higher than $\alpha$ (positive influence).
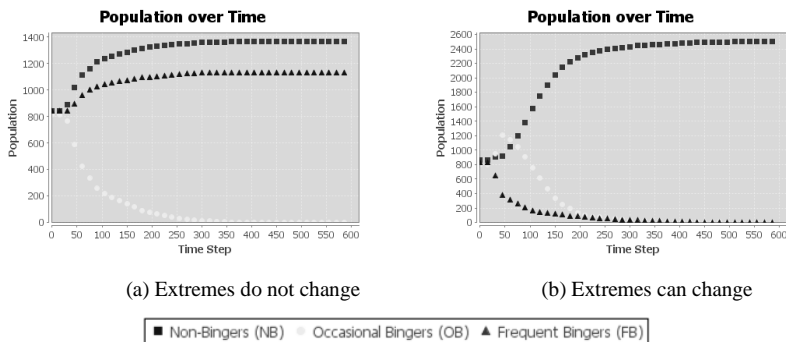


(a) Extremes do not change  (b) Extremes can change

■ Non-Bingers (NB)  ○ Occasional Bingers (OB)  ▲ Frequent Bingers (FB)

Figure 4: Experiments on influence strength, $\alpha = 0.02$, $\beta = 0.03$

In the base model, OB have no influence on similar neighbors. One alternate to this is for OB to have an effect equal to $\alpha$-$\beta$. Thus, they have a positive effect on each other if $\alpha$ is greater than $\beta$, and a negative effect if the reverse is true. However, this alternate rule simply accelerates any overall change in cell value. OB cells drift towards extreme values more quickly, and the overall state of the system approaches a steady state rapidly. This is true whether or not extreme values can be influenced.

## Conclusions

The models included in this paper present initial exploratory experimentation that is part of ongoing research into the social factors associated with binge drinking behavior. The cellular automata approach proves to be a promising method for investigating peer influences as it allows for both local and global population effects to be considered while taking into account the dynamics of various types of social and environmental influences. In the current work we adopted a simple approach that allows us to vary the flexibility of binge drinking classifications, the distribution of initial behavior classifications, and the strength of positive and negative types of influences.

Results of the experiments revealed several interesting patterns of social behavior including considerable variation in the speed at which individuals change their binge drinking habits. Such findings are encouraging at this early stage as they could lead to more significant discoveries in future research. For example, with further refinement to the model including the specification of positive and negative influences, the results of experimentations could lead to important policy implications for effective intervention strategies. It can also be used to support research employing more traditional methods, such as by suggesting what kind of questions should be asked in future surveys. We hope that this shows how simulation modeling can be used even during exploratory phases of research.

## References

[1] Cyders, M.A., K. Flory, S. Rainer, G.T. Smith (2009), The Role of Personality Dispositions to Risky Behavior in Predicting First Year College Drinking. Addiction, 104(2), pp. 193-202.

[2] Engs, R.C., D.J. Hanson, B. Diebold (1997), The Drinking Patterns and Problems of a National Sample of College Students, 1994: Implications for Education. Journal of Alcohol and Drug Education, Spring 1997.

[3] Gibson, C., C.J. Schreck, J.M. Miller (2004), Binge Drinking and Negative Alcohol-Related Behaviors: A test of Self-Control Theory. Journal of Criminal Justice, 32, pp. 411-420.

[4] Gorman, D.M., J. Mezic, I. Mezic, P.J. Gruenewald (2006), Agent-based modeling of drinking behaviour: a preliminary model and potential applications to theory and practice. American Journal of Public Health, 96(11), pp. 2055-2060.

[5] Hingson, R.W., T. Heeren, M.R. Winter (2006), Age at Drinking Onset and Alcohol Dependence: Age at Onset, Duration and Severity. Archives of Pediatrics and Adolescent Medicine, 160, pp. 739-746.

[6] Hingson, R.W., T. Heeren, M.R. Winter, H. Wechsler (2005), Magnitude of Alcohol-Related Mortality and Morbidity Among U.S. College Students Ages 18-24: Changes from 1998 to 2001. Annual Review of Public Health, 26, pp. 259-279.

[7] Hingson, R.W., T. Heeren, R.C. Zakocs, A. Kopstein, H. Wechsler (2002), Magnitude of Alcohol-Related Mortality and Morbidity among U.S. College Students Ages 18-24. Journal of Studies on Alcohol, 63, pp. 136-144.

[8] Kypri, K., J.D. Langley, R. McGee, J.B. Saunders and S. Williams (2002), High Prevalence, Persistent Hazardous Drinking Among New Zealand Tertiary Students. Alcohol and Alcoholism, 37(5), pp. 457-464.

[9] McCormick, A.V., I.M. Cohen, R. Corrado, L. Clement, C. Rice (2007), Binge Drinking Among Post-Secondary Students in British Columbia. BC Centre for Social Responsibility, Abbottsford, BC.

[10] McGee, R., K. Kypri (2004), Alcohol-Related Problems Experienced by University Students in New Zealand. Australian and New Zealand Journal of Public Health, 28(4), pp. 321-323.

[11] Ormerod, P. and G. Wiltshire (2008), 'Binge' drinking in the UK: A social network phenomenon. Mind and society: Cognitive studies in economics and social sciences, 8(2), pp. 135-152.

[12] Piquero, A.R., C. Gibson, S. Tibbets (2002), Does Self-Control Account for the Relationship between Binge Drinking and Alcohol Related Behaviours? Criminal Behaviour and Mental Health, 12, pp. 135-154.

[13] Sun, I.Y., J.G. Longazel (2008), College Students' Alcohol-Related Problems: A Test of Competing Theories. Journal of Criminal Justice, 36, pp. 554 - 562.

[14] Wechler, H., T.F. Nelson (2008), What We Have Learned From the Harvard School of Public Health College Alcohol Study: Focusing Attention on College Student Alcohol Consumption and the Environmental Conditions That Promote It. Journal of Studies on Alcohol and Drugs, 69(4), pp. 481-490.

[15] Weitzman, E.R., T.F. Nelson, H. Wechsler (2003), Taking Up Binge Drinking in College: The Influences of Person, Social Group, and Environment. Journal of Adolescent Health, 32, pp. 26-35.

[16] Alimadad, A., V. Dabbaghian, S.K. Singh, H.H. Tsang (2011), Modeling HIV spread through sexual contact using a cellular automaton. IEEE Congress on Evolutionary Computation, pp. 2345-2350.

[17] Chandler, S.J. (2003), Simpler games: using cellular automata to model social interaction. In P. Mitic (Ed.), Challenging the Boundaries of Symbolic Computation, Proceedings of the 5th International Mathematical Symposium, Imperial College Press, pp. 373-380.

[18] Dabbaghian, V., P. Jackson, V. Spicer, K. Wuschke (2010), A cellular automata model on residential migration in response to neighborhood social dynamics. Mathematical and Computer Modelling, 52, pp. 1752-1762.

[19] Hegselmann, R., A. Flache (1998), Understanding complex social dynamics: a plea for cellular automata based modeling. Journal of Artificial Societies and Social Simulation 1(3).

[20] Ilachinski, A. (2001), Cellular Automata: A Discrete Universe. World Scientific Publishing, River Edge.

[21] Borsari, B., K.B. Carey (2001), Peer influences on college drinking: A review of the research. Journal of Substance Abuse, 13, pp. 391-424.

[22] Durkin, K.F., T.W. Wolfe, G.A. Clark (2005), College students and binge drinking: an evaluation of social science learning theory. Sociological Spectrum, 25, pp. 255-272.

[23] Wechsler, H., J.E. Lee, M. Kuo, M. Seibring, T.F. Nelson, H. Lee (2002), Trends in alcohol use, related problems and experience of prevention efforts among U.S. college students 1993-2001: results from the Harvard School of Public Health College Alcohol Study. Journal of American College Health, 5, pp. 203-217.

[24] Del Boca, F.K., J. Darkes, P.E. Greenbaum, M.S. Goldman (2004), Up close and personal: temporal variability in the drinking of individual college students during their first year. Journal of Consulting and Clinical Psychology, 72, pp. 155-164.

[25] Bonabeau, E. (2002), Agent-based modeling: Methods and techniques for simulating human systems. Proceedings of the National Academy of Science, 99(3), pp. 7280-7287.

# Cellular automata based neural networks for modelling dual complex systems: Land-Use/Cover and transport networks.

**Reine Maria BASSE\*[1;] Hichem OMRANI[1]; Omar CHARIF [1,2;] Katalin BÓDIS [3] and Philippe GERBER[1]**

[1]CEPS/INSTEAD 3, avenue de la Fonte, L-4364 Esch-sur-Alzette, tel : (+352) 5858 55 325, Luxembourg

[2]Heudiasyc Lab., Université de Technologie de Compiègne, CNRS, Compiègne, France.

[3] EC JRC, IE, REU, 2749 via Enrico Fermi, TP450, 21027 Ispra (VA), Italy.

**Keywords:** Land use, land change modelling, cellular automata, artificial neural networks, transport systems, cross border region, The Greater Luxembourg.

## Abstract

When we take the time to observe nature, we often are surprised by the complex forms and behaviours that may emerge, surprised by the self reproduction and the self organisation phenomena that we notice, and we are compelled to acknowledge how difficult it is to understand this complex nature in perpetual state of evolution. By analogy to this nature, this paper deals with possible spatial evolution by combining two spatial systems: land use and the transport systems. However, underlying thi s evolution, there are processes that cannot be easily captured through the use of simple methods/statistical tools. Nevertheless, thanks to the emergence in the past few decades of artificial intelligence based models such as cellular automata and neural network models, this paper proposes to simulate future spatial evolution in Luxembourg and the Greater region up to 2020. The simulation results will act as the knowledge base which will make it possible to understand the functioning of complex cross-border areas.

## Introduction

Well aware of the stakes involved in understanding the processes that lead to the innovation of spatial systems as well as the innovation in diffusion strategies that often accompany them, geographers have mobilised diverse methodological approaches that could facilitate better understanding of land use as well as transport systems. Both these systems are complex, interdependent and complementary and they both play a specific and instrumental role in spatial dynamics, and particularly in urban dynamics.

Over the last few years, one of the most pertinent methodological approaches that has addressed the issue of spatial dynamics has combined land-use and transport systems in one single dynamic model. This approach particularly seeks tounderstand how transport and land use systems encroach upon each other, and

by doing so, determine the processes that influence land-use and land cover changes. Combining these two systems within one dynamic model was facilitated by the development of geographical information systems (GIS). However, to be fully aware of the spatial and temporal dynamics of these structures, it has been necessary to combine the GIS with artificial intelligence models such as cellular automata [1] or neural networks [2].

Cellular automata are known for their ability to model spatial interactions at different spatial levels (macro and micro) [3] [4]. Neural networks on the other hand have the advantage, when combined with cellular automata, of facilitating the development of spatial transition rules, and in particular, when these rules must take several types of land use classes into account [2]. Moreover, neural networks make it possible to determine the model's parameters. Nevertheless, the challenges associated to this type of hybrid model are at three levels: (1) definition of the evolution rule, (2) model calibration and (3) model validation.

This contribution seeks to provide a better understanding of the stakes, challenges and opportunities arising from a hybrid model and is structured around three main sections. The first section describes key insights and places our research within the context of previous studies on cellular automata and neural networks. In parallel, it makes explicit the advantages of CA models in geography and spatial modelling. Section two focuses specifically on the data and the methodological approach. It shows how machine learning algorithms like neural networks are designed as development models for cellular automata transition rules. The third section addresses the application of a neural-network based on cellular automata in Luxembourg and in the areas adjacent to its borders. This last section draws conclusions and proposes discussion around this hybrid model while placing a strong emphasis on the innovative aspects, perspectives, as well as on the issues that need further development in order to improve the model and optimise the results.

## 1. General background and related work

### 1.1. Cellular Automata based model as a framework for urban modelling

Scientists such as Alan Turing [5], Stanislaw Ulam [6], John von Neumann [7], and later John Conway [8] contributed to the cellular automata theory which considers cellular automata to be universal and complex tools [9]. The current paper goes beyond the tool factor and considers cellular automata as appropriate for modelling dynamic processes of complex systems and formalising them through a "bottom-up" approach. This approach considers that it is at the local level, via a well defined (local) neighbourhood, that complex structures at the global neighbourhood level arise. The interaction between local and global neighbourhoods is what led to the popularity of cellular automata in geography as from the 1970s. The famous law of the American geographer Waldo Tobler: *Everything is related to everything else, but near things are more related than distant things* [10], accompanied later by his vision of space as a grid of cells [11]-law and vision that would be taken up by other geographers [12] [13] [14]-marked the beginning of an interest in the cellular automata concept in geography and urban

planning [15]. However, it was the development of geographical information systems (GIS) which, through raster data formats, would facilitate comprehension [16] as regards cellular automata and urban simulation [17] [18]. While simulating land-use changes, the existence of multiple classes makes it difficult to set up transition rules based uniquely on elementary cellular automata. If the classes are binary (built-up land and not built-up land) a simple rule can be easily applied. But if additional classes as well as variables are taken into consideration, setting up a transition rule becomes complex. To alleviate this difficulty, some researchers have proposed more complex cellular automata [19] [20] or have used machine learning methods such as the support vector machine [21] and neural networks as the basis for generating transition rules of cellular automata [2].

## 1.2. ANN as the framework for CA model transition rule

The neural network model was developed parallel to cellular automata, and, like its predecessors, belongs to the family of artificial intelligence models [22]. As opposed to cellular automata, neural networks are not bound by a grid of regular cells. Theoretically, they are capable of accomplishing complex probabilistic, logical and mathematical functions. This is possible as their architecture (Figure 3) is based on a finite set of relations, connections, connectivities, interconnections and feedback loops (for more complex neural networks) between neurons, in a random manner [2]. Neural networks have a large capacity to learn data regardless of its quality, as well as the ability to grasp complex non linear input-output relations in the modelling process. They have different properties. (1) The neural network is constituted of a directed, weighted graph in which the nodes represent (2) the neurons. Each layer/group of neurons has what is known as an (3) activation function. It is this activation function that leads to neuron interconnectivity and also allows a neuron to influence other neurons. The connections between neurons are known as synaptic connections which are responsible of diffusing weighted neural activities also known as the synaptic weights. These synaptic weights are optimized by the (6) the learning algorithm, an additional property of neural networks which, through their analogy for living biological networks, simulate brain synaptic plasticity. The synapses' concept is fundamental in neural networks as it is on the basis of what we call synaptic coefficients (defined in the learning phase) that the network is calibrated. In our opinion, while synapses can be considered as transmission and/or information reception channels, neurons represent "zones" where the information transmitted or received by the synapses is stocked.

## 1.2.1. Why ANN? : Utility in land use changes and CA-based model

This section highlights the reasons that led us to use neural networks as the basis for generating transition rules for cellular automata.
The first reason is linked to the networks' ability to simulate complex functions due to their capacity to extract patterns from data and learn them thus, to facilitate the capturing of complex non linear relationships between different input variables and the output in an explicit manner. As we are well aware, land use is one of the most complex global spatial systems and this is linked, among other things, to (1) the

existence of numerous land use classes; (2) to the complex and non linear relationships between the classes (action, interaction, feedback loop); (3) to the existence of dependent, independent and interdependent variables which influence directly or indirectly the evolution of the land-use structure. Understanding this evolution and the changes in particular, implies that simulation and spatial modelling frameworks must take into account a variety of parameters. In addition, it is necessary to emphasise that the more the land use class categories, the harder it is to understand the land-use changes through spatial modelling. As a consequence, on the basis of this complexity, the simulation of land-use changes becomes one of the most arduous modelling tasks. This complexity cannot be captured through elementary cellular automata. The second reason is linked to the difficulty in determining transition rules in cellular automata. Neural networks offer a very attractive alternative in generating transition rules [2]. The latter is one of the most difficult characteristics to define in the cellular automata model especially when inputs are numerous and share a particularly complex relationship. The third reason is that neural networks have been successfully applied in Geography [23] [24] and compared to other models (e.g. Logit, SVM) neural networks produce better results [25] [26]. However, as in all artificial intelligence models, neural networks have shortcomings primarily based on the time factor which is necessarily important for setting up the model's parameters for convergence as well as for generalisation. In addition, it is often very difficult to find a "theoretical framework"/ an empirical explanation of the "interaction decision" between the neurons. Why is a neuron attracted to a particular neuron and not to another? It is nevertheless certain that the decision to interact leads to the emergence of complex structures with each passing moment, and in a non linear manner.

1.2.2. Details of the transition rules

This section gives details of how transition rules function. It also explores ANN's potential for CA-modelling. The transition rules presented here allow us to investigate possible land use changes of the study area between 2000 and 2020. Basically, the neural networks model functions in three phases. The first phase is relative to the construction of the model's structure on the basis of a database randomly split in two phases: the training phase and the testing phase. The second phase concerns network configuration based on the training data. During the first phase, an algorithm known as the learning algorithm is mobilised to serve as a weight optimization tool for the different synaptics connecting the network nodes. This algorithm is fundamental as it determines the learning capacity of the model. Learning is complete only when the algorithm has attained what we call a stable state. The recognition phase is the last phase. We could also speak of the network's restitution phase. This refers to analysing, in relation to the inputs injected into the model (input layers); whether the outputs correspond to expected outcomes (output layers). This step is also relevant in verifying the model's generalisation capacity.

Below is an example of a standard algorithm, the "multilayer perceptron" (ANN-MLP) with the standard back- propagation learning algorithm used to develop the model transition rules and the model's structure**.** The standard Back- propagation consists of minimising, using the gradient descent method, the mean square error given by:

$$E_p = \sum_{p=1}^{n_p} \sum_{j=1}^{n_L} \frac{1}{2}(d_j^L - y_j^L)^2 \qquad (1)$$

Where $d_j^L$ and $y_j^L$ are respectively the desired and the actual outputs for the $j$th neuron, $n_p$ is the number of patterns in the training data set and $n_L$ is the number of output neurons. $y_j^l$ is given by:

$$y_j^l = f(u_j^l) = \frac{1}{1 + e^{-u_j^l}} \qquad (2)$$

$$u_j^l = w_{j0}^l + \sum_{i=1}^{n_{l-1}} w_{ji}^l y_i^{l-1} \qquad (3)$$

Where $l = 1 \dots L$ denotes the number of corresponding layer S, $w_{jo}^l$ is the threshold (or bias) of the $j$th node in the layer $l$, $y_i^{l-1}$ is the input coming from the previous layer. In equation (2), the sigmoid has been chosen as the activation function.

The gradient descent method consists of minimising the error by updating the weights. The training ends after reaching an acceptable error or when processing the maximum number of iterations. The weights are updated using equation (6), first the error signals of the output and the hidden layers should be calculated and, subsequently, they are given by:

For the output neurons:

$$e_j^L = f'(u_j^L).(d_j^L - y_j^L) \qquad (4)$$

For the hidden layers:

$$e_j^l = f'(u_j^l) \sum_{r=1}^{n_{s+1}} (e_r^{l+1} w_{rj}^{l+1}) \qquad (5)$$

The weights in the hidden and output are updated using the following equation:

$$w_{ji}^l(k+1) = w_{ji}^l(k) + \alpha e_j^l y_i^{l-1} \qquad (6)$$

Where $\alpha$ denotes the learning rate, generally $\alpha \in [0,1]$. The bigger is the learning rate the faster is the training. A big learning rate may produce an unstable training process.

Below is presented the algorithm of an ANN-MLP trained using a "standard backpropagation algorithm" algorithm for a neural network with one hidden layer.

1) Define the network structure, assign initial weights randomly.

2) Chose a pattern to process.

3) For each node in the hidden layer

      evaluate the linear (1) and nonlinear outputs (2).

4) For each node in the output layer

      i. using the results of step3, evaluate the linear (1) and the non linear outputs (2)

      ii. calculate the error signals (4)

5) For each node of the hidden layer

      evaluate the error signals (5)

6) Update the weights of the hidden and output layers (6)

7) Repeat steps 3 - 6 for all patterns

8) Evaluate network error as well as the stopping criteria. If stopping criteria is not reached, repeat steps 2-5.

## 2. Materials and Methods

### 2.1. Study area, main inputs and data sources

Our case study area is Luxembourg and the greater region that constitutes a part of French (Lorraine), Belgium (Wallonia) and German (Rhineland-Palatinate and Saarland) territory, corresponding to a total population of more than 11 million inhabitants, that is, 3% of the EU-15 Member States' population covering 60 401 km². Thus, using a 100m×100m (one hectare) as a spatial resolution led us to deal with a grid of more than 6 million cells. The Greater region over the past few decades has become one of the most attractive regions in Europe [27] with Luxembourg emerging as an economic engine; this country comprises approximately 500 000 inhabitants and covers 2586 km². Even though Luxembourg is a small country, it has positioned itself as a "real core" within the European Union due to a strong economy that is primarily based on finance and industry. This economic strength impacts the migration flows which result in significant residential and daily mobility [28].

Different factors characterise the model's inputs. The first input is land-use in 1990 and in 2000, based on the Corine Land use classification in 100-m resolution [29]. Five land-cover classes are used for simulation; these are urban, industrial, water, agriculture and forest (table 1). It is at the land-cover level that we find interactions and feedback mechanisms between the different land-cover class categories. The second input is the physical factor which we refer to as *slope map*. It is given as a percentage calculated using a 100-m resolution Digital Elevation Model (DEM) [30]. The third input is related to the transport network which will enable us to evaluate the potential impact of the network on urban dynamics and to measure the distance from the cell to the given infrastructure (Table 1). In addition to these different inputs, we have used the Moore neighbourhood which comprises a grid of regular cells with a 3×3 window where each cell has 8 neighbours (table 1). As a

first step, the inputs of the cellular automata model are generated externally. In more precise terms, they are generated using a Geographical Information System tool (ARC-GIS-10 in this case) and Java before being "learned" by the neural network. They are then integrated in the cellular automata as is shown in figure 1 which gives precise details on the conceptual modelling approach.

Table. 1. Description of the model's inputs

| Category | Variable | Description |
|---|---|---|
| Spatial | Urban–neighbours | Amount of urban cells in the 3×3 Moore neighbourhood |
| | Industrial–neighbours | Amount of industrial cells in the 3×3 Moore neighbourhood |
| | Agriculture–neighbours | Amount of agriculture cells in the 3×3 Moore neighbourhood |
| | Forest–neighbours | Amount of agriculture cells in the 3×3 Moore neighbourhood |
| | Water–neighbours | Amount of water cells in the 3×3 Moore neighbourhood |
| Transport | Transport–neighbours | Amount of transport cells in the 3×3 Moore neighbourhood |
| | Distance–bus–station | Distance to the closest bus station (meters) |
| | Distance–train–station | Distance to the closest train station (meters) |
| | Distance–highway | Distance from cell to the nearest highway access point (km) |
| | Number–bus–station | Number of bus stations located 2km away from cell |
| | Number–train–station | Number of train stations located 2km away from cell |
| Physical | Slope | Slope value of cell (%) |
| | State | State of cell (1: built-up cell, 0: not built-up cell) |
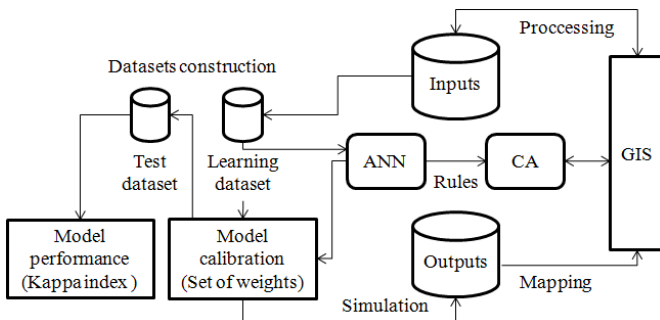


Figure 1. Conceptual CA based neural network model

### 2.2. Data preparation for model calibration and learning database construction strategy:

Table 2 summarises the data base for the periods 1990 and 2000 used for simulation. Different types of evolution are elucidated: increase, decrease or no change at all, as is the case with the transport network which remained unchanged

due to the fact that there was no new highway between the period 1990 and 2000. While growth is experienced in some of the land use classes such as the urban and the industrial classes, other classes such as agriculture and forest register a slight decrease. This decrease can be explained by the fact that the growth of built-up surfaces (industrial and urban) generally takes place to the detriment of undeveloped zones such as agricultural or forested areas. The class representing all the humid (water) zones registers very slight growth. This growth cannot be easily explained, but this could be as a result of measurement errors or of flooding which could have occurred during the two periods studied. While table 2 highlights the reality of the class evolutions observed between 1990 and 2000, table 3 presents the second phase which consists in cleaning up the data so as to ensure model convergence within minimal calculation time. This is known as the screening process and it makes it possible to eventually work on a real screened base of 71422 observations. To better adjust the model, it is essential to optimise the learning database. The simplest way to achieve this is to proceed by random sampling (50% of observation for the learning database and 50% for the testing phase) from the entire data base. However, in the case study presented here, a 50/50 random sampling is not ideal; on one hand, we run the risk of not taking into account the under represented classes which nevertheless determine the changes and the urban dynamics as is the case for urban and industrial classes, and on the other hand, we could under-estimate their role in the realism of the model. Subsequently, to attain the objective of a realistic model, we propose a learning database construction strategy. This consists of targeted sampling (table 4) concerning the urban and industrial classes, thereby guaranteeing their representativity in the calibration phase. To avoid choosing one particular division (vagaries), the base division screened in two parts (training phase and testing phase: the construction method is described here below) is repeated *n* times. This mechanism is known as *cross-validation* and it makes it possible to validate the model.

Table 2. Land use and transportation statistics (proportion) in observed periods 1990 and 2000

| Year | Urban | Industrial | Agriculture | Forest | Water | Transport |
|------|-------|------------|-------------|--------|-------|-----------|
| 1990 | 6.62  | 1.36       | 52.87       | 36.76  | 0.60  | 1.79      |
| 2000 | 6.75  | 1.54       | 52.57       | 36.74  | 0.61  | 1.79      |

Note: Configuration of the raster grid: squared grid with a resolution of $100 \times 100$ meters (cell size of 1ha) and Moore neighbourhood.

In the neural model, determining the number of units in the hidden layer is essential as the efficiency of the model depends on this parameter. To find the "optimal" number of units, we vary the number of units in the hidden layer between 2 and 20, and then select the number that minimises the error rate. The ANN-MLP model is repeated 10 times in order to estimate the error variation (mean and standard deviation) depending on the number of units (figure 2).
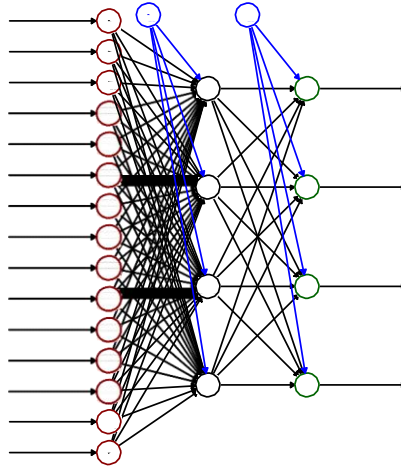
Figure 2: Architecture of ANN-MLP (outputs: V1, V2, V3, V4 correspond respectively to urban, industrial, agriculture and forest at time t1=2000; inputs: V5, V6, V7, V8, nbbus: number of bus stations, nbtrain, nburban, nbindustrial, nbagriculture, nbforest, nbwa ter, nbtransport, slope, dist_bus_station, dist_train_station) correspond to all variables/outputs at time t0=1990 ; described in table 1.

Table 3. Summary of land use classes, in the dataset, in observed periods 1990 and 2000

| Class | Total dataset | | | | Clean dataset | | | |
|---|---|---|---|---|---|---|---|---|
| | 1990 | | 2000 | | 1990 | | 2000 | |
| Class | # | % | # | % | # | % | # | % |
| Urban | 434574 | 6.62 | 442964 | 6.75 | 14735 | 20.63 | 16065 | 22.49 |
| Industrial | 89373 | 1.36 | 100994 | 1.54 | 7111 | 9.96 | 8437 | 11.81 |
| Agriculture | 3468229 | 52.87 | 3448154 | 52.57 | 21197 | 29.68 | 18773 | 26.29 |
| Forest | 2411034 | 36.76 | 2410159 | 36.74 | 15582 | 21.81 | 15187 | 21.26 |
| Water | 39042 | 0.60 | 39981 | 0.61 | 3077 | 4.31 | 3240 | 4.54 |
| Transport | 117228 | 1.79 | 117228 | 1.79 | 9720 | 13.61 | 9720 | 13.61 |
| Sum | 6559480 | 100 | 6559480 | 100 | 71422 | 100 | 71422 | 100 |

Note: We want a dataset with all the unique observations. Thus a preliminary step was conducted to remove the duplicate observations from the whole dataset (6559480 observations). As result, we obtain a clean dataset with unique patterns with 71422 observations

Table 4. Summary of land use classes, in the dataset, after cleaning

|  | Total dataset | | Training dataset | | Test dataset | |
|---|---|---|---|---|---|---|
| Land use | # | % | # | % | # | % |
| Urban | 16057 | 27.49 | 9575 | 27.33 | 6482 | 27.75 |
| Industrial | 8410 | 14.40 | 5109 | 14.58 | 3301 | 14.13 |
| Agriculture | 18773 | 32.14 | 11316 | 32.29 | 7457 | 31.92 |
| Forest | 15161 | 25.96 | 9040 | 25.80 | 6121 | 26.20 |
| Sum | 71422 | 100 | 35040 | 100 | 23361 | 100 |

In the table below (table 5) (confusion matrix), we present the prediction results (ANN-MLP (h*=4)) for the testing phase. This matrix makes it possible to merge the observed and the predicted data. The overall rate of correct prediction is 88.76%.

Table 5: Confusing matrix from ANN-MLP model using test dataset

|  | Urban | Industrial | Agriculture | Forest | Accuracy (%) |
|---|---|---|---|---|---|
| Urban | 3741 | 63 | 342 | 59 | 88.96 |
| Industrial | 76 | 3363 | 556 | 210 | 79.97 |
| Agriculture | 26 | 191 | 3835 | 153 | 91.20 |
| Forest | 2 | 135 | 76 | 3992 | 94.93 |
| Reliability (%) | 97.29 | 87.46 | 79.74 | 90.43 | 88.76 |

Note: Accuracy and reliability are two common measures obtained from the confusion matrix (details are given in the next sub -section). The diagonal elements in the matrix represent the number of correctly classified pixels of each class and the off-diagonal elements represent misclassified pixels or the classification errors.

### 2.3. Kappa index method for land use accuracy assessment: preliminary analysis

We have used the Kappa Index of Agreement (KIA) method to validate the model [31] [32] [33]. This method allows us to show the agreement between observed and simulated accuracy/data. The table 6 represents the confusion matrix of the observed and the simulated data for the period 2000. The diagonal of the matrix represents the number (also expressed as a percentage) of the accurately predicted cells. The values outside the diagonal represent the simulation errors for the period 2000. The results represented in table 7 generally confirm a good model calibration and show the model's capacity to replicate the observed reality, that is to say, the situation in the year 2000.

Table 6: Confusing matrix between the observed and the simulated land uses in 2000 (in %)

| | | Simulated land uses in 2000 | | | | |
|---|---|---|---|---|---|---|
| | | Urban | Industrial | Agriculture | Forest | Total |
| Observed | Urban | 434135 | 12 | 8556 | 253 | 442956 |
| land | | (98.009) | (0.003) | (1.932) | (0.057) | (100) |
| uses | Industrial | 435 | 87731 | 10852 | 1940 | 100958 |
| in 2000 | | (0.431) | (86.899) | (10.749) | (1.922) | (100) |
| | Agriculture | 35725 | 446 | 3411132 | 851 | 3448154 |
| | | (1.036) | (0.013) | (98.926) | (0.025) | (100) |
| | Forest | 8 | 731 | 1419 | 2407845 | 2410003 |
| | | (0.000) | (0.030) | (0.059) | (99.910) | (100) |

Note: For the confusion matrix table we have used the value of 0.44 as the cut off threshold. This threshold allowed us to calibrate the model: we assign the cell the land use class with maximum probability if this maximum probability exceeds the given threshold and if not the cell keeps it previous state.
Kappa Index of Agreement (KIA) for Overall Kappa:

$$KIA = (p_o - P_c)/(1 - p_c) \qquad (7)$$

where, $p_o$ represents the observed accuracy or the proportion of agreement. $p_c$ represents the chance agreement.
Kappa Index of Agreement (KIA) for the category Kappa:

$$KIA = (p_{ii} - p_i * p_i) / (p_i - p_i * p_i) \qquad (8)$$

where, $P_{ii}$ represents the proportion of unit agreement in row [i] at column [i]. $P_i$ represents the proportion of unit agreement for expected chance agreement in row [i].
As regards the Kappa results, table 7 presents two types of results. One shows the model's performance in relation to the entire database studied, that is, the overall result based on equation (7) and other more detailed results which show the same model's performance in different land use categories base on equation (8). The KIA results range from 0 to 1 where the values 0 and 1 signify respectively, poor and perfect agreement. Globally speaking, as table 7 has shown, there is an almost perfect agreement between the observed and the simulated situations (table 7).

Table 7: Detailed Kappa results, overall and per land use class

| | Overall | Urban | Industrial | Agriculture | Forest |
|---|---|---|---|---|---|
| Kappa | 0.983 | 0.978 | 0.867 | 0.976 | 0.998 |

Land use maps are considered to be *categorical maps* and consequently, the kappa index and other derivative approaches (eg. Fuzzy set approach [34]) are thought to be useful methods for assessing the similarity between observed and simulated datasets [35]; [36]. However, the kappa method has been highly criticised for

failing to distinguish whether land use/cover class changes during the transition phase are drastic or not. Moreover, regardless of the level of change that a given land use/cover class undergoes, the values remain extremely high. This is problematic when simulating territories where the urban system is far from equilibrium (in other words, a city with a phase of exponential urban growth). However, when simulation is carried out in spaces where the urban systems are in equilibrium (urban and/or constant growth) as is the case in most European cities where anticipating exponential urbanisation is no longer feasible, using the kappa index remains a valid and interesting method to distinguish the differences between observed and simulated situations. This method is also valid when comparing results within a comparable study area, in other words, a similar study area. However, even though the results are good in general, the kappa index remains inadequate as a validation method and must be compared with other methods of validation. It is for this reason that we propose, in a more detailed contribution, to use other validation alternatives based on existing models that have already been tried and tested such as Receiver Operating Characteristic (ROC), cross validation or the pattern based analysis (eg. cluster analysis [37]).

## 3. Simulation results

The analysis of the results shows that the automata based neural network model presented in this paper functions well in general. Indeed, table 8 which summarises the observed and simulated results up to 2020 shows reasonable results concerning the evolution of each land use class as well as coherency in simulation. Some of the land use classes expand to the detriment of others. This is the case of the urban and industrial classes over the agricultural class (Table 8). This table also shows that relationships between land use classes appear to be very complex. This is especially true for the urban and the industrial classes which are sometimes difficult to dissociate. Both classes represent artificialised areas and often interconnect in order to constitute continuous, discontinuous or mixed settlements, a fact that complicates spatial modelling. In addition, even if these two classes are interconnected, they do not have the same level of influence over each other because, if it is true that an industrial class can "easily/frequently" become an urban zone (after a decrease in industrial activities in a region for example) the contrary is less frequent. The results also show that if the expansion of urban and industrial classes was continuous, it became stable with time. This can be easily explained: the land reserves which were available 20 years ago and which led to a dispersed urbanisation no longer exist. In addition, as the cartographic results show, urbanisation in 2020 only points to a continuation of previously observed trends and is located in already urbanised areas as well as along transport axes (Figure 4).

Actually, urban growth is particularly significant around transport infrastructures. Undoubtedly, interdependence exists; urban growth is stimulated by the presence of a transport infrastructure and depends on the distance of the land use class from the transport infrastructure in question (Table 1). The neural networks as well as the cellular automata seem to have effectively highlighted

this interaction between these two complex systems namely land use and transport networks. Moreover, this urban structuring around transport axes explains (Figure 4) the metropolitan urban organisation of the Greater Luxembourg in different axes/ parts of the territory. A first, highly urbanised, North-West axe corresponds to the Belgian part of the territory. It is here that we find the largest urban areas such as Liège or Charleroi. Next, there is a second Centre-South axe which corresponds to the Luxembourg and French part of the study area; with linear urbanisation, it is also represented by large urban centres such as Luxembourg, Metz and Nancy. Finally there is a third axe that is less linear which corresponds to the German-Luxembourg part of the Greater Region with the polarised area on the German side through Saarbrücken. Close to the polarised areas, there is a large urban sprawl over the whole territory. Generally speaking, most of the urban growth takes place on desirable spaces, that is to say, spaces well adapted for urban growth as they have less steep slopes (Table 1). Nevertheless, it is important to highlight the fact that even if there are higher levels of urbanisation in this region, forested and agricultural lands take up most of the territory (Table 3 and table 8). The simulation results also confirm that, in addition to the transition rules (good convergence/coupling between CA and ANN), the cell states and the neighbourhood configuration, the influence of spatially roads and there derivative distances are also fully determinant in cellular automata based models and can induce urban growth [38].

However, as regards figure 4, by comparing the different situations taken into account (observed and simulated situations in 2000), it appears that the model indicates a highly urbanised zone which was inexistent in the situation observed in 2000 and which will persist until 2020. Several questions arise: why is this urban growth situated at this level (and not elsewhere) of the study area? Why will it persist up to 2020? Why is the urban class that is hardly present in this area overestimated and not the forest class which is very close-by and which also dominates this particular part of the territory? Is it due to the fact that the forest class is located on a highly steep slope considered to be repulsive to urbanisation? We can propose a few answers but these must be treated with caution. First, as regards the model, and more specifically at the model calibration level which uses a neural network which clearly overestimates urbanisation in this part of the territory compared to the situation observed. This suggests that the neural network proposes a stronger attraction between the urban class and the agricultural class than with the other classes in the immediate vicinity and that it is undoubtedly necessary to stabilise the connections between the urban class and the agricultural class so as to maintain over time a more realistic model. However, this does not explain why we observe this here and not elsewhere. This calls for further reflection and discussion in our current and future research projects. Secondly, beyond the model, it appears that this urban growth, even though nonexistent in the situation observed, is not unrealistic as it takes place close to a vast transport network where the industrial classes are also located. Moreover, this urban growth (which is discriminatory) takes place to the detriment of agricultural spaces as the latter are highly desirable and favourable for urban development (high suitability area for

urbanisation). This is a phenomenon that we have observed in our different studies and which is a daily reality in our regions.

Table 8: Simulated land use changes by class in hectares (%)

| Land use | Observed situation | | Simulated situation | | |
|---|---|---|---|---|---|
| | 1990 | 2000 | 2000 | 2010 | 2020 |
| Urban | 434 574 | 442 964 | 470 314 | 470 320 | 470 320 |
| Industrial | 89 373 | 100 994 | 89 375 | 89 417 | 89 478 |
| Agriculture | 3 468 229 | 3 448 154 | 3 432 422 | 3 432 356 | 3 432 289 |
| Forest | 2 411 034 | 2 410 159 | 2 411 099 | 2 411 117 | 2 411 123 |
| Road | 39 042 | 39 981 | 39 042 | 39 042 | 39 042 |
| Water | 117 228 | 117 228 | 117 228 | 117 228 | 117 228 |
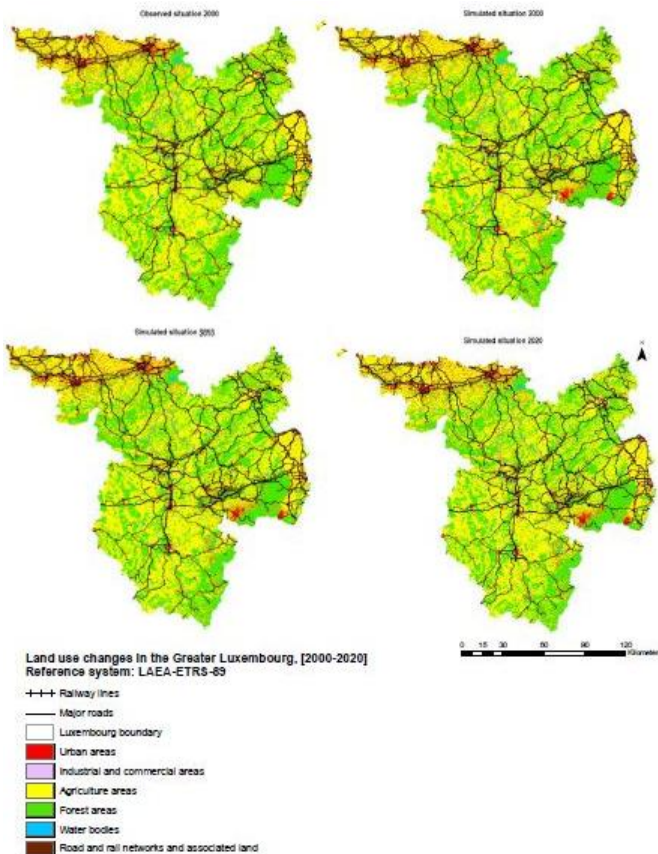


Figure 4: Cartographic simulation results: The Greater Luxembourg in 2020.

## 4. Conclusions and discussions

The results presented in the different tables show that the relationships and interactions between the different land use classes are often complex and difficult to understand. All the classes do not function in the same manner and some classes have an impact on the development of others. This is especially true for the urban and industrial classes; for example, the majority of the growth observed in industrial and urban classes occurs to the detriment of agricultural classes. Ultimately, what the model developer seeks to achieve, regardless of the model used, is to simulate land use changes, is to emphasise/reproduce real urban structures/patterns.

The paper presents a model which integrates neural networks into a cellular automata model and shows that these two tools are complementary and able to provide significant results for analysing complex systems. However, it is still extremely difficult to calibrate this type of model even if its structure appears to be simple. Moreover, taking into account several variables in addition to the land use classes accentuates this difficulty and lengthens the time necessary to implement the model. The neural networks in this work made it possible to: (1) elaborate cellular automata transition rules, to (2) determine the parameter values, (3) to make a non linear prediction of the land use changes all the while (4) minimising the input level errors of the model. However, this type of model raises questions: Are we really in the presence of a cellular automaton? Would it not be more appropriate to speak of a Neural Automaton (NA)? In future studies, we hope to improve the model by applying, for example, other validation tools such as the multi-class Receiver Operating Characteristics (ROC). Taking into account new variables, such as population, distance from the border, could, in the near future, make it possible to better analyse the robustness of the model. Finally, to better understand the urban phenomenon in the Greater Region, we will also consider the integration of variables such as *suitability maps* in order to get around the problem of zoning unavailability (impossible to attain in such broad border cases) on one hand and on the other, we will propose an urban development of the Greater Region and of Luxembourg which is as close as possible to the reality.

## References

[1] Batty, M., Xie, Y. (1994). "From cells to cities. " Environment and planning B: Planning and Design, 21: 531-538.

[2] Li, X., Yeh, A.G.O. (2002). "Neural-network-based cellular automata for simulating multiple land use changes using GIS." International Journal of Geographical Information Science, 16 (4): 323-343.

[3] White, R., Engelen, G. (2000). "High-resolution Integrated Modeling of the spatial Dynamics of Urban and Regional System." Computer, Environment and Urban Systems, 24: 383-400.

[4] White, R. (2005). "Modelling Multi-scale Processes in a Cellular Automata Framework". In J. Portugali, ed.: Complex Artificial Environments, Springer-Verlag (2005), pp.165-178.

[5] Turing, A. (1950). " computing machinery and intelligence." Mind 59(236): 433-460.

[6]  Ulam, S. (1952).  "Random  processes  and  transformations." International Congress ofMathematics.

[7]  von Neumann, J. (1966). Theory of Self-Reproducing Automata, University of Illinois Press, Urbana.

[8]  Gardner, M. (1970). "The fantastic combination of John Conway's new solitaire game life." Scientific American. 223: 120–123

[9]  Wolfram, S. (1984). "Cellular automata: A Model of Complexity." Nature 31: 419-424.

[10] Tobler, W. R. (1970). "A computer movie simulating urban growth in the Detroit region." Economic Geography 46(2): 234-240.

[11] Tobler, W. R. (1979). "Cellular geography" in Philosophy in Geography, S.Gale, G.Ollson (Eds), Reidel, Dordrecht: 279-386.

[12] Couclelis, H. (1985). "Cellular Worlds: A framework for modeling micro-macro dynamics." Environment and Planning A (20): 99-109.

[13] Phipps, M. (1989). "Dynamical Behavior of Cellular Automata under the constraint of Neighborhood Coherence." Geographical Analysis 21: 197-204.

[14] White, R., Engelen, G. (1993). "Cellular automata and fractal urban form: a cellular modelling approach to the evolution of urban land use patterns." Environment and Planning A: 25: 1175-1199.

[15] Benenson, I, Torrens, P M. (2004). "Geosimulation: object-based modeling of urban phenomena." Computers, Environment and Urban Systems 28(1-2): 1-8.

[16] Clarke, K. C., Gaydos, L. (1998). "Loose coupling a cellular automata model and GIS: long-term growth prediction for San Francisco and Washington/Baltimore." International Journal of Geographical Information Science, 12: 699-714.

[17]  Batty, M., Xie, Y., Sun. Z. L. (1999). "Modeling urban dynamics through GIS-based cellular automata. " Computers, environment and urban systems, 23(3):205–233.

[18] Torrens, P. M., O'Sullivan, D. (2001). "Cellular automata and urban simulation: where do we go from here." Environment and Planning
B: Planning & Design 28(2): 163-168

[19] White, R., Engelen, G. (1997). "Cellular Automata as the basic of integrated Dynamic Regional Modelling." Environment and Planning B 24: 235-246.

[20] Barredo, J. I., Kasanko, M., McCormick, N., Lavalle, C. (2003). "Modelling dynamic spatial processes: simulation of urban futur e scenarios through cellular automata." Landscape and Urban Planning 64(3): 145-160.

[21] Yang, Q., Li, X., Shi, X. (2008). "Cellular automata for simulating land use changes based on support vector machines." Computers & geosciences, 34(6):592–602.

[22] McCulloch, W.S, Pitts, W. H. (1943). "A logical calculus of the ideas immanent in nervious activity." Bulletin of Mathematical Biophysics 5: 115-133.

[23] Openshaw, S., Openshaw, C. (1997). Artificial Intelligence in geography. Chichester, England: John Wiley & Sons.

[24] Wang, F. (1994). "The use of artificial neural networks in a geographical information systems for agricultural land-use suitability assessment." Environment and Planning A: 26: 265-284.

[25] Zhou, J., Civco, D. (1996). "Using genetic learning neural networks for spatial decision making in GIS. " Photogrammetric Engineering & Remote Sensing, 62, 1287-1295.

[26] Omrani, H.,. Charif, O., Gerber, P., Bodis, K., Basse, R. M. (2012). "Simulation of land use changes using cellular automata and arti ficial neural network. " Technical report, CEPS/INSTEAD working paper series.

[27] Sohn, C., Reitel, B., Walther, O. (2009). "Cross-border metropolitan integration in Europe. The case of Luxembourg, Basel and Geneva. " Environment & Planning C. 27: 922–939.

[28] Omrani, H., Charif O., Klein O., Gerber P., Trigano P. (2010). "An Approach for spatial and temporal data analysis: application for mobility modeling of workers in

Luxembourg and its bordering areas." In: IEEE-SMC. IEEE International Conference on Systems, Man, and Cybernetics. ISTANBUL, 2010, pp.1437-1442.

[29] EEA (2000). CORINE land cover technical guide—Addendum 2000. Technical report No 40, European Environment Agency, Copenhagen, pp. 105. Documentation: URL: http://reports.eea.europa.eu/tech40add/en       Data       source:       URL: http://dataservice.eea.europa.eu/dataservice/metadetails.asp?id=1103.

[30] Farr, T. G., Rosen, P. A., Caro, E., Crippen, R., Duren, R., Hensley, S., Kobrick, M., Paller, M., Rodriguez, E., Roth, L., Seal, D., Shaffer, S., Shimada, J., Umland, J., Werner, M., Oskin, M., Burbank, D., Alsdorf, D. (2007). The Shuttle Radar Topography Mi ssion, Reviews of Geophysics, Volume 45. RG2004, doi:10.1029/2005RG000183. Available at the website of Consultative Group for International Agriculture Research (CGIAR), CGIAR Consortium for Spatial Information (CGIAR-CSI): http://srtm.csi.cgiar.org/

[31] Cohen, J.A., (1960). "Coefficient of agreement for nominal scales." Educational and Psychological Measurement 20: 37-46.

[32] Congalton, R., Mead, R A. (1983). "A Quantitative Method to Test for Consistency and Correctness in Photo interpretation." Photogrammetric Engineering and Remote Sensing. 49(1): 69-74.

[33] Rosenfield, G H., Fitzpatrick-Lins, K.(1986). "A coefficient Agreement as a Measure of Thematic Classification Accuracy." Photogrammetric Engineering and Remote Sensing. 52(2): 223-227.

[34] Hagen, A. (2003). "Fuzzy set approach to assessing similarity of categorical maps." International Journal of Geographical Information Science 17(3): 235.

[35] Foody, G.M. (2002). "Status of land cover classification accuracy assessment. " Remote Sensing of Environment, 80: 185-201.

[36] Pontius, R. (2002). "Statistic methods to partition effects of quantity and location during comparison of categorical maps at multiple resolutions. " Photogrammatric Engineering and Remote Sensing.

[37] White, R. (2006). "Pattern based map comparison. " Journal of Geographical System, 8: 145-164.

[38] Sembolini, F. (2000b). "The growth of urban cluster into a dynamic self-modifying spatial pattern." Environment and Planning B- Planning & Design 27 (4): 549-564.

# Simulating land-use degradation in West Africa with the ALADYN model

## Yulia GRINBLAT[1,2], Giora J KIDRON[1], Arnon KARNIELI[3], Itzhak BENENSON[1$]

[1]Department of Geography and Human Environment, Tel Aviv University
[2]Porter School of Environmental Studies, Tel Aviv University
[3]Jacob Blaustein Institutes for Desert Research, Ben Gurion University of the Negev
[$]Corresponding Author: bennya@post.tau.ac.il

## Abstract

West Africa faces rapid population growth and subsequent demand for food production. Despite increasing demand, local farmers still follow traditional practice and to overcome low productivity, continuously expand cultivated areas. To estimate the consequences of this process we developed a spatially explicit agent-based ALADYN model of agriculture land-use in the savannah around Kita, Mali. The model is based on the remote sensing data on the agriculture land-use in the Kita area, Mali and field surveys there. The ALADYN simulations clearly demonstrate that traditional agriculture is not sustainable. Even under the optimistic scenario of declining rate of population growth, the current agricultural practice results in including all available lands into agriculture towards 2015-2025. The agriculture production thus reaches its maximum and from then on, every household will experience, every 15-20 years, a period of 1-3 years during which field fertility will be too low for allowing cultivation. Emigration will be the only way to avoid starvation in these circumstances. The model highlights the great need for new agricultural practices in West Africa.

## 1. Land degradation in West Africa

The West African environment is believed to undergo a continuous crisis due to an excessive population pressure. According to previous studies in the region [1-4], degradation of croplands is most extensive in Africa. Land degradation and decline of soil fertility lead to decreasing yields and low food production in farming systems of Sub-Saharan Africa [5], where agriculture remains the main engine of the economical growth of these countries [6]. We investigate these processes in Mali, where current annual population growth is close to 3% [4, 7] and food sustainability in the nearest future may be at risk.

Since the late 1950s, production of cotton has increased immensely in West Africa and specifically in Mali, which is today the largest producer of cotton in Sub-Saharan Africa [4]. Cotton cultivation in Mali takes place in rotation with cereal and groundnut. The typical cycle begins with a year of cotton cultivation followed by a

year of cereal (sorghum, millet or corn), and an additional year of cereal or groundnut [8]. Whereas cereal is cultivated for domestic use, cotton is planted to provide cash, while the groundnut serves for both cash and domestic use. During cultivation, manure and chemical fertilizers are added to the fields, however not consistently. They are added primarily for cotton cultivation, mostly containing the major nutrients of nitrogen (N), phosphorus (P), and potassium (K) [8].

Extensive agriculture aimed to support the constantly growing population needs leads to low productivity of soils[9]. Soil in most parts of Mali is sandy-textured, characterized by the lack of significant soil profile. Following wind erosion soils may intermingle with basement rocks or indurate iron stone [10]. Given their excessive permeability and low nutrient content, agricultural use of these soils requires careful management [3].

In order to avoid exhaustion of the soil, farmers in Mali used to divide their land to 2-3 fields: While one is cultivated, the others are left fallow until regaining fertility. Recent observations reveal that Malian farmers intensify land-use by reducing the period of time that the lands are left fallow between cultivation periods, thus decreasing an overall fraction of the fallow lands. In parallel, the use of chemical fertilizers is still low [8, 9]. More and more lands are approaching the threshold fertility level, below which the agriculture production becomes essentially vulnerable [8]. The only way to ensure food production in this situation is to cultivate the lands that are further away from the settlement and are not yet included in the agriculture cycle.

To investigate the limits of the current agricultural practice, we have developed Agricultural Land DYNamics (ALADYN) model and employed it for assessing soil degradation given current population growth and agriculture practice. ALADYN belongs to a class of spatially explicit agent-based (AB) model that explore relationships between changes in socioeconomic parameters and changes in landscape pattern [11, 12] and are increasingly being used to simulate land use/cover changes [13-15]. ALADYN is based on the field research of soil degradation in Kita area, in 2004 and 2006, and on the space borne data of the Kita area during 1976–2004 [8].

## 2. Conceptual model of land degradation in Mali

Conceptual model of soil degradation in Mali was introduced by Kidron et al. (2010). They studied the relations between the soil organic matter (SOM), the major nutrients (N, P, K), and cotton yield and evaluated the rate of soil degradation.

Since 1960s, the CMDT (Compagnie Malienne pour le Développement des Textiles) company controls cotton production in Mali, and supplies chemical fertilizers to farmers. In 1981, the Malian government signed an agreement with the International Monetary Fund and the World Bank to join the structural adjustment program that led to a dramatic reduction in subsidies for the chemical fertilizers and immediate reduction in their use [4, 16]. This drop further promoted the expansion to new fields and accelerated soil degradation.

According to Kidron et al. (2010) soil fertility is defined by the amount of SOM in soils and the threshold below which a field becomes unproductive is ca 18 t/ha.

Kidron et al. (2010) have estimated the rates of SOM degradation in the cultivated fields and the rate of SOM restoration in the fallow field: the rate of SOM restoration is lower than that of the degradation during cultivation. With the help of simulation model, Kidron et al. (2010) have demonstrated that if the farmers are not able to extend their lands, then each of their fields eventually enters the land-use cycle characterized by the 10 - 12 years of cultivation and, then, 12 -16 years of fallow that are necessary to restore the SOM in the field. The period of 12-16 years is, however, insufficient for the full restoration of field's fertility and, as a result, all family fields simultaneously become unproductive after 25-30 years of the land-use and the farmer is forced to leave the lands for 1-3 years, until fertility of one of them will be regained. These results fit to Kita's reality, characterized by gradual expansion of the cultivated lands. This is the aim of this paper is to develop and evaluate spatially explicit model of agriculture land dynamics in typical for West Africa, Kita area, and to employ the model for investigating the sustainability of traditional agriculture there. For this end, we exploit remote sensing data and data on soil degradation and combine them within the framework of an agent-based spatially explicit model of agriculture land-use.

## 3. Land-use dynamics in the Kita area during last 30 years

### 3.1 Site description

Our research site (~26x26 km) is located to the northeast of Kita (Figure1). The area is characterized by geographical inter-tropical climate with a dry season and a rainy season that makes the agriculture rain-dependent. Precipitation in the area is about 800 mm, falling mostly between May and November. The geomorphology is that of a plain with low hills and narrow valleys. The natural landscape represents grassland and bushes with scattered individual trees that is described as a savannah type [17]. Agricultural fields are located in the flat areas, while the rocky areas are unsuitable for agriculture.



Figure1: Test site in Kita, Mali

### 3.2 Analysis of remote sensing data on agriculture land-use in Kita area

To investigate the dynamics of the agricultural land-use in the Kita area we rely on remote sensing data. The cultivation period of cotton begins with the onset of the rainy season and continues until the first two months of the dry season. It is difficult to detect cropland by remote sensing techniques during the cultivation period - both because of cloudy sky and continuous vegetation cover. We therefore identified cultivated fields with the images taken after the harvest, when the fields appear as bare soils. Fallow fields are identified as those that were cultivated in the past but are currently covered by savannah vegetation.

Two sets of multi-spectral satellite images were used in the analysis (Table 1). The first consists of Landsat MSS, TM, and ETM+ images taken in 1976, 1985, and 2003, in the middle of the dry season (February and March). The second, QuickBird image for 2004 (February), was employed for verifying the Landsat-based classification. The Landsat images were initially geometrically corrected (L1G product), and we further corrected them radiometrically and atmospherically.

Table1: Characteristics of Landsat and QuickBird multi-spectral sensors

| System | Date | Spatial Resolution | Bands |
|---|---|---|---|
| Landsat-2 MSS | February 28, 1976 | 80 m | 4 (green, red, NIR, SWIR) |
| Landsat-5 TM | February 3, 1985 | 30 m | 6 (blue, red, NIR, SWIR) |
| Landsat-7 ETM+ | March 17, 2003 | 30 m | 6 (blue, red, NIR, SWIR) |
| Quickbird | December 4, 2004 | 2.4 m | 4 (blue, red, NIR, SWIR) |

QuickBird image facilitates visual identification of the landscape objects that are necessary for our research, such as individual trees, bushes or agriculture constructions [18]. Based on the visual interpretation, we constructed a vector land-use map for 2004, with each parcel classified as a fallow field, cultivated field, or non-agriculture. The band features of the QuickBird and Landsat sensors are similar, and we thus used the QuickBird signatures of fallow and cultivated fields for supervised classification of the Landsat images.

First, we employed maximum likelihood algorithm to construct binary maps of agricultural/non-agricultural areas. The areas classified as agriculture in any of these maps were considered as "suitable" for agriculture and, based on three Landsat images, three maps of land suitability for agriculture for 1976, 1985, and 2003 were constructed. The pixel is marked as suitable for agriculture if classified as agriculture in any of these maps (Figure 2). Vector layers of settlements and road networks in 2003 were then overlapped with this map and served as a basis for simulation of agricultural land-use dynamics.

Second, to distinguish between the cultivated and fallow fields we employed Normalized Difference Vegetation Index (NDVI)*:*

$$NDVI = (\rho_{NIR} - \rho_{red}) / (\rho_{NIR} + \rho_{red}) \qquad (1)$$

where $\rho$ is the reflectance values in the respective spectral. The values of NDVI vary between -1 and +1, and generally negative NDVI values characterize water, for the bare soil NDVI values are less than 0.1, and for the vegetation greater than 0.16, depending on the vegetation density [19].

To separate between cultivated and fallow fields we estimated the value of NDVI in the cultivated and fallow fields that were visually recognized on the QuickBird image and then marked at the same part of the Landsat ETM+ image. The values of NDVI below 0.176 in the ETM+ image that was taken in February represent bare soils, and we interpreted these areas as cultivated fields that had been harvested short time before the image was taken. The fallow fields are covered in February by vegetation and the NDVI value over these fields in the ETM+ image is above 0.176.
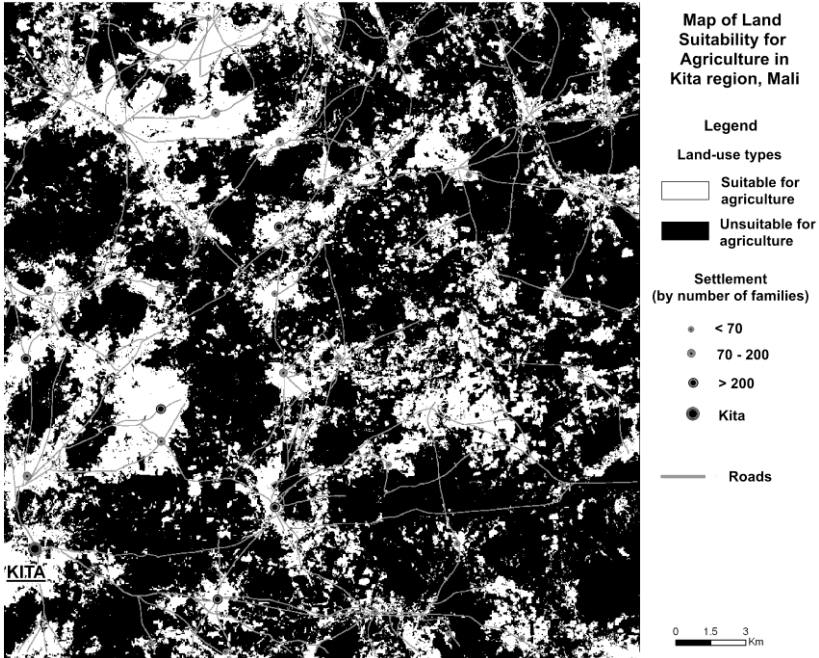


Figure 2: Lands suitable for agriculture in Kita area, overlapped with the layers of settlements and roads.

It is important to note that different sensors are sensitive to different wavelengths and thus, systematic bias of the NDVI values derived from the Landsat images taken in different years has to be corrected. According the calibration study of [20], the NDVI from the Landsat sensors employed in 1976 (MSS), 1985 (TM) and 2003 (ETM+) can be standardized as follows:

$$NDVI_{MSS}=0.924 * NDVI_{ETM+} + 0.025 \qquad (2)$$

$$NDVI_{TM}=0.979 * NDVI_{ETM+} + 0.002 \qquad (3)$$

Applying this correction to the threshold value of NDVI as established for the ETM+ images, we obtain the NDVI thresholds for distinguishing between cultivated and fallow fields: 0.187 in 1976, 0.174 in 1985, and 0.176 in 2003 and obtained the maps of three land-uses: non-agriculture, cultivated, and fallow (Figure 3).
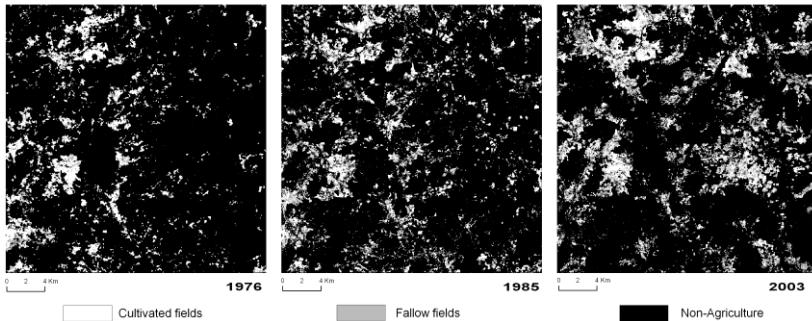


Figure 3: Classified land-use maps in Kita region, Mali, by years

We estimated the accuracy of our classification with the error matrix [21, 22] obtained by comparing the land-use maps derived from Landsat ETM+ and QuickBird images. The estimates of the overall accuracy and the kappa coefficient are 82.2% and 0.703, respectively.

Figure 4 shows the dynamics of agricultural land-use and cultivated areas in Kita region. During 1976-2003, the total area that once used for agriculture has expanded to 28163 ha. In 1976, the share of the agricultural area was 9607 ha (or 34.1% of total agricultural area). From 1976 to 1985, 3193 ha (11.3%), and between 1985 and 2003, 4121 ha (14.6%) were added. In contrast to the rapid expansion of overall agriculture area, the cultivated area has increased between 1985 and 2003 by 839 ha (2.9%).

Figure 5 presents the total cultivated area, as a fraction of the total agriculture area and the area cultivated within three 1 km rings around the settlements. We consider three such rings, following the fact that the average distance between agriculture settlements in Kita is about 5 km. As for the total amount of cultivated lands, it expanded between 1976 and 1985 by 9% and towards 2003 by 3% (Figure 5a). By rings, cultivated area has expanded during 1976-1985, by rings, 1.4%, 9.8% and 12.6%, respectively; between 1985-2003, the cultivated area expanded in the outer ring only (6.9%), while in the inner and middle rings the cultivated area decreased by 7.4% and 0.9%, respectively (Figure 5b).
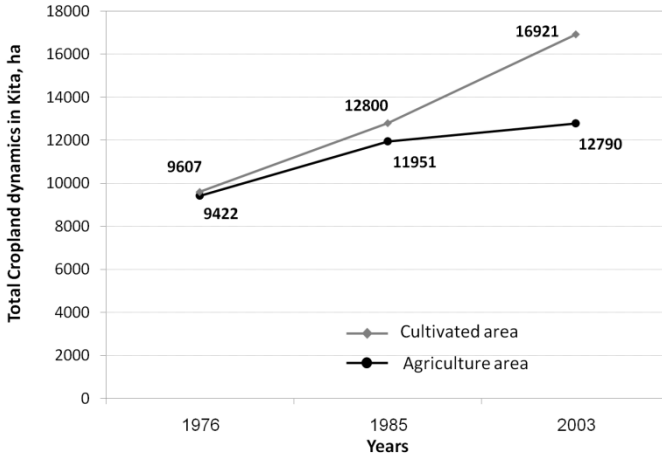
Figure 4: The dynamics of agricultural and cultivated lands in Kita region during 1976 – 2003



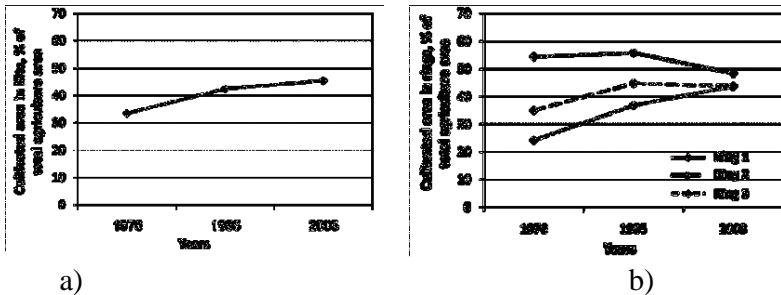a)                                                    b)

Figure 5: Temporal dynamics of cultivated area during 1976- 2003: (a) of entire area, as a percentage of the total agriculture area; (b) by rings of 1 km width from the settlements, as a percentage of the total agriculture area.

Expansion of agriculture further away from the settlements is a strong sign of land overexploitation and loss of fertility. In what follows we employ remote sensing data for comparing model results to reality.

## 4. ALADYN model of the agriculture land-use dynamics in Kita, Mali

ALADYN, spatially explicit AB model simulates agricultural land dynamics as an outcome of the farmer decision that regard land-use and crop choice. The model is developed within the NetLogo modeling environment [23].

### 4.1 ALADYN's overview

The model is based on the field data collected in Kita area, Mali in 2003 and 2005 [8]. The Kita area (26x26 km) is represented in the model by 30x30m grid. Each

grid cell is described by island-use. Land-uses are of six types, three of which are non-agricultural - settlements, roads, and lands unsuitable for agriculture, and three agricultural - virgin fields, cultivated fields and fallow fields. In the Kita area, the average distance between settlements is ca. 5 km. We thus assume in the model that the fields of each farmer are at a distance of up to 3 km from the settlement. The amount of agricultural land at up to 3 km distance is that considered as its agricultural capacity.

Settlement's population consists of farmers and grows at a rate defined by the model scenario. If the settlement's population exceeds settlement's capacity for agriculture, new farmers migrate to the other settlements. If all settlements are full, new farmers can establish a new settlement at a point located at 3 km or further from any of the existing settlements. The fertility of the agriculture lands is characterized in the model by amount of SOM.

### 4.2 Objects and agents in ALADYN

*Settlement* is characterized by location of its center (as a cell), initial number of farmers and population growth rate.

*Field* is spatially continuous set of land cells and characterized by the distance to the nearest settlement and the amount of SOM.

*Farmer* belongs to the settlements, possesses fields and cultivates cotton or crop there. In the beginning of the agriculture season, the farmer decides on the future land-use of each of his fields: whether it will be cultivated and with which crop. The farmer decides to cultivate the field if the amount of SOM is above the threshold level, otherwise the farmer will leave the field for fallow.

### 4.3 ALADYN structure

The ALADYN model consists of four main modules: Initialization, Agriculture, Prognosis and Demography (Figure 6). After the Initialization is performed, the major loop is repeated until the end of the modeled period (60 year in this paper). Model time step is one year.

*Initialization module:* Settlements are populated by farmers. The initial number of the farmers in the settlement is established as 60% of their number in 2003, the latter available from Kidron et al. (2010). This estimate is based on remote sensing data, according to which about 60% of the 2003 agriculture area was cultivated in 1976. Each farmer obtains two fields, each 1 ha in size, within a distance of 3 km from the settlement. One of the fields is set as being used for agriculture and the other left for fallow.

Each cultivated field is randomly assigned the number of years from the start of the period of cultivation, between 0 and 11, and each fallow field is randomly assigned the number of years from the start of the fallow period, between 0 and 17. Initial amount of SOM in the cultivated and fellow fields depends on a year within the cultivation cycle/period of the fallow. We assume that the amount of SOM in the beginning of the cultivation period is maximally possible 43 t/ha (Kidron et al, 2010), while the amount of SOM in the fallow field in the beginning of the fallow period is 18 t/ha. Then we apply formulae (4) – (6) of the Agriculture module below in respect to the initially assigned year of the cultivation or fallow.
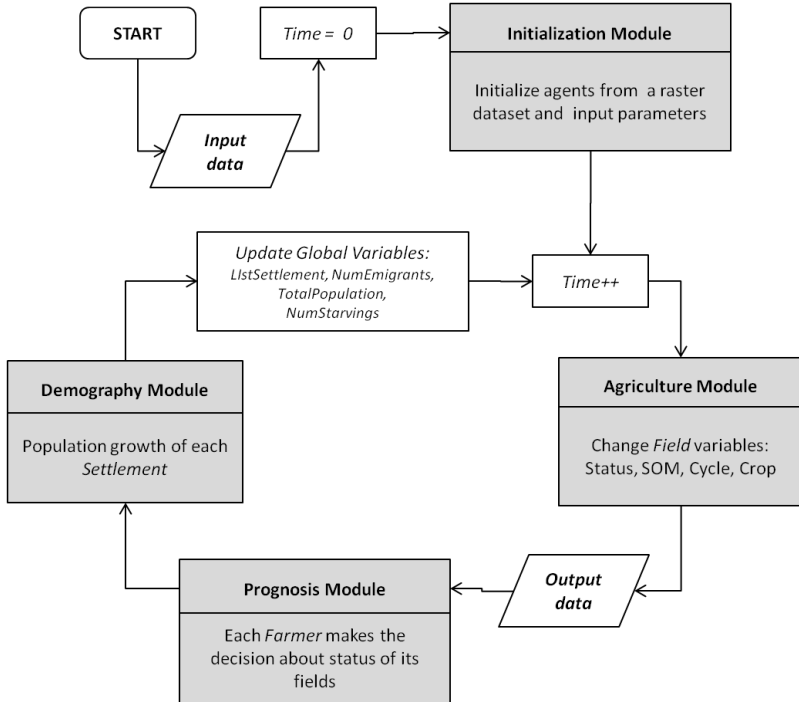
Figure 6: Basic blocks and processes of the ALADYN model

*Agriculture module*: The model simulates cotton and cereal production, by fields. The field status (cultivated/non-cultivated) and the amount of SOM in the soil are updated every year, during the years of cultivation in respect with the crop choice of the farmer. Based on Kidron et al. (2010), the decrease of SOM during cultivation and its increase during the years of fallow are described by linear equations:

SOM decline during a year of cotton cultivation

$$\text{SOM}_{T+1}(t/ha) = \text{SOM}_T(t/ha) - 2.38 \qquad (4)$$

SOM decline during a year of non-cotton crop cultivation

$$\text{SOM}_{T+1}(t/ha) = \text{SOM}_T(t/ha) - 1.19 \qquad (5)$$

SOM restoration during a year of fallow

$$\text{SOM}_{T+1}(t/ha) = \text{SOM}_T(t/ha) + 0.963 \qquad (6)$$

where T denotes time in years.

The initial amount of SOM in the cultivated/fellow field depends on a year within the cultivation cycle/period of the fallow. This year is assigned randomly between 0 and 11 for the cultivated and between 0 and 17 for the fallow field. The SOM level

for the cultivated field is then assigned according to equations (4) and (5), assuming that in year 0 the amount of SOM is 43 t/ha and the cotton is cultivated. The initial amount of SOM in the fallow field is assigned according to equation (6), assuming that in year 0 the level of SOM is 18 t/ha. As shown below, 12 years is a typical length of the cultivation and 18 years of the fallow period.

*Prognosis module*: Based on the amount of SOM in the soil, the farmer decides whether the field will be cultivated next year. If the amount of SOM decreases below 18 t/ha, the farmer leaves it for fallow. I f not, the farmer decides on the future crop. The amount of SOM in the fallow field is restored according to equation (6); the field can be exploited again if the SOM exceeds 25 t/ha.

*Demography module*: The rate of the population growth depends on the model scenario. Below we consider two scenarios – of constant 3% annual growth rate and of the growth rate that linearly declines during 60 years from 3% to 1% per year. In the course of a time, population in each settlement may exceed its capacity. In this case, new farmers attempt to migrate to the one of the existing settlements. If all existing settlements are full, new farmers may establish a new settlement. The latter happens if Kita agricultural area still contains virgin lands that are suitable for cultivation at a distance of 3 km or more from the existing settlement and is accessible by existing roads. In this case, each farmer is assigned two 1 ha fields, adjacent to each other, as close as possible to the new settlement.

According to the visual inspection of the QuickBird image, minimal number of households in Kita settlements in is six. We thus assume that a new settlement can be established if the virgin area suffices for at least six farmers. When all agriculture land is occupied, new farmers emigrate out of the system.

We consider land-use dynamics at annual resolution and investigate scenarios for 60-year period, 1975-2035. Parameters of the ALADYN model are represented in Table 2.

Table 2: Parameters of the ALADYN model

| Parameter | Default value |
|---|---|
| Length of cultivation cycle | 3 years |
| Amount of SOM in a virgin field above | 43 t/ha |
| Cultivation starts when SOM is above | 25 t/ha |
| Cultivation stops when SOM is below | 18 t/ha |
| Overall area of farmer's fields | 2 ha |
| Population of a settlement in 1976 (as a percentage of settlement's capacity in 2003) | 80% |

Model GUI is presented in Figure 7.

In what follows, we employ ALADYN for investigating dynamics of the agriculture land-use in Kita under two different scenarios of the population growth.
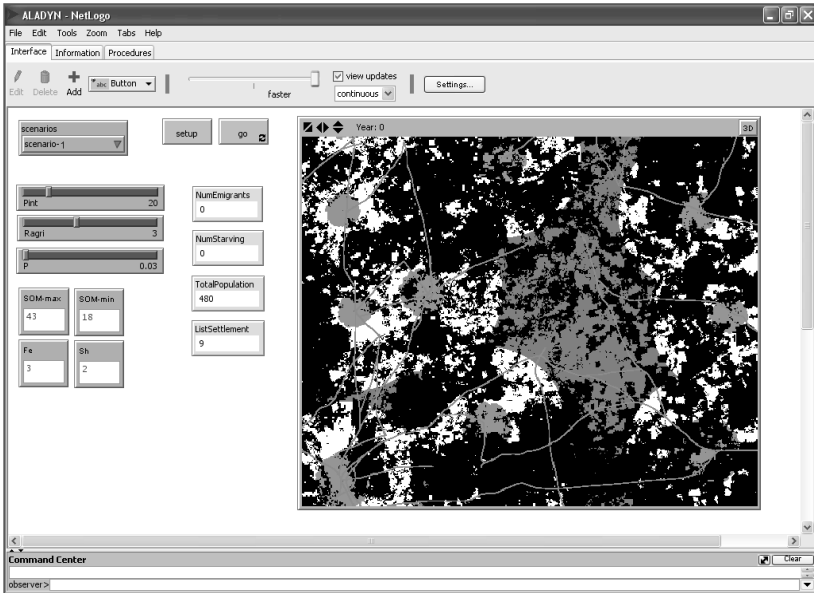
Figure 7: Interface of ALADYN model

## 5. Analysis of ALADYN results

### 5.1. Basic scenario of agriculture land-use dynamics in Kita

The basic ALADYN scenario employs the parameters presented in Table 2 and assumes constant 3% rate of population growth. The dynamics of SOM in the fields of a single farmer are presented in Figure 8. As can be seen, after the first 40 years, the amount of SOM in the farmer's fields stabilizes and varies between 15-25 t/ha. During 60 years, three periods of infertility of 1-3 year length are observed.

Figure 9 presents the model dynamics of agriculture and cultivated area over the entire Kita area as percentages of total agricultural area and three experimental points estimated according the satellite images. As can be seen, agricultural area expands until 2015 and then stabilizes; the cultivated area reaches maximum towards 2001, and then slightly declines. Towards 2035, more than half of agricultural land is left for fallow.

Generally, the cultivated area increases until ~2000 and then slowly declines; as it can be expected, the dynamics of the cultivated lands differ at different distances from a settlement (Figure 10a). ALADYN makes it also possible to estimate the fraction of farmers that cannot cultivate their fields due to soil degradation (Figure 10b).
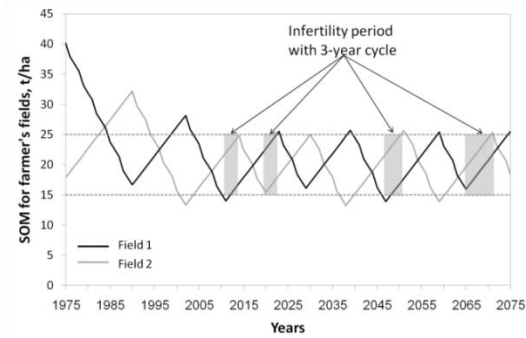
Figure 8: Amount of SOM in two farmer's fields, basic scenario of 3% population growth
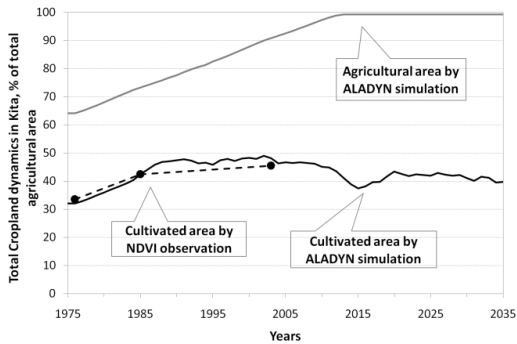


Figure 9: ALADYN dynamics of agricultural and cultivated area in Kita during 1975- 2035, for the basic scenario of 3% population growth, as percentages of total agriculture area with the experimental data superimposed
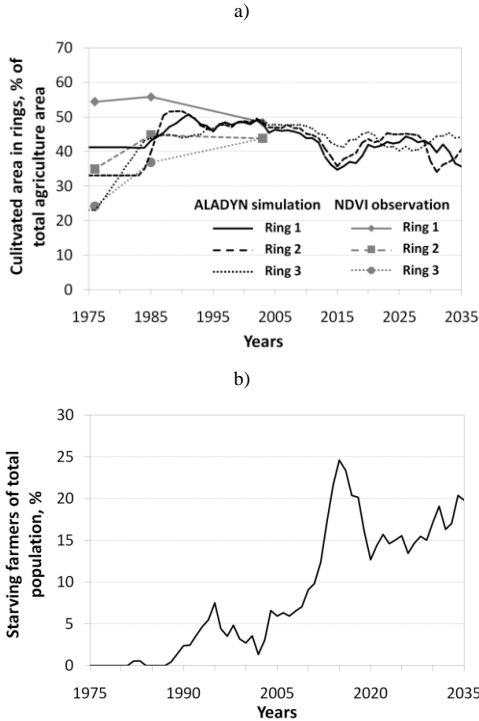
a)



b)



Figure 10: ALADYN dynamics basic scenario of 3% population growth - (a) the cultivated area within rings as a percentage of agriculture area in rings; (b); the percentage of potentially starving farmers.

**5.2. Sensitivity to the population growth rate**

While the current annual population growth rate in Mali is about 3% [4, 7], the UN prognosis is that in 3-5 generations the growth rate in developing countries, like Mali, will decrease to 1% [24]. We thus consider an additional scenario, in which population growth rate decreases, linearly, from 3% to 1% during 1975 – 2035 (0.0333% decrease per year).

Figure 11 presents overall land-use dynamics in Kita for these two scenarios. As can be expected, they are both characterized by overexploitation of the agriculture land.
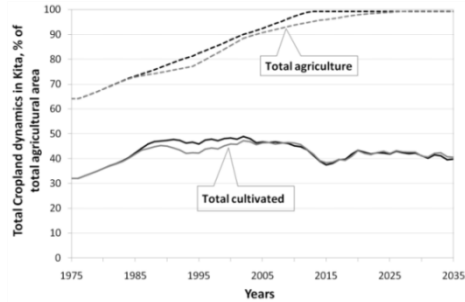
Figure 11: ALADYN dynamics of the total agriculture and cultivated area in Kita during 1975-2035, as percentages of the total agriculture, for two scenarios of population growth rate, 3% (black curves) and 3-1% (gray curves).

The same is true for the land use dynamics at different distances from a settlement (Figure 12). In both scenarios, towards 2015, about 20-25% of the farmers should leave the area.
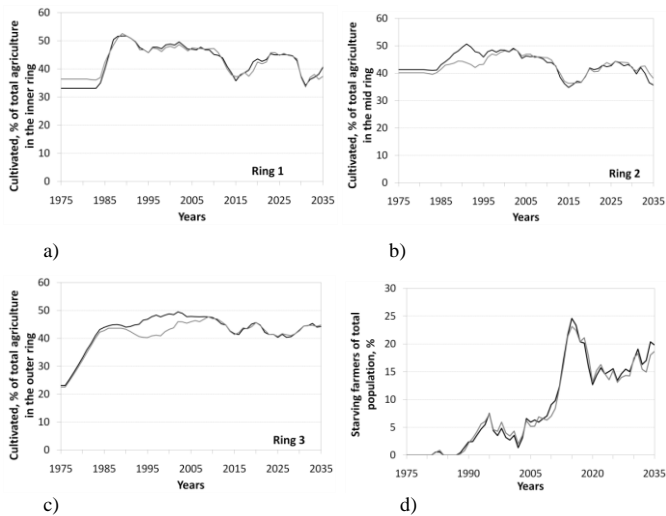


Figure12: ALADYN dynamics of cultivated area for population growth scenarios with 3% (black curves) and 3-1% (gray curves) during 1975-2035, as a percentage of total agriculture area in rings within (a) 1 km, (b) 2 km, and (c) 3 km rings and (d) the fraction of potentially starving farmers.

## 6. Discussion

Soil degradation in West Africa is a known phenomenon, resulting in a substantial decrease of crop yield per hectare in the second half of the 20th century [25]. In Niger for instance, sorghum and pearl millet yield per hectare decreased respectively by 62% and 12% from 1960 to 1999 [26]. At the same time, all researchers report a sharp increase in the cultivated land during the last decades. Thus, according to Fox and Rockstrőm [27] only 40% of the land was cultivated in the Yetenga region of northern Burkina Faso in 1973, while by 1996 it reached 80%.

High population growth rate is the main reason of the sharp increase in cultivated land in West Africa. However, local factors may also contribute to this phenomenon. The 1982 decision of the Malian government to stop subsidizing the chemical fertilizers caused a sharp decrease in their use, and the farmers preferred to clear virgin soil for cultivation, which in turn substantially increased the cultivated area [28, 29]. Additionally, the use of marginal fields [25] further enforced increasing soil degradation [30]. Lack of available agriculture lands resulted in an increase in the cultivation period of the fields and reducing fallow period [28, 31]. The researchers agree that the current practice of agriculture and high level of soil degradation do now allow to decrease the size of the field or duration of fallow period. This, in turn, limits the options for the new farmers.

Taking the Kita area as an example, we explore the dynamics of agriculture land-use with the ALADYN model. In agreement with other publications that regarded SOM as a key proxy for soil degradation [32-34], our model was based on the SOM decay during field cultivation and restoration during the fallow period. The amount of available land in Kita area was estimated based on the satellite data (from 1976, 1985 and 2003), which show steady increase in the agricultural land from 1976 to 2003 in agreement with other reports from other regions in Africa [27]. The potential use of fields which are close to the existing settlements is no longer relevant as these fields are already fully exploited towards 1985. This outcome is in agreement with the FAO (2010) report, according to which, since the 1990s, cotton yields have declined, while agricultural area has expanded.

Assuming that the current agricultural practice will continue, ALADYN predicts a substantial increase in the fallow fields and a reduction in the cultivated areas, no matter if the population growth rate will remain at a current level or decrease in accordance with the UN forecast. Depending on the scenario, towards 2015-2025, the system will reach a persistent level of production, when less than 50% of available agriculture lands is cultivated, and the production is 20-25% lower than maximally observed. Once in 10-20 years each household should pass a 1-3 year period when all their fields are non-productive and this poses an extra burden on the economical wellbeing of the farmer household. Decrease in population growth may decrease the pressure but does not provide, by itself, a solution. While the overall agriculture lands is growing slower, the cultivated lands and, thus, agriculture production, remains at the same level as obtained in the model for constant 3% population growth. As a result, the fraction of farmers that are not able to cultivate their fields every year remains about 20-25% starting from 2015.

In agreement with previous reports [3], our model simulation indicates that current agricultural practice in Mali will not suffice to sustain the population. Development of the infrastructure by building roads may alleviate the situation by facilitating the expansion of more agricultural land. In addition, the adaption of new cultivation methods is called for.

## Acknowledgements:

## References:

[1]  Tappan, G. and M. McGahuey, Tracking environmental dynamics and agricultural intensification in southern Mali. Agricultural Systems, 2007. 94(1): p. 38-51.

[2]  Bah, M., et al., Changing rural–urban linkages in Mali, Nigeria and Tanzania. Environment&Urbanization, 2003. 15(1).

[3]  Shapiro, B.I. and J.H. Sanders, Fertilizer use in semiarid West Africa: Profitability and supporting policy. Agricultural Systems, 1998. 56(4): p. 467-482.

[4]  Benjaminsen, T.A., The population-agriculture-environment nexus in the Malian cotton zone. Global Environmental Change, 2001. 11(4): p. 283-295.

[5]  Kaya, B., P.E. Hildebrand, and P.K.R. Nair, Modeling changes in farming systems with the adoption of improved fallows in southern Mali. Agricultural Systems, 2000. 66(1): p. 51-68.

[6]  Benjaminsen, T.A., Enclosing the land: cotton, population growth and tenure in Mali. Norwegian Journal of Geography, 2002. 56: p. 1 - 10.

[7]  FAO, FAOSTAT Statistical Database. 2010, Food and Agriculture Organisation (FAO) of the United Nations: Italy, Rome.

[8]  Kidron, G.J., I. Benenson, and A. Karnieli, Degradation of soil fertility following cycles of cotton-cereal cultivation in Mali, West Africa: A first approximation to the problem. Soil and Tillage Research, 2010. 106(2): p. 254-262.

[9]  Butt, T.A. and B.A. McCarl, An analytical framework for making long -term projections of undernourishment: A case study for agriculture in Mali. Food Policy, 2005. 30(4): p. 434-451.

[10] Laryea, K.B., P. Pathak, and M.C. Klaij, Tillage systems and soils in the semi-arid tropics. Soil and Tillage Research, 1991. 20(2-4): p. 201-218.

[11] Parker, D.C., T. Berger, and S.M. Manson, Agent-Based Models of Land-Use and Land-Cover Change, in LUCC Report. 2001.

[12] Lambin, E.F.G., H. J., Global land-use and cover change: What have we learned so far? Global Change Newsletter, 2001: p. 27 - 30.

[13] Berger, T., Agent-based spatial models applied to agriculture: a simulation tool for technology diffusion, resource use changes and policy analysis. Agricultural Economics, 2001. 25(2-3): p. 245-260.

[14] Kamusoko, C., et al., Rural sustainability under threat in Zimbabwe – Simulation of future land use/cover changes in the Bindura district based on the Markov-cellular automata model. Applied Geography, 2009. 29(3): p. 435-447.

[15] Balmann, A., Farm-Based Modelling of Regional Structural Change: A Cellular Automata Approach. European Review of Agricultural Economics, 1997. 24(1): p. 85 - 108.

[16] Benjaminsen, T.A., J.B. Aune, and D. Sidibé, A critical political ecology of cotton and soil fertility in Mali. Geoforum, 2010. 41(4): p. 647-656.

[17] Butt, B., et al., Use of MODIS NDVI to evaluate changing latitudinal gradients of rangeland phenology in Sudano-Sahelian West Africa. Remote Sensing of Environment, 2011(0).

[18] Turner, W., et al., Remote sensing for biodiversity science and conservation. Trends in Ecology &amp; Evolution, 2003. 18(6): p. 306-314.

[19] ackson, R.D. and A.R. Huete, Interpreting vegetation indices. Preventive Veterinary Medicine, 1991. 11(3-4): p. 185-200.

[20] Steven, M.D., et al., Intercalibration of vegetation indices from different sensor systems. Remote Sensing of Environment, 2003. 88: p. 412-422.

[21] Næsset, E., Testing for marginal homogeneity of remote sensing classification error matrices with ordered categories. ISPRS Journal of Photogrammetry and Remote Sensing, 1995. 50(2): p. 30-36.

[22] Stehman, S.V., Selecting and interpreting measures of thematic classification accuracy. Remote Sensing of Environment, 1997. 62(1): p. 77-89.

[23] Wilensky, U., NetLogo. http://ccl.northwestern.edu/netlogo/. 1999, Center for Connected Learning and Computer-Based Modeling, Northwestern University, Evanston, IL.

[24] UN-DESA, Trends in sustainable development: Africa report. 2008, Division for Sustainable Development, Department of Economic and Social Affairs, United Nations: New York.

[25] Bationo, A. and A.U. Mokwunye, Alleviating soil fertility constraints to increased crop production in West Africa: The experience in the Sahel. Nutrient Cycling in Agroecosystems, 1991. 29(1): p. 95-115.

[26] Pandey, R.K., T.W. Crawford, and J.W. Maranville, Agriculture Intensification and Ecologically Sustainable Land Use in Niger: A Case Study of Evolution of Intensive Systems with Supplementary Irrigation. WJSA, 2002. 20(3): p. 33-55.

[27] Fox, P. and J. Rockström, Supplemental irrigation for dry-spell mitigation of rainfed agriculture in the Sahel. Agricultural Water Management, 2003. 61(1): p. 29-50.

[28] Kouyaté, Z., et al., Tillage, crop residue, legume rotation, and green manure effects on sorghum and millet yields in the semiarid tropics of Mali. Plant and Soil, 2000. 225(1): p. 141-151.

[29] Pol, F. and B. Traore, Soil nutrient depletion by agricultural production in Southern Mali. Nutrient Cycling in Agroecosystems, 1993. 36(1): p. 79-90.

[30] Reenberg, A., T.L. Nielsen, and K. Ramussen, Field expansion and reallocation in the Sahel- land use pattern dynamics in a fluctuating biophysical and socio-economic environment. Global Environ. Change, 1998. 8: p. 309-327.

[31] Chappell, A., et al., Soil flux (loss and gain) in southwestern Niger and its agricultural impact. Land Degradation & Development, 1998. 9(4): p. 295-310.

[32] Bationo, A., F. Lompo, and S. Koala, Research on nutrient flows and balances in west Africa: state-of-the-art. Agriculture, Ecosystems &amp; Environment, 1998. 71(1–3): p. 19-35.

[33] Zougmoré, R., et al., Effect of stone lines on soil chemical characteristics under continuous sorghum cropping in semiarid Burkina Faso. Soil and Tillage Research, 2002. 66(1): p. 47-53.

[34] Oenema, O., et al., *Nutrient management in tropical agroecosystems.* Agric. Ecosyst. Environ., 2006. 116: p. 1-3.

# An activity-based CA model for Flanders, Belgium

Robustness analysis and improved distance computation in a variable grid representation

**Tomas CROLS[1,2]; Roger WHITE[3]; Inge ULJEE[2]; Guy ENGELEN[2];
Frank CANTERS[1]; Lien POELMANS[2]**

[1]Vrije Universiteit Brussel, Cartography and GIS Research Group, Department of Geography
Pleinlaan 2, 1050 Brussel, Belgium
+32 14 33 67 58, tcrols@vub.ac.be (correspondent author);
+32 2 629 33 81, fcanters@vub.ac.be

[2]Flemish Institute for Technological Research, Unit Spatial Environmental Modelling
Boeretang 200, 2400 Mol, Belgium
+32 14 33 67 34, inge.uljee@vito.be;
+32 14 33 67 37, guy.engelen@vito.be;
+32 14 33 67 92, lien.poelmans@vito.be

[3]Memorial University of Newfoundland, Department of Geography
St. John's, NL A1B 3X9, Canada
+1 709 864 8193, roger@mun.ca

## Abstract

Cellular automata (CA) models are increasingly applied for simulating land-use change in urban areas. However, in areas with strongly mixed land uses, like Flanders, Belgium, different types and intensities of human activity occur within a single dominant land use. This is in conflict with the discrete and dominant land-use states applied in CA. The direct modelling of the intensity of activities (population density and employment in different sectors) within a CA grid environment is an interesting alternative to model mixed and multifunctional land use.

In this research, an activity-based cellular automata (ACA) model, developed by White et al., will be further enhanced, applied and calibrated for Flanders. It also uses a variable grid approach: linking with a regional model is not necessary because the neighbourhood is expanded to the entire modelling area. The model should be able to cope with the complex multi-nodal structure and messy morphology of Flanders, typified as it is by multifunctional land use and diffuse, fragmented urban development strung out along roads.

In this paper we firstly show the results of a robustness analysis carried out to investigate whether the model behaves as expected under extreme circumstances. Secondly we propose a method to compute and store distances between cells in the variable grid ACA. This calculation should be based on the existing transportation network rather than on simple Euclidian distances applied in classical local CA neighbourhoods.

## Introduction

Classical CA, like other land-use change models, have strictly discrete land-use categories – one cell is in one state. Regions with mixed land uses, like Flanders, Belgium, however are better served by a model with distinct activities (population and economical activity per cell) instead of fairly abstract land-use types. Population and jobs can indeed grow gradually within most types of land uses even when the dominant land-use does not change. Many applications focusing on economic and environmental problems will also benefit from more detailed information on the location of activities. Multi agent systems (MAS) can predict direct interactions between actors but are not useful for large regions as they are computationally slow [1]. Therefore activity-based cellular automata (ACA) can be a solution to model the interactions between multiple types of activity, and between activities and land uses [2, 3]. As such, population and employment levels and their associated land uses can be predicted at a high spatial resolution.

Another problem is that long distance spatial interactions are not covered by classical CA models. Therefore CA models are usually linked to a spatial-interaction based model representing dynamics among larger administrative regions [4, 5]. This strategy leaves a number of problems unsolved: (1) intermediate spatial scales are not represented, (2) to calibrate and couple both models, additional parameters are needed, and (3) the regions are compacted into their usually unrepresentative centroids [3]. The expansion of the neighbourhood to the entire modelling area, using a variable grid approach, can be a good solution [6, 7]. It uses rings of "super-cells" which become increasingly larger for longer distance interactions. Each super-cell of level $L$ consists of 9 (super-)cells of level $L - 1$, and of $3^{2L}$ cells of the basic grid ("unit-cells").

In the next section we will describe the ACA model upon which this research is based. This model is being applied to, and calibrated for, Flanders, Belgium. Further, we will discuss some general data collection and application issues dealt with in the early stage of this research. Next, we will report on a robustness analysis of the model carried out for a sub-region centred on Antwerp. Finally, we will describe some possible approaches to work with transport network distances in the variable grid CA instead of simple Euclidian distances.

## A multiple activity-based cellular automaton

A schematic representation of the ACA model used in this research and developed by White *et al.* [3] can be found in figure 1. Some land uses are associated with an activity: e.g. residential land use is associated with population. Each land use can host several activities, but the associated activity is considered the primary activity and other activities present on the cell are secondary. Land uses not associated with an activity are considered to be their own primary activity (e.g. the primary activity of a forest cell is forest), but they will generally also host secondary activities (a forest cell may also house people). For each activity $K$, the proportion $q_K$ to be located as primary activity (i.e. on the associated land use) is calibrated. The rest of the activity proportion $(1 - q_K)$ will be located on other land uses as secondary

activity. Compatibility factors between activities and all land uses are calibrated to this effect. To calculate transition potentials for land uses and associated activities, the neighbourhood effect of all activities and land uses on all activities, as well as several other factors are needed. The latter include: the zoning status and suitability for each activity, an accessibility measure, a random factor and a diseconomies of agglomeration factor accounting for high land costs and congestion in densely settled areas. The activity potential is calculated as:

$$V_{Ki} = r\, Z_{Ki}\, R_{Ki}\, S_{Ki}\, N_{ki} \qquad (1)$$

with $V_{Ki}$ the activity potential for activity $K$ on cell $i$, $r$ a random perturbation, $Z_{Ki}$ the zoning status for activity $K$ on cell $i$, $R_{Ki}$ the accessibility measure for activity $K$ on cell $i$, $S_{Ki}$ the suitability of cell $i$ for activity $K$, and finally $N_{Ki}$ the neighbourhood effect. The random perturbation $r$, representing the stochastic component of the model, is generated as:

$$r = 1 + (- \ln (rand))^{\alpha} \qquad (2)$$

with *rand* a uniform random variate and $\alpha$ a parameter that controls the skewness of the function. Next, land-use transition potentials are calculated as:

$$VT_{Ki} = D_{Ki}\, (V_{Ki})^{mK} + I_{Ki} \qquad (3)$$

with $VT_{Ki}$ the land-use transition potential for activity K on cell i, $D_{Ki}$ the diseconomies factor, $mK$ a parameter to be calibrated and $I_{Ki}$ the inertia value for activity K on cell i. Briefly, the transition process can be described as follows [3]: for each cell, transition potentials for different land uses are ranked, and then all cells are ranked on the basis of the highest value for each cell. Starting with the highest ranked cell, each cell is assigned the land use for which it has the highest transition potential until the demand for the particular land use is satisfied and no further cells are assigned to that use. Next, for each cell with a land use corresponding to an activity, primary activity is allocated in proportion to the cell's activity potential. Finally, secondary activities are allocated proportionally to activity potentials, as adjusted in accordance with the compatibility factors.
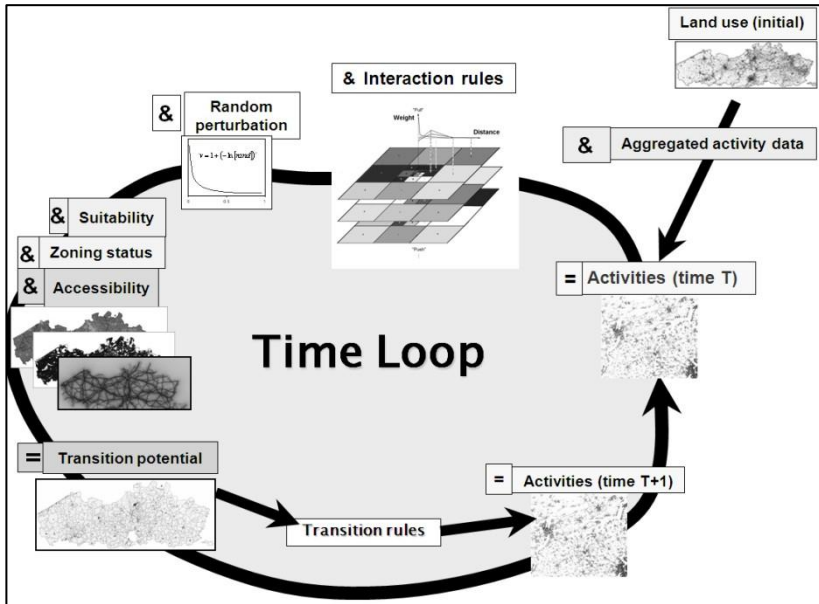
Figure 1: Scheme of the activity-based CA model.

## Application of the ACA model to a test area in Flanders

Several problems arose when applying the model of White *et al.* [3] to Flanders. Firstly, applying an ACA model at a 1 ha resolution for an area as large as Flanders (1,350,000 ha) is computationally heavy given the number of runs required for calibration and validation. Therefore we developed and tested a preliminary model on a region centred on Antwerp, in the central northern part of Flanders, consisting of Antwerp province and the neighbouring arrondissements of Sint-Niklaas and Dendermonde to the west (East Flanders province) (Map 1). This test area was chosen because its mix of activities and land uses are representative for Flanders as a whole and because extra data sets, including remote sensing products, are available that could be useful for solving a second problem, namely the lack of activity data at the detailed spatial resolution of the model.
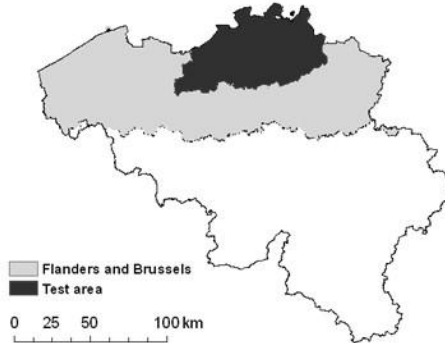
Map 1: Location of the test area around Antwerp within the targeted modelling area (Flanders and Brussels) and Belgium.

Good input data on the distribution of activities are indispensable for the appropriate functioning of the ACA model. Population and employment numbers for different economic sectors are needed for every cell, yet data are only available from official sources on an aggregated level (municipalities or statistical sectors). Dasymetric mapping, a multiple regression based spatial allocation technique, is applied on the aggregated data with a view to obtain the required cellular representation. In this approach, the individual cell (activity) values are the dependent variable, while other, known, cell-based geographical data (e.g. land use, distance to city centres) are used as independent variables [8, 9]. So far we have used a simple dasymetric mapping technique with only the input land-use map of the model as the independent variable. An improved dasymetric mapping is an important research goal at a later stage.

In our research we make use of a 10 m resolution land-use map of Flanders for the year 2010 with 45 land-use classes, developed by VITO [10]. For the initial modelling work described in this paper we rescaled the cells to 1 ha entities and grouped the land uses into 9 classes: two activity-driven land uses (the *residential urban fabric* associated with population, and the *industrial and commercial areas*, associated with employment in all economic sectors), two area-driven land uses (*protected nature* and *agriculture*), two passive land uses (*unprotected nature* and *other*, a rest category), and three static land uses (*recreational areas*, *infrastructure* and *water*). The resulting initial land-use map is shown in Map 2. Zoning maps, physical suitability maps and transport network maps were available from earlier studies [11]. Forecasted population and employment trends for the Belgian arrondissements, obtained from the Federal Planning Agency, were used as future total activities. In the absence of a second land-use map, the model was not historically calibrated on the past, rather run forward from 2010.
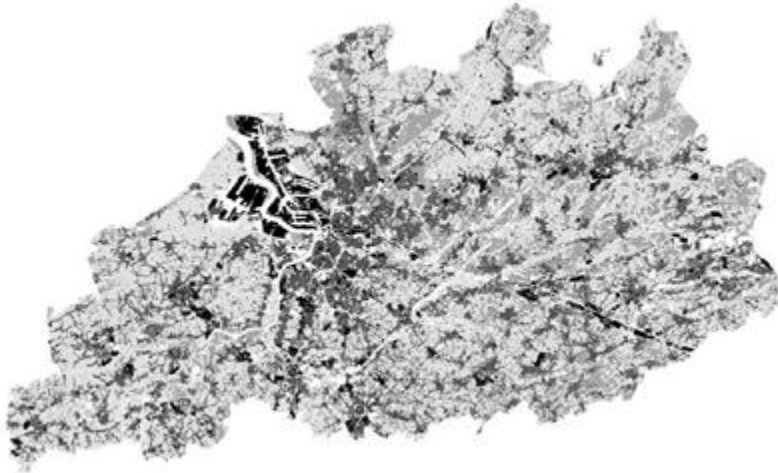
Map 2: Actual land use around Antwerp in 2010. Industrial and commercial areas (black), residential urban fabric (dark grey), protected nature (medium grey), agriculture (light grey), and static and passive land uses (white).

**Robustness analysis**

The goal of a robustness analysis is to find out whether the model behaves as expected under extreme circumstances. Four scenarios were tested: (1) a strong decrease of built-up categories, followed by a strong increase (or vice versa), (2) atypical neighbourhood rules for residential activities, (3) major influence of railways on the accessibility for the residential activity, and (4) a very strong random perturbation. The scenarios were run until 2025 or 2040, depending on whether a longer run still made a big difference or not.

When the built-up land use strongly decreases (scenario 1), only the centres of the cities remain as residential urban fabric which seems to be a logical result. However, forecasting industrial and commercial land use based on its associated activity (number of employees) does not always lead to good results. In the port area of Antwerp for example, the number of workers per cell is quite limited. In the case of a shrinking industrial sector (even for a small decrease), the model tends to eliminate port cells prior to other industrial cells, thus ignoring the huge economical importance of the Antwerp port (Map 3, top). When the amount of built-up area increases again, the port returns to its original location because the zoning map prevents the area from becoming residential. The residential urban fabric grows mainly around existing cities, which is logical. Smaller villages near the model edges, however, do not return (Map 3, bottom).
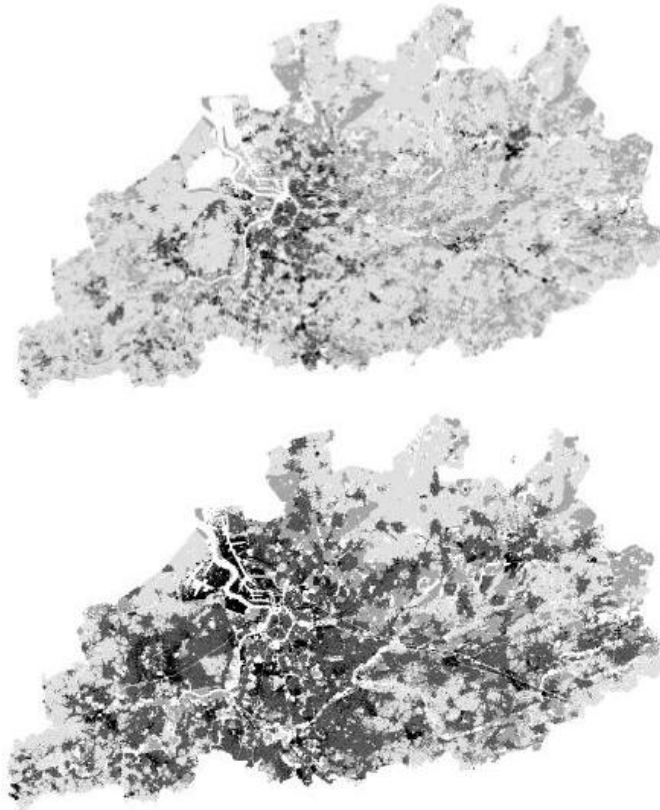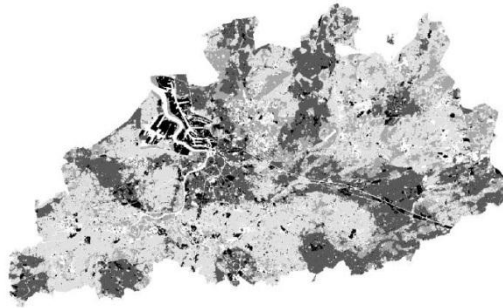
Map 3: Predicted land use around Antwerp in 2025 for an extreme decrease of urban areas scenario (top), followed by an extreme increase in 2040 (bottom). Legend as in map 2.

In scenario 2 atypical neighbourhood rules for residential activities were tested. A negative weight for residential activity at medium distance from residential areas was assumed. After an unstable period lasting some years, this results after 15 years into a spatial configuration consisting of new cities, interspaced by a given distance (Map 4). This again is what could be expected.

In the third scenario, raising the influence of the accessibility parameter determining the impact of railways on residential activity did not have a strong effect on the results obtained. With standard neighbourhood rules and average diseconomies of agglomeration, the interaction rules seem to dominate the accessibility parameters. Only in the case of low diseconomies of agglomeration, low inertia values for all land uses (especially natural categories) and in the absence of a zoning map, growth of new residential urban fabric is a little bit stronger near towns situated in a buffer zone around railways (Map 5). In general however, we can conclude that

accessibility parameters in the current model seem to have an insufficient effect This is one of the arguments for including network accessibility directly into the neighbourhood rules, as discussed in the next section.



Map 4: Predicted land use around Antwerp in 2025 if residential activity repels itself at medium distances. Legend as in map 2.



Map 5: Predicted residential land-use change around Antwerp in 2040 with a high railway accessibility parameter and a zero value for other accessibility parameters. Areas that remain residential urban fabric from 2010 to 2040 (light grey), new residential areas in 2040 (black), railways (dark grey lines).

Finally we tested the impact of a high random perturbation effect (see equation 2) as part of scenario 4. Extreme random perturbation (values for $\alpha > 55$) results in numerical instability. For values just below this critical value, new residential urban cells are mainly found scattered in agricultural zones, and also in a concentric zone at a certain distance around Antwerp due to the diseconomies of agglomeration effect (Map 6). This is as could be expected. As in scenario 1, the port area disappears because the employment activity values get too low.
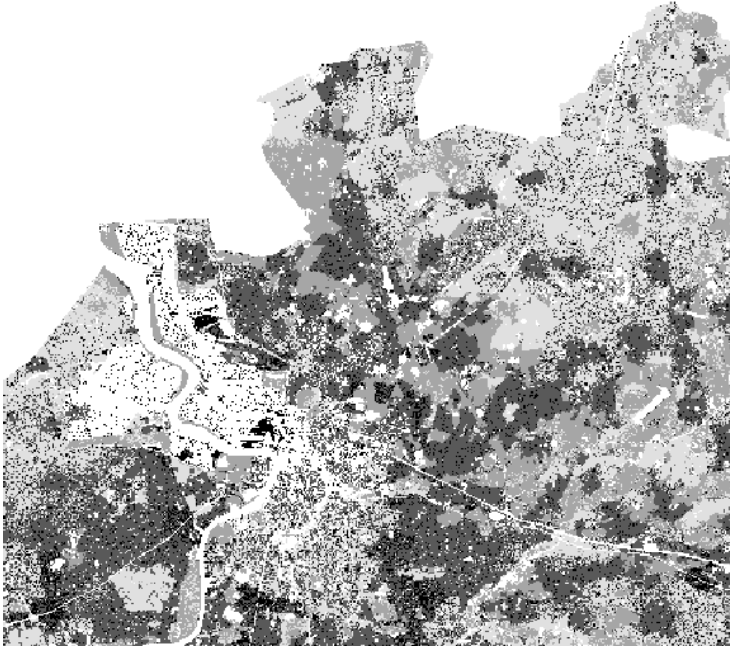
Map 6: Predicted land use north of Antwerp in 2040 with a high random perturbation. Legend as in map 2.

## Calculation of distances in the variable grid model

To calculate the neighbourhood effect, distances between the central cell and the other cells in its neighbourhood are needed. These distances should be measured over a transport network if we want to approximate as closely as possible real spatial interactions. It may even be better to use the relative time needed to travel between cells. However, a classical CA neighbourhood consists of a limited number of immediate neighbouring cells, hence, simple Euclidian distances are generally used. For example, the Spatially-Dynamic Land-Use Model for Flanders (RuimteModel Vlaanderen) has a circular neighbourhood of eight 100 m cells [11]. Hence, distance (or time) between the central cell and its neighbours is so small that the error made by using Euclidian distances is negligible. Moreover, the application of a cell-based accessibility measure to the central cell in the transition rule, is correcting for potentially over- or underestimated access to the cells in the neighbourhood.

In the variable grid environment dealing with distance based interaction gets more complicated though [6]. Distances are now needed between the central cell and the centre of each super-cell in its neighbourhood, extending to the entire modelling area. Thus, using the classical Euclidian approach may introduce substantial errors. On the other hand, the calculation of network distances between all cells of the

modelled area is computationally very intensive, and/or requires the storage of large distance matrices.

It is therefore a goal of our research to develop a "time-distance model" representing network distances with a minimum of (re)computation during the simulation. The chosen method should enable predicting anisotropic urban growth patterns depending on the integral accessibility between cells, rather than the opening up of a cell by the nearest links of the transportation system, as represented by the accessibility factor in the model. Possible methods include "detour factors" per region (and/or distance length class), and the storage of a distance matrix between a number of important major transportation nodes (or centroids of aggregated cells). A "detour factor" is a coefficient calibrated for a specific region that is multiplied with the Euclidian distance to approximate real network distances [12]. The use of a simple detour factor for the entire modelling area has no sense. We are only interested in relative distance (or time) differences, and such a factor would not change them. A different factor for different regions and/or distance length classes in the model could work but has also some disadvantages. Firstly, in a large region with mixed land uses like Flanders, it will probably be much more difficult to find appropriate factors than in single cities or in large rural areas. Secondly, if we would divide Flanders into a lot of sub-regions with different detour factors, this still implies the storage of a large set of factors. The method would therefore hold little advantages compared to storing a network distance matrix directly.
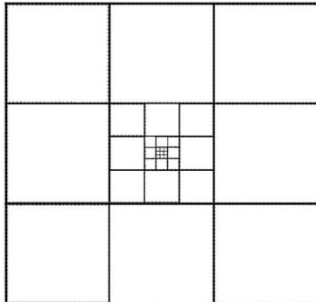


Figure 2: Neighbouring cells of level 0 through level 3 around a unit-cell in the variable grid approach.

Storing matrixes of network distances could be done in several ways. Distances between all cells are not needed, rather, the model requires distances between a unit-cell and the centres of all its super-cell neighbours. For a model at the 1 ha resolution, the total area of Flanders can be covered by variable grid (super-)cells ranging from level 0 until level 7, meaning 8 levels times 8 (super-)cells of each level around a centre level 0 cell (unit-cell) (Figure 2).

Additionally, Euclidian distances could still be used for levels 0 and 1, as these distances are in the same range as the ones in classical CA neighbourhoods (e.g. the RuimteModel Vlaanderen). For larger distances ($L \geq 2$), we need the average time between points on the network, as close as possible to the centre of the cells. If there is no network point within the cell, a time according to a very low speed should be

added to reach the cell. To implement and test this new approach, we will initially assume average speeds per road type, and replace them later by speeds taking into consideration local conditions including congestion.
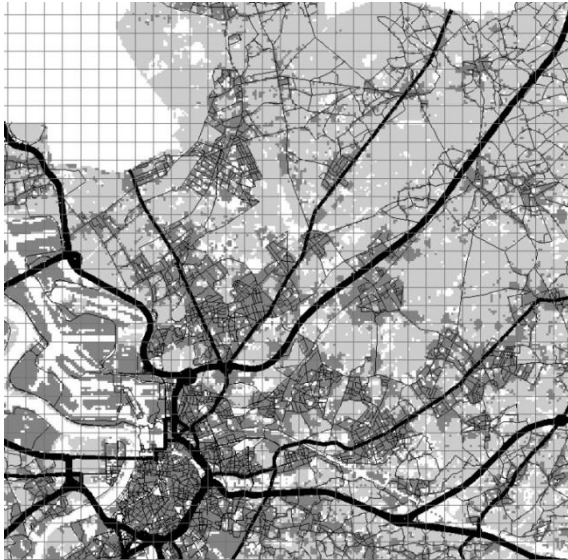


Map 7: Roads and land use northeast of Antwerp with a 900 m grid background. Motorways (thick black lines), major roads (medium black lines), minor roads (thin black lines); built-up areas (dark grey), agriculture and protected nature (light grey), other land uses (white).

Still, storing all travel times from every unit-cell to its super-cells ($L \geq 2$) would involve a lot of data. However, the time-distance from a unit-cell to a super-cell in a particular direction would in general be very similar to the time-distance from a neighbouring unit-cell to its corresponding super-cell in the same direction. This idea is also supported by the concept of a detour factor calibrated for very small regions and different distance length classes. Hence an efficient solution could consist in defining a regular grid of level 2 super-cells (a 900 m grid cell in our model as the unit-cell resolution is 100 m) – we will call this the stored distance grid – and calculating and storing time-distances between the centre unit-cell ($L = 0$) of each 900 m grid cell and the centre unit-cells of all its neighbouring super-cells ($L \geq$ 2). All the other unit-cells within this 900 m grid cell can then make use of these stored time-distances.

However, not every 900 m grid cell is connected to the road network (Map 7) and the nearest point on the network will not always be representative for larger super-cells if they are highly urbanised. Therefore we will experiment with different distance models: we can make use of the nearest major transport node to the centre cells, or just the nearest point on the network. We have to evaluate whether these models tend to over- or underestimate actual travel times.

Finally, we have to define a relationship between the distance used in the neighbourhood rules themselves (expressed as a level of super-cells *L*) and the calculated times *T*. In the current ACA model, the level *L* that has to be used can be calculated from the Euclidian distance *D* (in m) and the cell resolution *R* (in m):

$$L = \log_3(D/R) \qquad (4)$$

In this research *R* = 100 m. Then the level *L* in the variable grid that has to be used, according to the calculated time-distance *T* is:

$$L = L_G + \log_3(T/T_G) \qquad (5)$$

with $L_G$ the level of the stored distance grid (2 in this research) and $T_G$ the time needed to travel the width of one cell of the stored distance grid at a local travelling speed.

## Conclusions

In this paper we discussed some critical issues related to the implementation of the activity-based cellular automata (ACA) model proposed by White *et al.* [3] for Flanders. Results of an ACA model at a high spatial resolution (1 ha) can be instrumental to explore future states of the Flanders region, characterised as it is by a large variety of built-up areas with mixed land uses. The modelling of activities at high resolution will also be of great value for several socio-economic and ecological applications [3].

Several problems remain to be solved: running a complex model for a large region like Flanders is computationally demanding. An efficient implementation is therefore required. Also, a better method is required to disaggregate activity input data to the resolution of the model.

The results of a robustness analysis discussed in this paper are promising as most model components behave in line with the expectations. However, network accessibility should be incorporated into the model in a more realistic way. Alternative methods were discussed to compute or store network distances outside the time-loop of the ACA model in an effective and computationally efficient manner. The storage of a network time-distance matrix will probably be the best solution. The method discussed will be implemented in the next phase of this research.

## Acknowledgments

## References

[1]   Parker, D.C., S.M. Manson, M.A. Janssen, M.J. Hoffman, P. Deadman (2003), Multi- Agent Systems for the simulation of land-use and land-cover change: A review. Annals of the Association of American Geographers, 93, pp. 314–337.

[2]   van Vliet, J., J. Hurkens, R. White, H. van Delden (2011), An activity based cellular automaton model to simulate land use dynamics. Environment and Planning B., 29, pp. 431-450.

[3]   White, R., I. Uljee, G. Engelen (2012), Integrated Modelling of Population, Employment, and Land Use Change with a Multiple Activity Based Variable Grid Cellular Automaton. International Journal of Geographical Information Science, DOI:10.1080/13658816.2011.635146

[4]   White, R., G. Engelen (2000), High resolution integrated modelling of the spatial dynamics of urban and regional systems. Computers, Environment and Urban Systems, 24, pp. 383-400.

[5]   Engelen, G., C. Lavalle, J. Barredo, M. van der Meulen, R. White (2007), The MOLAND modelling framework for urban and regional land use dynamics. In Koomen, E., J. Stillwell, A. Bakema, H. Scholten (Eds.), Modelling Land-Use Change: Progress and Applications, pp. 297-320, Springer.

[6]   White, R. (2005), Modelling multi-scale processes in a cellular automata framework. In J. Portugali (Ed.), Complex Artificial Environments, pp. 165-178, Springer.

[7]   van Vliet, J., R. White, S. Dragicevic (2009), Modeling urban growth using a variable grid cellular automaton. Computers, Environment and Urban Systems, 33, pp. 35-43.

[8]   Langford, M., D.J. Maguire, D.J. Unwin (1991), The areal interpolation problem: estimating population using remote sensing in a GIS framework. In Masser, I., M. Blakemore (Eds.), Handling Geographical Information: Methodology and Potential Applications, pp. 55-77, Wiley, New York.

[9]   Wu, S., X. Qiu, L. Wang (2005), Population estimation methods in GIS and remote sensing: a review. GIScience and Remote Sensing, 42, pp. 80-96.

[10]  Van Esch, L., G. Engelen, A. Gobin, I. Uljee (2010), Landgebruikskaart Vlaanderen en Brussel. VITO Report 2010/RMA/R/158, Flemish Institute for Technological Research (VITO), Mol, Belgium.

[11]  Gobin, A., I. Uljee, L. Van Esch, G. Engelen, J.-L. de Kok, H. van der Kwast, M. Hens, T. Van Daele, J. Peymen, W. Van Reeth, S. Overloop, F. Maes (2009), Landgebruik in Vlaanderen, MIRA 2009 and NARA 2009 Scientific Reports, VMM, INBO. R.2009.20, www.milieurapport.be, www.nara.be.

[12]  Berens, W. (1988), The suitability of the weighted $l_p$-norm in estimating actual road distances. European Journal of Operational Research, 34, pp. 39-43.

# Modeling and simulation of periurban dynamics

Using CA to explore the peripheral growth on southern Brazil

## C. P. TORALLES[1,2,3]; M. V. P. SARAIVA[1,4]; M. C. POLIDORI[1,5]

[1]Programa de Pós-Graduação em Arquitetura e Urbanismo - PROGRAU,
Laboratório de Urbanismo - LabUrb, Universidade Federal de Pelotas - UFPel
[2]Instituto Federal do Rio Grande do Sul - IFRS, Campus Rio Grande
Pelotas, RS, 96010-020, Brazil
55 53 32845500
[3]kicotoralles@gmail.com
[4]marcus.saraiva@gmail.com
[5]mauricio.polidori@terra.com.br

**Keywords:** peripheral growth, periurban dynamics, urban modeling, geosimulation, cellular automata

## Abstract

Urban growth has been the subject of several studies in recent decades. Many studies is dedicated to the issue of segregation and production of peripheries in cities. Peripheral growth is understood as the socio-spatial phenomenon that occurs at the edges of the interface between city and natural environment (or rural), distinguishing two types of urban fabric expansions: the peripherization, related to occupations for residential use of low-income populations; and closed urbanizations, related to residential use production oriented for higher income groups. Considering that formal structure of physical space and society are closely interrelated, this investigation addresses the issue from urban morphology. Studies with morphological approach, though techniques and tools of modeling and GIS support, have used the cellular automata technique for urban growth simulation, assisting the production of knowledge about their processes and their dynamics. In this way, this paper aims to identify relationships between urban morphology and dynamics of peripheral growth, assuming operational hypothesis of the association of periurban spatial patterns with indicators of urban facilities concentration and buildings densities, with features of natural environment and socioeconomic similarities of neighborhoods. In order to demonstrate the procedures for peripheral growth simulation from the model implemented in software CityCell, we propose an exploratory case study in a medium-sized city in southern Brazil: Pelotas. The results demonstrate the importance of considering aspects of city and natural environment in an integrated way, as well as neighborhoods that can attract types of consumers, allowing the simulation of peripheral formation for future scenarios.

## Introduction

In recent decades, studies about urban growth have drawn models and theories about socio-spatial phenomena in order to represent and interpret inherent logics of the configuration of cities and their dynamic processes. One of these phenomena is the peripheral growth, which consists of urban fabric expansions in the edges of interface between city and the natural (or rural) landscapes, primarily for residential use, in a rapid dynamic of interaction and conversion of natural areas in urban ground. This phenomenon is associated with urban segregation problem and we can detach two peripheral types in Brazil: a) peripherization, related to concentration of low-income population [1], b) closed urbanizations, related to residential nuclei for high-income population [2] (including those that are not closed). From this reality, urban growth and natural environment changes have been understood as the greatest challenge to humanity for the XXI century [3].

With the computing development and increasing expansion of its storage capacity and data processing, and the development of geographic information systems (GIS), were possible advances in studies about related processes of urban phenomena. Efforts on urban modeling and simulation, with morphological approach and using the cellular automata technique enabled the incorporation of environmental, socioeconomic and politic dimensions in urban models [4-5]. These are important advances on spatial and temporal representation to modeling urban dynamics, increasing the use of models and simulators as scientific instruments.

In this way, the goal of this research is identify relationships between urban morphology and the dynamics of peripheral growth phenomenon, aiming to capture patterns that are related to the fabric production of these two peripheral types. From this, the relationships are translated into an urban growth model implemented in a software called CityCell [6-7], enabling the periurban growth simulation. The study assumes an operational hypothesis related to the association of periurban spatial patterns with indicators of urban facilities concentration and buildings densities, with features of natural environment and with socioeconomic similarities of neighborhoods.

Thus, this work starts presenting morphological characteristics of the peripheral types studied. Then we provide a brief theoretical review of urban models, urban modeling and the cellular automata technique for urban dynamics simulation. After, we present the urban growth model implemented on CityCell and their procedures to simulate the peripheral growth through an exploratory study applied to the case of a medium-sized city in southern Brazil: Pelotas.

## Morphological characteristics of peripheral formations

Urban growth and peripheral nuclei formation, for high or low income population, have been observed in cities of different sizes in all Earth regions. In developed countries this phenomenon of peripheral growth is understood like urban sprawl [1], as the suburbs and edge cities. In underdeveloped or developing countries we also found similar formations to urban sprawl, such as the closed urbanizations. However, in these countries, peripheral growth phenomenon is mainly related to the

peripherization process, generating nuclei with concentrations of low-income population. In addition to income factor, there are other factors which characterize these peripheral types. We posted here those related to morphological dimension in the Brazilian case.

Closed urbanizations is associated with the movement of elites from center towards the periphery [1] and may be characterized by: auto-segregation (looking groups with similar income levels and prevent different groups) [8-9-10]; diffuse and decentralized pattern in relation to central business district (CBD) [9]; occupy large urban areas [1]; low population densities [1-9]. Low income nuclei are more numerous and can be characterized by: buildings concentration (small, but close each other) and larger population densities; occupy areas close to natural landscape structures which are restrictive to urbanization [2-8], the dynamic of nuclei growth occurs through expansion by successive additions of similar types, in a continuous increase of occupations [1-11]. These morphological features, related to dynamics and production patterns of peripheral urban fabric, help to compose the operational hypothesis and the model procedures, which will be seen throughout the text.

## Modeling and simulation: using cellular automata to urban dynamics studies

Urban modeling is the process of translation of urban theories into mathematical models, tested through experiments and simulations in computational environment, which functions as a laboratory [5-12]. The model objective should lead to choice the appropriate methodology for its construction, not vice versa [13]. Thus, according to its goal, models may have different representation, descriptive systems and technical approaches.

One representation type used to understanding the urban morphology configuration is the cell grid, representing the surface like a matrix or a lattice of evenly spaced points, favoring the neighborhood contextual relationships and integrating Euclidian approach to the Leibnitzian [14]. This type of spatial representation allows complex data to work in spatially homogeneous way and it's one of main features of cellular automata models.

CAs are objects of a computational cellular universe whose characteristics change systemically from simple rules, depending on neighboring objects characteristics [15-16]. The possibility to simulate systemical processes which local actions (neighborhood) generate reflections in global order allows incorporate complexity in modeling [15].

Portugali [16] defines the self-organization as one of the fundamental properties of complex systems, being a phenomenon that occurs when a system organizes its internal structure independent of external causes. To Johnson [17], in a similar manner, the complexity is in these systems that adapt through an emergent behavior. When a system has multiple components interacting dynamically in different ways, following local rules and without any perceived higher-level instruction, there is complex behavior. When these local interactions generate a pattern that can be perceived in macro scale, there is an emergent behavior. From it, is formed a self-organization network, with different components creating order without deterministic intervention and creating a system that emerges from the bottom-up.

CA models are able to replicate complex behaviors and self-organizing patterns of spatial phenomena. Thus, the results of simulations can be similar to real cities morphology, allowing construction of future scenarios [3].

Currently there are several CA models in use for urban applications. Most of them are proposed as a scientific tool for academic use. These are some examples of models used to simulate the land use changes or urban growth [5-12-18]: Dinamica EGO, developed by the Remote Sensing Center of Federal University of Minas Gerais (UFMG); Metronamica, developed by Research Institute for Knowledge Systems (RIKS); and SLEUTH, developed by the U.S. Geological Survey's Urban Dynamics Research Program (USGS).

## CityCell: the urban growth simulator

To simulate urban growth, focusing on peripheral growth, this study uses a software called CityCell - Urban Growth Simulator, developed by the research group of Urbanism Laboratory (LabUrb) at the Federal University of Pelotas (UFPel) [7]. CityCell has incorporated the SACI - Simulador do Ambiente da Cidade (City Environment Simulator) [18], that is a dynamic urban model, which integrates CA and GIS; considers urban, natural and institutional attributes; and simulates urban growth through centrality and potential measures - adapted by Polidori [18] from Krafta [19] studies - and accumulated resistance (or constrictions) to urbanization. According Polidori [18], the urban planning has traditionally worked with isotropic environments, separating the city and nature. While many urban models have efforts to represent the city only by its effectively urbanized area, ecological models have difficulties to include the influence of cities, often treated as static and deterministic. The model incorporated in CityCell recognizes the need to overcome the isotropic approaches to study expansion of cities, considering urban and natural attributes. City and the nature are modeled in computational environment support by CA, graph theory, geotechnologies and adaptive modeling (allowing adjustments by user and input data according to the objective of study) [18]. Thus, the model enables to explore future scenarios by directing urban growth in order to make speculations about possible morphologies and approaching real cases.

As model input data, are chosen spatial variables that are considered relevant to the process under study. They are linked to system cells and called attributes, which can be classified as: a) natural, which describe the environment undeveloped; b) urban, describing the urbanized environment; c) institutional, representing plans and policies that are capable to intervening in the urban growth process. Attributes are elements that can generate tensions of attraction or resistance to urbanization that be relevant to simulate the dynamics of changing reality.

Tensions are abstractions associated with various types of flows (energy, people, vehicles, information) and represent investments in actions or modifications of space. In model, the city is reproduced from the distribution of five different types of tensions (Figure 1): a) axial, along paths or axes; b) axial buffer, around the paths or axes; c) polar, around nuclei; d) diffuse 1, randomic distributed, inversely proportional to its centrality and environmental resistance, and associated with formal production of high-income population (closed urbanizations); e) diffuse 2,

distributed randomly and also inversely proportional to its centrality, but directly proportional to environmental resistance and are associated with informal production of lower-income strata (peripherization).
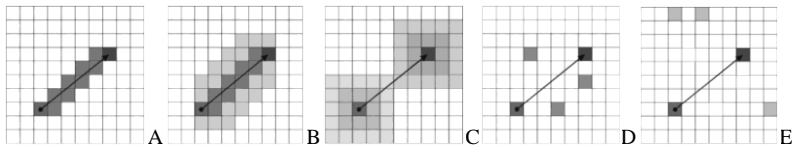


Figure 1: CA diagrams representing the types of tensions [18]: A) axial, B) axial buffer; C) polar; D) diffuse 1, E) diffuse 2.

The logic used in the model follows the understanding that centrality measure (considered an indicator of urban facilities) is able to describe potential change of urban space, creating locational imbalance in the system [20]. High values of centrality suggest areas of interest, movement and urban value, while low values indicate the opposite. The potential for change is found at the interface of the biggest difference between highest and lowest values from one location and its neighborhood. It is understood that this area combines locational advantages with lower cost of land, maximizing the income of achievement. Thus, the potential is used to increase the urban cell loading (urban load). This change process is iterative, continuous and complex, because locational opportunities are assimilated by other agents and the system is constantly changed.

Even with presence of diffuse tensions in the urban growth simulation, the outputs of original CityCell are not sufficient to identify the peripheral types in resulting morphology. With these model limitations and seeking contribute to overcome them, simple procedures have been proposed for modeling and simulation of peripheral growth of cities, assisting the identification of peripheral types and the dynamics of its formation. These procedures compose a prototype of a transition rule called Periurban Growth Tendency (PGT) and will be presented below.

## Periurban Growth Tendency: a prototype transition rule

The PGT rule is composed by following tendencies: 1) Diffuse Tendency, which explores the possibility of innovation, simulating the formation of new nuclei; 2) Neighborhood Tendency, which explores the positive feedback and the segregation logics to existing settlements expansion; 3) Final Tendency, which assumes the highest values of the two previous tendencies, corresponding the percentage of each peripheral type in city structure, making conversion of urban fabric. In this way, the diffuse tensions, as proposed by Polidori [18] and implemented in CityCell, allow a first approach for simulation patterns of urban peripheries. Their logics consider characteristics of urban morphology (low centrality) and natural environment (high resistances for peripherization; lower resistances for closed urbanization).

Following the assumed operational hypothesis and considering the characteristics of natural environment are already part of the calculations of diffuse tension distribution, was formulate that identification can be obtained from the combination of measures that indicate concentration of urban facilities and buildings densities.

Are used the CityCell outputs corresponding to morphological measures of centrality and urban loads respectively, through programmed map algebra operations typical of GIS.

The calculations proposed to find the Diffuse Tendency follow this logic: a) the peripherization is associated with lower centralities (where there is less supply of urban facilities) and a higher concentration of buildings (with smaller grain of urban land division and buildings closer each other); b) the closed urbanizations are also related to lower centralities, but not the smaller ones (where you can find more urban facilities), and the lower density of buildings.

$$DTPeriph = Urban\ Load\ /\ Centrality\ R2 \qquad (1)$$

where DTPeriph corresponds to diffuse tendency for peripherization; Urban Load corresponds to urban load value, normalized by maximum between 0 and 1; and Centrality R2 corresponds to cellular centrality normalized from logarithm with base-10, with values between 0 and 1.

$$DTClurb = Centrality\ R1\ /\ Urban\ Load \qquad (2)$$

where DTClurb corresponds to diffuse tendency for closed urbanization; Centrality R1 corresponds to cellular centrality, normalized by maximum between 0 and 1; e Urban Load corresponds to urban load value, normalized by maximum between 0 and 1.

The operational hypothesis also indicates association between spatial patterns and the socioeconomic similarities of neighborhood. Therefore, is important include the pre-existing peripheries in the system input data, acting as masks. The cells surrounding the mask take the urban load and the centrality values as variables what define the Neighborhood Tendency, using a distance-decay parameter representing actions-at-a-distance.

However, the emergence of one peripheral type does not generate only positive feedback to the same type. High income people tend to not settle close to the peripherization. It can be understood how a negative feedback. And this negative effect can also happen in inverse way, when the valorizing of the proximities of high incomes settlements not permitting the occupancy by poor people. To replicate this effect of segregation in periurban growth process is included the parameter called repel radius, which consists in a buffer where the tendencies (diffuse and neighborhood) to opposite type of periphery are zero.

$$NTPeriph = Urban\ Load\ /\ (r+1)\ .\ decay \qquad (3)$$

where NTPeriph corresponds to neighborhood tendency for peripherization; Urban Load corresponds to urban load value, normalized by maximum between 0 and 1; r corresponds to the radius (or the amount of cells from the edge of the mask); and decay corresponds to distance-decay constant.

$$NTClurb = Centrality\ R1\ /\ (r+1)\ .\ decay \qquad (4)$$

where NTClurb corresponds to neighborhood tendency for closed urbanization; Centrality R1 corresponds to cellular centrality, normalized by maximum between 0

and 1; r corresponds to the radius (or the amount of cells from the edge of the mask); and decay corresponds to distance-decay constant.

The Final Tendency of cellular conversion is found by union of diffuse and neighborhood tendencies, prevailing the greater value when some cells have both tendencies. From the amount of cell of peripherization and closed urbanization masks, the system calculates the percentage of cells with each peripheral type in relation to total urban cells. In each iteration, the amount of urban cells increases and the peripherization and closed urbanization cells increases too according the calculated percentage (this percentage can be edited by the user, enabling the creation of scenarios), converting the cells with higher Final Tendency. So the initial masks are changed, feeding back the system to calculate the Neighborhood Tendency in the next iteration and generating dynamic to the model.

$$FTPeriph = \max{(DTPeriph; NTPeriph)} \qquad (5)$$

where FTPeriph corresponds to final tendency of land use conversion for peripherization;
NTPeriph corresponds to neighborhood tendency; and DTPeriph corresponds to diffuse tendency.

$$FTClurb = \max{(DTClurb; NTClurb)} \qquad (6)$$

where FTClurb corresponds to final tendency of land use conversion for closed urbanization;
NTClurb corresponds to neighborhood tendency; and DTClurb corresponds to diffuse tendency.

The PGT prototype may be applied to all urban cells of the system or only to new cells brought with the urban growth process. In order to demonstrate the procedures included in CityCell model to peripheral growth simulation, through the PGT rule, is established an exploratory case study for the city of Pelotas, in southern Brazil.

## Exploring the periurban growth: the case of Pelotas, Brazil

Pelotas has 327,778 inhabitants (according to Census 2010), with 93% living in urban areas. Its urban area is located in the coastal plain with low altitudes. The spatial clipping includes the effectively urbanized area of the city and its surrounding natural environment (and rural), in order to allow the model simulates expansion considering urban attributes and nature attributes. This study area (Figure 2A) has 33.018 km in east-west and 19.139 km in north-south direction, bounded by the following coordinates in UTM WGS 1984 datum, zone 22 south: 6500195.75 northern boundary; 6481. 668.97 southern boundary; 393,807.48 eastern boundary; 360,802.84 western boundary. The resulting grid of spatial disaggregation has 96 rows by 165 columns, resulting 15,840 cells with 200m x 200m.

To describe the study area were used three groups of attributes, corresponding the system input data and the constraints related to urban growth: urban attributes (effectively urbanized area (EUA) and central area) (Figure 2B); natural attributes (lagoon, waterways, lentic waters, drainage lines, wetlands, forests,

dunes, fields, and a random layer) (Figure 2C and 2D); and institutional attributes (prohibition to urbanize in lagoon and waterways). Besides the attributes, are also considered the masks of pre-existing peripheries: low-income settlements (LIS) and high-income settlements (HIS) (Figure 2E and 2F). The simulation was set to 40 iterations (corresponding to 40 years), with growth rate approximately 1% per year and tension distribution called isotension (20% for each of five tensions). The PGT rule was applied to all cells of system and the parameters were set as follows: decay equal to 1; repel radius with 2 cells; the percentage of each periphery type based on mask.

As can be observed, the result highlights an increase of peripherization on seaport area (at south), on Barro Duro balneary (at east) and the closer the Pelotas River (watercourse between center of city and the coast of the lagoon) (Figure 3A, marked with arrows). For the closed urbanization, mainly the result shows a vector directing toward the Laranjal balneary (at east) (Figure 3B, marked with arrows), which nowadays is empirically observed. This was only an exploratory study, aiming to demonstrate the procedures of PGT rule. The procedures need follow the validation steps and so could give more accurate results in simulations and future scenarios.
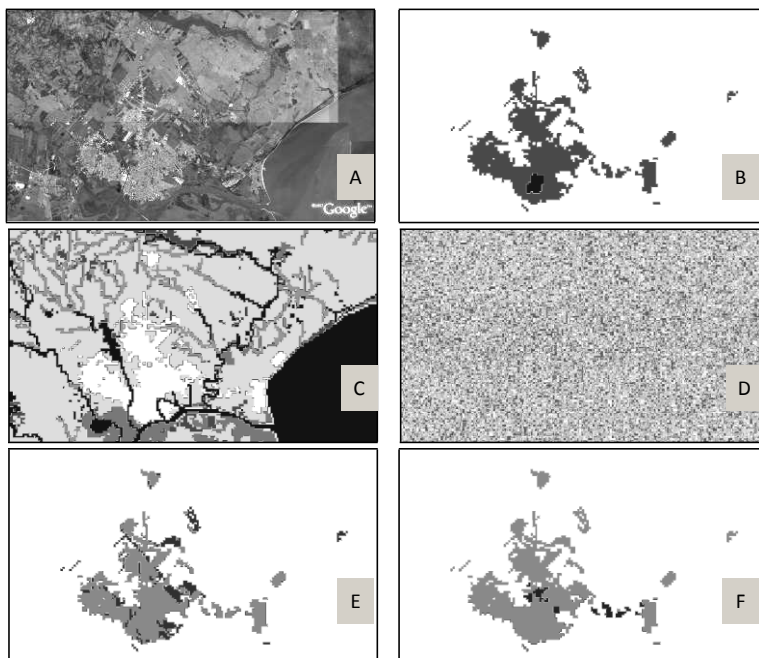


Figure 2: Pelotas input data for 2010: A) Google Earth base; B) urban loads (EUA and center); C) environmental resistences (lagoon, waterways, drainage lines, wetlands, forests, dunes, fields); D) random resistences; E) mask of LIS (over EUA); F) mask of HIS (over EUA).

Figure 3: masks of peripheral types for Pelotas, respectively for iterations 13, 26 and 40, over EUA, with tendencies for the type formations: A) peripherization; B) closed urbanizations.

## Remarks and continuities

Modeling with cellular automata techniques for urban studies and geosimulation have enabled simulate the morphological dynamic of urban growth, incorporating the current ideas of systems, complexity, emergencies and self-organization [3-16]. The periurban growth is a phenomenon associated with the urbanization process, having a strong relationship with natural environment changes and socio-spatial segregation in cities. Therefore, is important that studies about socio-spatial dynamic, especially when related to production of urban fabric in peripheral edges, consider aspect of city and natural environment in an integrated way. The urban growth model implemented in software CityCell considers both current ideas and aspects of the city and the natural environment, allowing to simulate dynamical changes of reality and to speculate about future scenarios.

To model and simulate the periurban growth was constructed an operational hypothesis indicating that urban peripheries are associated with the concentration of urban facilities, buildings densities, natural environment features and socioeconomic similarities of neighborhoods, developed in a prototype transition rule called Periurban Growth Tendency. From results found for present study, can be made the following observations: a) the distribution of diffuse tensions proposed by Polidori [18] and related to centralities and natural environment resistences allows to simulate spatial patterns of the peripheral types; b) the Diffuse Tendency, that considers indicators of concentration of urban facilities and of buildings densities, allows identify tendencies of fuzzy urbanizations around the edges of city; c) the Neighborhood Tendency, from pre-existing peripheries, allows identify possible tendencies geared to attracting similar types; d) the Final Tendency, joining the two previous tendencies and consider all items involved in operational hypothesis, allows identify the conversion directed towards the peripherization and closed urbanizations. For better accuracy to periurban growth simulation is indicated apply procedures of validation (evaluating with patch measures and spatial correlation) and sensitivity tests. Finally, it is expected that the studies allow explore future scenarios, increasing discussion of peripheral growth and helping to strengthen the model as a scientific tool to decision-making processes for urban planning.

## Acknowledgments

## References

[1]    Barros, J. X. (2004), Urban growth in latin american cities - Exploring urban dynamics through agent-based simulation, PhD Thesis, University of London, London.

[2]    Buzai, G. D., Marcos, M. (2012), The social map of Greater Buenos Aires as empirical evidence of urban models. Journal of Latin American Geography, 11 (1), 2012, Conference of Latin Americanist Geographers, pp. 67-78.

[3]    Li, X. (2011), Emergence of bottom-up models as a tool for landscape simulation and planning. In Landscape and Urban Planning, n. 100, Elsevier, pp. 393-395.

[4]    Almeida, C. M., Monteiro, A. M. V., Câmara, G. (2007), Perspectiva histórica de modelos de dinâmicas urbanas e regionais. In C. M. Almeida, G. Câmara, A. M. V. Monteiro (orgs.), Geoinformação em urbanismo - Cidade real x cidade virtual, pp. 254- 285, Oficina de Textos, São Paulo.

[5]    Furtado, B. A., Van Delden, H. (2011), Modelagem urbana e regional com autômatos celulares e agentes - Panorama teórico, aplicações e política pública. In Texto para discussão, n. 1576, IPEA, [Brasília].

[6]    Polidori, M. C., Peres, O. M., Saraiva, M. V. P., Toralles, C. P., Cardoso, A. O., Morelatto, N. B. (2011), Atualização do modelo de crescimento urbano e emergência de padrões sócio-espaciais urbanos, Relatório de pesquisa, Universidade Federal de Pelotas, Pelotas (Brasil).

[7]    Saraiva, M. V. P., Polidori, M. C., Peres, O. M., Toralles, C. P. (2011), CityCell – Urban Growth Simulator, software, Laboratório de Urbanismo, FAUrb, UFPel, Pelotas (Brasil).

[8]    Davis, M. (2006), Planeta favela, Boitempo, São Paulo.

[9]    Torrens, P. M. (2006), Simulating sprawl. In Annals of the Association of American Geographers, n. 96, Association of American Geographers, Washington D. C

[10]  Villaça, F. (2001), Espaço intra-urbano no Brasil, Studio Nobel, FAPESP, Lincoln Institute, São Paulo.

[11]  Domingues, Á. (1995), (Sub)úrbios e (sub)urbanos - O mal estar das periferias ou a mistificação dos conceitos. In Revista da Faculdade de Letras – Geografia, I Série, Vol. X/XI, Porto (Portugal), pp. 5-18.

[12]  Batty, M. (2009), Urban modelling. In R. Kitchin, N. Thirft (eds.), International encyclopedia of human geography, [Elsevier].

[13]  Benenson, I., Torrens, P. M. (2004), Geosimulation - Automata-based modelling of urban phenomena, Wiley, New York.

[14]  Polidori, M. C., Krafta, R. (2005), Simulando crescimento urbano com integração de fatores naturais, urbanos e institucionais. In GeoFocus (Artículos), nº 5, Madri.

[15]  Batty, M. (2005), Cities and complexity - Understanding cities with cellular automata, agent-based models, and fractals, MIT Press, Cambridge.

[16]  Portugali, J. (2000), Self-organization and the city, Springer, Berlim.

[17]  Johnson, S. (2003), Emergência - A vida integrada de formigas, cérebros, cidades e softwares, Jorge Zahar Ed., Rio de Janeiro.

[18] Polidori, M. C. (2004), Crescimento urbano e ambiente - Um estudo exploratório sobre as transformações e o futuro da cidade, Tese de Doutorado em Ecologia, PPGECO, Universidade Federal do Rio Grande do Sul, Porto Alegre.

[19] Krafta, R. (1994), Modelling intraurban configurational development. In Environment and planning B - Planning and desing, vol. 21, Pion, London.

[20] Granero, J. C., Polidori, M. C. (2002), Simulador da dinâmica espacial com representação em um ambiente SIG. In Anais do IV Simpósio Brasileiro de Geoinformática – GeoInfo 2002, Caxambu (Brasil), GeoInfo, pp. 17-23.

# An Irregular and Multi Scale Cellular Automata

Tessellation to Model Surface Water

## H. SAMMARI[1]; M.A. MOSTAFAVI[1,2]; B. MOULIN[1,3]

[1]Centre for Research in Geomatics, Laval University, Canada hedia.sammari.1@ulaval.ca
(correspondent author)

[2]Dept. of Geomatics, Laval University, Quebec, Canada
mir-abolfazl.mostafavi@scg.ulaval.ca

[3]Dept. of Computer Sciences and software Engineering, Laval University, Canada
bernard.moulin@ift.ulaval.ca

**Keywords:** water flow, geosimulation, cellular automata, multi-scale, Voronoi diagram.

## Abstract

Geographic information systems (GIS) are a powerful tool to handle spatial information and are widely used to represent, manage and analyse spatial data in many disciplines including geosciences, agriculture, forestry, metrology and oceanography. In GIS, considerable efforts have been carried out for the representation and management of the spatial data, based on the object view of the space. However, they are still limited when it comes to representation and simulation of spatiotemporal processes. Examples of such processes in the geographic domain include global warming, inundation, erosion, land cover change, urban growth and traffic. GIS have been criticized for not being able to provide the necessary functionalities for representation, analyzing and predicting effectively the behaviour of those processes. The integration of Cellular Automata (CA) and geospatial models represents a potential solution for understanding and representing spatiotemporal processes. In this paper, we are exploring the potentials of a Voronoi lattice based CA as an alternative to improve GIS capabilities to represent surface water flow as a spatiotemporal process. In addition, we propose a hierarchical perspective of the built lattice that may be essential to easy move between scales and then to better understand the complex behaviour of the whole system.

## Introduction

During the past decades, considerable efforts have been devoted to the representation and management of spatiotemporal processes. Examples of such processes in the geographic domain include global warming, flood, erosion, land cover change, urban growth and traffic. The integration of Cellular Automata (CA) and geospatial models represents a potential solution for modeling and representation of spatiotemporal processes for better understanding of their complex behavior. However, because of the irregularity and the multi-scale nature of these

processes, a classical Cellular Automata model may not be able to simulate their complexity.

The aim of this paper is to propose a Cellular Automata approach using an irregular hierarchical tessellation. For this purpose, we propose to develop an irregular lattice of cells based on Voronoi diagram for discretization of the space that is hierarchical in order to better represent the multi-scale behavior of spatiotemporal processes. As a case study we will apply the developed tessellation for the simulation of surface water flow which has a very irregular behavior in the space and time and it is also necessary to study its behavior in more than one scale for hydrologists. This paper is thus organized as follows: The first part primarily deals with the cellular automata construction. In this part, we explain how we build a lattice of cells using Voronoi diagrams, how we define specific neighborhood and transition rules and how we can move from one scale to another to better represent the process behavior. In the second part of the paper, the proposed approach is applied to a specific spatiotemporal process in the hydrologic domain. We describe the CA transition rules equations in order to simulate surface water flow. Finally, we present some preliminary simulation results corresponding to a watershed located near Quebec City and we discuss the potentials and limitations of the proposed approach.

## I. Cellular Automata Construction

In the context of Cellular Automata theory [17], our model consists of three primary components: a lattice of cells or grid, the neighborhood of each cell and the transition rules that determine the changes of cells properties. In fact, each of these components influences the state of each individual cell and in turn the global behavior of the phenomenon. In this section, we present the characteristics of our Cellular Automata Model and how its components can be organized hierarchically.

### 1. The Grid Geometry

[10] [1] and [ 2] argue that most of traditional Cellular Automata are based on regular grids which are known to be less complex and easier to operate than irregular ones [16]. Examples of these include rectangular, triangular and hexagonal tessellations. Although the regular grids Cellular Automata are simple to construct, they are less adapted to the irregularities of real world phenomena that they are supposed to represent. [4] and [9] suggest that the Voronoi diagram, and its dual Delaunay triangulation, can be a good choice for the representation and simulation of continuous dynamic fields.

Following some early researches on irregular Cellular Automata [15] using a Voronoi-based spatial discretization, we propose to use Voronoi diagram as an alternative Cellular Automata lattice of cells that can effectively support a more realistic representation of spatial dynamic processes such as surface water flow. Briefly, a Voronoi diagram may be defined as a particular kind of space decomposition based on points or objects called generators. This decomposition leads to a number of Voronoi cells, each associated with one generator. In our approach each Voronoi cell corresponds to an automaton.

One of the main issues in generation of Voronoi diagram for cellular automata based simulation is to determine on which set of points or objects the diagram should be created. The answer is strongly dependent on the studied process as well as on the available data. The spatial decomposition should allow a realistic representation of spatial process and allow considering its irregular and complex behavior in the space and time. In our case, surface water flow and its behavior is strongly related to topography. Hence, the altitude is the most relevant parameter on which can be based a point selection to construct the Voronoi diagram. That's why we use terrain elevation data points as generators of Voronoi cells. We can apply a point selection approach to any kind of original elevation data set in order to have multi resolution representation of the terrain topography. More specifically, terrain data is initially obtained from topographic maps. LIDAR point clouds are also very well suited to the construction of such irregular tessellations. Regular square grid elevation model can also be used as initial data set. However, in order to eliminate unnecessary points with appropriate algorithms and keep more relevant points for generation of Voronoi lattice. The procedure consists in making successive point selections from this original grid. Each selection's output is a set of irregular distributed data points suitable to construct a Voronoi diagram. The first selection keeps a maximum number of points and generates our cellular automata initial data set. Then, the following selections reduce the number of points, allowing less and less Voronoi cells in each diagram or grid and defining different levels of scale. Details of point selection algorithm are given in Section 3 which presents the multi-scale character of the grid. Once the grid of Voronoi cells is built, the issue is to define the necessary rules that formalize the interactions between neighbors and dictating the update of cells' states.

In the next subsection, we propose our own definition of the neighborhood relationship between cells and we explain what kind of transition rules can be used in the case of surface water flow CA simulation.

## 2. Definition of an Oriented Neighborhood and Transition Rules

Traditional square CA grid usually uses Moore and Von Neumann's neighborhood where the degree of neighborhood relationships is either 1:4 or 1:8 [3].

In the case of a Voronoi partition, the number of neighbors is different from one cell to another depending on the spatial distribution of data points in the space. Furthermore, the distance between the cell and each of its neighbors and the length of the common boundary cannot be fixed. However, the Delaunay triangulation associated with the spatial discretization may be used to provide the links that define the neighborhood, which is an important component of the CA approach. In fact Voronoi diagram creates a space partition into regions such that any location is associated with its nearest Voronoi generator [5]. According to Gold [6], this allows for an automated discretization of space and provides an adjacency structure from which a topology table can be generated.

More specifically, a Voronoi data structure is defined so that each Voronoi cell is associated with a vector containing information about its vertices, edges and neighborhood's generators. This structure allows for reaching parameters and states of the neighbor cells in order to establish the transition rules and update the general

grid state. In our case, we define a specific neighborhood based on terrain elevation and the studied phenomenon. As a matter of fact, a cell *A* is considered to be a neighbor of a cell *B* not only if it is a geometric neighbor on the Voronoi diagram, but also if water can move from *B* to *A*. Hence, in this case, *B* is not necessarily a neighbor of *A*. One cell may have no neighbor if its elevation is lower than the elevations of its Voronoi neighbors (Figure 3). This specific neighborhood is predetermined before running the simulation algorithm. It is an output of the space decomposition as well as the surface slope, two inputs which are strongly related to the terrain elevation in the case of a surface water flow. Knowing that transition rules are applied to neighbor cells, we can talk about oriented transition rules because the interactions between cells agree with the water direction: Water movement defines between which cells exist interactions and in which direction the flow is authorized.
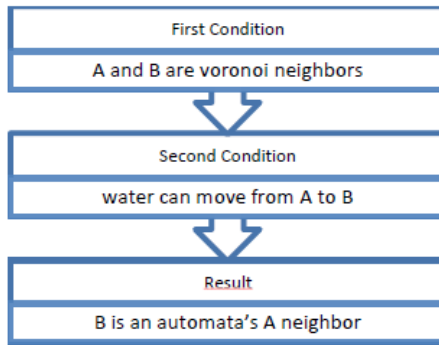


Figure 3: Oriented CA Neighborhood Definition

The following subsection deals with building space scales using a Voronoi diagram decomposition and explains the algorithm we use to select points for each scale level in order to have a multiscale space discretization.

### 3. Spatial Hierarchy

Generally, considering a multi-scale Cellular Automata, we need a grid refinement method. This is useful when the real-world phenomena and associated behavior can be studied and simulated at several levels of detail (or scales).

One important innovation of our Cellular Automata approach is the multiscale aspect of the irregular grid of cells. In Geographic Information Systems, spatial hierarchy of regular square grids is usually based on a quadtree data structure that allows to recursively subdivide the space into quadrants. Hence, each internal node has exactly four children. However, this kind of spatial hierarchy is rarely discussed in the case of irregular space decomposition, and more specifically in relation to a CA model. Indeed, the issue is to find a method to build different levels of space scales based on Voronoi diagrams. In the literature, [5] propose to construct Voronoi cells for the whole data set which constitutes the micro level of the details. Moving to higher levels is accomplished by reducing the number of Voronoi cells.

However, no algorithm was proposed to reduce the number of Voronoi cells. Indeed, a similar approach was used by [11] who proposed a structure where the index generators were local maxima of a given attribute (such as elevation). Our solution is to go from a micro scale to a meso and then a macro scale by selecting points from the original data set and constructing a Voronoi diagram for each scale using a reduced number of points. Hence, we propose an approach that allows us to identify and sort important points for each scale and then construct one Voronoi diagram for each scale. Certainly, depending on the type of spatiotemporal process and its characteristics, there may be different methods to select data points or objects for each space scale representation. Terrain generalization algorithms are well suited for multiscale representation of terrain topography and its morphology. Several generalization algorithms exist in terrain modeling domain. We selected one of them, the VIP algorithm ("Very Important Points") that can be related to surface water flow processes. Actually, it is specifically used to store elevation data points in order to eliminate less important points and to keep only the points that are necessary to reproduce a topography model closest to reality. To apply the VIP algorithm we need a Digital Elevation Model (DEM) of the studied area, which has to be a raster square grid DEM. Then, the method assesses how important is a given point by calculating how its elevation can be approximated by the elevation of its direct eight grid neighbors. More precisely, a three by three filter is used to define a kind of Moore neighborhood. So, each point has 8 neighbors forming 4 diametrically opposite pairs. The procedure consists in examining each of these pairs in turn for each point of the DEM: we connect the two neighbors by a straight line and compute the perpendicular distance of the central point from this line. For example, in Figure 5, we show how to compute the perpendicular distance for N1 and N2 the north and south neighbors of a point P. It is assumed that the greater the difference between a real point's elevation and the estimated elevation from its grid neighborhood, the more important the point is in term of surface significance.
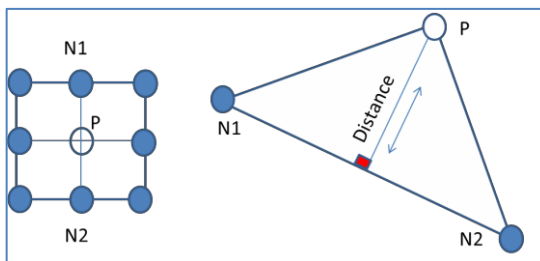


Figure 5: distance between diametrically opposite pairs

Then, we average the four distances to obtain what we call a significance measure for the point. After that, selecting very important points is done by deleting points of the DEM in order of increasing significance (deleting the least significant first). We carry on the deletion until meeting one of the two following conditions: either the

number of points reaches a predetermined limit, or the significance value reaches a predetermined limit (Figure 6).
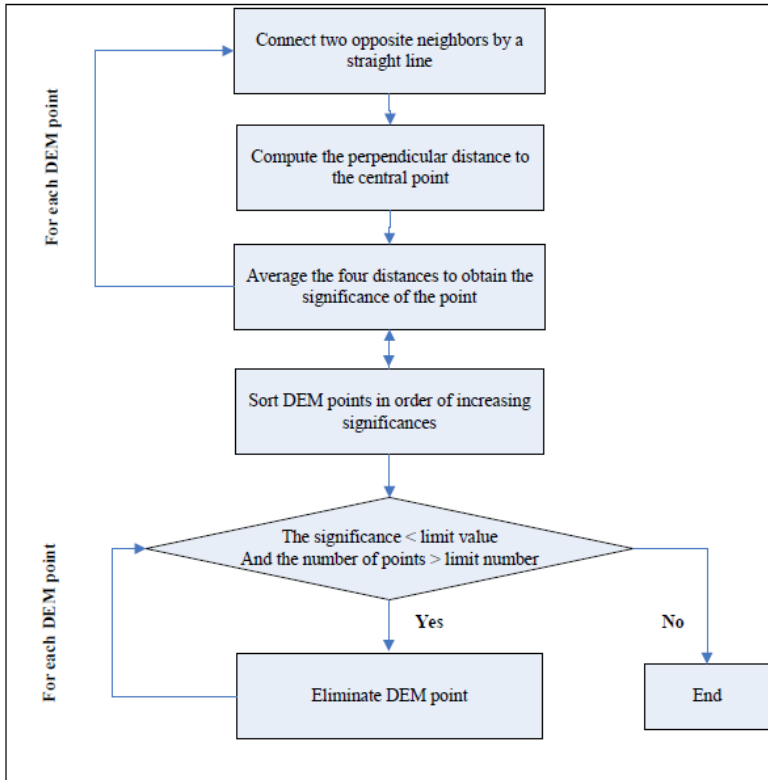


Figure 6: VIP Algorithm

In practice, once the different Voronoi diagrams levels (or scales) are built; the approach is to couple grids of different scales and define their overlap regions. Indeed, as the basic geometry of the grid is a Voronoi cell, its shape is different from one cell to another and also from one scale to another. Furthermore, when we slip through scales; we cannot predefine the final shape of an aggregation of a set of Voronoi cells because the boundaries of one level do not necessarily correspond to the higher level boundaries. Hence, our future approach's attempt is to examine the degree of overlapping between grids of different scale and to propose a solution to aggregate parameters values from low to high levels.

## II. CA Transition Rules for Surface Water Simulation

Watershed runoff simulations have been traditionally based on numerical computations solving momentum and energy equations. While simulations based on these methods generally simplify the constitutive equations in order to allow for a closed solution [13], our cellular automata approach is a different alternative to simulate water flow because unlike in traditional simulations it only computes local processes from which emerges the global behavior that is not linked to the model [11].

Surface water flow between cells is based on physical processes involved in water movements. Hence, in order to maintain the conservation of mass, Cellular Automata rules should specify the added quantity of water to each cell as a result of precipitation (rain) as well as the loss of water due to infiltration in the soil. The method is specified as follows: In each cell, we calculate the water velocity using a rule based on Manning's equation (Equation 1) [12] where the velocity depends on the water surface slope **S** and the input roughness **n** depends on the type of soil and vegetation.

$$velocity = depth^{2/3}.S^{1/2}/n \qquad (1)$$

Typically, Manning's equation is an empirical formula for open channel flow calculations. Hence, as we simulate an overland flow, the water depth is an approximation which corresponds to the normally-used hydraulic radius in Manning's equation. The same approximation was used by [11].

The velocity is then used to compute the time **T** needed for the water to traverse the cell (Equation 2). Until the time condition is met, the simulator keeps the water in the cell. This time is then reset once the water in the cell is released to its neighbouring cells.

$$T = width/velocity \qquad (2)$$

The simulation procedure that we use to update the grid state is explained in Figure 4. Firstly, we choose a time step so that water will not cross the cell in less than one time step. Another condition is that the simulation time step cannot be less than available data time step. For each cell of the grid we calculate the traverse time T as explained in the CA algorithm (Figure 7) using equations 1 and 2. When the traverse time T is completed, the amount of moveable water leaves the cell. However, before that, this amount is stored in a buffer layer until we cover all the grid cells. Then, the updating of the entire grid is applied simultaneously. The distribution of the moveable volume of water is dictated by the elevation of the neighbourhood's cell.

In fact, the neighbours share the moveable water of the centre cell if its surface water elevation is higher than them. In other terms, the model allows to transfer the movable volume of water to the downstream neighbours in proportion to the difference in water surface elevation. The following example is given by [13]: if two neighbours have lower water elevation than the centre cell, and if one of them is twice as low as the other, than two thirds of the centre cell's movable water would

go to the lowest downstream neighbour and a third would go to the other downstream neighbor.
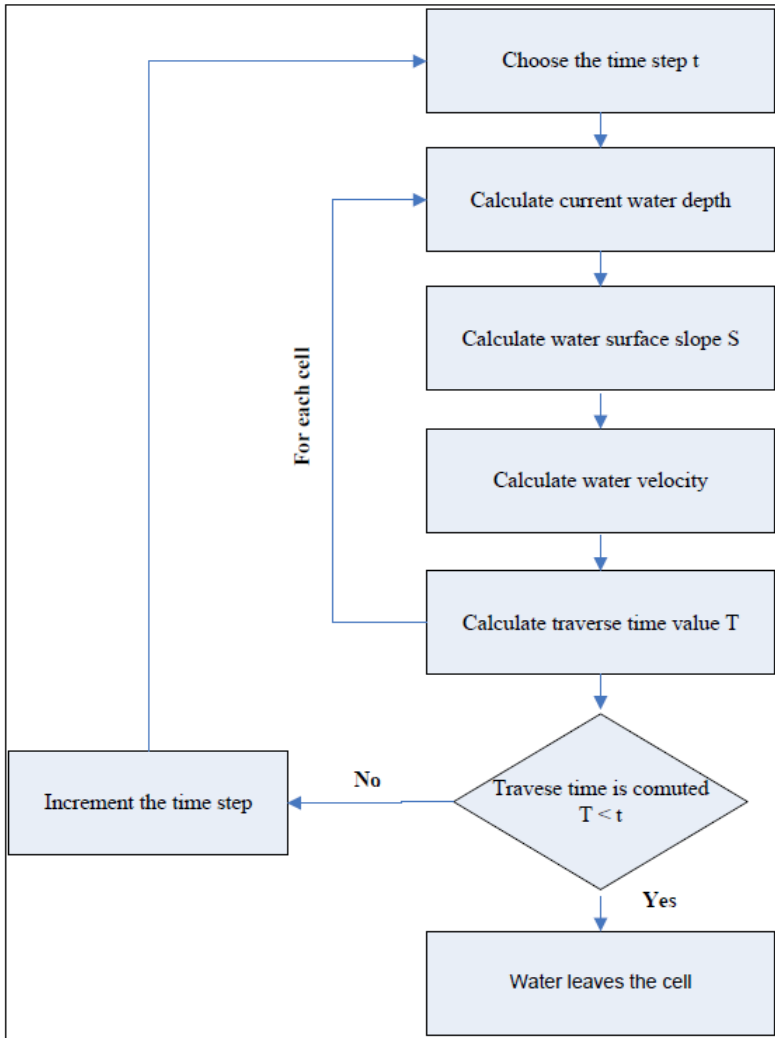


Figure 7: Simulation CA Algorithm

Currently, we have implemented the proposed CA approach for surface water flow simulation. The simulation engine has been be developed in C++ programming

language which is selected as the development language due to its compatibility with the CGAL (*Computational Geometry Algorithm Library*) library chosen for the geometric lattice building.

Data about terrain elevation, precipitations, type and occupation of the soil are collected in Montmorency River watershed in Quebec City region where Laval University has an experimental watershed named "Eaux Volées" with a huge amount of data available and observed in a regular base for more than forty years (Figure 5).
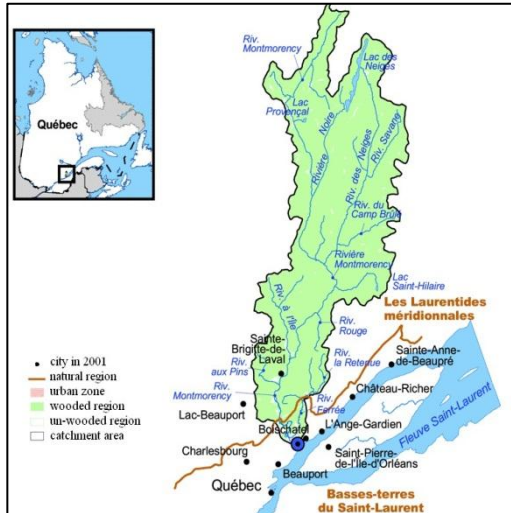


Figure 5: Location map of the Montmorency river watershed [14]

This data can be used not only for the calibration of the simulation engine but also to validate the simulation results. Data inputs into our model are in forms of raster layers exported from GIS text files. As a matter of fact, firstly, Voronoi diagram of the micro scale is constructed with the prototype using CGAL functions. Then, the generators coordinates are exported to ArcGIS where we interpolate other simulation inputs: a layer of water depth (precipitation values minus infiltration) to be used in equation (1), a layer of slope values which can be derived from elevation layer and a layer of roughness coefficients derived from type and soil occupation layers. Finally, in order to apply equations (1) and (2), the attribution of parameters to each automata cell is done by our simulation engine which takes the Voronoi structure as an input.

A major consideration of CA models is the computational resources needed to run simulations. We are working on improving computational time, which is currently about 30 seconds per time step for a grid of 800 Voronoi cells. The result of a first simulation shows how the model reacts to a constant 0.01 Manning's n roughness value (Table 1). This shows that the model produces realistic watershed simulation: the same order of magnitude of real data.

Table 1: Simulated and in situ Velocity values comparaison

| Period | Simulated Velocity (m$^3$/s) | In situ Velocity (m$^3$/s) |
|--------|------------------------------|----------------------------|
| June 2010 | 0.0643 | 0.0741 |
| July 2010 | 0.0862 | 0.0566 |

In this step, multiple simulations are still to be performed to determine the impact of varying the unknown parameter of roughness rate. Nevertheless, a better computational time is necessary to allow such tests. That's why, what is pressing right now is to reduce the simulation running time.

## III. Conclusion and Challenges

In this paper we have presented our research on a hierarchical irregular lattice based Cellular Automata using Voronoi diagram for the simulation of spatial dynamic processes such as surface water flow. It has been argued that the traditional CA approaches based on regular tessellations are not suitable for very irregular varying real world phenomena; we have proposed to use a Voronoi hierarchical lattice instead of traditional regular grids which are commonly used both in CA simulation methods and GIS raster models. We have suggested the Voronoi diagram as an alternative space discretization model within GIS in order to improve GIS capabilities for spatiotemporal processes presentation and simulation. Showing the utility of different scales representation of spatiotemporal processes, we propose a hierarchical approach that allows to merge Voronoi cells based on the data attributes values, and then to move to higher scales. We have then detailed different components of a CA simulation approach and described how it can be practically applied to the simulation of the dynamic phenomenon of surface water flow. Finally, we have detailed different procedures for the simulation of surface water flow in a given watershed in Quebec region using the proposed approach. An algorithm defining the CA rules was presented based on hydrologic equations in order to define the interactions between CA cells. The required information for the simulation process was identified using this equation which mainly includes Digital Terrain Model, slope, soil type, vegetation, information on precipitation and etc. There are numerous challenges that we need to study in details in order to adequately adapt the proposed method for the simulation of a dynamic process such as surface water flow. Firstly, spatial resolution for the micro level is an important point to be considered. It is clear that the proposed method can adapt itself to any resolution that is required by the application. In addition, in contrast to the existing regular grid based CA, we can create a multi-resolution adaptive grid to better represent the spatial variability of the dynamic process in any level of hierarchy. Another challenge is the selection of the temporal resolution for the simulation process that needs to be decided. The third challenge consists on the attribution of the initial states to each cell. Validation of the simulation process is another challenge that we need to address. Finally, the aggregation process needs to be done more carefully, knowing the fact that

aggregated cells surface does not exactly correspond to the higher level cell surface. This introduces some uncertainties in aggregated data in higher levels. Hence, we need to consider the propagation of these uncertainties to higher levels of aggregation and try to reduce their impact on final results. To sum up, several experimentations would be also necessary in order to more rigorously evaluate the potentials of the proposed method.

## Acknowledgement

## References

[1]   Barros, J., (2004), Urban Growth in Latin American Cities: Exploring Urban Dynamics
Through Agent-Based Simulation. PhD Thesis. University of London, pp. 1-285.

[2]   Batty, M., (2005), "Agents, Cells and Cities: New Representational Models for Simulating Multi-Scale Urban Dynamics." Environment and Planning A 37(8) pp. 1373-1394.

[3]   Benenson, I and Torrens, P., (2004), Geosimulation: Automata-based mo0deling of urban phenomena, 287 pp.

[4]   Gold, C.M. and Condal, A.R., (1995), "A Spatial Data Structure Integrating GIS and Simulation in a Marine Environment." Marine Geodesy 18, pp. 213-228.

[5]   Gold C. and Angel P. "Voronoi hierarchies" GIScience 2006 LNCS 4197 (2006): 99-111.

[6]   Gold, C. M., (2000), "An Algorithmic Approach to Marine GIS, In Marine and Coastal Geographical Information Systems". Ed.: Wright, D. and Bartlett, D. London, England: Taylor and Francis, pp. 37-52.

[7]   Goodchild, M., (1992), "Geographical data modelling." Computers & Geosciences 18, pp. 401-408.

[8]   Goodchild, M.F., Yuan, M., Cova, T.J. (2007), "Towards a General Theory of Geographic Representation in GIS." International Journal of Geographic Information Science 21 pp. 239-260.

[9]   Mostafavi Mir Abolfazl, Christopher M. Gold., (2004), "A global kinetic spatial data structure for a marine simulation." International Journal of Geographical Information Science 18(3) pp. 211-227.

[10]  Nara, A., Torrens, P.M., (2005), "Inner-City Gentrification Simulation Using Hybrid Models of Cellular Automata and Multi-Agent Systems". Proceedings of the Geocomputation 2005 conference. University of Michigan, Michigan, USA, pp. 1-23.

[11]  Nicholas, AP. (2005), "Cellular modelling in fluvial geomorphology". Earth Surface Processes and Landforms 30, pp. 645–649

[12]  Okabe, A., and Sadahiro, Y., (1996), "An illusion of spatial hierarchy: Spatial Hierarchy in a Random Configuration". Environment and Planning, A 28 pp.1533-1552.

[13]  Parson Jay A. and Fonstad Mark A., (2007), "A Cellular Automata Model of Surface Water Flow." Hydrological Process 21, pp. 2189-2195.

[14]  Hubert, S., (2007) "Faits saillants 2004-2006 État de l'écosystème aquatique - Bassin versant de la rivière Montmorency." Ministère du développement durable, de l'environnement et des Parcs. Gouvernement du Québec, pp. :1-7.

[15] She, Wenzhong, Pang Matthew Yick Cheung., (2005), "Development of Voronoi-Based Cellular Automata - an Integrated Dynamic Model for Geographical Information Systems". International Journal of Geographical Information Science 14, n. 5, pp. 455-474.
[16] Sullivan, O. (2001), "Exploring Spatial Process Dynamics Using Irregular Cellular Automaton Models". Geographical Analysis 33.1 pp. 1-18.
[17] Wolfram, Stephen (1983), "Statistical mechanics of cellular automata". Reviews of Modern Physics 55 (3): pp. 601–644.

# Mining of CA based land transition rules through self-adaptive genetic algorithm for urban growth modeling

## Yan LIU[1] and Yongjiu FENG[2]

[1]School of Geography, Planning and Environmental Management, University of Queensland
Chamberlain Building, St. Lucia Campus, Brisbane, QLD 4072, Australia
Phone: 3365 6483 Email: yan.liu@uq.edu.au (correspondent author)
[2]College of Marine Sciences, Shanghai Ocean University, China
Email: yjfeng@shou.edu.cn

## Abstract

This paper presents a method for mining the land use transition rules and parameters of a cellular automata urban growth model using a self-adaptive genetic algorithm (SAGA) method. It builds on the evolutionary computation technique to search for and optimize a set of spatial parameters representing various spatial factors impacting on urban land use change. The application of the SAGA-CA model to simulate the spatio-temporal processes of urban land change in Southeast Queensland's Gold Coast City, Australia from 1991 to 2006 demonstrates that the self-adaptive genetic algorithm can be integrated within a conventional urban CA model to improve the performance of the model, therefore enhance our understanding of urban landscape dynamics.

## Introduction

There is a long-standing interest in understanding urban dynamics through the use of computer generated simulation models [1-10]. Compared to modeling approaches developed with the exclusive use of mathematical formulae, such as those based on gravity theory to model transportation networks and land-use planning, models based on cellular automata (CA) have been favored due to their ability to capture the systematic spatio-temporal process and the stochastic behavior or characteristics of land use change [8, 11-13].

Central to a CA based urban model is the definition of the model's transition rules which determine how the state of a cell changes over time [4, 12-14]. Cellular automata models are simple in nature and are flexible at incorporating various transition rules that may impact on urban development into the model. This type of model is intuitive and capable of incorporating different driving factors to urban land use change into the simulation process. However, the challenge remains in the identification of appropriate parameter values to quantify the effect of various driving factors on urban growth [15, 16].

The development of genetic algorithms (GAs) has provided researchers with new ways to identify and search for suitable transition rules and their defining parameters in urban modeling [17, 18]. A genetic algorithm can be used to search for an optimal solution to a problem based on the mechanics of natural genetics and natural selection [19]. Compared with other evolutionary methods such as particle swarm optimization [20, 21], GA's unique feature exists in its operators, including selection, crossover, and mutation. Substantively, GA is a randomized method rather than a simple random operation because historical information is used to speculate on new candidate solutions [19].

This paper presents a method for mining the land use transition rules and parameters of a cellular automata urban growth model using a self-adaptive genetic algorithm (SAGA) method. The model was applied to simulate the spatio-temporal processes of urban land change in Southeast Queensland's Gold Coast City, Australia. The following section presents the modeling framework, followed by a description of the study area where the proposed CA model is tested and calibrated. Next, the results generated from the application are presented and discussed. Conclusions are drawn in the last section.

**The Modeling Framework**

The modeling framework consists of a generic CA urban growth model which is linked to an optimization module using SAGA to search for an optimal set of transition rules and parameters for the CA model to simulation the dynamic process of urban growth (Figure 1).
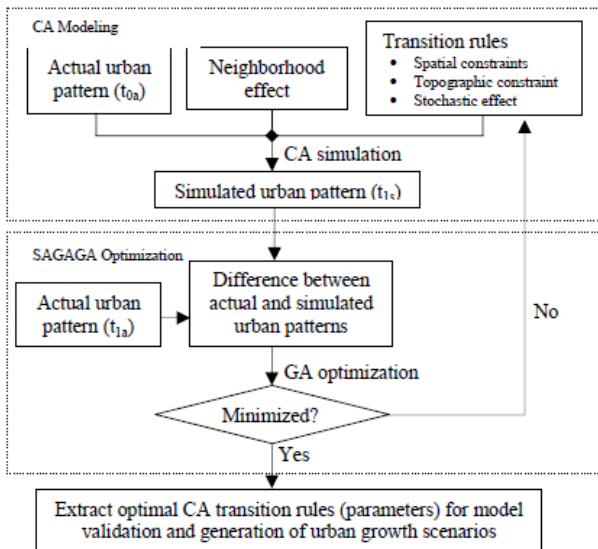


Figure 1: The SAGA-CA modeling framework

## The generic CA urban growth model

The generic CA urban growth model was initially configured using logistic regression approaches [22], where the land use conversion probability of a cell at location i at time t is represented as:

$$P_i^t = P_{di}^t \times \overline{P_{Ni}^t} \times C \times R \tag{1}$$

Where:

$P_i$ represents the land use conversion probability of cell i at time t; $P^t$ is a land use conversion probability due to its spatial proximity to facilities and services. This is controlled by a set of spatial proximity factors $d_j (j = 1,..., k)$, including the distance of each cell to the key regional and regional centers, distance to sub-regional and district centers, distance to highways, distance to main roads, distance to the coastal line and the prime agricultural land $P_{di}^t$ can be written as:

$$P_{di}^t = \frac{1}{1 + e^{-(a_0 + \sum_{j=1}^{k} a_j d_j)}} \tag{2}$$

The parameters $a_0$ and $a_j$ ($j = 1,..., k$) representing the impact of each distance factor on land conversion probability are to be mined and optimized using the SAGA optimization approach.

$P^t$ is a land use conversion probability due to neighborhood support. In this research, a square neighborhood with $m \times m$ cells was adopted; the probability a cell develops from one state to another is defined as a proportion of the accumulative state of urban cells within the m×m neighbourhood in total neighbouring cells. For the case study implemented in this paper, the neighbourhood size is 5×5 cells.

C represents a (set of) land suitability constraints where urban growth cannot occur. *R* is a stochastic disturbance factor on urban development.

The temporal scale is set to one year for each iteration of the model. Details regarding the logistic regression based CA model can be found in [22].

## Self-adaptive genetic algorithm for mining of transition rules

GA represents a possible solution by a chromosome. Each chromosome consists of a set of genes or parameters that need to achieve an optimal solution to the problem the GA is trying to solve. In the CA based urban modeling practice, all possible CA transition rules affecting urban land use change are considered as chromosomes and their defining parameters are the genes.

To search for an optimal solution which minimize the difference between simulated and observed land use patterns, GA uses a fitness function to evaluate and quantify the optimality of a solution [23]. This search and optimization process is achieved according to natural selection rules, including selection, crossover and mutation. However, standard GAs use fixed selection, crossover and mutation rates; this can be problematic as such operators and their parameters cannot be modified during the search and optimization process. A SAGA can overcome this problem; it not only keeps population diversity effectively but also improves the performance of

local and premature convergences [24, 25]. Such genetic diversity is important to ensure the existence of all possible solutions in the solution domain and the identification of an optimized solution. In addition, the SAGA improves the search speed and precision of the standard genetic algorithm and hence, accelerating the search and optimization process for problem solutions.

Selection is the key operation of the SAGA in which individual genomes are chosen from a population of candidate solutions for later breeding, including recombination and crossover. Individual solutions are selected through a fitness-based process during each successive generation where solutions with better fitness values (that is, the difference between the simulated and observed results is smaller) are more likely to be selected. The crossover and mutation operators are adopted from [24], which were defined through a probability measure which changes in accordance with the fitness values.

## Study Area and Data

Gold Coast City in South East Queensland, Australia was selected as the case study site to apply the SAGA-CA model to simulate its land use change from 1991 to 2006. Gold Coast City is situated in the southeast corner of Queensland; it extends north to the southern fringe of metropolitan Brisbane, the state's capital city, south to the border with the state of New South Wales, and west to the Lamington National Park, the foothills of the Great Dividing Range (Figure 2). It has a total area of 1400 square kilometers. The current urban structure consists of a range of suburbs, localities, towns and rural districts which, according to the Gold Coast Planning Scheme, will evolve into key regional centers, regional centers, sub-regional centers and district centers [26].



Figure 2: The City of Gold Coast (right) and its location in Australia (left)

Gold Coast City has grown from a small beachside holiday town to the second largest city in Queensland and the sixth largest city in Australia over the past fifty years. From 1996 to 2006 it has seen a population increase from 375,000 to 472, 000 [27]. The rapid population increase has lead to phenomenal economic development in the city and the state and significant geographical expansion of urban areas. According to Ward et al. [28] urban areas in Gold Coast City increased by 32% from 1988 to 1995. Such rapid urban growth and change may present challenging issues in terms of social, environmental and economic sustainability [29].

Two Landsat Thematic Mapper (TM) imageries acquired in 1991 and 2006 were used to quantify the extent of land use change over this period in time. These data were re-sampled to 30m spatial resolution with 1402 rows by 1965 columns. Three types of land uses were classified from the imageries; urban, non-urban and water bodies. As the focus of this research is on land use change from non-urban to urban states, the presence of water bodies was considered as physical constraints to urban growth. In addition to the satellite imageries, data representing key regional and regional centers, sub-regional and district centers, highways, main roads, coastal line, natural conservation and prime agriculture land as well as a 9 second DEM were collected from the relevant government agencies. All data were re-processed to raster grids in 30m spatial resolution.

## Results and Discussions

### Optimal chromosome/CA transition rule parameters

To construct a fitness function and commence the searching and optimization process using the SAGA approach, a total of 20 000 sample cells were randomly selected from within the study area. The distances of each of these sample cells to the key regional and regional centers ($d_{ct}$), sub-regional and district centers ($d_{tw}$), highways ($d_{hw}$), main roads ($d_{rd}$), the coastal line ($d_{cl}$) and the prime agricultural land ($d_{ag}$) were extracted from the relevant distance data layers. The model achieved the best fitness value after 4,000 iterations. The convergence of the fitness track led to the identification of an optimized chromosome or solution (Table 1).

Table 1: Optimized chromosome of the GeneCA model

| Variables | Constant | $d_{ct}$ | $d_{tw}$ | $d_{hw}$ | $d_{rd}$ | $d_{cl}$ | $d_{ag}$ |
|---|---|---|---|---|---|---|---|
| Parameters | 0.779 | -0.668 | -0.471 | -0.227 | -0.304 | -0.003 | 0.592 |

The optimized chromosome demonstrated the different impacts of the spatial factors on urban land use change in the Gold Coast City. According to Equation (2), a negative parameter of $a_i (i = 0,1,...,6)$ leads to a larger $P_{gi}(t)$ value, that is, a positive impact on urban growth or higher probability for a cell to convert from a non-urban to an urban state. Likewise, a positive $a_i$ value results in a smaller $P_{gi}(t)$, hence, a negative impact on urban growth or lower probability for the cell to convert into an urban state in the next time step. The parameter values optimized by the

SAGA shows that the distance to the key regional and regional centers has the most significant impact on the development of cells within its neighborhood, followed by the impacts of distances to the sub-regional or district centers and the main roads. On the other hand, close proximity to prime agriculture land has negative impact on urban land use change. Hence, the closer a cell is to agricultural lands the less likely the cell is to be developed to an urban state. This is consistent with regional policies of conserving prime agricultural land.

**Simulation accuracy assessment**

To evaluate the simulation accuracy of the model, the error budget analysis as proposed by Pontius et al. [7] was applied to compare the simulated results with the land use classification data from the satellite imageries. This is to evaluate whether the observed agreement between the map pairs is attributable to chance ($C_{agr}$), quantity ($Q_{agr}$), or location ($L_{agr}$), and whether the disagreement between the map pairs is attributable to location ($L_{disagr}$) or quantity ($Q_{disagr}$). The five indicators were computed for 2006 (Figure 3).



a) 1991 reference map     b) 2006 reference map     c) 2006 simulated map
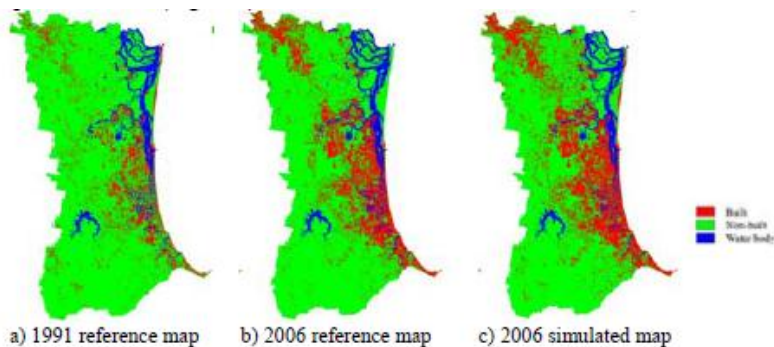
Figure 3: Actual and simulated land use patterns of Gold Coast in 2006

Comparing the percentages of agreement and disagreement between the 2006 simulated result and 2006 reference map (Figure 4), the model achieved a simulation of 85.0% match of cells between the two maps. Amongst these matching cells, 29.2% are locational matches and 27.1% are quantity agreement and the remaining 28.7% are agreement due to chance. On the other hand, there is 15.0% mismatch of cells between the two maps where 5.2% are due to quantity disagreement and 9.8% are locational disagreement (Figure 4).
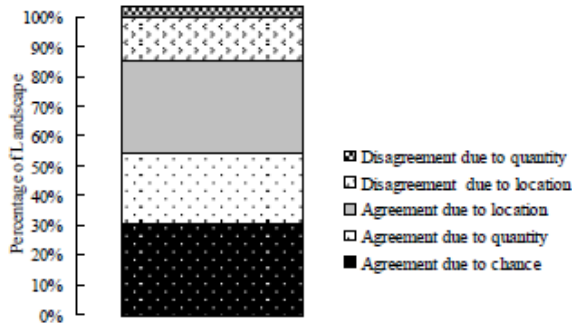
Figure 4: Error budgets between the reference and simulated result in 2006

**Discussions**

Previous studies show that the simulation accuracies of CA urban models are affected by the methodologies used in retrieving the transition rules, the spatial and thematic resolution of the model, as well as the physical, socio-environmental and institutional situations of the areas under study. In this research, three thematic categories (i.e. urban, non-urban, and water body) were extracted from satellite imageries to simulate the process of land use change from non-urban to urban. Given the complex land use types and conversions on the ground, it is challenging to apply a model with simplified land use categorization to simulate multiple land use change processes while still maintain high simulation accuracies.

The simulation accuracy of the CA based urban models is sensitive to the spatial scale or resolution of cells [30, 31]. CA models configured at a coarse resolution (e.g. 250m) usually generate low simulation accuracies whereas models configured at finer resolution (e.g. 30m) generate relatively high accuracy [31]. The low simulation accuracy of the model at a coarse scale is usually due to the isolation of urban cells at such scale, where only a small number of isolated urban cells can be identified in the initial input data [31].

Moreover, the methodology adopted in retrieving the CA's transition rules is crucial for good simulation results. A number of new methods have been developed to capture land use dynamics and improve simulation accuracy. Using an evolutionary computation technique the SAGA-CA model is a further improvement on conventional spatial statistical methods such as logistic regression based CA models; it optimizes the transition parameters of the CA model to improve the model's simulation accuracy. By applying the self-adaptive genetic algorithm method to a typical logistic regression based CA model, the model is capable of taking into account feedback from individual 'genes' during the modeling process. This leads to the identification of a set of optimized transition rules.

## Conclusion

Spatially-explicit simulation of urban land use change has attracted widespread interest in recent years with the focus on the spatio-temporal dynamics of urban system and its land use evolution. Many CA based urban models have been developed and applied in various situations. It is useful to apply such model to simulate the dynamic change of urban land use, provided that suitable transition rules reflecting the characteristics and driving factors on land use change are identified and built into the model. However, it remains a challenging issue for urban modelers to achieve such accomplishment in the modeling practice.

This paper contributes to this field by developing an urban CA model with its transition rules optimized by a self-adaptive genetic algorithm. It builds on the evolutionary computation technique [24, 25] by introducing a self-adaptive genetic algorithm to search for and optimize a set of spatial 'chromosomes' through a series of interactive and dynamic selection, crossover and mutation operations. The self-adaptive genetic algorithm was used to optimize the spatial parameters representing various spatial factors contributing to urban land use change. Consequently, a set of optimized transition rules and their defining parameters were identified and used to simulate the process of land use evolutions. The application of the SAGA-CA model to Gold Coast City demonstrates the effectiveness of the SAGA technique in optimizing the transition rules of an urban CA model, thereby contributing to human studies of urban landscape dynamics. The high simulation accuracy generated by the model demonstrate that the SAGA-CA model is a promising tool for simulating urban land use change and future land use scenarios.

Further research will focus on introducing other spatial factors, such as land values and income differentiated socio-economic factors, into the modeling process, as well as considering multiple types of land use changes. This will evaluate whether the SAGA technique is capable of searching for and extracting more complex transition rules on urban land use evolution.

## References

[1]  Batty, M. and Y. Xie (1994). From cells to cities. Environment and Planning B: Planning and Design, 21, pp. 531-548.

[2]  Couclelis, H. (1997). From cellular automata to urban models: New principles for model development and implementation. Environment and Planning B: Planning and Design, 24, pp. 165-174.

[3]  Batty, M., Y. Xie, and Z. Sun (1999). Modelling urban dynamics through GIS-based cellular automata. Computers, Environment and Urban System, 23, pp. 205-233.

[4]  Li, X. and A.G.-O. Yeh (2002). Neural-network-based cellular automata for simulating multiple land use changes using GIS. International Journal of Geographical Information Science, 16(4), pp. 323-343.

[5]  Wu, F. (1998). SimLand: a prototype to simulate land conversion through the integrated GIS and CA with AHP-derived transition rules. International Journal of Geographical Information Science, 12(1), pp. 63-82.

[6]  Liu, Y. and S.R. Phinn (2003). Modelling urban development with cellular automata incorporating fuzzy-set approaches. Computers, Environment and Urban Systems, 27, pp. 637-658.

[7] Pontius, R.G., D. Huffaker, and K. Denman (2004). Useful techniques of validation for spatially explicit land-change models. Ecological Modelling, 179(4), pp. 445-461.

[8] Stevens, D. and S. Dragicevic (2007). A GIS-based irregular cellular automata model of land-use change. Environment and Planning B: Planning and Design, 34, pp. 708-724.

[9] Al-Ahmadi, K., et al. (2009). Calibration of a fuzzy cellular automata model of urban dynamics in Saudi Arabia. Ecological Complexity, 6(2), pp. 80-101.

[10] Pinto, N.N. and A.P. Antunes (2010). A cellular automata model based on irregular cells: application to small urban areas. Environment and Planning B: Planning and Design, 37(6), pp. 1095-1114.

[11] White, R.W. and G. Engelen (1993). Cellular automata and fractal urban form: a cellular modelling approach to the evolution of urban land use patterns. Environment and Planning A, 25, pp. 1175-1193.

[12] Stevens, D., S. Dragicevic, and K. Rothley (2007). iCity: A GIS–CA modelling tool for urban planning and decision making. Environmental Modelling & Software, 22(6), pp. 761-773.

[13] Liu, Y. (2008). Modelling urban development with geographical information systems and cellular automata.

[14] Al-kheder, S., J. Wang, and J. Shan (2008). Fuzzy inference guided cellular automata urban-growth modelling using multi-temporal satellite images. International Journal of Geographical Information Science, 22, pp. 1271-1293.

[15] Wu, F. (2002). Calibration of stochastic cellular automata: the application to rural-urban land conversions. International Journal of Geographical Information Science, 16(8), pp. 795-818.

[16] Li, X., J.Q. He, and X.P. Liu (2009). Intelligent GIS for solving high-dimensional site selection problems using ant colony optimization techniques. International Journal of Geographical Information Science, 23, pp. 399-416.

[17] Bies, R.R., et al. (2006). A genetic algorithm-based, hybrid machine learning approach to model selection. Journal of Pharmacokinetics and Pharmacodynamics, 33, pp. 196-221.

[18] Li, X., Q. Yang, and X. Liu (2007). Genetic algorithms for determining the parameters of cellular automata in urban simulation. Science in China Series D: Earth Sciences, 50(12), pp. 1857-1866.

[19] Schmitt, L.M., C.L. Nehaniv, and R.H. Fujii (1998). Linear analysis of genetic algorithms. Theoretical Computer Science, 208, pp. 111-148.

[20] Kennedy, J. and R.C. Eberhart (1995). Particle swarm optimization, in IEEE International Conference on Neural Networks, Perth, Australia. pp. 1942-1948.

[21] Feng, Y. J., Y. Liu, and Z. Han (2011). Land use simulation and landscape assessment using genetic algorithm based cellular automata under different sampling schemes. Chinese Journal of Applied Ecology, 22, pp. 957-963.

[22] Liu, Y., and Y. J. Feng (2012). A logistic based cellular automata model for continuous urban growth simulation: A case study of the Gold Coast city, Australia. In Alison J. Heppenstall, Andrew T. Crooks, Linda M. See and Michael Batty (Ed.), Agent-based models of geographical systems (pp. 643-662) Dordrecht, Netherlands: Springer.

[23] Muzy, A., et al. (2008). Modelling landscape dynamics in an Atlantic Rainforest region: Implications for conservation. Ecological modeling, 219, pp. 212-225.

[24] Srinivas, M. and L.M. Patnaik (1994). Adaptive probabilities of crossover and mutation in genetic algorithms. IEEE Transactions on Systems, Man and Cybernetics, 24, pp. 656-667.

[25] Angeline, P.J. (1995). Adaptive and self-adaptive evolutionary computation, in Computational intelligence: A dynamic system perspective, IEEE Press. pp. 152-161.

[26] Gold Coast City Council (2010). Our living city: Gold Coast Planning Scheme 03 Version 1.2 Amended Oct 2010. Available at: http://www.goldcoast.qld.gov.au/gcplanningscheme_1010/overview.html. Last accessed 1 Apr 2012.

[27] Australian Bureau of Statistics (2006). Census products 1996, 2001, 2006, Australian Bureau of Statistics: Canberra.

[28] Ward, D.P., A.T. Murray, and S.R. Phinn (2000). Monitoring growth in rapidly urbanizing areas using remotely sensed data. Professional Geographer, 52(3), pp. 371-386

[29] Ward, D.P., A.T. Murray, and S.R. Phinn (2003). Integrating spatial optimization and cellular automata for evaluating urban change. The Annuals of Regional Science, 37(1), pp. 131-148.

[30] Kocabas, V. and S. Dragicevic (2006). Assessing cellular automata model behaviour using a sensitivity analysis approach. Computers, Environment and Urban Systems, 30(6), pp. 921-953.

[31] Feng, Y., et al. (2011). Modeling dynamic urban growth using cellular automata and particle swarm optimization rules. Landscape and Urban Planning, 102(3), pp. 188-196.

# Evolutionary computing & CA models

A genetic algorithm tool to optimize the Bayesian calibration of an urban land use change model

## Cláudia M. ALMEIDA[1]; Britaldo S. SOARES-FILHO[2]; Hermann O. RODRIGUES[2]

[1]National Institute for Space Research – INPE, Division for Remote Sensing - DSR
Av. dos Astronautas, 1758, SERE – I, PO Box 515, 12227-010 São José dos Campos, Brazil
+55-12-3208-6428, almeida@dsr.inpe.br (correspondent author)
[2]Federal University of Minas Gerais – UFMG, Centre for Remote Sensing – CSR/IGC Av.
Antônio Carlos, 6627, 31270-900, Belo Horizonte, Brazil
+55-31-3409-5449, {hermann, britaldo}@csr.ufmg.br

## Abstract

Empirical models meant to simulate and predict urban land use change are commonly dependent on the utilisation of statistical methods to estimate the probabilities of land use change. As opposed to such probabilistic methods, genetic algorithms (GA) arise as an ancillary heuristic tool to refine and optimize such probabilities by means of non-parametric approaches. This work introduces a simulation experiment on urban land use change in which a GA-optimized Bayesian calibration model has been employed in the parameterisation of several infrastructure variables considered for simulation. The estimated spatial land use transition probabilities drive a cellular automaton (CA) simulation model, based on stochastic transition rules. The model has been tested in a medium-sized town in the Midwest of São Paulo State, Bauru. A series of simulation outputs for the case study town in the period 1988-2000 were generated, and statistical validation tests were then conducted for the best results by means of multiple resolution fuzzy similarity measures.

## Introduction

The employment of evolutionary (or Darwinian) premises for automated problem solving is not new and dates back from the 1950s. Nearly a decade afterwards, three different interpretations of this approach started to be developed in parallel by three distinct researchers. Lawrence J. Fogel [1] in the US was the first one to introduce the concept of evolutionary programming. John Henry Holland [2], on his turn, called his method a genetic algorithm. In Germany, the domain of evolution strategies arose with Ingo Rechenberg and Hans-Paul Schwefel [3]. It was only in the beginning of the 1990s that these three areas were merged under one major field called evolutionary computing. Also at this time an alike fourth

stream had emerged – genetic programming. In this way, evolutionary computing turned out to embrace the sub-areas of evolutionary programming, evolution strategies, genetic algorithms, and genetic programming.

The field of evolutionary computing has presented linkages with Artificial Life, especially since the 1990s, with the swarm-based computation and nature-inspired algorithms. Genetic algorithms in particular gained popularity with the work of John Holland [2]. According to [4], the increasing academic interest in this field led to meaningful advances in the computers processing capacity for practical applications, including the automatic evolution of computer programs. Evolutionary algorithms, as stated in [5], "are now used to solve multi-dimensional problems more efficiently than software produced by human designers, and also to optimise the design of systems".

As [6] reported, the use of genetic algorithms in cellular automata (CA) models started at the end of the 1990s with the work of [7]. Other works in the same line were produced, as in [8] and [9], which used GA for parameter estimation of complex urban dynamic models, as well as in [10], [11], [12], and [13], in which transition rules of CA models have been optimized by genetic algorithms (GA).

More recently, there has been a profusion of articles dealing with GA for calibration and optimization of urban CA models [14], [15], [16], [17].

In all above-mentioned cases, a binary approach (urban x non-urban) has been adopted. In a diverse way from the previously reported works, the purpose of this paper is to deal with the simulation of multiple urban land uses (e.g. residential, commercial, industrial, etc.) by means of a GA tool employed to optimize a Bayesian calibration of a CA urban land use change model.

## GA fundamentals

As stated by [18], evolutionary algorithms form a subset of evolutionary computation in that they generally only involve techniques implementing mechanisms inspired by biological evolution such as reproduction, mutation, recombination, natural selection and survival of the fittest. In this process, there are two main forces that form the basis of evolutionary systems: Recombination and mutation create the necessary diversity and thereby facilitate novelty, while selection acts as a force increasing quality [18].

Genetic algorithms, in brief, are methods that simulate the processes of natural and genetic evolution through computational routines, aiming to solve optimization problems in situations where the search space is huge and conventional methods have demonstrated to be inefficient. GA are basically structured in an analogous way to the biological chromosomes, as initially exposed. The first step consists in the generation of a population of individuals, which are characterized by their chromosomes, corresponding to numerical values representing a possible solution to a given problem. During the evolutionary process, this population is evaluated, and each chromosome is awarded a grade that reflects its adaptation capacity to a certain environment. The fittest chromosomes are selected, and the least fit ones are discarded, in accordance with Darwinian laws. The selected individuals are subject to cross-over (recombination) and mutation, generating offspring to the next

generation, which corresponds to a complete iteration of the genetic algorithm. This process is repeated until a satisfactory solution is found [19].

Cross-over basically consists in combining the genetic material of two individuals, generating two new descendents, which inherit the parents´ characteristics. In order to avoid the anticipated convergence of the genetic algorithm, it is necessary to conduct a mutation operation, introducing new regions in the solutions search space. Many aspects of such an evolutionary process are stochastic. Changed pieces of information due to recombination and mutation are randomly chosen. On the other hand, selection operators can be either deterministic, or stochastic. In the latter case, individuals with a higher fitness have a higher chance to be selected than individuals with a lower fitness, but typically even the weak individuals have a chance to become a parent or to survive [18].

In order to assess the quality of a candidate solution, an objective function is used. It provides to the genetic algorithm a measure of fitness of each individual belonging to the population [19]. The choice of an appropriate objective function is crucial for the success of the GA performance. A detailed explanation on the objective function (or fitness function) employed in this work is presented in the next section.

## Application

### Study Area and the GIS Database

The GA-optimized CA simulation model was applied to a medium-sized city, Bauru, located in the Midwest of São Paulo State, southeast of Brazil. The city comprised a total of 236,740 inhabitants in the initial time of simulation (1988), which increased to 309,531 inhabitants in 2000. In this period, the annual population growth rate was around 1.34%, and it was marked by the expansion of the existing residential areas together with the mushrooming of peripheral residential settlements, which have been mostly incorporated to the main urban tissue (Figure 1).
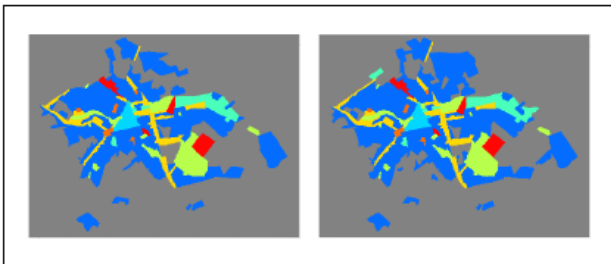


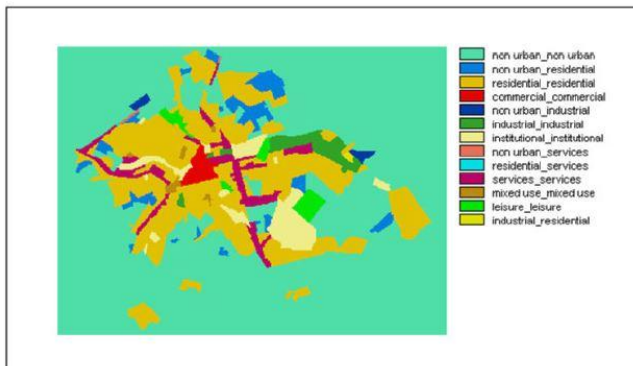Figure 1: Land use map in Bauru in 1988 (left) and 2000 (right)

Figure 2: Cross-tabulation map between Bauru land use maps of 1988 and 2000, indicating permanence and changes in land use

Besides experiencing a considerable development concerning the residential use, Bauru also witnessed intra-urban land use changes like the increase in industrial and services areas (Figure 2).

The assessment of the total amount of land use change from 1988 to 2000, commonly known as global transition rates, was directly derived from a cross-tabulation operation between the initial and final land use maps, which provided the figures presented in Table 1, associated with the five types of observed land use change.

Table 1: Global transition rates for Bauru: 1988–2000

| Land Use | Non-Urban | Resid. | Comm. | Ind. | Inst. | Services | Mixed | Leis./Recr. |
|---|---|---|---|---|---|---|---|---|
| Non-urban | 0.9615 | 0.0333 | 0 | 0.0043 | 0 | 0.0009 | 0 | 0 |
| Resid. | 0 | 0.9997 | 0 | 0 | 0 | 0.0003 | 0 | 0 |
| Comm. | 0 | 0 | 1 | 0 | 0 | 0 | 0 | 0 |
| Industr. | 0 | 0.0438 | 0 | 1 | 0 | 0 | 0 | 0 |
| Instit. | 0 | 0 | 0 | 0 | 1 | 0 | 0 | 0 |
| Services | 0 | 0 | 0 | 0 | 0 | 1 | 0 | 0 |
| Mixed | 0 | 0 | 0 | 0 | 0 | 0 | 1 | 0 |
| Leis./Recr. | 0 | 0 | 0 | 0 | 0 | 0 | 0 | 1 |

After the identification of land use transitions and their respective rates, the next step concerned the determination of the different sets of infrastructure variables governing each of the five types of change, based on heuristic procedures. These procedures basically regard the visualization of distinct maps of variables (distances in grey scale) superposed on maps of land use transition, so as to identify those more meaningful to explain the different types of land-use change. The variables selected for modeling are listed in Table 2, and the sets of variables assigned to explain each of the five transitions are indicated in Table 3.

Table 2: Independent variables defining land use change in Bauru: 1988–2000

| Notation | Physical or Socioeconomic Land Use Change Variable |
|----------|----------------------------------------------------|
| dist_ind | Distances to industrial zones |
| dist_res | Distances to residential zones |
| dist_com | Distances to the central commercial zone |
| main_res | Distances to residential areas belonging to the main urban agglomeration |
| dist_serv | Distances to services corridors |
| serv_axes | Distances to the services and commercial axes |
| exist_rds | Distances to main existent roads |

Table 3: Selection of variables determining land use change in Bauru: 1988–2000

| Notation | Nu_Res | Nu_Ind | Nu_Serv | Res_Serv | Ind_Res |
|----------|--------|--------|---------|----------|---------|
| dist_ind |        | ◆      |         |          |         |
| dist_res | ◆      |        |         |          |         |
| dist_com | ◆      | ◆      | ◆       |          | ◆       |
| main_res |        | ◆      | ◆       |          |         |
| dist_serv |       |        |         | ◆        |         |
| serv_axes |       | ◆      | ◆       | ◆        | ◆       |
| exist_rds | ◆     |        |         |          |         |

All data used in this application had a resolution of 100 x 100 m and composed grids containing 487 lines and 649 columns, there being a total of 316,063 cells defining the region for simulation.

**The GA-optimized Bayesian model of land use change**

The GA-optimized Bayesian model of land use change was implemented in Dinamica EGO, a modeling environment that embodies neighborhood-based transition algorithms and spatial feedback approaches in a stochastic multi-step simulation framework. The parameterization method available at EGO is based on the theorem of conditional probabilities. For estimating the land use transition probabilities in each cell, represented by its coordinates x and y, an equation converting the logit formula into a conventional conditional probability was used. The logit corresponds to the natural logarithm of odds, which consists in the ratio of the probability of occurring a given land use transition to its complementary probability, i.e. the probability of not occurring the transition. This concept derives from the Bayesian weights of evidence method, from which the land use transition probability can be obtained through algebraic manipulations of the logit formula, as follows [20]:

$$P(T_i^{\alpha}/V_i^1,...,V_i^{m_a}) = O(T_i^{\alpha}).e^{\sum_{v=1}^{m_a} W^+_{i,v}} / 1 + \sum_{\alpha=1}^{\eta} O(T_i^{\alpha}).e^{\sum_{v=1}^{m_a} W^+_{i,v}} \,,$$ (1)

where P corresponds to the probability of transition in a cell; i corresponds to a notation of cells positioning in the study area, defined in terms of x,y coordinates; $\alpha$ represents a type of land use transition, e.g. from a class c to a class k, within a total of $\eta$ transitions; $V_i^1$ corresponds to the first variable observed in cell i, used to explain transition $\alpha$; $V^{m_a}$ corresponds to the m-th variable observed in cell i, used to explain transition $\alpha$; $O(T_i^{\alpha})$ represents the odds of transition $T^{\alpha}$ in the i-th cell, expressed by the ratio of the probability of occurrence of $T_i^{\alpha}$ over its complementary probability, i.e., $P(T_i^{\alpha})/P(T_i^{\alpha})$; and $W^+_{i,v}$ corresponds to the positive weight of evidence for the i-th cell regarding the v-th variable range, defined as:

$$W^+_{i,v} = \log_e P(V_i^{m_a}/T_i^{\alpha}) / P(V_i^{m_a}/\overline{T_i^{\alpha}}) \,,$$ (2)

where $P(V^{m_a}/T^{\alpha})$ is the probability of occurrence of the m-th variable range observed in cell i, used to explain transition $\alpha$, in face of the previous presence of transition $T^{\alpha}$, given by the number of cells where both $V^{m_a}$ and $T^{\alpha}$ are found divided by the total number of cells where $T_i^{\alpha}$ is found; and $P(V^{m_a}/T_i^{\alpha})$ is the probability of occurrence of the m-th variable range observed in cell i, used to explain transition $\alpha$, in face of the previous absence of transition $T_i^{\alpha}$, given by the number of cells where both $V_i^{m_a}$ and $T_i^{\alpha}$ are found, divided by the total number of cells where $T_i^{\alpha}$ is not found.

The $W^+$ values represent the attraction between a determined land use transition and a certain variable range. The higher the $W^+$ value is, the greater is the probability of a certain transition to take place. On the other hand, negative $W^+$ values indicate lower probability of a determined transition in the presence of the respective variable range. Using the $W^+$ values concerning the several distances ranges of the static variables employed in the analysis, the Dinamica EGO model calculates the cells transition probabilities according to equation 1. The grid cells are assigned a value of probability and a probability map is then generated. In order to evaluate if the model is well calibrated, i.e. if the employed explaining variables are appropriate and if the categorization of the numerical grids is optimal, this map must present the area with the highest transition probability values as close as possible to the areas that actually underwent land use change.

The GA tool in Dinamica EGO retrieves the $W^+$ values and assembles them into tables. Each model parameter ($W^+$) represents an allele and will be a record in a table that corresponds to a gene. This group of tables is an input to the GA tool. GA tool spawns a population based on the genotype passed within a group of tables. Inside GA tool, a routine (or functor) called Get current individual is placed to get the genes from the individuals of a generation. Other functors are sequenced to get the parameters and pass them on to the model. An evaluation (fitness) function is coupled with the model output and its result is passed to a functor called Set fitness,

which returns the fitness value to the GA tool for the selection process [21]. The internal sequence of functors will iterate a number of times as specified by the user. When the GA tool terminates, it outputs the fitness of the overall best individual as well as the group of tables that comprises its genes. Additional parameters of the GA tool are: number of generations; population size; convergence stopping criteria, which forces the GA tool to terminate if evolution becomes asymptotical, as defined by the convergence limit, which must be achieved within the span of generations set by the number of generations; default lower and upper bounds, which set default values within which all allele values may vary; customized lower and upper bounds, defined by the user; amongst others [21].

The GA tool engine is based on the EO computation library and selects parental individuals for the next generation using one-to-one deterministic tournament. Individuals that take part in it are randomly drawn from the current population without depleting it. Cross-over creates 70% of the new generation individuals. Any allele in a gene of an individual chosen for mutation can be altered upon 1% probability. A new generation is completed by passing it the remaining 29% of parental individuals that were submitted to neither crossing-over nor mutation. Figure 3 illustrates the graphical user interface of the Dinamica EGO GA tool.
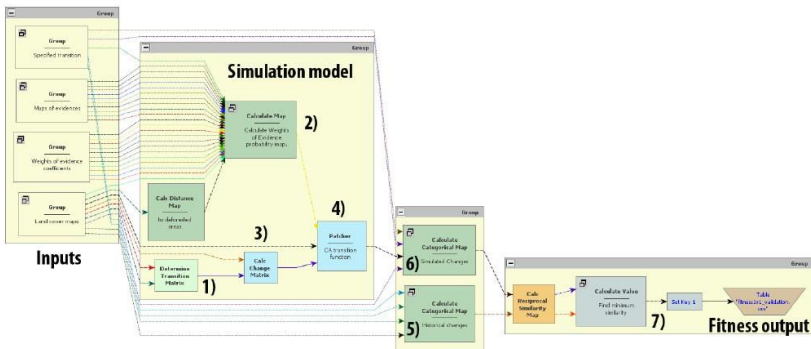


Figure 3: Graphical user interface of the GA model embedded in the Dinamica EGO

**Objective Function and Validation**

For assessing the fitness of the GA tool outputs as well as the accuracy of the CA simulation model performance, fuzzy similarity measures applied within a neighborhood context were used. The fuzzy similarity method employed in this work is a variation of the fuzzy similarity metrics developed by [21], and has been implemented in the Dinamica EGO platform.

Hagen´s method is based on the concept of fuzziness of location, in which the representation of a cell is influenced by the cell itself and, to a lesser extent, by the cells in its neighborhood. Not consider ing fuzziness of category, the fuzzy neighborhood vector can represent the fuzziness of location. In the fuzzy similarity validation method, a crisp vector is associated to each cell in the map. This vector has as many positions as map categories (land uses), assuming 1 for a category = i,

and 0 for categories other than i. Thus, the fuzzy neighborhood vector (Vnbhood) for each cell is given as:

$$
V_{nbhood} \;=\; \begin{bmatrix} \mu_{nbhood\ 1} \\ \mu_{nbhood\ 2} \\ \vdots \\ \mu_{nbhoodC} \end{bmatrix} \tag{3}
$$

$$
\mu_{nbhood\ i} \;=\; \left| \mu_{nbhood\ i,1} * m_1,\ \mu_{crisp\ i,2} * m_2,\ \ldots,\ \mu_{crisp\ i,N} * m_N \right|_{Max} \tag{4}
$$

where μ nbhood i represents the membership for category i within a neighborhood of N cells (usually N=n$^2$); μ crisp $_{i,j}$ is the membership of category i for neighboring cell j, assuming, as in a crisp vector, 1 for i and 0 for categories other than i (i ⊂ C); m$_j$ is the distance-based membership of neighboring cell j, where m accounts for a distance decay function, for instance, an exponential decay (m = 2-d/2). The selection of the most appropriate decay function and the size of the window depend on the vagueness of the data and the spatial error tolerance threshold [21]. As it is intended to assess the model spatial fit at different resolutions, besides the exponential decay, a constant function equal to 1 inside the neighborhood window and to 0 outside can also be applied. Equation 5 sets the category membership for the central cell, assuming the highest contribution is found within a neighborhood window n x n. Next, a similarity measure for a pair of maps can be obtained through a cell-by-cell fuzzy set intersection between their fuzzy and crisp vectors:

$$
S(V_A, V_B) \;=\; \left[\ \left| \mu_{A,1},\ \mu_{B,1} \right|_{Min},\ \left| \mu_{A,2},\ \mu_{B,2} \right|_{Min},\ \ldots,\ \left| \mu_{A,i},\ \mu_{B,i} \right|_{Min}\ \right]_{Max} \tag{5}
$$

where V$_A$ and V$_B$ refer to the fuzzy neighborhood vectors for maps A and B, and μ$_{A,i}$ and μ$_{B,i}$ are their neighborhood memberships for categories i ⊂ C in maps A and B, as in equation 4. According to [22], since the similarity measure S (V$_A$,V$_B$) tends to overestimate the spatial fit, the two-way similarity is instead applied:

$$
S_{twoway}(A, B) \;=\; \left|\ S\left(V_{nbhoodA},\ V_{crispB}\right),\ S\left(V_{crispA},\ V_{nbhoodB}\right)\ \right|_{Min} \tag{6}
$$

The overall similarity of a pair of maps can be calculated by averaging the two-way similarity values for all map cells. However, when comparing a simulated map to the reference map (real land use in the final time of simulation), this calculation carries out an inertial similarity between them due to their areas that did not suffer any change. To avoid this problem, the Dinamica EGO team introduced a modification into the overall two-way similarity method of DINAMICA, using two maps of differences, which present value 1 for the cells that underwent change, and 0 for those that did not change. In this way, each type of change is analyzed separately using pair-wise comparisons involving maps of differences: (i) between the initial land use map and a simulated one, and (ii) between the same initial land use map and the reference one. This modification is able to tackle two matters. First,

as it deals with only one type of change at a time, the overall two-way similarity measure can be applied to the entire map, regardless of the different number of cells per category. Second, the inherited similitude between the initial and simulated maps can be eliminated from this comparison by simply ignoring the null cells from the overall count. However, there are two ways of performing this function. One consists of counting only two-way similarity values for non-null cells in the first map of difference, and the other consists in doing the opposite. As a result, three measures of overall similarity are obtained, with the third representing the average of the two ways of counting. As random pattern maps tend to score higher due to chance depending on the manner in which the nulls are counted, it is advisable to pay close attention to the minimum overall similarity value. This method has proven to be the most comprehensive when compared to the aforementioned methods, as it yields fitness measures with the highest contrast for a series of synthetic patterns that depart from a perfect fit to a totally random pattern.

**Simulations and Discussion**

The GA-optimized simulation and the land use change probabilities maps are respectively presented in Figures 4 and 5, demonstrating a good performance of the model.
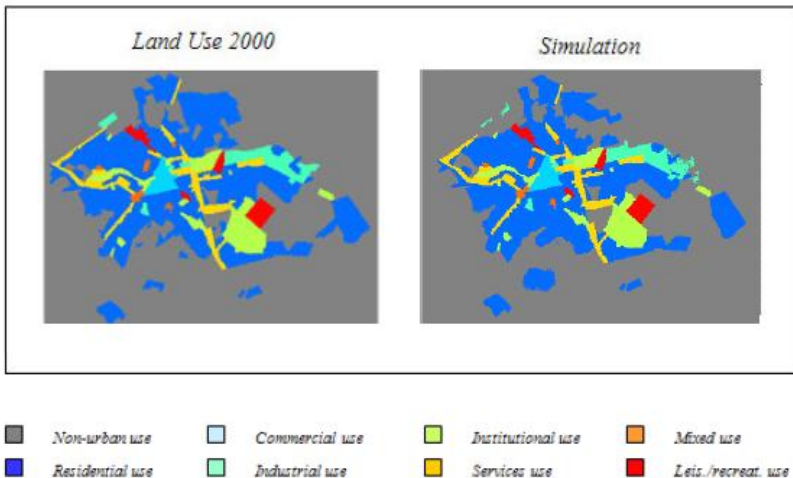


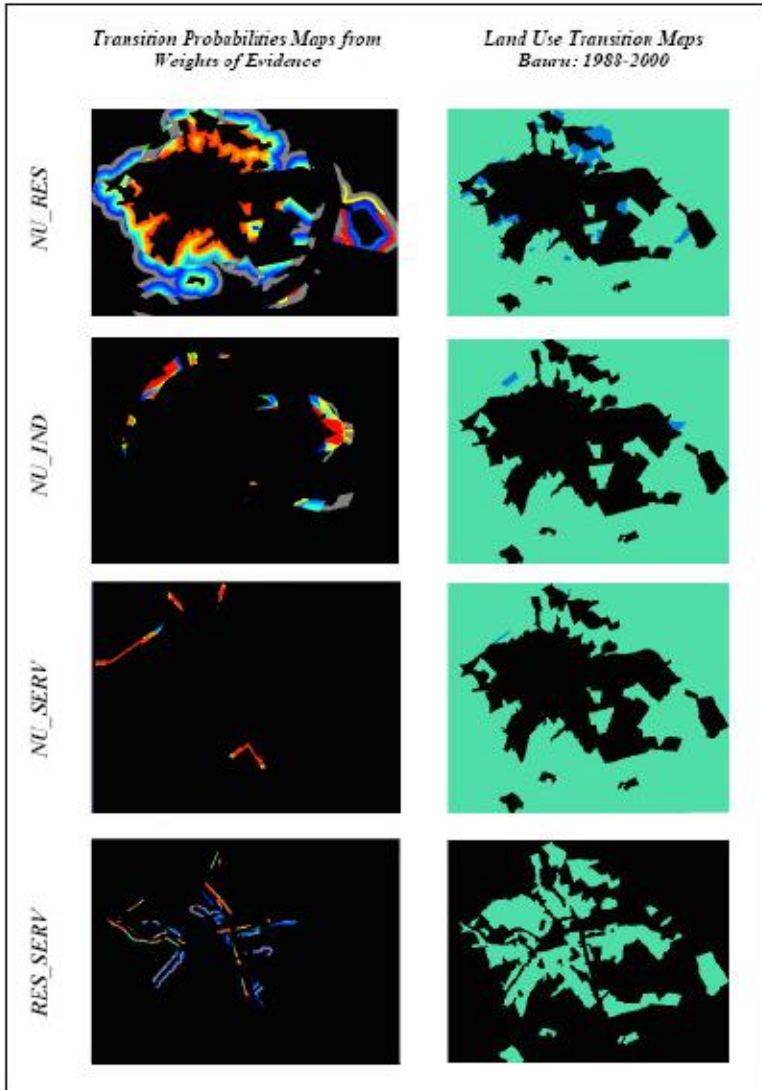Figure 4: The GA-optimized simulation compared to the actual land use in 2000

Figure 5: Estimated transition probability surfaces and land use change: 1988-2000
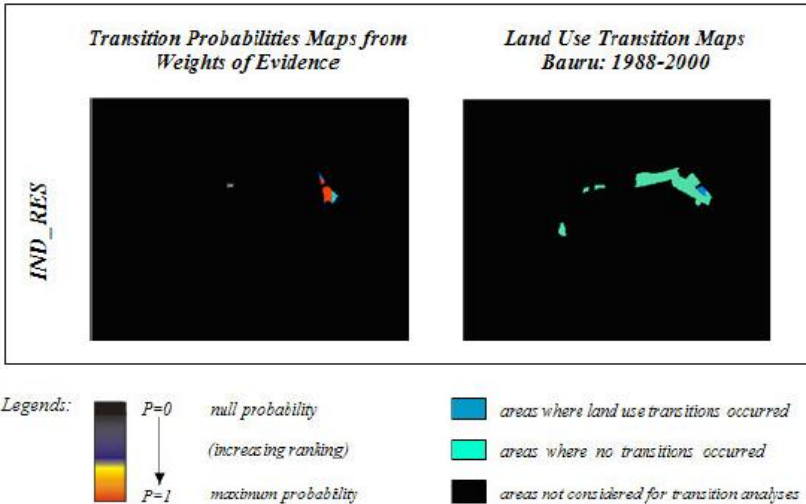
Figure 5 (Cont.): Estimated transition probability surfaces and land use change: 1988-2000

## Final Remarks

Although there is a criticism towards genetic algorithms in the sense that they require manifold parameters, the GA tool of Dinamica EGO already provides the modeler with default input parameters, which have been previously tested and shown to be optimal. Genetic algorithms must be regarded as a heuristic to find an ideal solution for a problem, conducted by parallel research and not by an exhaustive and troublesome process of trial and error.

## Acknowledgments

## References

[1]   Fogel, L. J., A. J. Owens, M. J. Walsh (1966), Artificial Intelligence through Simulated Evolution, John Wiley, New York

[2]   Holland, J. H. (1975), Adaptation in natural and artificial systems, Ann Arbor, University of Michigan Press

[3]   Rechenberg, I. (1973), Evolutionstrategie: Optimierung Technisher Systeme nach Prinzipien des Biologischen Evolution, Stuttgart, Fromman-Hozlboog Verlag

[4]     Koza, J. R. (1992), Genetic Programming, Boston, MIT Press

[5]     Jamshidi, M. (2003), Tools for intelligent control: fuzzy controllers, neural networks and genetic algorithms, Philosophical transactions, Series A, Mathematical, physical, and engineering sciences, v. 361, n. 1809, pp. 1781–808

[6]     Wu, N., Silva, E. A. (2010), Artificial Intelligence Solutions for Urban Land Dynamics: A Review, Journal of Planning Literature, v. 24, n. 3, pp. 246-265

[7]     Papini, L., G. A. Rabino, A. Colonna, V. Di Stefano, S. Lombardo (1998), Adaptation Learning cellular automata in a real world: The case study of the Rome metropolitan area in natural and artificial systems. In Proceedings of the Third Conference on Cellular Automata for Research And Industry, - ACRI'96, Milan, Italy, October 16-18, Springer-Verlag, pp. 165-183

[8]     Goldstein, N. C. (2005), Brains versus brawn - Comparative strategies for the calibration of a cellular automata-based urban growth model. In P. M. Atkinson (Ed.), GeoDynamics, pp. 249-272, CRC Press, Boca Raton, FL, USA

[9]     Al-Kheder, S., J. Wang, J. Shan (2007), Cellular automata urban growth model calibration with genetic algorithms. In Proceedings of the Urban Remote Sensing Joint Event, Paris, France, April 11-13, Kansas City, Institute of Electrical and Electronics Engineers (IEEE)

[10]    Li, X., Q. S. Yang, et al. (2007), Genetic algorithms for determining the parameters of cellular automata in urban simulation, Science in China Series D-Earth Sciences, v. 50, n. 12, pp. 1857-1866

[11]    Jenerette, G. D., J. G. Wu (2001), Analysis and simulation of land use change in the central Arizona-Phoenix region, USA, Landscape Ecology, v. 16, n. 7, pp. 611-626

[12]    Xu, X., J. Zhang, X. Zhou (2006), Integrating GIS, cellular automata and genetic algorithm in urban spatial optimization: A case study of Lanzhou, Geoinformatics 2006: Geospatial Information Science, v. 6420, pp. 1-10

[13]    Liu, Y., Y. Feng (2006), An optimised cellular automata model based on adaptive genetic algorithm for urban growth simulation. In E. Guilbert, B. Lees, Y. Leung (Eds.), Proceedings of the Joint International Conference on Theory, Data Handling and Modelling in GeoSpatial Information Science, Hong Kong, May 26-28, pp. 45-50

[14]    Wu, N., Silva, E. A. (2009), Integration of Genetic Agents and Cellular Automata for Dynamic Urban Growth Modelling, In Proceedings of the 10th International Conference on GeoComputation, Sydney, Australia, November 30 – December 02, Cambridge, UK, Department of Land Economy and Darwin College of the University of Cambridge

[15]    Zhang, F., (2010), Calibration of cellular automata model with adaptive genetic algorithm for the simulation of urban land-use, In Proceedings of the 18th International Conference on Geoinformatics, Beijing, China, June 18-20, Kansas City, Institute of Electrical and Electronics Engineers (IEEE)

[16]    Fourotan, E., M. E. Delavar (2012), Urban growth modeling using genetic algorithms and cellular automata; A case study of Isfahan Metropolitan Area, Iran, In Proceedings of the GIS Ostrava 2012 - Surface models for geosciences, Ostrava, Czech Republic, January 23-25, Ostrava, Technical University of Ostrava

[17]    Koenig, R., D. Mueller (2011), Cellular automata-based simulation of the settlement development in Vienna. In A. Salcido (Ed.), Cellular Automata – Simplicity behind Complexity, pp. 23-46, INTECH Open, Rijeka, Croatia

[18]    Ashlock, D. (2006), Evolutionary Computation for Modeling and Optimization, Springer, Berlin

[19]    Goldberg, D. E. (1989), Genetic algorithms in search, optimization, and machine learning, Addison-Wesley, New York

[20]    Bonham-Carter, G. (1994), Geographic Information Systems for Geoscientists: Modelling with GIS, Pergamon, Ontario, Canada

[21]    Hagen, A., 2003, Multi-method assessment of map similarity. In Proceedings of the 5th AGILE Conference on Geographic Information Science, Palma, Spain, April 25–27,

2002, Palma, Universitat de les Illes Balears, pp. 171–182

# Exploring complex dynamics with a CA-based urban model

## J. PARTANEN[1]

[1] Tampere University of Technology
School of Architecture
Urban Planning and Design
POB 600, 33101 Tampere, FINLAND
Tel. +358405184405
jenni.partanen@tut.fi

**Keywords:** Cellular Automata, Urbanity, CA dynamic states, Local Scale, Complexity

## Abstract

This paper presents a dynamic urban land-use model using cellular automata. The premise of the model is that urban activities interact with each other according to their proximity, especially in certain type of areas which have a high potential for self-organizing behaviour. The local dynamics of these highly adaptive enclaves affect the dynamics of the urban region on a global scale.

In complex systems the flexibility and adaptivity to changes are crucial for the systems dynamic stability. In this study the main focus is on temporal dynamics of the pattern formation process, which is studied using an irregular CA-based model. It is assumed that by exploring the dynamic states of the model resulting from different border conditions it is possible to discover favourable set(s) of rules which encourage the existing self-organizing dynamics in the modelled area.

The results indicate that the different values of the parameters impact greatly on the model's dynamics, and generate different dynamic states of the system. The resulting stagnated and various types of dynamic states which emerged with different parameter values were analogical to the prior studies among one-dimensional automata. Most importantly, it seemed that the model could produce favourable, dynamic states which may refer to self-organization of the area in the model world. The model provides a tool for exploring and understanding the effects of boundary conditions in planning process as various scenarios are tested, and helps to identify planning guidelines that will support the future complexity of these areas.

## Introduction

The number of dynamic CA-based modelling applications exploring the complex urban phenomena, such as growth or land-use dynamics, has increased in recent decades [1], [2], [3], [4], [5]. Most of these models have operated on a rather large, regional scale. Despite the well-known lower-scale models of Schelling, Benenson

et al. and Portugali, local-scale applications are limited and mainly deal with social dynamics [6], [7], [8].

Dynamic complexity is considered essentially important for the evolution of complex urban systems. In the model world, analogically, evaluating the dynamic states of the model could help us to understand the premises affecting systems' dynamic, and support the continuity of modelled urban processes [9]. This type of dynamics, which results from the different sets of CA rules, has been widely studied among mathematical and computational studies, mainly contemplating 1D CA (see, for example, [10], [11], [12]). An interesting example of this in urban studies is White et al.'s study of self-organisation in urban systems using fractal or radial dimension [13], which explicated the process of simultaneously evolving the progress of complex and order states using a CA model, and discovered that spontaneously emerging nuclei determine future urban patterns. Nevertheless, urban models that explore the dynamic states of the system are surprisingly limited, considering that complex cities evolve constantly in a continuous, unpredictable process that balances between dynamically stabile and unstable phases, and that this type of dynamics can be considered as a necessary condition for such systems. In particular, there is a lack of approaches that have studied the re-organisation of urban contexts in reference to White et al.'s approach.

A broad range of literature in urban economics and economic geography contemplates *agglomeration economics*, which refers to synergetic or competitive activities' tendencies to form clusters on a regional, nationwide, or global scale. The spontaneous agglomeration tendency is important, especially in an innovative economy [14], [15]. The location dynamics of several types of activities have not been widely studied on the local scale. Several authors have referred to specific types of local-scale-demarcated areas in cities, which emerge and self-organise according to the agents' interactions. The authors suggest that these areas can have an impact on urban dynamics at a higher level.

Thus, empirical local scale studies would be of relatively high importance in reference to these generative areas. Here, generative features refers to the area's ability to adapt and self-organise: certain mechanisms of autonomous order can be perceived. These features are important to all industries, since they enhance the economic viability and innovation. We need to study how to support these features and study how the changes in the local rules of interaction affect their dynamics. Due to their complexity and bottom up-nature of the mechanisms, the computer model would be a relevant tool.

**The question in this study is what kind of a dynamic model could be able to simulate the self-organising dynamics of this type of generative area.**

I will answer this question by using a modified CA model to explore the dynamic states in the model's temporal pattern formation processes resulting from differently emphasised transformation rules, which simulate various 'planning decisions' in this urban simulation game. The main dynamics of the model are based on empirically perceived tendencies towards agglomeration of similar activities and regeneration resulting from over-crowded clusters. The model is relaxed in certain ways. For

example, the irregular cell space follows the actual site division, and quantitatively (volumes) and qualitatively (activity types) defined transition rules simulate the gradual urban processes. The model can help to build different scenarios in planning processes, evaluate the impact that planning decisions have on the general dynamics of the area, and provide the degree of freedom needed for the crucial self-organisation of activities.

The performance of the model was tested using two areas – the Nekala old industrial area in Tampere, and the Vaasa old garrison area in Western Finland – as case studies. Both are in a process of transition towards a diverse mix of activities. Nekala also contains a remarkable proportion of working places of Tampere region, and has thus larger economic importance.

## The theoretical framework

David Graham Shane considers certain type of 'islands', the heterotopias of illusion, as a dominant element in today's multinodal city. These areas are self-organising and flexible formations within porous boundaries, which are able to order the society through flexible and bottom-up-generated norms. Franz Oswald and Peter Baccini introduced the term "urban fallow" to refer to areas that emerge from sudden changes in society, such as transition of modes of production. They suggested that these areas form important resources in city as they can often form a breeding ground for the self-organisation of various cultural or economic actors. A certain degree of freedom is required to maintain and support the adaptivity, dynamic and diversity of these actors. [16], [17], [18], [19]. The target areas are typical fallow land in a dynamic process of transforming to a heterotopia of illusion.

The clustering tendency of firms that occurs on a regional-scale, as cited in the literature, is a basic principle of agglomeration economies and has been studied widely [20],[21],[22],[23]. Studies have examined the impacts of this tendency at different scales, contemplating nationwide, regional or more local concentrations of firms. Systematic studies of location logics of different types of activities in one specific area are limited. Nevertheless, the empirical findings in Nekala area indicate this type of tendency. The premises of the model in the present paper are based on these findings [24]. In addition, this dynamic is continuous in time; the area is capable of adapting to temporal ruptures in society [25]. Given these results, the present study contemplates how the dynamic evolution of the area could also be guaranteed in the future.

## A proposed cellular model

The majority of urban models concentrate on exploring the spatial dynamics of regional scale patterns that result from various societal-economic conditions [26]. The present paper, on the other hand, contemplates the dynamic states of these pattern formation processes in the neighbourhood scale by using a modified CA model that operates in a GIS environment. Note that concentrating on the local scale interaction does not exclude the obvious principles of location theory in economics. It is assumed that basic characteristics of the area, such as good accessibility, low

land price and low quality of the environment, have already 'filtered' the most suitable activities entering the area according to their preferences. The aim is to study the dynamics of these 'filtered activities', not to find, for example, optimal locations to them in general.

I assume that this specific case of self-organisation enhances the innovations and creativity required in all industries today. Here, self-organisation refers to the location choices of activities in the model world, resulting from their individual decision making in a certain regulatory framework. This generative process occurs in a most desirable way within the models' dynamic, complex state. The system transforms and adapts constantly during the iteration. A system that is so far from equilibrium oscillates unpredictably between steady and unsteady states. Therefore, I propose using a dynamic model to explore the features of the dynamic processes during the simulations resulting from various emphases in the transformation rules representing different planning decisions. The variables are the urban activities, which are grouped into six categories: housing (U1), retail (U2), services (U3), offices (U4), small industry (U5) and warehouses (U6). The type and volume of the new actor depends on the type and volume of the activities in the neighbouring site. These principles are based on previous empirical studies [27].

## Dynamic cellular states

Since the 1980s, the dynamic states of one-dimensional CA have been studied widely in the fields of mathematics and computational sciences (see, for example, [28], [29], [30]) but there have been limited applications in urban studies [31]. In the present study, I have applied classifications of dynamics states of Wolfram, Braga, Wuenche and Langton. According to these classifications, I re-formulated a two-fold classification of various favourable continuous, dynamic states (complex or periodic) and stagnating states (infinitely oscillating or completely stagnating states). Langton and Wuenche's concepts of entropy provide a measure of the unpredictability, implying the dynamics that can be applied in an analogical manner [32], [33].

## The model configurations: The neighbourhood and cell states

The lattice of irregular cells in the model follows the legal site division. The cell's neighbourhood contains parcels within 24 meters of the central cell. This measurement follows the traditional block size in the area, providing the optimal distance for pedestrians, which implies that firms benefit from the proximity of competition or synergy between similar activities.

The floor area of the site is merged into the feature of the cell. The cell's qualitative state results from the combination of six different activities. Each activity has an individually defined volume. The quantitative cell states are defined according to the utilisation rate, which is a ratio of the used floor area to the current building right at the site (Equation 1).

$$\sum_{j=1}^{N} s_j \log_2 s_j$$

Equation 1. $R_j$ = utilisation rate (site j). $\sum$ FA i,u = sum of the floor area ( u1…u6) on the site I and ej is the town plan's building efficiency on the site j. Aj is the total area of the site j.

The building right varies between 0.5 and 1.25, following the current plan. The state of the cell is then classified according to the utilisation rate into four categories: empty, half-empty, half-full and full (Figure 1, Table 1). The quantitative cell state affects the site's future mode of transformation.

Table 1. Transformation rule 2: The type of transformation of the site depends on the state of the site.

| state of the site | | most probable procedure | the motive |
|---|---|---|---|
| *vacant* | | build a new building | to use the building right |
| *half-empty* | *<10%* | demolish (fill up) | to use the building right more effectively: low demolishing costs |
| *half-full* | | fill up (change) | to use the building right more effectively: demolishing costs above the threshold*1 |
| *full* | | remain/change/fill/reconstr. **2e.g 0.6/0.3/0.01/0.99 | certain inertia on the full site; tendency to change if one use starts to dominate the neighborhood=lot of FA (empiria) |
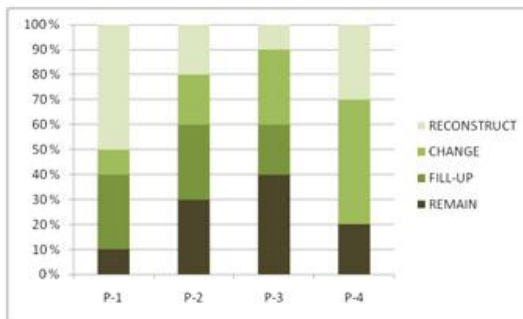


Figure 1: Cells' mode of transformation according to their utilisation rates. P-1: 'empty', FAR=0-0.1; P-2: 'half-empty', FAR=0.1-0.3; P-3: 'half-full', FAR= 0.3-0.7; P-4: 'full', FAR= 0.7-1.

## Transformation rules

The basic mechanism the transformation rules are empirically based: synergetic or similar activities tend to gravitate to within proximity of each other until the clustering exceeding the threshold value causes 'overpopulation', leading to re-location of some activities.

The site's mode of transformation is defined according to the current cell state. Sites are grouped into four categories with potential values (P-1 to P-4) indicating the probability of different types of changes. The type of future change depends on the site's category. The site may remain as it is (RM), it may fill up (F) according to the percentage growth rate (GR) defined by the user, activities on the site may change (C) while volume remains the same, or the volume and activities may be totally reconstructed (RC) (Figures 1 and 2). The premises are (1) that vacant sites tend to fill up mainly with actors similar to their neighbours and the sites are built to use the building right efficiently, and (2) that the buildings are eventually replaced as the demolition/construction costs become theoretically profitable.
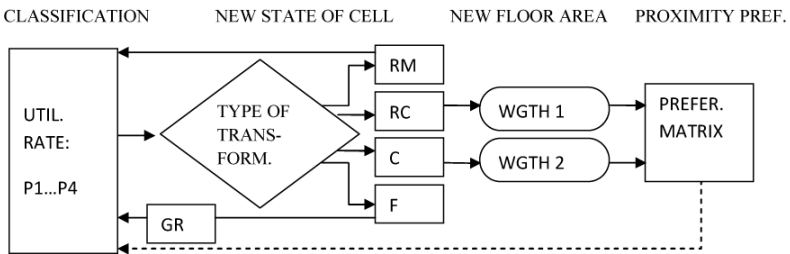


Figure 2: Model's operation.

**Nekala case**

Firstly, the model was constructed and tested in a case area of the Nekala industrial area in Tampere, Finland. This area of approximately 80 sites was planned in the 1930s for heavy industry and the processing of agricultural products. The area used to be in the outskirts of the city, but active urban growth in recent decades has caused the area to become surrounded by a dense city structure; its current location can be considered quite central. Housing surrounds the area, which forms a unique enclave within the urban fabric. The area has proven surprisingly capable of self-organisation. It has also been able to flexibly adjust itself to the current mode of production, from mainly industrial to a gradually more complex mixture of service, information technology and cultural industry [34].
Features and former empirical findings in Nekala [24] have offered adequate information for outlining the rules and dependencies for modelling.

**Vaasa case**

The second case study, in which the model was further developed, was an old garrison area in Vaasa, Finland. This area is located inside the central area of old Vaasa, where the transition from military use to diverse range of other activities has occurred quite recently. The area consists of different types of gradually fulfilled or historically valuable buildings, large empty sites and buildings beyond repair. A wide range of temporary and permanent actors have gradually settled in to the old

buildings at the lower price levels. Original and vital culture has started to appear in the area, according to the actors' reciprocal interactions.

Data on these actors comes from the Tampere and Vaasa Municipality. Numeric data (Excel matrix) was combined with location information using GIS. Electrical maps (spatial data) are from the Tampere and Vaasa Municipality offices. The volumes of activities are from the building permit archives of the Tampere and Vaasa municipality.

## Computer runs

The first simulations were run in a pilot study in Nekala. The resulting pattern formation process was relatively dynamic, but it was rather hard to observe the dependences between these built-in control parameters and resulting dynamics. Consequently, a preference matrix (Table 2) was introduced in the second phase of the project in Vaasa. The weight values defining preferred proximity between actors could vary within this experiment between 1 and 20, and they were iterated by trial and error, which simulated the planning decisions.

As a result of negotiation process among shareholders in a planning process, two sets of rules were chosen for computer runs; one set mainly supported new housing, and the other emphasise more mixed uses. The shifts in dynamics were traced heuristically using various weight values for each pair of activities. The lengths of the iteration were mainly between 500 and 2000.

Table 2. Preference matrix. μ= 1…20.

| | U1 | U2 | U3 | U4 | U5 | U6 |
|---|---|---|---|---|---|---|
| U1 | μ | μ | μ | μ | μ | |
| U2 | μ | μ | μ | μ | ... | |
| U3 | μ | μ | μ | ... | | |
| U4 | μ | μ | ... | | | |
| U5 | μ | ... | | | | |
| U6 | ... | | | | | |

## Results

The resulting dynamics varied between iterations and depended heavily on the initial values of the matrix. The emerging dynamics can be classified into two main categories according to the end state, and two sub-categories describing the behaviour in greater detail using the classifications of CA's dynamic states are described in Table 3.

Table 3. Dynamic states of the model.

|  | Type 1 | Type2 |
|---|---|---|
| **Static** | *Stagnation* | *Oscillation* |
| **Dynamic** | *Cyclicity* | *Complexity* |

Two types of non-dynamic behaviour were perceived for the iterations that ended up in a certain end state; the system could either end up to a certain permanent end state, or oscillate infinitely between two or three values on certain sites. Despite these few 'blinking' cells, the dynamics can be considered static. In both cases, the volumes and the sites at issue varied. These dynamics seemed to be correlated with high impact from the surrounding housing area, which occurred with relatively low matrix values for the housing. The model quite accurately reflected the urban reality. Surrounding housing caused pressure on housing development. The stagnating progress seemed plausible, yet not desirable.

As the relative emphasis of the matrix values was shifted from U1xn1…6 to U4…U5, the behaviour of the model changed remarkably. First of all, the volumes for all activities started to increase gradually and decrease in time, resulting in a pulse of higher and lower utilisation rate on the sites; a certain order started to emerge within the system. The lengths of these cycles were measurable, and the dynamics of these periods depended heavily on the rule set (matrix values). With certain rule sets, the system gravitated towards dynamics that were periodic but non-uniform. These dynamics were diverse, which was contrary to the cases introduced above (Figure 3).
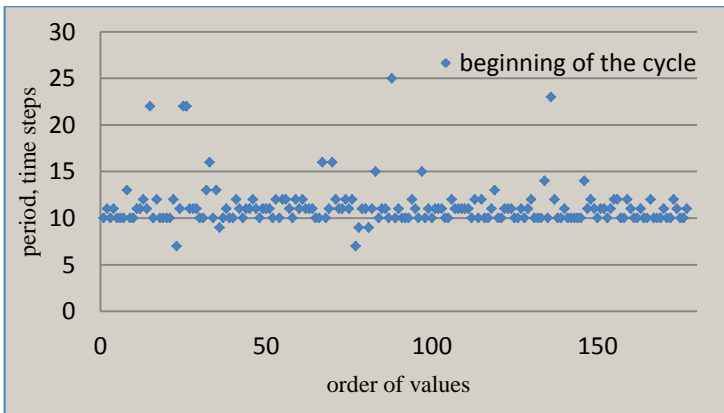


Figure 3. Example: Dynamic, periodic states.

With a very particular set of matrix values, the behaviour of the model changed radically again. The uses U2–U6 remained periodic, although the lengths of the cycles and the degree of predictability seemed to slightly change for different activities. The most remarkable transition towards a higher degree of complexity was perceived with U1. Similarly to the periodic states, the system's dynamic seemed rather stochastic at the start of the iteration, but it soon started to gravitate towards a certain cycle. The period could reoccur only twice, but did so for as many as 18 times. Several different cycles could occur during one iteration (Figure 4). Despite these short, constantly emerging and disappearing cycles, the overall dynamics of the system were highly unpredictable, and this oscillation seemed to continue infinitely even with remarkably long iterations (up to 2000 time steps).
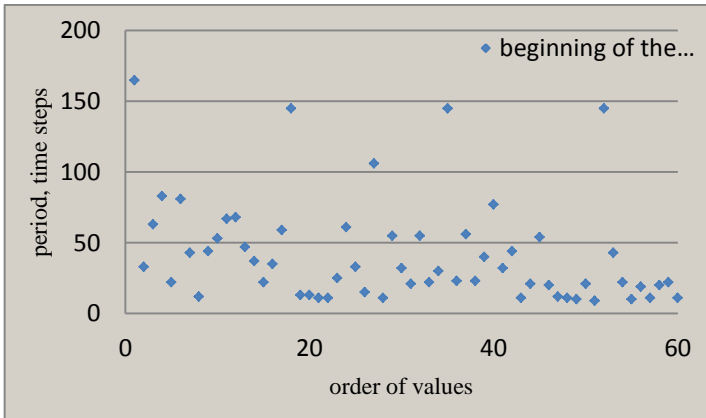


Figure 4. Example: Dynamic, complex states.

Although these dynamic states were easy to perceive visually, I also used a more exact measurement for validation. Langton found that complex states appear only with a very limited set of intermediate entropy values. According to Wuenche, the degree of input entropy of the system implies its dynamic state in a similar manner. In a totally chaotic system, the entropy is extremely high; in an ordered system, rather low; and in a complex system, between these extremes.

Within this study, entropy values were calculated for the whole system after iteration in order to perceive the differences in overall diversity and predictability.

Six examples of periodic and six of complex behaviour were chosen at random from the 60 iterations that passed a visual evaluation test. The entropy for the system was calculated according to equation 2.

$$\sum_{j=1}^{N} s_j \log_2 s_j$$

Equation 2. Given $s_j$ is the relative share $t/t_{all}$ of the entities; $t$ = length of the regeneration cycle of an activity measured in time steps.

The results indicate a clear dispersion between highly ordered and periodic states and more unpredictable, complex states. All of the entropy values resulting from periodic states were 100 or below, while they varied for complex states from 150 to 300 (Figure 5).
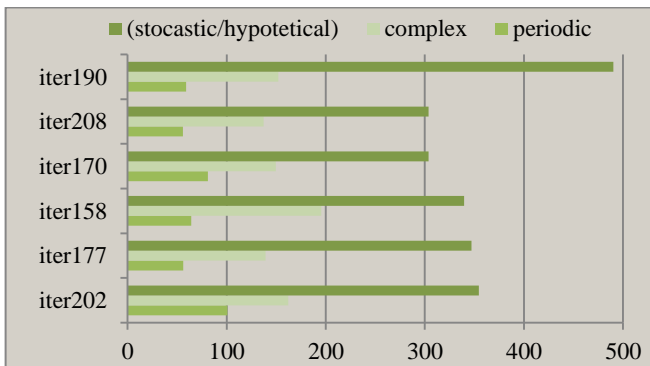


Figure 5. Entropy values (i) for six iterations visually classified as "periodic"; 50 > i > 100 "complex"; 150 > i > 200 and with maximal stochasticity; i > 300.

Since the chaotic state was not perceived within this study, a stochastic set was created for comparison purposes, indicating a maximum value (above 300) of entropy in the system (Figure 5).

**Concluding remarks**

The static states can be considered analogical with traditional, hierarchical planning processes, in which the plan consolidates a certain static position. In the context of complex cities, this could imply a burdensome process of constantly updating plans. Tolerable plans and dynamic simulations could provide a more flexible planning procedure. This modelling experiment indicates that a certain degree of steering is necessary in order for the process to achieve the most desirable outcome, such as high diversity that enhances the city's evolution.

**Discussion**

Complex systems evolve constantly, balancing near a critical point. Only a few urban modelling approaches have concentrated on the CA's ability to produce transient, highly organised, complex and constantly evolving structures. In this paper, I have introduced a CA-based urban model with which to explore whether such a model can discover certain critical states analogical to Langton's phase transitions, and to explore the optimal range of restriction for enabling these self-organizing dynamics. The results indicated that this model was indeed able to produce different type of stable and dynamic, even highly organised states:certain initial values supporting the self-organisation and future evolution of the area can be discovered.

The model could provide a useful tool for communicating in the planning process. Despite its inevitable inability to predict accurately, it can provide guidelines for a future balance between restrictions and freedom, and to identify the dynamic features that should not be hindered or over-controlled. The accuracy of the model is quite relevant for this general purpose. The model could be used for exploring the urban dynamics on the general level, to enhance the understanding of the role of restriction to self-organisation and city evolution.

**References**

[1]    Batty, M. and Xie, Y., From cells to cities. *Environment and Planning B,*1994*:* Planning and Design. 21: p. 531–548.

[2]    Clarke, K.C. and L.J. Gaydos, Loose-coupling a cellular automaton model and GIS: long-term urban growth prediction for San Francisco and Washington/Baltimore. *International Journal of Geographical Information Science*, 1998. 12(7): p. 699–714.

[3]    White, R., Engelen, G. and Uljee, I., The use of constrained cellular automata for high resolution modelling of urban land use dynamics. *Environment and Planning B*, 1997: Planning and Design 24: p. 323–343.

[4]    White, R. and Engelen, G., Cellular automata and fractal urban form. *Environment and Planning A*, 1993. 25: p. 1175–1199.

[5]    Wu, F. and Webster, C. J., Simulation of land development through the integration of cellular automata and multicriteria evaluation. *Environment and Planning B*, 1998: Planning and Design. 25: p. 103–126.

[6]    Schelling,T.C., Dynamic Models of Segregation. *Journal of Mathematical Sociology*, 1971 1: p. 143–186.

[7]    Portugali, J. , *Self-organization and the city*. Springer-Verlag, Berlin Heidelberg New York, 1999.

[8]    Benenson, I., Omer, I. and Hatna, E., Entity-based modeling of urban residential dynamics: the case of Yaffo, Tel Aviv. *Environment and Planning B: Planning and Design*, 2002. 29: p. 491–512.

[9]    Langton, C.R., Computation at the edge of chaos: Phase transitions and emergent computation. *Physica D*, 1990. 42: p. 12–37.

[10]  Wolfram, S.*,* Universality and Complexity in Cellular Automata. *Physica D,* 1984. 10: p. 1–35.

[11]  Braga, G., Cattaneo, G. , Flocchini, P and Quaranta V.C., Pattern growth in elementary cellular automata. *Theoretical Computer Science*, 1995. 145: p. 1–26.

[12] Culik II.K., Hurd, L.P. and Yu, S., Computation theoretic aspects of cellular automata. *Physica D, 1995.* 45: p. 357–378.

[13] White, R. and Engelen, G., Cellular automata and fractal urban form. *Environment and Planning A*, 1993. 25: p. 1175–1199.

[14] Florida, R., *The Rise of the Creative Class and how it's Transforming Work, Leisure, Community and Everyday Life.* Basic Books, New York, 2000.

[15] Hautamäki, A., *Luova talous ja kulttuuri innovaatiopolitiikan ytimessä.* Opetusministeriön julkaisuja, 2009: 30.

[16] Oswald, F. and Baccini, P., *Netzstadt – designing the urban.* Birkhäuser, Basel-Boston-Berlin, 2003.

[17] Portugali, J., *Self-organization and the city*. Springer-Verlag, Berlin, 1999.

[18] Allen, P., *Cities and regions as self-organizing systems.* Taylor&Francis, Oxon, 2004.

[19] Shane, D.G., *Recombinant Urbanism – Conceptual Modeling in Architecture, Urban Design and City Theory.* John Wiley & Sons Ltd., London, 2005.

[20] Marshall, A., *Principles of Economics*. Macmillan, London, 1920.

[21] Porter, M., Clusters and The New Economics Of Competition Source. *Harvard Business Review,* 1998. 76 (6): p. 77–90.

[22] Fujita, M., Thisse, J.-F., *Economics of Agglomeration*. Cambridge University Press, Cambridge, 2002.

[23] Glaeser, E.L., Kallal, H.D., Scheinkman, J.A., Shleifer, A., Growth in cities. *Journal of Political Economy,* 1992. 100 (6): p. 1127–1152.

[24] Partanen J., Modeling Urban Dynamics in Self-organizing Enclaves: The Cases of Nekala and Vaasa. *Conference proceedings in 17$^{th}$ ECQTG2011, Athens, Greec*e.

[25] Partanen, J., Indicators for Self-organization in Urban Context. 2012, in progress.

[26] Stevens, D., Dragicevic, S., A GIS-based irregular cellular automata model of land-use change . *Environment and Planning B: Planning and Design,* 2007. 34, p. 708 – 724.

[27] Partanen J., Modeling Urban Dynamics in Self-organizing Enclaves: The Cases of Nekala and Vaasa. *Conference proceedings in 17$^{th}$ ECQTG2011, Athens, Greec*e.

[28] Braga, G., Cattaneo, G. , Flocchini, P and Quaranta V.C., Pattern growth in elementary cellular automata. *Theoretical Computer Science*, 1995. 145: p. 1–26.

[29] Culik II.K., Hurd, L.P. and Yu, S., Computation theoretic aspects of cellular automata. *Physica D, 1995.* 45: p. 357–378.

[30] Wolfram, S., Universality and Complexity in Cellular Automata. *Physica D 10,* 1984. p. 1–35.

[31] Caruso, G., Peeters, D., Cavailhès, J., Rounsevell, M., Space–time patterns of urban sprawl, a 1D cellular automata and microeconomic approach. *Environment and Planning B, 2009: Planning and Design*. 36: p. 968–988

[32] Langton, C.R., Computation at the edge of chaos: Phase transitions and emergent computation. *Physica D*, 1990. 42: p. 12–37.

[33] Wuensche, A., Discrete Dynamical Networks and Their Attractor Basins. *Santa Fe Institute Working Paper 98-11-101*, 1998.

[34] Castells, M., The Information Age: Economy, Society and Culture. Volume 1. The Rise of Network Society. Blackwell Publishing,Oxford, 2000.

# Preliminary Design and Implementation of DSL3S – a Domain Specific Language for Spatial Simulation Scenarios

## Luís DE SOUSA[1], Alberto Rodrigues DA SILVA[2]

[1]Resource Centre for Environmental Technologies, Public Research Centre Henri Tudor
66 Rue de Luxembourg, Esch-sur-Alzette, L-4221 Luxembourg
+352 42 59 91 3356, luis.a.de.sousa@gmail.com
[2]Instituto Superior Técnico
Lisbon, Portugal alberto.silva@acm.org

**Keywords:** spatial simulation; domain specific language; mode driven engineering; cellular automata; agent based modelling

## Abstract

Spatial Simulation in the context of Geographic Information Systems has been used in the past decades to assess the evolution of spatial variables over time. Two main techniques have been applied to perform this kind of spatial analysis: Cellular Automata and Agent-based modelling.

A spectrum of spatial simulation tools exists today to aid implementing a model of this genre, ranging from code libraries (Program-level tools), that support the coding activity, to pre-built models (or Model-level tools), that can be used by simple parametrisation. Somewhere in the middle of this spectrum lay Domain Specific Languages (DSL). Nevertheless, the choice of a simulation tool still entails a trade off between flexibility and the need of programming skills

This article presents a different approach to spatial simulation in the GIS domain, through the employment of standards from the Object Management Group (OMG) to produce a graphical simulation language - DSL3S. This language provides a way to describes simulation models at higher level of abstraction, allowing faster development, reducing coding errors and increasing model readability.

## Introduction

Spatial Simulation in the context of Geographic Information Systems (GIS) is used primarily to assess the evolution of spatial variables over time. Since the 1990s two main techniques have been applied to perform this sort of spatial analysis: Cellular Automata [1] and Agent-based modelling [2]. The simulation models produced with these methods tend to be quite specific, only usable within the particular field of application, largely due to the multi-dimensional and heterogeneous character of spatial data. Mainly for this reason, modern multi-purpose GIS packages, such as GRASS[1] or ArcGIS[2], largely lack tools dedicated to this technology.

---

[1] http://grass.osgeo.org/

Developing a spatial simulation model using a general purpose programming language presents several burdens. Besides implementing the model, the program has to control the flow of execution, manage system resources, and manipulate data structures. This leads to several problems [3]: (i) difficulties verifying correct implementation; (ii) limited model generality due to difficult modification and/or adaptation; (iii) difficulty comparing computer models, usually restricted to their inputs and outputs [4]; (iv) problematic integration with other models or tools (e.g. GIS or visualisation packages).

Beyond general purpose programming languages, a spectrum of Spatial Simulation tools exists, ranging from code libraries (referred to as Program-level tools), that support the coding activity, to pre-built models (or Model-level tools), that can be used by simple parametrisation [3] (see Figure 1). Somewhere in the middle of this spectrum lay Domain Specific Languages (DSL).
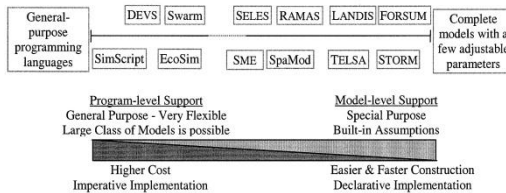


Figure 1: The Spatial Simulation tools spectrum devised by Fall and Fall [3].

In spite of this wide spectrum, spatial analysts are still constrained by the trade off between the burdens of programming and the strictness of pre-built models; with existing DSL not yet exactly freeing the analyst from coding.

This article presents a different approach to spatial simulation in the GIS domain, through the employment of standards from the Object Management Group[3] (OMG) to produce a graphical DSL. Starting is a short review of the types of simulation tools available today, their strengths and shortcomings; then, present difficulties are identified and the approach stated. The language is then presented in conceptual terms and closing its implementation is detailed.

**Spatial simulation tools**

As stated in the Introduction, three main categories of tools can be devised: Program-level, Model-level and DSL-level. This section describes each and briefly discusses its main characteristics. A more detail review is provided by de Sousa and da Silva [5].

Program-level support tools extend the facilities available in general-purpose programming languages, usually providing code libraries for building specific classes of simulation models. Examples of these tools are Swarm[4] RePAST [6] and MASON [7]. Higher-level code, usually in a general-purpose object-oriented

---

[2] http://www.arcgis.com/
[3] http://www.omg.org/
[4] http://www.swarm.org/index.php/Main\_Page

programming language, specifies how objects are used to produce the desired behaviour. The main advantage of this type of tools is the encapsulation of the model from functionality, relieving the modeller from banal programming tasks and potentially producing leaner and easier to read code. These tools are tendentiously open source, operational on several computer platforms and providing good level of integration with GIS packages. Coupling this characteristic to their wider application scope, Program-level tools usually gather around them large communities of users, that provide informal, but extensive, support. On the downside, these tools require an extra learning effort for their proper use. Beyond requiring relevant knowledge on the programming language itself [8], the modeller must learn to some detail the behaviour of functions, objects and methods provided by the tool kit, something that may require several months of practice [9].

Model-level support tools allow the employment of spatial simulation without requiring programming. These tools provide pre-programmed simulatio models, designed for specific application fields that can be parametrised by the end user. They provide fairly straightforward and rapid mechanisms for implementation, but invariably constraint the modeller to a specific application framework. Examples of such tools are SLEUTH [10], TELSA [11] and AnyLogic[5]. These tools tend to be quite specific, and much of the model behaviour and assumptions are hidden by the framework; their use in other application fields is largely impossible. They also tend to lack GIS interoperability, in best cases requiring specific data formats. Traditionally, they take advantage of market niches providing for the needs of a restricted group of users. Thus, in most cases, they are commercial products and their users community tend to be weak or non-existent, more often support is a paid service.

Midway between Program-level and Model-level are DSL-level tools that provide a specific language specialised for a simulation domain. Compared to Model-level tools, these languages make fewer assumptions about the underlying simulation model structure. Examples include NetLogo[6], SELES [3] and MOBIDYC [12]. The use of DSL facilitates modelling and reduces the build-up time of simulation models. The programming environment is more constrained that in Program-level tools, with behaviour described using simple constructs. Still, the user has to understand keyword meaning and how to compose a set of instructions into a program. In general this category of tools doesn't provide much support for GIS integration, some even totally lacking such functionality. Users communities tend to be larger than those of Model-level tools, but on the other hand platform dependency is often an issue.

**Difficulties and Approach**

When using a tool for spatial simulation a GIS analyst is faced with some important challenges, namelly:

▪ Most spatial simulation tools require advanced programming skills;

---

[5] http://www.xj tek.com/anylogic/why_anylogic/

[6] http://ccl.northwestern.edu/netlogo

- Those that do not require such knowledge are narrow scoped and invariably lack GIS interoperability;
- There's no standard or common language to describe spatial simulation models.

Analysts working with spatial data either come from GIS related areas, like Geography or Geodesy, or from the scientific areas of application, such as Biology or Economics. In spatial simulation projects is almost mandatory the involvement of programmers, skilled in advanced methods like object-oriented technologies. This creates a further communication step from model concept to its implementation.

The adoption of pre-compiled Model-level tools also imposes its burdens. The correct implementation of such models is often hard or impossible to verify, since most are commercial, or otherwise closed source tools. Their static structure imposes strict compliance to their conceptual framework. Experiments with different behaviours or the input of alternative spatial information is impossible.

A simulation model that can only be described by the underlying source code becomes inaccessible to most GIS analysts. Source code specificities, such as data input/output or control structures, produce a layer of obfuscation that complicates the comparison of different models. There are a number of concepts that are common to any spatial simulation, such as the succession of time, spatial variables, agents or spatial location, but two implementations of a same model can appear entirely different if based on different tools, that impose different software architectures.

Our work attempts to address these issues through the development of the DSL3S, a Domain Specific Language for Spatial Simulation Scenarios. This language takes spatial simulation as a branch of the wider Spatial Analysis GIS field, where model inputs originate at least partially from a GIS and whose outputs may also have geo-referenced relevance. The same approach shall be taken to models that are traditionally implemented with cellular automata and to those based on agents, seeking a language abstracted from such technical differences.

DSL3S is design as a UML profile[7] because it allows the development of simulation models through UML class diagrams (to which stereotypes from the profile are applied and parametrised with properties). These models are then feed to a model-to-code transformation facility producing a ready-to-run simulation model on top of a Program-level tool. Then the analyst can chose to either perform tuning at model level or further refine the corresponding source code with the assistance of a developer.

The improvements with this approach are:

- *Faster development*, reducing the lag from prototype conception to testing;
- *Reduction of errors*, by reducing (or even eliminating) coding activities;
- *Increased readability*, with models described by graphical diagrams;
- *Improved GIS interoperability,* by using the modern Program-level tools
- *One model, several implementations*, code generation templates can be developed for different target Program-level tools.

---

[7] http://www.omg.org/technology/documents/profile_catalog.htm

The following section describes the concepts underlying the DSL3S.

**The DSL3S Meta-model**

Three main pillars have been identified as the underpinning concepts of a spatial simulation: Spatial Environment Variables, Animats and Behaviour. **Spatial Environment Variables** are spatial information layers that have some sort of impact on the dynamics of a simulation, e.g. slope that deters urban sprawl, biomass that feeds a wildfire. **Animat** is a term coined by S. W. Wilson [13] signifying *artificial animal*; in the context of DSL3S it is used more widely, representing all types of agents of change, such as wildfires, urban areas or agents in a predator-prey model. **Behaviour** associates the former two concepts, defining how Animats react to their surrounding environment and internal state, examples can be movement or replication.

Beyond these core concepts, other elements can also be found in a simulation, particularly context variables. **Global Variables** define information that is constant across the whole space of simulation, such as wind direction in a wildfire model. Global variables can eventually change with time, simulating changing environment conditions (again wind direction is a good example). Animats can have variables themselves, called **State Variables** that detail their internal state.

A **Simulation** is composed by a set of Spatial Environment variables, Animats and Global variables; Animats may be composed by series of State variables. Animats are also composed by Behaviours that determine how it's internal state evolves; behaviours can be function of global variables, spatial environment or the state of other animats (see Figure 2). All these concepts are stereotypes in the DSL3S profile (see Figure 3).
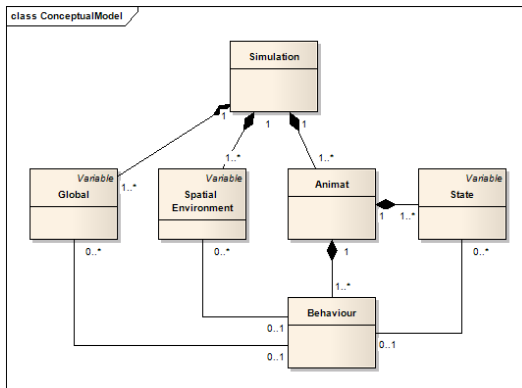


Figure 2: The core concepts of DSL3S

The Global Variable is intended to be a simple scalar value that may vary with time. It can for instance be set randomly at simulation start and/or made to vary randomly

each time step; it can also be fed into the model as a pre defined time-series of values, for instance read from an input text file.

The stereotype for Spatial Environment Variable is essentially a stub for the input of geo-referenced data. Each instance shall correspond to a spatial layer with the characteristic of having an unequivocal value for each location in space. No reference system is made explicit, it is assumed that all spacial data imputed to the simulation is bound to the same system and the model effectively operates in an ordinary Cartesian plane. For now no distinction between vector and raster data is being considered in the meta-model.
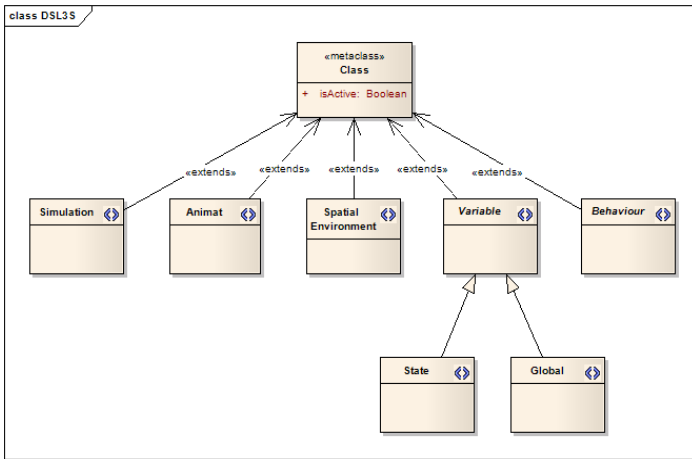


Figure 3: The main stereotypes of DSL3S.

Animats are essentially an aggregation of state variables residing at a perfectly identifiable location in space. Different types of Animat can model specific genres of actors, e.g. wolves and sheep in a predator-prey simulation. The initial number of animat instances and their spatial positioning can be provided by a specific geo-referenced data set such as a raster map. By similar mechanisms the initial values of state variables can too be set with geo-referenced data.

The elements presented so far focused on retaining the information needed to run a spatial simulation. But more than that is required to capture spatial dynamics, the way animats act has to be made explicit. In DSL3S this aspect is modelled with specialisations of Behaviour, more precisely: **Initiate**, **Move**, **Replicate**, **Harvest** and **Perish**.

Initiate captures the conditions under which a new instance of an animat can appear in the simulation, the act of "birth". An example may be an urban development simulation where the emergence of a new urban spot is possible in an area that meets a certain set of criteria like distance to transport infrastructure or topography. Probabilities of birth can also be defined with properties.

Move relates an animat with one or more spatial environment variables or other animats, determining the locations that are more or less favourable to be in. Specific

properties allow to weight the relevance of each class related to a Move behaviour. For instance, in a predator-prey simulation the movement of a "sheep" animat may be positively weighted in a relationship with a "grass" class and negatively weighted in a relation with a "wolf" animat.

Replicate captures behaviours where an animat replicates itself to an adjacent location, such as a wildfire spreading or an urban area sprawling. Just as with previous behaviours, the objective is to capture the conditions under which an animat may originate a sibling into its neighbourhood. Properties may weight the influence of spatial environment variables (e.g. fire spread) or set thresholds against the animat's internal state (e.g. biological reproduction).

Harvest an act on which an animat may change other elements in the same spatial location; it can act on a spatial environment variable, such as a wildfire consuming bush, or by seizing another animat as in a predator-prey simulation. In this class properties parametrise the changes of this action on both harvester and harvested.

Perish defines the circumstances under which an animat instance may cease to exist during the simulation (e.g. "starve"). This class defines minimum thresholds related to animat internal state that determine conditions for the endurance of its existence. It may be associated with the animat class itself to set conditions by which an instance may cease to exist due to crowding. Associations with spatial environment variables may provide further conditions for existence.
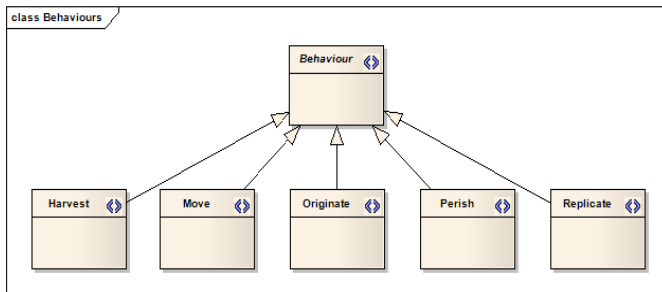


Figure 4: The five behavioural stereotypes.

This is just a selection of behaviour classes that provide a set of core procedures for animat conduct. In their seminal work, Epstein and Axtel [14] conceive a considerably larger set of behaviours in a spatially bound agent based simulation, including elaborate processes such as trade and cultural exchange. While interesting, these intricate behaviours are less common in pure GIS applications (where the dynamics is captured at a higher level of geographic abstraction) and more keen to Social or Economics studies. However, the addition of further behaviours will be the main process of extension of DSL3S, answering to new requirements if necessary.

**Views and Icons**

DSL3S models can become visually intricate if a single diagram would de used to represent a complex spatial simulation scenario. To avoid such difficulties distinct Views are proposed to better organise models (see Figure 5):

- **Global View** - contains the simulation settings that do not have spatial realisation. Includes Simulation and Global classes, defining parameters such as the number of time steps to run, spatial extent or result output.
- **Spatial View** - where all the Spatial Environment variables are configured, defining the geographic inputs to the simulation.
- **Animat View** - defining animat internal state. In simulations scenarios with more than one animat several animat views can be used.
- **Behaviour View** - contains only the classes with specialisations of the Behaviour stereotype applied on, but also showing composition links to all classes that parametrise each behaviour. A dedicated view for each different behaviour is proposed.
- **Simulation View** – a simple package diagram that aggregates all other views.
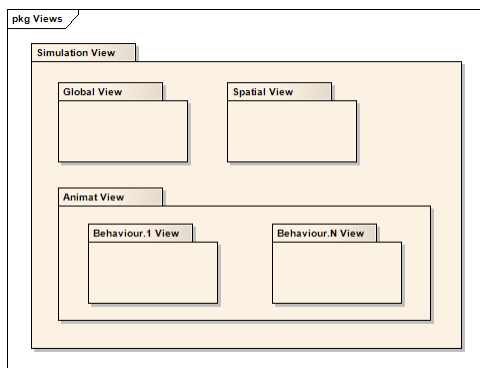


Figure 5: The proposed Views scheme for DSL3S.

Beyond these views a set of icons is also proposed to make the language visually explicit (see Figure 6). For Simulation, Global Variable and Spatial Environment Variable direct pictorial representations of their concepts are used. For the stereotypes Animat, State and Behaviours are proposed abstract symbols intending to create mental associations with a simulation model.
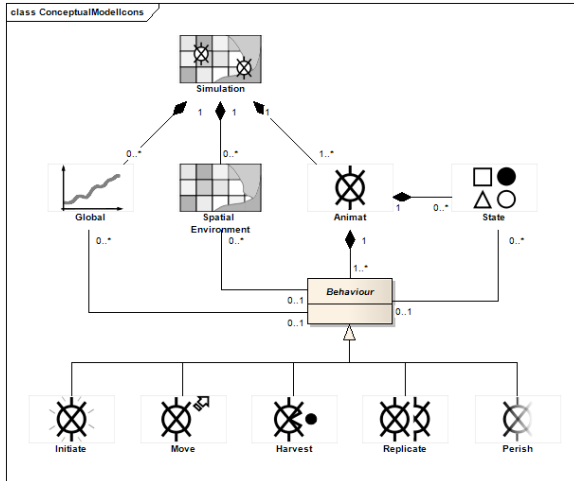
Figure 6: The proposed icons for DSL3S stereotypes.

## Implementation

The reference architecture for the DSL3S language defines three components, all based on open source technologies (see Figure 7):

- the UML profile, supported by the Papyrus add-on for the Eclipse[8] IDE;
- MASON, a Program-level tool supporting the generated code;
- Model-to-code generation templates, developed with Acceleo, another Eclipse add-on.

### Papyrus

Papyrus[9] was a project started by the *Commissariat à l'Énergie Atomique* in France, with the aim of producing an advanced graphical editor for the UML language, supporting particular DSL, especially SysML[10], a language for systems engineering. It evolved as an open source product based on the Eclipse Modelling Framework[11] (EMF), a tool-kit that supports the edition and visualisation of structured models defined in the XMI language and provides a set of Java classes that facilitate its manipulation. Papyrus eventually evolved to support the development of ad *hoc* DSL, through the definition of UML profiles.

---

[8] http://www.eclipse.org
[9] http://www.eclipse.org/modeling/mdt/papyrus/
[10] http://www.sysml.org/
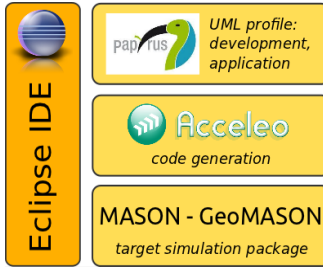[11] http://www.eclipse.org/modeling/emf/

Figure 7: The technologies used to implement DSL3S.

In 2009 Papyrus merged with Eclipse altogether, becoming the forefront graphical UML editor add-on for this popular IDE, replacing other assorted tools with fewer capabilities. It is presently close to fully support the version 2 of the UML language, coming to be one of the most advanced tools available for the purpose. Beyond SysML, Papyrus includes a series of other DSL dedicated to domains like embedded systems or automotive systems.

**Acceleo**

Acceleo[12] is an open source code generator created by the French company Obeo, first released in 2006, as a plug-in to Eclipse 3.0 and 3.1. It is also built on EMF, facilitating the interoperability with several other modelling tools based on the same technology. The following year the Eclipse Foundation took Acceleo as an official project. In latter versions Acceleo adopted the MOF Model to Text Transformation Language[13] (MOFM2T), another OMG standard. Though not yet fully implementing this standard, the model-to-code generators produced with Acceleo are today some of the closer to the scheme proposed by the OMG.

The code generation mechanism is based on special files called templates, which define the text output to produce from a graphical model. They are composed by regular text plus a series of annotations that are substituted by values and names of model elements during generation time (see Table 1). Traditional computational operations such as branches or loops are also possible to include with specific annotations, allowing the production of more complex outputs. Templates can be articulated through an inclusion mechanism, whereby a master template can make use of several other templates creating a generation chain. When fully developed, a generation chain can be transformed into an independent plug-in for Eclipse, facilitating its portability and application.

Acceleo 3 fully supports code generation from meta-models, identifying stereotypes applied on classes and providing access to properties. The later isn't based on MOFM2T, but provided by a service, essentially a Java method that browses through the UML2 object model associated with each class.

---

[12] http://www.acceleo.org/pages/introduction/en
[13] http://www.omg.org/spec/MOFM2T/1.0/

Table 1. A simple Acceleo template and its output when used on a class named "Clients" with the stereotype "Table" applied on. The "hasStereotype" query is an external service.

| Acceleo code template | Sample output |
|---|---|
| ```[comment encoding = UTF-8 /][module generateProf(    'http://www.eclipse.org/uml2/3.0.0/UML')/][template public generateProf(c : Class) ?(c.hasStereotype('Table'))][comment @main /] [if (c.hasStereotype('Table'))] [file (c.name.concat('.test'), false, 'UTF-8')]   File for a class with the stereotype Table.   The name of the class is: [c.name/]. [/file] [/if][/template]``` | File for a class with the stereotype Table.The name of this class is Clients. |

## MASON

MASON (the acronym for "Multi-Agent Simulator Of Neighbourhoods") aims to be a light-weight, highly-portable, multi-purpose agent-based modelling package [15]. MASON is a relatively new tool, with the first version coming to light in 2003; being somewhat different for tools developed in the 1990s. Its objects are architected in such a way that simulation models are totally isolated from visualisation and input/output mechanisms. MASON is fully written in Java and freely distributed, hence it produces programs that are highly portable between different operating systems, not only running alike but also presenting identical results. Comparative results have shown that in general MASON is likely the fastest of the main Program-level tools.

MASON was initially used for artificial scenarios, evolving as a text input/output tool, lacking graphical facilities [7]. These features are now fully available, and improved with the usage of Java3D. Supported by extensive documentation and a relevant comunity[14], MASON has been adopted more widely.

GeoMason[15] is a rather complete extension for geo-referenced data. Input and output functionality is available for both raster and vector data, relying on third party packages: the Java Topology Suite for geometry manipulation, GeoTools for vector interaction and GDAL for raster formats.

Its light-weight infrastructure, extensive documentation, and easy of integration through Eclipse made MASON an obvious choice for validating DSL3S.

## Summary and future work

The application of spatial simulation techniques to the GIS realm is still today locked in the choice between versatile tools that require advanced programming skills and easy to use pre-built models that force relevant compromises of transparency and scope. Several DSL, such as NetLogo or MOBIDYC, have been

---

[14] http://cs.gmu.edu/~eclab/projects/mason
[15] http://cs.gmu.edu/~eclab/projects/mason/extensions/geomason/

tried in this field but invariably producing imperative languages with compromises of their own.

DSL3S proposes a new approach to this subject, with the development of a UML profile language and a code-to-model transformation infrastructure, producing simulation models based on a Program-level tool. This scheme promotes faster model development, reduces coding errors and increases model readability through graphical m o d e l s . Relying on MASON, it guarantees interoperability w i t h geographic data, while largely dispensing coding activities. The language is being developed on the Eclipse IDE, using the modelling ad-ons Papyrus and Acceleo.

In the near future DSL3S will be assessed through its application to real world scenarios. This interative process will allow to understand how far it can go in its current form and how necessary new behavioural stereotypes may be.

## References

[1]   Wuensche, A. and M. Lesser (1992). "The Global Dynamics of Cellular Automata".Addison-Wesley.

[2]   J. Ferber (1999). "An Introduction to Distributed Artificial Intelligence", chapter Multi-Agents Systems, Addison-Wesley.

[3]   Fall, A. and Fall, J. (2001), "A domain-specific language for models of landscape dynamics", Ecological Modelling, 141, pp. 1–18.

[4]   Olde, V. and Wassen, M. (1997), "A comparison of six models predicting vegetation response to hydrological habitat change", Ecological Modelling, 101, pp. 347–361.

[5]   de Sousa, L. and da Silva, A. (2011), "Review of Spatial Simulation Tools for Geographic Information Systems" in SIMUL 2011, The Third International Conference on Advances in System Simulation, ThinkMind.

[6]   N. Collier, T. Howe, and M. North (2003). "Onward and upward: the transition to Repast 2.0", In First Annual North American Association for Computational Social and Organizational Science Conference, Pittsburgh, Pa.

[7]   Luke, S., C. Cioffi-Revilla, L. Panait, K. Sullivan, and G. Balan. (2005) "Mason: A multi-agent simulation environment". Simulation: Transactions of the society for Modeling and Simulation International, 82(7), pp. 517–527.

[8]   Tobias, R. and C. Hofmann. (2004) Evaluation of free java-libraries for social-scientific agent based simulation. Journal of Artificial Societies and Social Simulation, 7(1).

[9]   Samuelson, D. and C. Macal. (2006) "Agent-based simulation comes of age". OR/MS Today, 33(4), pp. 34–38.

[10]  Mladenoff, D. (2004) "Landis and forest landscape models". Ecological Modelling, 180(1), pp. 7 – 19.

[11]  Merzenich, J. and L. Frid. (2005) "Projecting landscape conditions in southern Utah using VDDT". In M. Bevers and T. M. Barrett, editors, Systems Analysis in Forest Resources: Proceedings of the 2003 Symposium, pp. 157–163, Portland, OR. U.S. Department of Agriculture, Forest Service, Pacific Northwest Research Station.

[12]  Ginot, V., C. Le Page, and S. Souissi. (2002) "A multi-agents architecture to enhance end-user individual based modelling". Ecological Modelling, 157, pp. 23– 41.

[13]  S. W. Wilson (1991), "The animat path to AI". In J. A. Meyer and S. Wilson, editors, From Animals to Animats, pp. 15–21, Cambridge, MA. MIT Press.

[14]  Epstein, J. M., and R. Axtell. (1996) "Growing Artificial Societies". MIT Press.
      S. F. Railsback, L. L. Steven, and J. K. Jackson (2006), "Agent-based simulation platforms: Review and development recommendations". Simulation, 82, Issue 9.

# Effects of peri-urban structure on air pollution

Using CA models to understand the link between urban structure and air pollution

## M. SCHINDLER[1]; G. CARUSO[1]

[1]Geography and Spatial Planning Research Centre, University of Luxembourg
Campus Walferdange, BP2, Walferdange, 7220, Luxembourg
+352 621314898, Mirjam.Schindler.001@student.uni.lu (correspondent author)

**Keywords:** urban structure, air pollution, cellular automata, residential choice

## Abstract

Air quality is a major concern in urban areas worldwide not only because of its severe health impacts but also due to its influence on living quality and residential behaviour. The subsequent increasing demand for residential areas in the greener fringes of urban agglomerations fuels the discussion about sustainability in future cities. As traffic emissions are acknowledged to be the major source of pollutants in an urban environment this residential trend has triggered research to further understand the influence of urban structure on air quality. In order to meet sustainable growth, many researchers argue that in a global perspective a compact city is the desirable urban form due to less traffic distance, just in contrast to the trend towards urban sprawl. However, quantifying the link between urban structure and air pollution has only been the aim of few research studies so far. Thus, our objective is to deepen the understanding of this link by coupling a micro-economic CA urban growth model with a traffic emission model and a CA air pollution model while focussing on the impact on residential population.

In order to simulate peri-urban growth of a theoretical city we use the CA economic model S-GHOST, which takes into account residential preferences for green space and social externalities and accordingly generates the spatial pattern of houses, green space and road network. Based on calibrated self-organized long-run urban forms, the emitted traffic pollutant concentrations caused by commuters to the CBD are estimated within the generated road network and dispersed using a CA dispersion model. The CA approach accounts for the dynamic behaviour and the substantial spatial variability of the pollutants. Based on gravity, wind velocity and the characteristics of neighbouring cells, the lattice gas CA simulates pollutant transportation, collision and dispersion. Since we are interested in the effects of urban structure on the population in the residential locations, resulting exposure concentrations are calculated and compared for different equilibrium urban forms.

Not only the global perspective on exposure are of interest to us but essentially the local perspective to understand the factors influencing air quality within urban structures. How do the residential preferences like green space and social amenities influence air quality besides, for instance, transportation costs? Additionally, the question of scale and time is addressed: which urban structure provides sustainability of cities in a long-term perspective on city but also population level?

## Introduction

Air quality is a major concern in urban areas worldwide not only because of its severe health impacts but also due to its influence on living quality and residential behavior. The subsequent increasing demand for residential areas in the greener fringes of urban agglomerations fuels the discussion about sustainability in future cities. As traffic emissions are acknowledged to be the major source of pollutants in an urban environment this residential trend has triggered research to further understand the influence of urban structure on air quality. In order to meet sustainable growth, many researchers argue that in a global perspective a compact city is the desirable urban form due to shorter travelling distances, just in contrast to the trend towards urban sprawl. However, if energy consumption (e.g. [1]) and total emissions (e.g. [2]) can be shown to be reduced with more compact urban forms via reduced car use at regional scale, compactness is still debated ([3],[4],[5]). Moreover, population exposure to traffic pollutants is rarely directly considered, while it might well increase with compactness due to joined concentration of traffic flows and population and because of shorter trips thus with colder and more polluting engines. In addition to triggering health problems, the compact city might therefore well reduce the attractiveness of the more central areas and favor exurban residential choice, in contrast to an anti-sprawl policy. Modeling the link between urban structure and air pollution has only been the aim of few research studies so far [6], [7]. Our objective is to deepen the understanding of this link. We assume that how cities are locally designed is key to resolving the aforementioned compact city contradiction. We also believe that residential preferences should be explicitly considered in order, in the longer run, to assess how households trade-off pollutants and other locational attributes. In this paper we couple a micro-economic CA urban growth model with both a traffic emission model and a CA air pollution model while focussing on the impact of residential preferences and local designs on air pollution exposure of residents.

## Methodology

We chose a purely theoretical modeling approach, combining factors we found most relevant in a sequence of four models: (i) residential choice (ii) traffic generation and pollutants emission, (iii) pollutants dispersion and (iv) population exposure model.

### Residential Model

In order to simulate peri-urban growth of a theoretical city we use the CA economic model S-GHOST [8], which takes into account residential preferences for green space and social externalities and accordingly generates the spatial pattern of houses, green space and a road network. Urban structures result from the process of people choosing a residential location by maximizing their utility subject to a budget constraint. The process reflects a trade-off between a location with surrounding green space and proximity to public goods amenities, while minimizing transportation costs to work in the CBD. The model uses a cellular automata

approach in the sense that the land uses of neighbouring cells partly determine (the conversion of) the state of each cell simultaneously. In each step, household's utility and bids are calculated (in line with Alonso [9]) and accordingly originally agricultural land is either converted to residential areas or roads or remains green space. The city is an open system with free in-migration that eventually reaches a long-run equilibrium where all agents have maximized utility so they have no incentive to move into or out of the area. A final structure represents the results of a growth process considering residential preferences. The model has been calibrated on parameters for a typical French city [10] with a resolution of 730m. Figure 1 shows the land use obtained from this benchmark calibration as well as a situation where residential prefrences for green space are higher, thus leading to more sprawl.
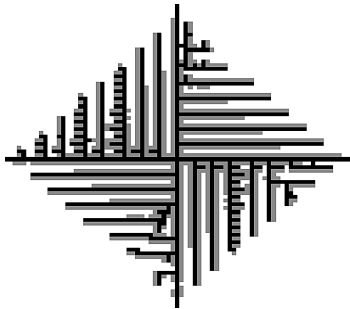


Figure 1: Resulting urban structures around a CBD for benchmark calibration in S-GHOST model after Caruso [8]; white: green spaces, grey: residential areas, black: road network

For this study, the model is disaggregated to a 146m resolution in order to improve its approximation towards reality and to allow for the simulation of different local designs. These designs are related to how households would prefer to position themselves in relation to the main distributor road. A conditional disaggregation process is applied on the residential areas in the S-GHOST model output so that local and city-wide residential choices are considered, resulting in structures of varying degrees of compactness (Figure 2).
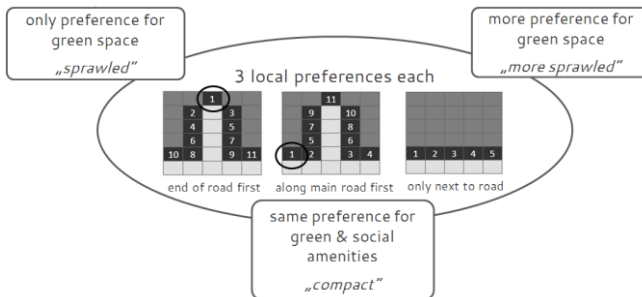


Figure 2: Illustration of residential preferences on city-wide (social & green) and local (relation to main road) scale; local preferences termed short as "back", "front" and "road" respectively

### Traffic and Emission Model

Based on these self-organized urban forms, the emitted traffic pollutant concentrations caused by (one-way) commuters to the CBD are estimated within the peri-urban environment. Traffic emissions are modeled based on average speed, traffic activity defined by population densities, trip length as the shortest path to the CBD from each residential cell and engine operation mode. The respective equations for hot and cold emissions are taken from the MEET Project [11] and, where necessary, European averages are chosen as reference values for emission calculations.

Air quality is modeled by looking at pollutant concentrations in different discrete time steps, meaning during a time window[1] up to the moment when every resident has reached the CBD. Thus, we simulate the commuting process by sending the residents to work in a staggered process and calculate the emissions respectively: we assume that the residents living the furthest away from the CBD leave first since it takes them more time. However, in order to avoid arrivals in the CBD all at the same time and, thus, to reduce congestion potentials, staggered numbers of people at other distances start as well in the same time step[2].

### Pollutants Dispersion Model

Next, transport, dispersion and removal processes are modeled which the pollutants undergo after being emitted on the road network. Earlier studies point at the complexity of the modeling process which also inspired many researchers to look out for more simplistic approaches with nonetheless comparable results. One of such attempts is the cellular automata air pollution model developed by Guariso and Maniezzo [12] and further elaborated by Marín et al. [13]. The CA approach accounts for the dynamic behavior and the substantial spatial variability of the pollutants. Based on gravity, wind velocity and the characteristics of neighboring cells, the CA simulates pollutant transportation, collision and dispersion. Due to its simplistic and flexible representation based on a few numerical relations and its nonetheless proofed comparability to standard complex air quality models [12] this model serves as an inspiring approach to proceed with the calculated emission concentrations on the roads. Instead of originally three dimensions, it has been modified to be applied on 2D.

Inputs to the dispersion model are the emissions on the road network in each time step, added to the current dispersed emissions. For each time step when cars are passing through one cell the new situation is calculated[3]. Considering a Moore

---

[1] We assume an imaginary time window of ~45 min in the morning between 8:00 and ~8:45 since it takes one car 13 seconds to pass one cell (146 m) at an average speed of 40 km/h.

[2] Starting at the largest distance with all people living this far from the CBD, staggered in 5%-steps with smaller distances: residents living the maximum distance away ALL start in the first time step while staggered numbers (5% steps) of residents at all other distances start respectively as well; in the second time step, residents at the second largest distance. ALL start while 5% less start at the third largest distance and so on.

[3] Due to simplistic reasons, it is assumed that one time step (vehicles passing one cell) is identical to one iteration of pollutant dispersion. This seems justifiable since vehicles move

neighborhood on 2D an update rule is applied in each time step on each cell in order to model horizontal, Gaussian-like transport based on wind speed, wind direction and (isotropic) diffusivity [14]. Vertical transport is indirectly accounted for by assuming a certain amount of concentration being removed in one time step due to gravity and buoyancy. Building effects, meaning diversion of air flow due to obstacles, is treated as well in order to consider land uses and urban structures. In residential cells a percentage partition of the modeled concentration (based on wind and diffusivity) into the neighboring cells which are not occupied by buildings is assumed. This partition depends on the magnitude of building effects (scaled logarithmically and based on population densities) and is, thus, indirectly linked to building height and distances. Chemical processes are not included.

**Exposure Model**

Exposure is then estimated per residential cell. Since air flow is diverted by each residential location (obstacle), exposure cannot be derived directly but by considering the air quality in all its surrounding locations: calculated is the average concentration from the neighbouring cells of each residential location (applying an averaging filter) and the average across all time steps (Equation 1).

$$\bar{E}_{ij} = \frac{1}{nj} \sum_{n=1}^{d} \sum_{j=1}^{9} C_{jn} R_i \qquad \text{(Equation 1)}$$

where

| | |
|---|---|
| $\bar{E}_{ij}$ | is the mean exposure per residential cell $j$ in relation to the number of residents |
| $n$ | is the number of time steps |
| $d$ | is the maximum distance from the CBD of a residential location |
| $C_{jn}$ | is the emission concentration in one cell $j$ per time step $n$, considering also the 8 neighbouring locations (Moore) |
| $R_i$ | is the number of residents $I$ in the residential location |

**Results and discussion**

We ran the model for CO as one of the major air pollutants caused by road traffic. The analysis indicates that different *local* residential preferences implicate different overall exposure levels and alter the distribution of air pollution across the distances to the CBD. When people are only located along a main distributor road the air quality situation is worst. The further people live away from the CBD, the less they are in all designs exposed to air pollution. However, the compact scenario is linked to higher exposure levels at the same distances across the structures. More compact local designs implicate higher densities and less land cover change which implies a concentrated number of residents exposed to air pollution in one residential location. On the contrary, in a sprawled local development, few residents are exposed to air pollution per cell.

---

faster with the assumed parameters (vehicle speed, resolution) as pollutants could pass one cell (wind speed).

In short, compact structures expose more residents to higher emission concentrations but then vary to a larger extent with distance. Against the expectation that more compact structures reduce the need to travel, sprawled local arrangements outweigh this increased travel by their lower population densities and greater distance to main roads and, hence, also emission sources.

The distribution patterns of each local arrangement in relation to distance (see zoomed-in boxes in Figure 3) reveal that the exposure values vary not only with changing distance to the CBD but also within a local neighborhood: due to local design of land uses and population density, exposure values vary from one distance to another, seemingly more for the two dead-alley designs than for the more compact arrangement. This indicates that the residential location within a local arrangement is also influencing besides the distance to the CBD. Figure 3c) shows the average population exposure in function of distance which is simulated when residents only live along a main distributor road. Exposure varies here less within a local design due to the underlying constant local design and the distance decay is less strongly visible. This depicts clearly the influence of local design of population density and land uses, based on residential preferences. Distance to the CBD is a relevant factor in terms of population exposure but its influence varies also with the city structure and is not the only explanation for differences in population exposure within an urban area.
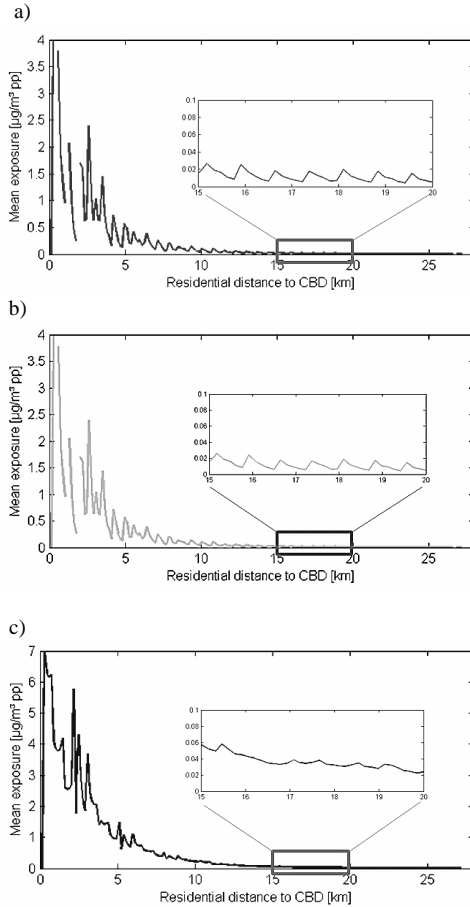
a)



b)



c)



Figure 3: Mean exposure to CO across all distances to the CBD in μgm⁻³pp, for the city-wide residential structure "sprawled" and the three local designs a) "back" b) "front" 3) "road" (as explained in Figure 2)

Figure 4 shows the average exposure to CO across an urban area and indicates as well that local design matters.
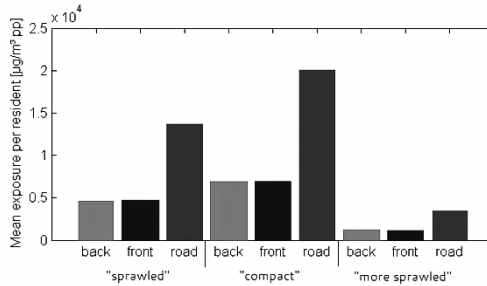
Figure 4: Mean exposure to CO per residential structure/local design, averaged across the entire urban area and all time steps

On *city-wide* scale, different preferences for social and green amenities show also that on average compact structures result in higher average exposure values whereas more sprawled structures are linked to lower exposure values, independent of the local arrangements. This means that moderate preferences for both, social and green amenities, depict the worst overall situation in terms of air quality. As the preference for green space increases, also in relation to the preference for social amenities, less residents are exposed to air pollution due to low population densities. The more sprawled an urban area, the lower the average exposure. This result lies in contrast to other studies (e.g. [6] and [7]) and triggers the discussion about both, findings and methodologies.

Compactness in other studies reveals lower exposure values because compactness is linked to change in mode of transportation and travel behaviour, whereas this study does not distinguish between different modes of travel and other factors like congestion linked to residential structures. Therefore, compact development induces more commuting traffic in a smaller area where also more people are affected due to higher population densities. These findings suggest that beneficial effects from compactness are on the one hand limited to a certain density threshold beyond which density reveals worse air quality and on the other hand are linked to changes in the composition of travel mode choices. Hence, residential structures influence exposure but important is also the link to other factors, such as travel behavior in order to reduce vehicle travel after Stone et al. [15]. This is akin to what Neumann [4] states: "conceiving the city in terms of form is not sufficient [...] instead, conceiving the city in terms of process holds more promise in obtaining the elusive goal of a sustainable city".

Figure 5 displays a comparison of average population exposure relative to the distance to the CBD in each structure and design. It shows the general trend of exposure, resulting from a regression analysis. Keeping in mind that the figure indicates a generalization, the same as above can be concluded: higher preferences for green space yield overall lower exposure levels whereas balanced preferences tend to expose residents to more emission concentrations, at least for compact local designs. Although compact structures expose more residents to higher emission concentrations close to the CBD, average values further away from the city are

lower due to less distance driven and an overall smaller expansion of the city boundaries. Exposure decreases faster with distance in compact development due to higher population densities but the same number of residents in the total area. On the contrary, more sprawled development implies relatively less variation across distance. Hence, up to a certain distance, sprawled development seems better but residents living in continuing sprawled development are more exposed at greater distances. Therefore, compact development limits the area where exposure levels are higher indicating a threshold to the benefits of sprawled development: up to some extend it results in better air quality but after a distance threshold this benefit is outweighed by increased exposure compared to compact structures. Sprawled development reduces overall exposure close to the city but does not decrease as much with increased distance. Not having considered congestion in the model is an explanation for the good result of sprawled development.
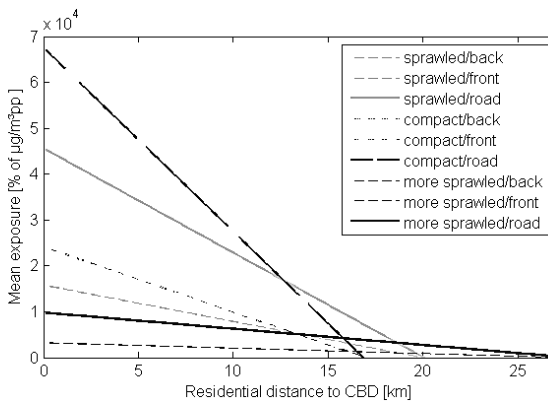


Figure 5: Regression on average exposure to CO per residential structure/local design and distance to the CBD

The scale at which compactness is favored does matter in the discussion of urban form and air quality and that the answer to the research question remains complex and twofold, preventing the provision of a best-practice solution.

A widely known discussion is held about the question whether air quality is *mainly* determined by the distance travelled, meaning compact structures reduce the need to travel and therefore directly provide overall better air quality situations than sprawled structures [15]. The here analyzed results comply partly with this discussion since exposure levels generally decrease with increased distance to the CBD, but additionally indicate the need for further distinction: although the distance travelled certainly influences the level of exposure, compact structures are linked to higher exposure despite less distance travelled. Further outside the CBD where population densities are lower, the distance travelled impacts greater, leading to higher exposure levels for sprawled development. Hence, the distance travelled determines the general level of exposure but is not the only criterion for local variations and is linked to congestion potentials and other factors. This goes along

with findings from, for instance, Clark et al. [16] who state that "urban form could play a modest but important role in achieving long-term air quality goals".

Still, within the modeling process certain parameters are already linked to distance. These are, for instance, the predefined departure schedule for the commuting trips, the emission calculation and the underlying cold distance per pollutant type as well as wind speed which influence the results but do not determine the discovered variations as such. Stone et al. [15] address travel speed and cold start distributions besides distance as explanations for varying emission concentrations which are, in turn, coupled with residential structures.

Analyzed is the interrelation between residential preferences, residential structures and average exposure. Although there is an influence detected and quantified, the degree of influence of urban form on air quality in relation to other factors is still to be discussed: are other social or socio-economic factors, meteorology, topography etc. more determining in relative terms? The promotion of public transport, for instance, is a favored strategy to reduce traffic emissions. In comparison to this strategy and to car-dependency, a deliberate residential structure might also seem relevant but may not be as effective without linkage to other factors, as the results of this study and the discussion show. Socio-economic factors have stronger bearings on mobility behavior than spatial characteristics, which is linked to residential choice and preferences [5]. The impact of residential structures can, thus, not be isolated from broader societal and technological trends as already explained in comparison with other studies [6].

Modeled are only traffic-emissions from residents commuting by car in the morning, based on a predefined departure schedule. Neither regular traffic passing through the area nor non-work trips are included in the simulation. Against this background, the seemingly small changes detected between the different structures appear relevant. Certainly, car dependency is due to simplifications overestimated which modifies the results but unchains the approach from travel mode dependencies and, therefore, points at the influence of the linkage of travel mode and urban structure. Local designs do not only influence the environment directly but also indirectly through travel behavior and spatial distributions of land cover which are mirrored in the trends of residential choices [16].

Likewise important are the resolution of the model and the grid size to which residential areas are disaggregated and therefore local designs are considered. This question of the degree of aggregation and, thus, scale has a noticeable influence on the model, reflected in the scale on which preferences are considered. This is an important finding and points at the necessity to distinguish in the discussion about residential choice. Further, emissions from all vehicle sources in each grid area are combined together into a larger area source, assuming that emissions are uniform over that particular area.

Placing the study within its limited context, it proofs the compatibility of the model types and the findings from the here presented simplified modeling approach open up the field for further discussion and extension of this research in spite of the assumptions discussed.

**Conclusion**

We investigated the link between residential preferences and traffic-induced air quality within the discussion about sustainability and the design of future cities. We analyzed whether the preferences for social and/or green amenities within residential choice and, thus, residential structures, impact air quality in an urban area. Following state-of-the-art research by e.g. [6], our work expands the research by modeling not only the influence of city-wide residential structures but also of local designs and their induced population exposure from commuter's traffic.

A theoretical modeling approach has been developed, coupling a residential choice, traffic generation and pollutants emission, pollutants dispersion and population exposure model. Running the model on different residential structures with varying degrees of compactness city-wide and locally for CO indicates that residential preferences do matter.

Driving factors are hereby scale and distance to the CBD at which preferences are considered, although distance is not the only determining factor. With increasing distance to the CBD, population exposure decreases, no matter the degree of compactness. However, the difference across distances is higher for more compact structures compared to sprawled development. Preferences for green and social amenities implicate different impacts on population exposure which points at the importance to distinguish between local and city-wide designs. Besides state-of-the-art findings that the overall city form impacts air quality, this study shows that also local designs do play a noticeable role. Our study suggests that the overall city form is most influencing on air quality, followed by intra-urban residential structures and local designs.

In contrast to findings from other studies compact development with high population densities entails on all scales highest population exposure to CO. This suggests a limit to the gains of compact structures due to e.g. more trips with colder engines. It triggers the discussion on the benefits of compactness in spatial planning and adds a critical viewpoint on the belief that more compactness in planning is directly linked to better air quality in urban areas. Structure needs to be linked with, for instance, varying travel mode respectively in order to reduce exposure to air pollution. Although elaborate urban structures comprise the potential to mitigate air pollution, they do not ensure better air quality alone but have to be coupled with other strategies.

**References**

[1]    Newman, P. and Kenworthy, J. (2000), Sustainable urban form: The big picture. In Williams, K., Burton, E. and Jenks, M. (Eds), Achieving sustainable urban form, pp. 109-120, Spon Press, London

[2]    Manins, P.C., Cope, M.E., Hurley, P.J., Newton, P.W., Smith, N.C. and Marquez, L.O. (1998), the impact of urban development on air quality and energy use. In Proceedings of the 14th International Clean Air and Environment Conference, Melbourne, pp. 331-336

[3]    Gordon, P. and Richardson, H. (1997), Are compact cities a desirable planning goal? In Journal of the American Planning Association, 63(1), pp. 95-107

[4]   Neumann, M. (2005), The compact city fallacy. In Journal of Planning Education and Research 25, pp. 11-26

[5]   Van der Waals, J. (2000), The compact city and the environment: a review. In Tijdschrift voor Economische en Sociale Geografie 91(2), pp. 111-121

[6]   Borrego, C., Martins, H., Tchepel, O., Salmim, L., Monteiro, A. and Miranda, A.I. (2005), How urban structure can affect city sustainability from an air quality perspective. In Environmental Modelling & Software 21(4), pp. 461-467

[7]   De Ridder, K., Lefebre, F., Adriaensen, S.,Arnold, U., Beckroege, W., Bronner, C., Damsgaard, O., Dostal, I., Dufek, J., Hirsch, J. IntPanis, L., Kotek, Z., Radamier, T., Thierry, A., Vermoote, S. Wania, A. and Weber, A. (2008), Simulating the impact of urban sprawl on air quality and population exposure in the German Rhur area. Part I: Reproducing the base state. In Atmospheric Environment, 42, pp. 7059-7069

[8]   Caruso, G., Vuidel, G., Cavailhès, J., Frankhauser, P., Peeters, D. and Thomas, I. (2011), Morphological similarities between DBM and a microeconomic model of sprawl. Journal of Geographic Systems 13, pp. 31-48

[9]   Alonso, W. (1960), A theory of the urban land market. In Regional Science, 6(1), pp. 149-157

[10]  Caruso, G., Cavailhès, J, Frankhauser, P., Peeters, D., Thomas, I. and Vuidel, G. (2010), S-GHOST, un modèle d'auto-organisation de l'étalement urbain et du réseau de transport. Chapitre 12 in Antoni, J.-P.(dir.) Forme urbaine et politiques de transport. Paris, Economica (Méthodes et approaches)

[11]  European Commission (1999), Methodology for calculating transport emissions and energy consumption (MEET). Transport Research Laboratory, Luxembourg

[12]  Guariso, G. and Maniezzo, V. (1992), Air quality simulation through cellular automata. In Environmental Software 7, pp. 131-141

[13]  Marín, M., Rauch, V., Rojas-Molina, A. López-Cajún, Herrera, A. and Castaño, V.M. (2000), Cellular automata simulation of dispersion of pollutants. In Computational Materials Science 18, pp. 132–140

[14]  Chopard, B. and Masselot, A. (1998), Cellular automata and lattice Boltzmann methods: a new approach to computational fluid dynamics and particle transport. In Elsevier, pp. 1-13

[15]  Stone, B.J., Mednick, A. Holloway, T. and Spak, S. (2007), Is compact growth good for air quality? In Journal of the American Planning Association 73(4), pp. 404-418

[16]  Clark, L., Millet, D. and Marshall, J. (2001), Air quality and urban form in U.S. urban areas: Evidence from regulatory monitors. In Environmental Science and Technology 45, pp. 7028-7035

# ABSTRACTS

# Calibration of cellular automata based land use models: lessons learnt from practical experience

## H. VAN DELDEN[1], J. DÍAZ-PACHECO[2], Y. SHI[3], and J. VAN VLIET[4],[¤]

[1,2,3,4]Research Institute for Knowledge Systems (RIKS)
P.O. Box 463, 6200 AL Maastricht, The Netherlands
+31 (043) 350 1750, [1]hvdelden@riks.nl; [2]jdiaz@riks.nl, [3]yshi@riks.nl,
[4]jaspervanvliet@gmail.com

**Keywords:** cellular automata, calibration, validation, land use change modelling.

## Abstract

With an increasing interest and use of CA-based land use models in the planning and policy practice, calibration and validation gain in importance. Calibrating CA models, however, remains an ongoing challenge. Despite several attempts to develop (semi-)automatic approaches [1, 2], manual calibration, especially for calibrating land use change models with multiple dynamic land uses, remains the common practise [3]. Although there are numerous papers that discuss CA models, only few cover their (manual) calibration process, and a common knowledge base seems to be lacking. This presentation aims to start such a knowledge base by presenting a method for calibrating CA-based land use models, which has been developed over the past 25 years and builds on work by a number of people who have calibrated the Metronamica land use model [4, 5, 6] in its current or preliminary forms [7, 8, 9, 10]. In this methodology the calibration process is approached broader than the setting and fine-tuning of parameters, and includes all steps related to finding an appropriate parameter set and assessing its quality.

The calibration process follows a number of steps in line with common calibration practices and the characteristics of CA-based land use models:

1. As part of the *data analysis* the current situation and historic developments are analysed. This includes analysing the temporal change in total area surface for various land uses as well as the change in landscape structure. Regarding the latter, metrics such as the clumpiness index [11] and the rank size distribution [12] are used in conjunction with a visual inspection of the developments. Furthermore, the enrichment factor is used to analyse the over- and underrepresentation of certain land uses in the neighbourhood of changed land uses [10].

2. *Model set-up* includes a set of choices relevant for setting up the model to a specific region and context. In CA-based land use modelling main

---

[¤] Institute for Environmental Studies and Amsterdam Global Change Institute, Amsterdam, The Netherlands

choices are related to the decision on the area extent, the applied resolution and the selection of land use classes to be modelled, where finding a balance between providing additional information and creating a false sense of accuracy is often a crucial point of discussion [13].

3. During the *calibration*, parameter values are set and fine-tuned and subsequently the model is assessed on its behaviour and results, frequently over a historic calibration period. Difficulties in calibrating CA-based land use models mainly relate to the large number of parameters that need to be set, the limited availability of time series of land use maps, and finding objective ways to assess the quality of the calibration. Regarding the latter, progress has been made over the past years, which has resulted in the use of neutral models to act as a benchmark for quality assessment [14], together with the use of objective measures to complement the more subjective visual assessment. To assess the quality of the calibration we take into account the *predictive accuracy*, which is the ability of the model to accurately simulate actual land use patterns; and the *process accuracy*, the extent to which the modelled processes are consistent with real world processes [15]. Main indicators used for assessing the quality of the calibration are indicators for location agreement, such as Fuzzy Kappa [16] and Kappa Simulation [17]; indicators for landscape structure agreement, such as the clumpiness index [11], the fractal dimension [18], the rank size distribution [12], and the enrichment factor [10]; and visual inspection.

4. During the *validation*, the model's behaviour and results, based on the parameters settings obtained during the calibration, are assessed over a data set independent from the one used as part of the calibration. This usually results in an evaluation of the model's behaviour over a different historic period; although other independent data sets are equally valid, see e.g. [19]. Assessment criteria are the same as for the calibration.

5. Finally the model is tested and evaluated on its *long-term behaviour*, which includes a long-term simulation with the calibration parameters, a number of tests with extreme scenarios to assess the robustness of the model and a number of tests to assess the sensitivity of model results on small changes to the parameter settings.

During the presentation the details of the methodology will be discussed using an application to Madrid, Spain.

## References

[1] Arai, T., T. Akiyama (2004), Empirical analysis for estimating land use transition potential functions – case study in the Tokyo metropolitan region. Computers Environment and Urban Systems, 28, pp. 65-84

[2] Straatman, B., R. White, G. Engelen (2004), Towards an automatic calibration procedure for constrained cellular automata. Computers, Environment and Urban Systems, 28, pp. 149-170

[3]   Van Vliet, J., H. van Delden (2011), Calibration of the neighborhood effect in cellular automata land use models. In Proceedings of the 17th European colloquium on quantitative and theoretical geography, Athens, Greece, September 2-5

[4]   White, R., G. Engelen (1993), Cellular automata and fractal urban form: a cellular modelling approach to the evolution of land use patterns. Environment and Planning A, 25, pp. 1175 – 1199

[5]   Van Delden, H., J. Hurkens (2011), A generic Integrated Spatial Decision Support System for urban and regional planning. Keynote presented at MODSIM11 International Congress on Modelling and Simulation, Perth, Australia.

[6]   www.metronamica.nl

[7]   White, R., G. Engelen (2003), A calibration procedure for constrained large neighbourhood cellular automata based land use models. In proceedings of the 13th European Colloquium on Theoretical and Quantitative Geography, Lucca, Italy

[8]   Hagen-Zanker, A., P. Martens (2008), Map comparison methods for comprehensive assessment of geosimulation models. In O. Gervasi, B. Murgante, A. Lagana, D. Taniar, Y. Mun and M. Gavrilova (eds.), Lecture Notes in Computer Science, Proceedings of the 2008 International Conference on Computational Science and Its Applications ICCSA, Springer, Berlin, Germany, pp. 194-209

[9]   Wickramasuriya, R.C., A.K. Bregt, H. van Delden, A. Hagen-Zanker (2009), The dynamics of shifting cultivation captured in an extended Constrained Cellular Automata land use model. Ecological Modelling, 220, pp. 2302-2309

[10]  Van Vliet, J., N. Naus, A.K. Bregt, R. van Lammeren, J. Hurkens, H. van Delden (submitted), Measuring the neighbourhood effect to calibrate land-use models. Computers, Environment and Urban Systems

[11]  http://www.umass.edu/landeco/research/fragstats/documents/Metrics/Contagion%20-%20Interspersion%20Metrics/Metrics/C115%20-%20CLUMPY.htm

[12]  Gabaix, X. (1999), Zipf's law for cities: an explanation. The Quarterly Journal of Economics, 114(3), pp. 739-767

[13]  Van Delden, H., J. van Vliet, D.T. Rutledge, M.J. Kirkby (2011), Comparison of scale and scaling issues in integrated land-use models for policy support. Agriculture, Ecosystems and Environment, 142(1-2), pp. 18-28

[14]  Hagen-Zanker, A., G. Lajoie (2008), Neutral models of landscape change as benchmarks in the assessment of model performance. Landscape and Urban Planning, 86(3-4), pp. 284-296

[15]  Brown, D.G., S., Page, R. Riolo, M. Zellner, W. Rand (2005), Path dependence and the validation of agent-based spatial models of land use. International Journal of Geographical Information Systems, 19(2), pp. 153-174

[16]  Hagen-Zanker, A. (2009), An improved fuzzy kappa statistic that accounts for spatial autocorrelation. International Journal of Geographical Information Science, 23(1), pp. 61-73

[17]  Van Vliet, J., A.K. Bregt, A. Hagen-Zanker (2011), Revisiting Kappa to account for change in the accuracy assessment of land-use change models. Ecological modelling, 222(8), pp. 1367-1375

[18]  Chen, Y (2011), Derivation of the functional relations between fractal dimension of and shape indices of urban form. Computers, Environment and Urban Systems, 35, pp. 442-451

[19]  Van Vliet, J., R. Vanhout, A. Saretta, C. Lavalle, H. van Delden (2010), MOLAND-Light: Supporting planners with a generic land use model for European regions, Paper presented at the International Conference on managing the Urban Rural interface, 19-22 October, Copenhagen, Denmark.

# Assumptions in cellular automata modeling:

Recent advances to meet them

## Danielle J. MARCEAU[1] and Yan LIU[2]

[1]Department of Geomatics Engineering, University of Calgary
2500 University Drive, Calgary, Alberta, Canada, T2N 1N4
Phone: 1-403-220-5314, Email: dmarceau@ucalgary.ca
[2]School of Geography, Planning and Environmental Management, University of Queensland
Chamberlain Building, St. Lucia Campus, Brisbane, QLD 4072, Australia
Phone: 336-56483, Email: yan.liu@uq.edu.au

**Keywords:** Land use change, cellular automata, assumptions, progress

## Abstract[¤]

The study of spatial systems, such as urban systems, and Land-Use Science have been profoundly transformed in the last two decades by the emergence and spread of cellular automata (CA) models designed to simulate future land-use patterns from a bottom-up perspective. The fundamental elements in CA models are individual spatial units defined by their location, geometry, and attribute that evolve through time and over space according to the influence of their neighbors and some external factors. The aim of CA modeling is to capture this influence through a set of rules in order to generate meaningful patterns that represent possible paths the spatial system being simulated can take in the future. If well designed, CA models can inform on the processes that govern urban growth and land-use dynamics and can be used to explore future outcomes through the testing of alternative scenarios. However, to be useful, the architecture and implementation of these models, along with their assumptions must be stated in an explicit way in order to be understood and evaluated by the scientific and users' communities. In addition, adequate techniques must be applied to verify to what extent the estimations of both quantity and location of change provided by CA models can be trusted. The objective of this paper is twofold: 1) to highlight some of the key assumptions in CA modeling, and 2) to describe the progress recently made in attempts to meet these assumptions.

*Assumption 1:* The spatial units used in CA models adequately represent the meaningful geographical entities that compose the system being simulated. *Recent advances:* Moving from the arbitrary, fixed cell grid representation to an irregular, flexible entity-based representation (Bithell and Macmillan, 2007; Pinto and Antunes, 2010; Wang and Marceau, in prep.).
*Assumption 2:* The neighborhood adequately corresponds to the zone of influence of each spatial unit composing the system being simulated. *Recent advances:* Moving from a rigid topologically-based neighborhood definition to a flexible semantic

---

[¤] This contribution has its references in an 'Author-Date' format.

definition adapted to each entity being represented (Moreno et al., 2009; Van Vliet et al., 2009).

*Assumption 3:* The historical dataset used for the empirical calibration of CA models is of good quality, i.e. is free of errors and has been acquired at the right time and at the right spatial scale. *Recent advances:* It has been demonstrated that the quality of the datasets used for the CA calibration can greatly affect the simulation results (Pontius and Petrova, 2010; Pontius and Li, 2010; Van Dessel et al., 2011).

*Assumption 4:* The transition rules built from historical datasets adequately capture the land-use dynamics; this involves an appropriate selection of driving factors (parameters), their values, and their combination. *Recent advances:* Numerous calibration techniques have been tested ranging from simple statistical and probabilistic methods to sophisticated computational intelligence techniques (Feng, et al. 2011; Feng and Liu, 2012). Systematic comparison of some methods is being done (Lin et al., 2011). Interactive and visual methods including some based on fuzzy logic that provide geographically-meaningful rules are being proposed (Hasbani et al., 2011; Stanilov and Batty, 2011; Liu, 2012; Mantelas et al., 2012). *Assumption 5:* The trends in land-use dynamics and the factors driving these changes detected from historical datasets remain constant over time. *Recent advances:* Studies illustrated that such temporal stationarity is uncommon in many land-use systems and that this may affect the performance of CA models (Bakker and Veldkamp, 2011).

Following this review and illustration, recommendations for future research in land- use CA modeling will be provided.

## References

Bakker, M., A. Veldkamp (2011), Changing relationships between land use and environmental characteristics and their consequences for spatially explicit land-use change prediction. Journal of Land Use Science, DOI:10.1080/1747423X.2011.595833

Bithell, M., W. D. Macmillan (2007), Escape from the cell: spatially explicit modelling with and without grids. Ecological Modelling, 200(1-2), pp. 59-78

Feng, Y. J., Y. Liu (2012), Modelling urban development with nonlinear cellular automata based on kernel principal component analysis. Environment and Planning B: Planning and Design (in press)

Feng, Y. J., Y. Liu, X. H. Tong, M. L. Liu, S. Deng (2011), Modeling dynamic urban growth using cellular automata and particle swarm optimization rules. Landscape and Urban Planning, 102(3), pp. 188-196

Hasbani, J.-G., N. Wijesekara, D. J. Marceau (2011), An interactive method to dynamically create transition rules in a land-use cellular automata model. In A. Salcido (Ed.), Cellular Automata: Simplicity Behind Complexity, InTech Publisher, Available from: http://www.intechopen.com/articles/show/title/an- interactive-method-to-dynamically-create-transition-rules-in-a-land-use-cellular- automata-model

Lin, Y.-P., H.-J. Chu, C.-H. Wu, P. Verberg (2011), Predictive ability of logistic regression, auto-logistic regression and neural network models in empirical land- use change modeling: a case study. International Journal of Geographical Information Science, 25(1), pp. 65-87

Liu, Y. (2012), Modelling sustainable urban growth in a rapidly urbanising region using a fuzzy constrained cellular automata approach. International Journal of Geographical Information Science, 26 (1), pp. 151-167

Mantelas, L., P. Prastacos, T. Hatzichristos, K. Koutsopoulos (2012), Using fuzzy cellular automata to access and simulate urban growth. GeoJournal, 77(1), pp. 13-28

Moreno, N., F. Wang, D. J. Marceau (2009), Implementation of a dynamic neighbourhood in a land-use vector-based geographic cellular automata model. Computers, Environment and Urban Systems, 33(1), pp. 44-54

Pinto, N. N., A. P. Antunes (2010), A cellular automata model based on irregular cells: application to small urban areas. Environment and Planning B, 37(6), pp. 1095-1114

Pontius Jr., R. G., S. H. Petrova (2010), Assessing a predictive model of land change using uncertain data. Environmental Modelling & Software, 25, pp. 299-309

Pontius Jr., R. G., X. Li (2010), Land transition estimates from erroneous maps. Journal of Land Use Science, 5(1), pp. 31-44

Stanilov, K., M. Batty (2011), Exploring the historical determinants of urban growth patterns through cellular automata. Transactions in GIS, 15(3), pp. 253-27

Van Dessel, W., A. Van Rompaey, P. Szilassi (2011), Sensitivity analysis of logistic regression parameterization for land use and land cover probability estimation. International Journal of Geographical Information Science, 25(3), pp. 489-507

Van Vliet, J., R. White, S. Dragicevic (2009), Modeling urban growth using a variable grid cellular automata. Computers, Environment and Urban Systems, 33(1), pp. 35-43

Wang, F., D. J. Marceau (2012), A patch-based cellular automaton for simulating land-use changes at fine spatial scale. Submitted to Transactions in GIS

# Modelling land use dynamics in support of Spatial Planning and Policy-making in Flanders, Belgium

## Guy ENGELEN[1]; Lien POELMANS[1]; Inge ULJEE[1]; Jean-Luc de KOK[1]

[1] VITO, Flemish Institute for Technological Research, Environmental Modelling Unit
Boeretang, 200 2400 Mol, Belgium
+32 14 33 67 37, guy.engelen@vito.be

**Abstract**

To support planners and policy makers in confronting the complexity of land use changes in Flanders, a dynamic, high-resolution land use model has been developed. It enables a better understanding of the main drivers and autonomous dynamics causing land use change and, as a prognostic instrument, it supports the design of planning instruments as well as the assessment of the potential effectiveness prior to the implementation. It allocates demands for space by the population, aggregated economic sectors, agriculture, and nature.

The model is a constrained cellular automata land use model (White and Engelen, 1993) consisting of linked sub-models representing spatial dynamics in Flanders at three geographical levels. At the *Global level*, Flanders and Brussels are represented as one entity subjected to exogenous influences and change. Trend lines determine growth in: population, employment in 10 aggregated economic sectors, land demand in 5 agricultural sectors and finally land demand for 11 natural land uses. These trends are obtained or computed external to the model as part of dedicated scenario exercises. At the *Regional level*, Flanders and Brussels are represented in terms of the 23 constituting arrondissements (EU-NUTS3 regions). A dynamic gravity-based model allocates and reallocates the populations and jobs, obtained from the global level, and computes the associated changes in population and employment densities. For each arrondissement, it passes on to the Local level the amounts of land needed to allocate the population and jobs per sector. Finally, at the *Local level*, Flanders and Brussels are represented as a regular grid of cells measuring 1 ha. Cells are in one of a maximum of 36 states representing their dominant land use. A cellular automata model determines the evolving land use of the individual cell based on the spatial interactions among the land uses within its immediate neighbourhood, constrained by institutional, physical and transportation characteristics. Apart from the changing land use, a series of custom-definable spatial indicators encapsulating economic, social and environmental qualities of the modelled spatial system are computed. Like the land use, these indicators are calculated on a yearly basis, thus resulting in time series of maps as well as aggregated synthetic index values.

The model makes extensive use of statistical and GIS data. In the absence of a map of sufficient quality, a dedicated land use map was compiled based on a rich set of GIS data layers obtained from various data providers in the Flemish, Belgian and

Brussels administrations. It represents land uses in Flanders and Brussels in 2010 classified in some 50 categories at a 10m resolution. The model has been extensively calibrated among others by means of hindcasting. It was further calibrated against the outcomes of the so-called PLANET model of the Federal Planning Bureau. Finally the morphogenetic capacity of the model and the spatial configurations generated are validated by applying Zipf's rule on the rank-size distribution of urban clusters.

During the past two years, the model has been used in several policy exercises requiring insights in land use developments as much as 40 years into the future. Impacts of current, intended or optional policies were assessed to raise new challenges for policy making and management in among others spatial planning, green energy production, flood prevention, and the estimation of ecosystems services provided by the Natura 2000 areas. New applications which are currently under development include dynamic coupling with feedback to a transportation model and a hydrological model in support of on the one hand mobility studies, and on the other, integrated river basin management.

In the presentation, the structure and underlying principles of this constrained cellular automata land use model will be briefly discussed. Results of a scenario exercise carried out for the Ministry of Spatial Planning will be presented. Four contextual scenarios 2010-2050 similar to the worldviews of IPCC-SRES were developed and analysed with a view to provide input for the new Spatial Policy Plan Flanders (Beleidsplan Ruimte).

# An Assessment of Cellular Automata Models in Urban Simulation

## Michael BATTY[1]; David O'SULLIVAN[2]; Paul TORRENS[3]

[1] CASA, UCL
Gower Street, London, WC1E 6BT, United Kingdom
++44-7768-423-656, m.batty@ucl.ac.uk
[2] Geography, University of Auckland,
Private Bag 92019,Auckland, 1142, New Zealand
d.osullivan@auckland.ac.nz
[3] Geography, University of Maryland
College Park, MD 1,United States of America
torrens@geosimulation.com

## Abstract

Urban cellular automata models were first developed as ways of operationalizing generative processes involving urban morphologies as, for example, in simulating fractal growth. In one sense, they have become part of the wider movement towards articulating cities as complex systems, and they tend to be part of the move from aggregate and static, cross-sectional models to those dealing with more disaggregate populations and dynamic behavioral processes. They currently tend to be associated with agent-based models for which they might be regarded as a special case but their comparative simplification and focus on the physical development of cities tends to have elevated them into a form that means that are being considered for use in prediction. In general however although there are many packages which have been fashioned to operationalize such models, their use in practice is patchy in that most urban agencies find them hard to use in that their predictive focus is highly physical and often non-numerical. In contrast to static, aggregative land use transportation models, their usage has been limited.

In this paper, we will review the state of the art of urban in CA models. We will in particular examine the assumptions involved in their validation and verification, arguing that most such models do not articulate the processes that relate to land development that should strictly be part of the changes of state in development that such models seek to represent. We will argue that the starting point for most such models which is physical development and morphology is the wrong point of departure and it is the processes of change *per se* that should be the focus, difficult though this is. The key problem is that although processes of development drive physical CA models, there processes are rarely made explicit or if they are they are highly simplified. They are not validated in any sense for the calibration of such models is against spatial outcomes, not against the fact that such processes can be examined in practice. In short, processes are assumed but not tested for often data is simply absent. Hence calibration against model outcomes can often be spurious in that we know that models with multiple processes and many

interactions can generate similar patterns in many different ways. This is part of the problem of equifinality which means that the same patterns might be reproduced using very different processes. Currently unlike in the case of land use transport and spatial interaction models where there has been substantial research into the modifiable areal unit problem, there is no equivalent analysis or approach in the development of CA models.

In the paper, we will catalogue these and many other problems, suggesting strategies for their resolution and suggesting changes in approach. We will list a series of issues with respect to their application and we will attempt to figure out what are the most appropriate conditions under which such models might be developed. This will involve not only scientific credibility but also practical applicability in the wider context of applications to policy making, prediction and planning support. In one sense, we take this paper as an updating of our earlier papers which have sought to review key problems in this filed [1, 2]. In this sense, we see this paper as a 'progress report'.

**References:**

[1] Batty, M. (2000) Geocomputation Using Cellular Automata, in S. Openshaw and B. Abrahart (Editors) Geocomputation Taylor and Francis, London, 95-126.

[2] Torrens, P. M., and O'Sullivan, D. (2001) Cellular Automata and Urban Simulation: Where Do We Go From Here? Environment and Planning B: Planning and Design, 28(2), 163 – 168.

# Urban land-use policy issues and geosimulation system in a lake watershed of the Yunan-Guizhou Plateau of Southwest China:

A case study of Lake Dianchi*

**Yaolong ZHAO[1]; Ke ZHANG; Yingchun FU**
[1]School of Geography, South China Normal University,
Guangzhou, 510631, P.R. China
TeL: +86-137-5186-9021, Email address: yaolong@scnu.edu.cn

**Keywords:** geosimulation system, urban land-use, policy issues, the Lake Watershed, SLEUTH

## Abstract

A rapid urbanization process in a lake watershed is always accompanied by great land use/cover change and its subsequent effects on the local eco-environment. Therefore, urbanization process in a lake watershed should be controlled to avoid serious deterioration of ecological system. The urbanization process control usually is carried out through establishing appropriate urban land-use planning and policy. Scenario, as a link of uncertain future with given policies, is a popular method in policy planning and make-decision. In region or urban areas, scenario is always connected with Cellular Automata (CA)-based geosimulation system, which can produce multi-scenario forecast for the future. SLEUTH is one of the famous geosimulation systems which have been used for policy make-decision in many cities around the world. The purpose of this study is to explore the feasibility of SLEUTH in land-use policy decision-making in a large lake watershed – the Lake Dianchi watershed in Yunan-Guizhou Plateau of Southwest China.
Lake Dianchi is located in the Yunnan-Guizhou Plateau of southwest China in the upriver area of Yangtze River. Lake Dianchi is the largest freshwater lake in the Yunnan-Guizhou plateau and is the sixth largest body of freshwater in China with a total area of approximately 300 km$^2$ and a total watershed area of approximately 2834 km$^2$. Since China adopted the well-known "open-door" policy and economic reform in later 1970s, the near-shore area of the lake Dianchi has experienced rapid progress in industrialization and urbanization which has resulted in regional eco-environmental degradation, loss of bio-diversity, extreme deterioration of water quality of Lake Dianchi, and so on. For example, water quality in Lake Dianchi is greatly polluted into serious eutrophication. Such degree of the deterioration of eco-environment and water quality is a great threat to the ecological safety and sustainable socio-economic development of the southwest region of China.
This study adopts a series of Landsat images, including Landsat Multispectral Scanner (MSS) images with a spatial resolution of 57 meters taken in January of 1974, and Landsat Thematic Mapper (TM) images with a spatial resolution of 30

meters taken in January of 1988, April of 1998 and 2008. These images have been processed through geometric and radiometric correction. The Landsat MSS image of 1974 was resampled into 30 meters to maintain the consistency of the image's resolution in the time series. Furthermore, a high-resolution image in 2008 covering the main urban area of Kunming city was collected as the reference of field work, real Region of Interest (ROI), and extraction of land use/cover pattern. Classification maps of the Dianchi watershed in 1974, 1988, 1998, and 2008 were produced to be used in system calibration for SLEUTH. Then, six land-use policy scenarios were established for land-use policy decision-making in the Lake Dianchi watershed: 1, to inherit past land-use policy without changes; 2, to use the least land for ecosystem protection; 3, to establish three ranks of urban development area for controlling urban sprawl; 4, to mix ecosystem protection and urban development control; 5, to control urban sprawl for agricultural land protection; 6, to promote urban develop through multi-centers. These six land-use scenarios were produced respectively from 2008 to 2028 for every year using the calibrated SLEUTH system. The produced scenarios for year 2013, 2018, 2023, and 2028 were assessed using landscape metrics and fractal dimension. The results show that the fourth scenario not only controls urban sprawl but also keeps appropriate urban morphology for the Lake Dianchi watershed. Other land-use scenarios also show themselves urban development characteristics. This study testifies the feasibility and advantage of CA-based geosimulation system for land-use policy decision-making in a lake watershed.

# Cellular Automata Model for the Urban Growth of the Metropolitan Area of Concepción (CAMAC).

**D. MALDONADO[1]; A. GAJARDO[1]; \*C. ROJAS[2]; P.VALDEBENITO[2]; C. CANTERGIANI[3]**

[¤1]Department of Mathematical Engineering, University of Concepción
Casilla 160-c, Concepción, Chile
[2]Department of Geography, University of Concepción
Casilla 160-c, Concepción, Chile
[3]Department of Geography, University of Alcalá
C/Colegios, 2 – 28801 – Alcalá de Henares, Madrid - España
\*Corresponding author's contact information:
Carolina Rojas. Phone +56412207230 ; E-mail crojasq@udec.cl.

**Keywords:** Cellular Automata, Urban Growth, Model, Metropolitan Area of Concepción, GIS

**Abstract[¤]**

Cellular Automata (CA) have been intensively used in the last decades to simulate urban growth in cities. This is based on the fact that the suitability of a given location for built-up areas is highly dependent on the characteristics of the neighbouring locations, particularly on whether they are already urbanised or not.

CA and Geographic Information Systems (GIS) have recently become an instrument for modelling the temporal dynamics of urban areas. Nevertheless, they have not yet been extensively used in Latin American cities.

The prediction approaches for urban growth in cities are diverse. Some use probabilistic CA, while others define appropriate deterministic rules by hand, or use statistical tools to determine the CA transition rule, etc. Calibration parameters usually are the neighbouring radius, the random degree, or the influence of a given geographical feature. But up to our knowledge, the influence of the time scale, *i.e.,* the number of years that a single CA iteration represents, has not yet been studied. Since accumulative effects of the CA dynamics are relevant in the CA theory, we think it important to explore the CA effect on urban growth models in different time scales.

In the present work, we adopt the approach of Aguilera (2006), who runs a Geographical Logistic Regression to estimate the probability of a cell to become urbanised, and then it will urbanise only the most probable cells up to fill the real amount of surface growth. We repeat this methodology iteratively, in order to look at the CA effects. We apply it to predict the urban growth the Metropolitan Area of Concepción, Chile (MAC), from 2000 to 2009, and we compare the results.

Description of the model

---

[¤] This contribution has its references in an 'Author-Date' format.

As independent variables, we considered
- $x_1$: the density of the cell (people/m$^2$).
- $x_2$: the altitude of the cell (m).
- $x_3$: the number of urbanised neighbouring cells in 2000.

In a previous work by Rojas & Plata (2010), the selected geographical factors were distance to urban centres and roads, density and altitude; but a statistical analysis showed a strong correlation between the distance to urban centres and roads, and the number of urbanised neighbouring cells, which is an important variable for the CA models. The neighbourhood was chosen as the Moore's square neighbourhood, and the radius was determined by analyzing the error of the model for several different options, being 3 the most accurate.
The data was obtained by:

- Urbanised cells: by Landsat satellite images from 2000 and 2009.
- Density: from 2002 census blocks data.
- Altitude: from Digital Elevation Model (DEM).

The dependent variable is the binary variable: urbanised or not between 2000 and 2009.

From this data we ran a Geographical Logistic Regression with the software Matlab in order to obtain a formula for the probability of a cell to be urbanised [3].

$$p(x_1,x_2,x_3)=\beta_0+ \beta_1 x_1+ \beta_2 x_2+ \beta_3 x_3 \qquad (1)$$

The software produced the following values (only 5 digits showed).

$\beta_0$=-1.6717
$\beta_1$=0.0002
$\beta_2$=-0.0146
$\beta_3$= 0.1248

Then we computed the total number of urbanised cells in 2000 and 2009, $n_0$ and $n_T$, and consider a linear growth model for this quantity.

$n_t= n_0+ \alpha t$, for $t$ varying from 0 to $T$.

We repeated the following steps $T$ times:

1: compute the probability distribution through Eq.(1),
2: choose the $\alpha$ most probable cells,
3: add them to the urbanised cells, and
4: compute, for each cell, the new number of neighbouring urbanised cells.

We restricted the cellular space to the set of allowed cells. As a consequence, we discarded some urbanised cells belonging to a disallowed surface.

We applied the method in one, three and nine steps and we compared the results. The next figure illustrates our results.
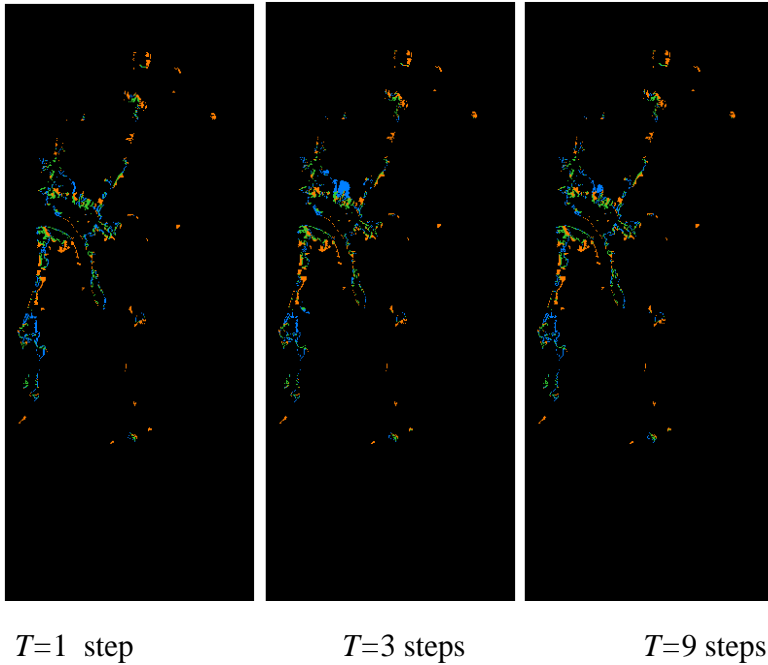


$T=1$ step $\qquad$ $T=3$ steps $\qquad$ $T=9$ steps

Figure 1. Comparison of actual and simulated urban area for three different values of T. Green colour represents the urban area which is correctly predicted; the urban surface which is not predicted appears in orange, and the blue colour is used for the wrongly predicted pixels.

As quality measure we have used the rate of correctly predicted cells over the total urban growth (success rate), and the areal fractal (Barredo et al., 2003; Tannier & Pumain, 2005). These indices are showed in the following table.

Table 1. Quality indices for the three experiments.

| *n* | 1 | 3 | 9 |
|---|---|---|---|
| **Success rate** | 46% | 50% | 51% |
| **Fractal dimension** | 1.3116 | 1.2908 | 1.2769 |

The figure and the table show how the success rate increases with the number of iterations, while the shape of the predicted urban area has smoother boundaries than the real one. The fractal dimension confirms this remark. We can see that this value decreases with the number of iterations, moving away from the real fractal dimension of the MAC urban area, which gives 1.3273 in 2000 and 1.3489 in 2009.

From ocular inspection, we see some orange persistent areas, which could be explained by the influence of variables that we had not used. Specifically, the *distance to roads* could explain the orange areas because these new urbanisations are entirely related to the tentacular model of growth. Blue areas which are wrongly predicted in the simulation on one step disappear when more steps are considered, because the highest number of steps are used, the smaller is the growth at each step, thus maintaining the new simulated cells near the urbanized area.

The use of a smaller time scale in the cellular automata model can reduce the error, but the present transition rule has a smoothening effect when applied iteratively. Maybe a similar study would give better result using other CA rules.

## References

Aguilera, F. (2006). Predicción del crecimiento urbano mediante Sistemas de Información Geográfica y modelos basados en Autómatas Celulares. Revista internacional de la ciencia y tecnología de la información geográfica, 81-112.

Barredo, J., Kasanko, M., McCormick. & Lavalle, C. (2003). Modelling dynamic spatial processes: simulation of urban future scenarios through cellular automata. Landscape and Urban Planning 64, 145-160.

Rojas, C. & Plata, W. (2010). Área Metropolitana de Concepción: Factores espaciales explicativos de su crecimiento urbano reciente (2001-2009) por medio de un Modelo de Regresión Logística Espacial. Actas I Congreso Internacional de Ordenamiento Territorial y Tecnologías de la Información Geográfica. 11 – 16 de Octubre de 2010, Tegucigalpa, Honduras. María Cristina Pineda & Joaquín Bosque Sendra (editores), Universidad de Alcalá, Obras colectivas Humanidades 26, Alcalá de Henares (España), 21 pág.

Maldonado, D. & Valdebenito, P (2012). Especificaciones y manual de usuario de GEOLAB. Informe Técnico Proyecto FONDECYT N11090163. Departamento de Geografía. Universidad de Concepción.

Tannier, C. & Pumain, D. (2005), Fractals in urban geography: a theoretical outline and an empirical example, Cybergeo: European Journal of Geography [en línea], Systèmes, Modélisation, Géostatistiques, article 307, Access: September 30th, 2012 URL : http://cybergeo.revues.org/3275

# The influence of the spatial scale in the applying CA models for urban land use change

## J. DÍAZ-PACHECO[1], H. VAN DELDEN[2], J. GUTIÉRREZ[3]

[1,2] Research Institute for Knowledge Systems (RIKS)
[1,3] Complutense University of Madrid
P.O. Box 463, 6200 AL Maastricht, The Netherlands
+31 (043) 350 1750, [1]jdiaz@riks.nl; [2]hvdelden@riks.nl;[3]javiergutierrez@ghis.ucm.es

**Keywords:** cellular automata, scale issues, sensitivity analysis, land use, dynamic modelling.

## Abstract

The problem of the modifiable areal unit (MAUP) is well known in geography and geostatistical analysis. The aggregation of the information in spatial units to build geographical models influences the final value assigned to these units. Raster models based on cellular automata are not free of this problem. In their application errors are introduced by aggregation the data and converting shape files into a regular grid. The choice for the grid approach, the selection of the cell size and the aggregation method used all influence the behaviour of the model and hence its simulation results.

In fact researchers concerned about the impact on analysis results of variation in spatial scale in cellular automata models have started to measure it. The objective of this study is to assess how spatial scale affects a dynamical urban land change model based on cellular automata. An application was developed for the Madrid metropolitan region using the Metronamica software. From a detailed land use geodatabase (1:5000) land use maps of three time periods (2000, 2006 and 2009) were available. This data was used to set up applications with a cell size of 25 m., 50 m., and 100 m., which were calibrated and validated, subsequently.

Calibration was performed based on an analysis of historic data (for the period 2000-2006) and expert judgement. Validation was performed over the period 2006-2009. In assessing the calibration and validation focus was given to the results as well as the shape of the interaction rules. To assess the results use was made of the Kappa Sim metric for the accuracy assessment of the locations and the Cluster - Size frequency distribution to assess the patterns of the urban clusters. To assess the shape of the interaction rules, we investigated the over and underrepresentation of land uses in the neighbourhood of locations that showed changes in land use between two periods. Comparing the measured over and underrepresentation against the simulated over and underrepresentation helps to fine-tune the interaction rules and assess the modelled process by looking at the agreement between both analyses. As part of the sensitivity analysis to test the impact of the selected scale, the following steps were conducted:
1.  Calibration of the application at 50 m.

2. Application of the neighbourhood rules obtained during the calibration under 1 to the applications using 25 and 100 m. resolutions and assessing the results.
3. Fine-tuning the calibration of the application at 25 m.
4. Application of the neighbourhood rules obtained during the calibration under 3 to the applications using 50 and 100 m. resolutions and assessing the results.
5. Fine-tuning the calibration of the application at 100m.
6. Application of the neighbourhood rules obtained during the calibration under 5 to the applications using 25 and 50 m. resolutions and assessing the results.

This analysis provides us with two types of information. Firstly we can evaluate at what resolution an application for Madrid obtains the best calibration and validation results (using information from steps 1, 3 and 5). Secondly we can evaluate the sensitivity of a rule set calibrated for a specific resolution to a different resolution. The presentation will focus on the process and the results of this study.

# An iterative economic residential choice ABM of urban growth in Luxembourg

## Geoffrey, CARUSO[1]; Cyrille MEDARD DE CHARDON[2]

[1]University of Luxembourg
Route de Diekirch, L-7220 Walferdange, Luxembourg
+352 46 66 44 6625, geoffrey.caruso@uni.lu (correspondent author)
[2] University of Luxembourg
Route de Diekirch, L-7220 Walferdange, Luxembourg
+352 46 66 44 9757, cyrille.medarddechardon@uni.lu

**Abstract**

We present a residential choice simulation for localizing existing ($P_0$) and future ($P_1$) household agents within the Grand Duchy of Luxembourg. MOEBIUS (MObilities, Environment, Behaviour integrated in Urban Simulation), a multi-institution project, aims to simulate Luxembourg's future (2025 / $T_1$) urban development across multiple policy driven scenarios. This presentation focuses on distributing existing populations ($P_0$ at $T_0$) and locating future growth ($P_1$ at $T_1$).

Luxembourg is experiencing rapid growth, high housing prices, large numbers of daily cross-border commuters and extensive road congestion. Recent urban growth has intensively consumed arable land in locations that road infrastructure is struggling to support. In this context our research partners upstream are providing spatial and synthetic population data for our work in determining urban population distributions, which we provide to our downstream partner to model potential future commuting and congestion patterns. This analysis flow is applied to integrated (sustainable) development, business as usual and pro-growth scenarios ($S_{1-3}$).

Localization of $P_0$ agents at $T_0$ is dependent on spatial attributes determined through a cellular automata (CA) kind framework and network distance accessibility. A synthetic population [1] containing 170,000 active (employed) agents within 110,000 households provides the data from which to determine agent location preferences. Households and individuals are allocated using an economic residential choice agent-based model, inspired from Caruso et al. [2] and adapted to heterogeneous households and finite population sets. This process is replicated at $T_1$ with population growth, $P_1$, across multiple scenarios, $S_{1-3}$, using more complex methodologies.

Agent placement is dependent on four factors: Spatial attributes, network accessibility, agent preferences and the remaining agents in the synthetic population.

Spatial attributes (e.g., green space, urban and population density) are calculated using neighbourhood functions. Accessibility is based on road network distance to services and work destinations. The economic residential choice model allows agents, based on their preferences, to weigh tradeoffs, such as distance to work, urban density and proximity to green spaces, in terms of utility in order to bid. The residential model uses a market clearing method adapted from Fujita [3], applied recursively across households groups, in order to generate agent locations, rents, and utility levels.

The implantation of future urban growth agents brings new challenges. Areas available for growth of various densities have been processed into empty residences arranged in an irregular spatial structure. The residences are then filled on demand by agents. We created the new residences using a recursive CA space filling algorithm. While initial population, $P_0$, are specified at communal scale, $P_1$ forecasts are national. In order to provide a balanced future population distribution we performed regressions on urban indicators that impact residential price and extracted communal residuals for the predictive model. We have also implanted a congestion model provided by our downstream partner based on our $T_0$ output to improve accessibility attributes. Although these new factors created new attributes and considerations for agent preferences, the economic model and market clearing mechanism remained the same. The final synthetic population allocation for each scenario shows spatial variations in rent and utility as well as differences in socio-economic class well-being.

This document is a template with the rules that must be considered for submitting a short paper to CAMUSS. The short papers will be peer-reviewed by the Scientific Committee of the Symposium. Authors of a selection of short papers will be invited to submit full papers that will go through a peer-review process and will be published in the associated journals. Short papers must follow the rules described to guarantee a high quality of the book of proceedings. Each short paper must not exceed 4000 words due to editorial reasons, including title, authors and their affiliations, and references. Page size must be A5 with the following margins: 2 cm on top, bottom, left and right. Title must be in Times New Roman bold, 14pt, centered. Authors must be listed with their names in Times New Roman bold, 10pt, and remaining information in Times New Roman, 8pt. The correspondent author must be clearly identified. Figures, maps, and tables should be kept to a minimum and identified in the document with proper caption and must be referenced in the body of the text. The maximum number of keywords is 5, written in Times New Roman, 9pt, left aligned.

The organizers will refuse short papers if they do not comply with this template.

## References

[1] Cornelis E., L. Legrain, P. Toint (2005), Synthetic populations: a tool for estimating travel demand. In Proceedings of BIVEC-GIBET Transport Research Day 2005, Vol. I, VUBPRESS Brussels University Press, pp. 217-235

[2] Caruso G., D. Peeters, J. Cavailhès, M. Rounsevell (2007), Spatial configurations in a periurban city. A cellular automata-based microeconomic model. Regional Science and Urban Economics, 37(5), pp. 542-567

[3] Fujita, M. (1989), Urban Economic Theory: Land Use and City Size. Cambridge University Press, Cambridge

# Reticular automata models: using non-regular neighborhoods to simulate segregation

## D. MORENO[1]; D. BADARIOTTI[2]; A. BANOS[3]

[1] ESPACE, UMR 6012, Université Nice Sophia Antipolis /CNRS
[2] Image, Ville, Environnement, ERL7230, Université de Strasbourg/CNRS
[3] Team PARIS, Géographie-Cités, UMR 8504 Université Paris 1/CNRS
arnaud.banos@parisgeo.cnrs.fr

**Keywords:** Network, Reticular CA, Segregation

## Abstract

An important issue in CA modeling is the impact of neighborhood structure on automaton dynamics. The Schelling's spatial proximity segregation model [1], [2] can be used to analyze this influence.

Schelling illustrated the emergence of a highly organized phenomenon, segregation, from the combination of individual behaviors based on a demand of similar neighbors. By varying neighborhood size, Schelling explained that the tendency to segregate is more attenuated in largest neighborhoods than in smallest one's, because satisfactory patterns are more easily found. Laurie & Jaggi [3] showed that this is true at intermediate levels of individuals demand. On higher levels of demand, an increase of the neighborhood size produces an increase in non-satisfied individuals, so the model stabilizes later and the final pattern is more segregated.

More recently, graph-based (or reticular automata) has been used to include non-regular neighborhoods in automata. In these models the regular lattice of cells is replaced by a graph describing the complexity of proximity relationships in urban environments [4], [5], [6], [7]. This relaxation of cellular automaton definition permits to integrate the anisotropy of urban space due to the spatial configuration of buildings and the transportation networks in local-scale studies.

SMArtSegreg model [8] was implemented to test the Schelling model in different theoretical graphs. Simulation results reveal that presence of cliques attractors in networks. Hierarchical networks, like scale-free or fractal networks are more likely to allow segregative structures at low-levels of individuals demand than regular or random graphs.

Remus model [6], [7], permits to include real urban patterns and road accessibility in a graph-based cellular automaton. The model replaces cells by buildings polygons in the cellular automata and it creates neighborhood graphs, based on road network accessibility between buildings, that are used to define their neighborhoods. Simulations on real urban patterns show that dense areas reach stable configurations later than sparse one's, confirming Schelling's and Laurie and Jaggi's hypothesis. But results show also that urban structure seems to have a strong influence on the spatial distribution of population clustering. The main crossroads, corresponding to the best-connected nodes in urban graph, represent attractors for clustering: buildings in the crossroads proximity are more connected, and aggregate in larger

clusters. Segregation dynamics are controlled by poorly connected zones separating well-connected ones.

This two models reveal the fact that segregation dynamics depends on the size of neighborhoods, but also in the spatial distribution of neighborhood sizes. This conclusion can be used by urban planners to conceive less segregative urban patterns. Reticular automata are useful tools to improve comprehension of phenomena constrained by proximity effects, like intra-urban processes.

## References

[1]    Schelling, T.C. (1969), Models of Segregation, American Economic Review, Papers and
       Proceedings, 59-2, 488-493
[2]    Schelling, T.C. (1971), Dynamic Models of Segregation, Journal of Mathematical Sociology, 1: 143-86
[3]    Laurie A.J.; Jaggi N.K. (2003), Role of 'Vision' in Neighbourhood Racial Segregation: A Variant of the Schelling Segregation Model. Urban Studies, 40, 13: 2687-2704
[4]    O'Sullivan, D. (2001), Exploring spatial process dynamics using irregular cellular automaton models, Geographical Analysis, 33(1): 1-18
[5]    O'Sullivan, D. (2001), Graph-based cellular automata: a generalised discrete urban and regional model, Environment and Planning B: Planning and Design, 28(5): 687-705
[6]    Badariotti D., Banos A., Moreno D. (2007), Conception d'un automate cellulaire non stationnaire à base de graphe pour modéliser la structure spatiale urbaine: le modèle Remus", Cybergeo, Sélection des meilleurs articles de SAGEO 2006, article 403
[7]    Moreno D., Badariotti D., Banos A. (2009), Graph based automata for urban modeling, in Handbook of Theoretical and Quantitative Geography, François Bavaud and Christophe Mager (dir.), FGSE, University of Lausanne, Lausanne, Switzerland, p.261-309
[8]    Banos A. (2012), Network effects in Schelling's model of segregation: new evidences from agent-based simulation, Environment and Planning B, Volume 39, n°2, 393 – 405

# Scalarity of local interaction in cellular automata models

## Sanna ILTANEN[1]; Anssi JOUTSINIEMI[2]

[1] Researcher, M. Arch., School of Architecture, Tampere University of Technology
PO BOX 600, FIN-33101 Tampere, Finland
+358 40 8490447, sanna.iltanen@tut.fi

[2] Associate Professor, Dr. Tech., M. Arch., School of Architecture, Tampere University of Technology
PO BOX 600, FIN-33101 Tampere, Finland
+358 40 5896223, anssi.joutsiniemi@tut.fi

**Keywords:** local interaction, cellular automata, gravitation, fractality, accessibility

## Abstract

The ambiguity of the spatial entitation is a fundamental issue in cellular automata models (CA). However, theoretical approaches to the issue are quite rare. This paper presents a new approach to local interaction in cellular automata models that links the theories of gravitation, accessibility, fractality and space syntax. In classical cellular automata (CA), spatial relations are defined through neighbourhood definitions, which determine the spatial structure of the CA system. In applied CA, strict definitions of neighbourhood in "pure" CA are often relaxed, but no extensive/uniform theoretical formulation has been presented on the means of relaxations. Typical relaxations include statistical rules used in larger neighbourhoods and macro-level spatial constraints, which are based on econometric models. This paper discusses how these different methodologies defining spatial relations can be applied to the interaction in cellular spaces. We suggest that a generic framework of spatial separation can be formulated by exploiting well-established spatial theories in order to strengthen the theoretical basis of implicit assumptions in the neighbourhood definitions of CA models.

By definition, local interaction creates another theoretically challenging issue; namely, the scalarity of the spatial interaction, how the interactions of different scales can be included in one model, and exactly how "local" the local activity really is. The fractal nature of urban networks can be a key to the interaction between the spatial networks of different scale levels. Certain spatial entities intuitively seem very "natural" from the CA model perspective (such as houses, lots or blocks), but the question remains as to whether they are suitable objects for describing the interactions of all levels. The ontological ambiguity becomes more obvious when we observe any model that manipulates larger region-based information. While the geometrical definition of a region is trivial, its corresponding geographical counterpart is far from that. Regions are formed on the basis of similarity of observed phenomenon, but the similarity-norm to create crisp entities does not automatically fit with the aggregation.

In terms of spatial separation, the long tradition of gravitation models defines the distance decay between the spatial entities. The gravity measure takes into account population or other attractive features of urban environment. There is a clear need to identify more sophisticated methods of forming the spatial representation other than abstract tessellation, such as rectangular or hexagonal grid, in order to achieve more sensitive results of the simulation. The paper discusses the extension potential towards a few classic theories that are all implicitly attached to neighbourhood and scale.

The best known examples of the spatial relativity phenomenon are gravitation models and their derivatives, which are more generally known as Spatial Interaction Models. The key idea and importance to geography of these models are expressed in the so-called Tobler's law, which states: "I invoke the first law of geography: Everything is related to everything else, but near things are more related than distant things"[1]. The same principle is behind concepts such as the attractiveness of the space, the friction of space or distance decay. Joutsiniemi [2] recently observed this principle in a crisp, street segment-based network model. Joutsiniemi also showed that the configurational approach of the so-called "space syntax school" [3] has similarities with gravitation models and how this can be interpreted as generic spatial accessibility.

The current paper presents an experimental sample model that uses the cellular space derived from a disaggregated transportation network instead of grid tessellation. The interaction in the model is based on the dynamically changing neighbourhood definitions. The disaggregated data and relaxed neighbourhood definitions enable the use of CA framework in a more concrete way and more realistic interaction rules. The restrictions set by the computational capacity to use more and more disaggregated data are gradually dying out. They are being replaced by an expanding variety of different parameter combinations that cannot be tested, not because of the capacity itself but because of the capacity of the model user to handle the variety of simulation results. This heightens the importance of the selection of parameter combinations.

## References

[1]  Tobler, A. (1970), A computer movie simulating urban growth in the Detroit region. Economic Geography. Vol. 46, pp. 234-240.
[2]  Joutsiniemi, A. (2010), Becoming metapolis - A configurational approach. Datutop Vol. 32.
[3]  Hillier, B., Hanson, J. (2011), The Social Logic of Space, Cambridge University Press.

# Exploration and exploitation in urban growth models

Optimizing CA-based urban growth models using a memetic algorithm

## William VEERBEEK[1,2]; Taneha BACHIN[1,2,3]; Chris ZEVENBERGEN[1,2]

1Flood Resilience Group, Dep. Water Science and Engineering,
Westvest 7, 2611 AX, Delft, Netherlands
+31 15 2151844, w.veerbeek@floodresiliencegroup.org
2Hydraulic Engineering, Faculty of Civil Engineering and Geosciences,
Delft University of Technology, Stevinweg 1, 2628CN, Delft, Netherlands
3Department of Urbanism, Faculty of Architecture, Delft University of Technology
Julianalaan 134, 2628BL, Delft, Netherlands

## Abstract

During the past century, spatially explicit urban growth models (UGM) have evolved from regional economic models, Markov-Chain driven probability matrices to machine learning driven cellular automata (CA) based models. Machine learning driven CA-based UGMs use supervised learning algorithm to optimize land use transition rules using regression techniques on historic geographic data. Although this method has achieved significant improvements during validation, the applied machine learning algorithms are often specifically designed to operate within the domain of urban simulations. Many UGMs that incorporate neural networks, support vector machines or genetic algorithms to 'learn' underlying rules of geographic pattern formation are 'off-the-shelve' products that are not especially optimized to deal with the specific constrains posed by within an UGM context. One of the major problems is the large number of candidate solutions provided by the algorithms needed for optimization. This is often due to the fact that many machine learning algorithms excel at exploration (searching through the search space) but show limited effectiveness in exploitation (finding local optima). For instance, to reach a satisfactory level of accuracy, a standard genetic algorithm requires an extensive population of differently parameterized UGMs in combination with a large number of iterations. Since, CA based UGMs for large metropolitan areas often consist of 10s of millions of individual cells, the validation sequence for an individual growth model that defines the model's fitness (e.g. kappa coefficient based similarity indices) is computationally expensive. This often limits the systematic development UGMs.

In search of higher levels of accuracy, in the past years CA based UGMs have been extended by agent-based models that mimic urban metabolic flows as well behavioural aspects of urban dwellers (e.g. traffic models). Although this might

seem intuitive, this also increases the model's complexity, the subsequent control and manageability. Yet, CA based models often do not exploit implicit patterns, rules and potential correlations that can be found within the geographic data used to drive CA based models. While it is fairly common to incorporate static morphologic data (e.g. elevation, slope), infrastructure related data (e.g. proximity to main roads) as well as other explicit urban drivers for growth, the use of 'hidden structures' like for the distribution of urban cluster locations are often limited. Yet, these 'hidden patterns' might provide additional information that improves the accuracy of the UGMs.

For this study we developed a so called memetic algorithm; a combination of a standard genetic algorithm and a local search 'hill climbing' function. While the genetic algorithm is used for the exploration of the search space using common techniques like arithmetic recombination and mutation, the 'hill climbing' algorithm searches for local optima by improving the candidate solutions (i.e. exploitation). In practice, this means that all candidate UGMs are optimized to provide the 'best' solution within a local search space. The model has been developed using the Dinamica-Ego platform for dynamic GIS and has been applied to greater Beijing, CN. Dinamica-EGO provides a Bayesian probability based 'weight-of-evidence' methodology to regress land cover transition rules. The model provides two constrained CA-based cell transitional modules: the 'expander' and 'patcher'. While the expander develops land patches from existing land cover classes (i.e. mimicking urban extension) the 'patcher' initiates disconnected land cover transitions (i.e. leapfrogging development). The modulation of growth rates for the two modules is controlled by a third module. All three modules require substantial parameterization. The optimization of the parameters is controlled by the mimetic algorithm. Apart from a set of common thematic layers (e.g. slope, proximity to infrastructure), the model uses a set of dynamically generated layers; during each iteration, a urban cluster analysis is performed that is used as input for the next iteration. An additional problem encountered during model development was caused by the independency of transition rules. While the model uses three land cover classes to identify urban areas (i.e. low, medium and high density built-up areas) the transitions to and between these classes were treated independently. Although high levels of accuracy were achieved during the validation stage, future projections showed extensive urban sprawl that did not comply with intuition or perceived growth trends. To overcome this problem, the model has been divided into 2 stages. During the first stage a so-called 'urban envelope' is calculated for prospective years. In the second stage the model diversifies the urban development into the three urban classes using the envelope as a growth extent.

The outcomes of this approach show significant improvement over the existing baseline model; the combination of using a memetic algorithm and the information provided by dynamic maps further increases the accuracy during UGM validation. The 2-stage approach on the other hand produces consistent growth scenarios for future years.

# Natural Hazards Impact and Urban Growth

Legitimacy and urgency for connecting urban growth models to natural hazard impact assessment

## William VEERBEEK[1,2]; Assela PATHIRANA[1]; Chris ZEVENBERGEN[1,2]

[1]Flood Resilience Group, Dep. Water Science and Engineering,
Westvest 7, 2611 AX, Delft, Netherlands
+31 15 2151844, w.veerbeek@floodresiliencegroup.org
[2]Hydraulic Engineering, Faculty of Civil Engineering and Geosciences,
Stevinweg 1, 2628CN Delft, Netherlands

**Keywords:** urban growth modelling, natural hazards, impact assessment, floods, business as usual

## Introduction

Over the past 30 years, a substantial body of scientific work has been developed in spatially explicit urban growth modelling. Using historical land use and land cover data as validation, the current-state-of-the-art in urban growth modelling uses sophisticated machine learning algorithms to 'learn' site-specific urbanization patterns in order to develop scenarios for future urban development. Although the accuracy of these models has reached a high standard, actual application of these models in strategic urban growth policies, urban containment and/or urban zoning and master plans is still limited. One could argue that urban growth models are facing a challenge in legitimacy; model outcomes are often treated with suspicion by city planners and other institutions involved in the urban planning. This is to some extent due to the inherent uncertainty associated to the development of drivers (e.g. local GDP growth, population changes) as well as constrains (e.g. top-down planning policies). Since the majority of urban growth models focus on the extrapolation of historic urban growth patterns into the future one could argue that model outcomes can be considered as Business-As-Usual (BAU) scenarios in the urban development domain.

During the past decades, the impact of natural hazards (e.g. flooding, drought, heat stress) on metropolitan areas exceeded all expectations. Climate change is likely to further exacerbate the frequency and intensity of natural hazards and their consequences. In natural hazards research, BAU scenarios are generally used to identify a long-term baseline from which the effects of climate change scenarios as well mitigation and adaptation policies are quantified. Within this domain, there is an increased awareness that the majority of natural hazard impacts are linked to urban growth and (the lack of) long term urban planning policies. Urban growth increases the exposure (e.g. increased concentration of people and assets located in flood prone areas) and sensitivity (e.g. slumification) of urban areas to natural

hazard impacts but also acts as a driver (e.g. increased surface runoff and precipitation).

To assess the impact of urban development, there is an increased demand for urban growth modelling in both the natural hazard research community and the environment agencies of local, regional and national governments. Within the fields of flood management, water resource management, heat impact assessment as well as urban climate mitigation and adaptation, insights into long term urban development are vital to develop robust 'climate-proof' urban policies. Since many stakeholders within these domains are familiar with uncertainty management, the intrinsic uncertainties within the domain of urban growth modelling are not necessarily treated with suspicion. On the contrary, the outcomes of urban growth modelling are embraced and treated as they should: as potential development scenarios instead of predictions. In that respect they are used as discussion support platform to better assess the consequences of long term strategies and 'what-if'-scenarios.

In this paper we will present three domains in which future natural hazard impact assessment and urban growth modelling are combined. The first project covers the impacts of urban growth on flooding in expanding megacities: Beijing, CN, Dhaka, BD and Mumbai, IN. For all three cities, constrained urban growth models have been developed that cover a mid-term horizon (2060). The urban growth models are connected to hydraulic and flood impact assessment models to identify future flood prone areas and changes in the subsequent impacts. Depending on the outcomes, alternative 'water-sensitive' long term urban development plans are developed that safeguard these cities against future flooding. The second project focuses the interaction between urban growth and changes in local precipitation for large metropolitan areas. Recent meteorological research shows that local changes in (monsoon driven) precipitation are strongly related to the intensity and extent of the urban heat island effect that most metropolitan areas suffer from. The study showed increasing extreme rainfall events as a consequence of urban growth for the city of Mumbai, IN, for a horizon of 50 years. Since Mumbai is already suffering from severe urban flooding, this evidence urges for a controlled urban development (currently 60% of Mumbai's population lives in slums) to at least maintain flood hazards at the current level. The last project evaluates the effects of future urban growth on the water quality and pollution loads in Lagos, NG. As the fastest growing megacity in Africa, Lagos is severely suffering from poor sanitary conditions that cause increasing stress on streams and rivers. Since more than half of the population lives in slums, the subsequent pollution loads significantly impact the local water quality and ecosystem. Due to urban growth, this trend will also expand to streams currently used as grey and black water drains. Since the surface water in Lagos is used extensively by the local population, the consequences of urban growth and the lack of good sanitation facilities might lead to immense strain on local resources and inhabitants and render the problems to an unmanageable scale.

# CA Apllied to Spatial Simulating Models in (LULUC) Multi-Temporals Images.

CA Applied to Spatial Models (LULUC)

## SUAREZ, A. F[1], CANDEIAS, A. L. B. [2]

[1]Federal University of Pernambuco - UFPE
Av. Acadêmico Hélio Ramos, s/n, CEP 50740-530, Cidade Universitária, Recife-PE, Brasil
+55 81 9809-5827, alerson.falieri@gmail.com
[2] Federal University of Pernambuco - UFPE
Av. Acadêmico Hélio Ramos, s/n, CEP 50740-530, Cidade Universitária, Recife-PE, Brasil
+55 81 2126-8981, analucia@ufpe.br

**Keywords:** Cellular Automata, Spatial Modeling, DINAMICA-EGO, Land Use, Land Use Change, LULUC

## Abstract

The man-made processes, boosted by the increasingly worldwide need of food, fiber, water and shelter, rule the changes of use and land cover [1]. The deforestation causes the loss of biodiversity and causes possible weather impacts [2]. With the valuation of natural resources, know its allocation in both spatial location and time and know how they interact in space is fundamental to create aid mechanisms to decision taking as well as planning future development [3].
The spatial modeling simulation help understand the causing mechanisms and development processes of environmental systems [4]. The spatial modeling simulation based on Cellular Automata (CA) have been used for assessing complex environmental issues, such as estimate pathways and impacts related to the greenhouse gases emissions [5], [6], integrated modeling of population, employment and land-use change [7], land-use change [8], predict possible trends in deforested areas, pastures and forests [9], among others [10].
This study proposes the development, calibration and outcomes analysis of a dynamic spatial modeling simulation Land Use, Land Use Change (LULUC), taking into consideration a time period, 1986, 2000 and 2008 ($t_1$, $t_2$ and $t_3$, respectively) where $t_3$ is used to assess quality of the simulated map from $t_2$. Work is focused on reduction rate of the forest remaining of Atlantic Rainforest of the Brazilian Municipality of Maragogipe located at 82 miles east of the State Capital Salvador in the State of Bahia. For so, a modeling platform was used (freeware) based on (CA) DINAMICA-EGO (http://www.csr.ufmg.br/dinamica).
Medium and high resolution satellite images were researched and purchased (Landsat-TM and CBERS-2B, sensor CCD; HRC) and other cartographical bases correlated to the study area. Information was cataloged according to its source, homogenized, and defining the work unit: degrees, cartographic and geodetic references, by performing conversions and geo-referencing if applicable. Satellite images were processed to equalization histogram and radiometric. They were classified by using the supervised method and the Bhattacharya algorithm. The

following classes were identified: rainforest, mangrove, grassland, regrow, urban areas and others. The thematic precision was assessed with the aid of 300 points acquired in technical visit and by high resolution images analyses, in both cases defined at random. The descriptive statistics of global accuracy reached the 89% ratio and the Kappa inter-rater agreement: 0.864 number that represents a high acceptance level according to scale suggested by Congalton and Green [3]. The classes were grouped in rainforest and non-rainforest.

Basically, the model was structured in the software, based on a simulation model suggested by Soares-Filho *et al.* [12]. An initial map ($t_2$) has its classes changed according to change rate "Transition Matrix" (TM). TM is the total amount of change for each land cover transition type of the maps classified, taking into account the time period of the simulation through a cross-tab operation. Such changes happen in the most likely areas, defined by the likelihood map, resulting from the calculus of Weights of Evidence (WofE). WofE are the local odds of a transition land use classes taking into account a range of spatial variables by stochastic methods, Bayesian statistical or conditional probability. The spatial variables were: altitude, slope, soil conditions, conservation areas, distance to major rivers, distance to small rivers, distance to urban patches, distance to roads, distance to deforestation, and distance to protected areas. In this study, analyzed transition was transformation of forest in deforested areas (deforestation). Stains of change (landscape disturbance) happened in quantity in accordance with TM and had their rate of appearance or aggregation according to the values arbitrated to certain software function operators, as well as the isometrics of stains. Applied to changes, the resulting landscape map was saved at every step of the model and retro-fed as initial map in the next step until reaching a compatible time variation with $t_3$, by making possible the validation of outcomes. Validation was performed by calculating the similarity between the simulated map and the real map ($t_3$) based on fuzzy logic, applied to a context of pixel vicinity, by means of an exponential decay function with an 11-pixel-window.

By visual analysis (Figure 1), it was noted that the heuristic process was successfully designed, as the deforestation standard was respected and are congruent with the local probabilities according to the likelihood map. The similarity reached by comparison between the model outcome and the real map ($t_3$) was 46% of minimal similarity and 77% of maximal similarity.
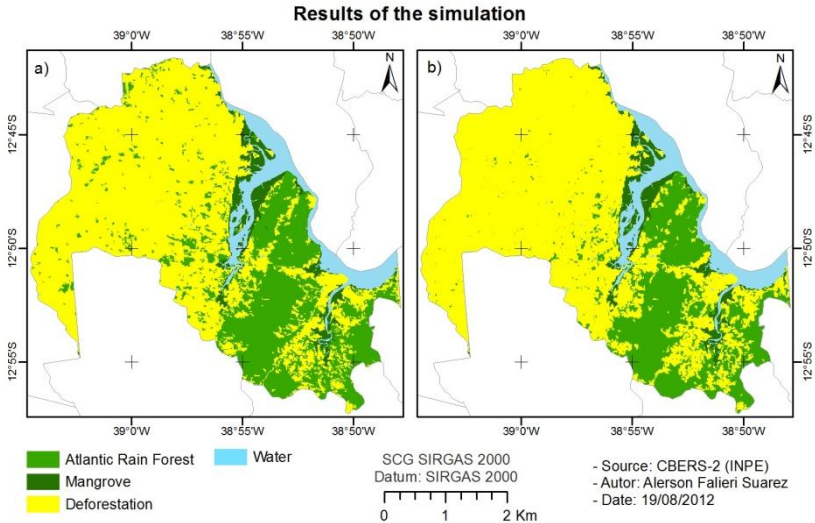
**Results of the simulation**



Figure 1: Results of the simulation: a) 2008 observed, b) 2008 simulated.

The outcomes reached in this paper show that the spatial model implemented and the software utilization, which use the methodology based on CA is a good tool for the analyzes of environmental complex systems and have robust potential to generate predictive or previous analyses within the ambit of LULUC studies, and the reliability level may also be assessed.

We thank Instituto Perene ("Perene Institute") for granting the data used for this study.

### References

[1] Foley, J. A., Defries R., Asner G. P., Barford C., Bonan G., Carpenter S. R., Chapin F. S., Coe M. T., Daily G. C., Gibbs H. K., Helkowski J. H., Holloway T., Howard E. A., Kucharik C. J., Monfreda C., Patz J. A., Prentice I. C., Ramankutty N., Snyder P. K, (2005), Global consequences of land use. Science, Vol. 309, pp. 570–574

[2] Metz, B., Davidson, O. R., Bosch P. R., Dave, R., Meyer, L. A. (2007), Contribution of Working Group III to the Fourth Assessment Report of the Intergovernmental Panel on Climate Change. In: IPCC Fourth Assessment Report: Climate Change. Cambridge University Press, Cambridge, United Kingdom and New York, NY, USA

[3] Congalton, R. G., Green, K (2009), Assessing the accuracy of remotely sensed data: principles and practices. Lewis Publishers, New York

[4] Rodrigues, H. O., Soares-Filho, B. S, Costa, W. L. S. (2007), Dinamica EGO, uma plataforma para modelagem de sistemas ambientais. In: Simpósio Brasileiro de Sensoriamento Remoto, 13. Instituto Nacional de Pesquisas Espaciais (INPE), São José dos Campos, SP., pp. 3089-3096

[5] Soares Filho, B. S., Nepstad, D, Curran, L., Voll, E., Cerqueira, G., Garcia, R. A., Ramos, C. A., Mcdonald, A, Lefebvre, P., Schlesinger, P. (2006), Modeling conservation in the Amazon basin. Nature, Vol. 440, pp. 520-523

[6]  Soares-Filho, B. S., Dietzsch, L., Mountinho, P., Suarez, A. F., Rodrigues, H., Pinto, E., Maretti, C., Suassuna, K., Scaramuzza, C. A., Vasconcelos, F. (2010), Protected Areas Helping to Reduce Carbon Emissions in Brazil. In: Arguments for Protected Areas - Multiple Benefits for Conservation and Use. London, Washington DC: EarthScan, Vol.1, pp. 205-218.

[7]  Wite, R., Uljee, I. Engelenb, G. (2012), Integrated modelling of population, employment and land-use change with a multiple activity-based variable grid cellular automaton. International Journal of Geographical Information Science, Vol. 26, pp. 0-30

[8]  Suarez, A. F., Soares-Filho, B.S., (in press). Aplicação de um modelo para estudo da mudança de uso e cobertura do solo na bacia do Rio Formiga – MG. Revista Brasileira de Cartografia. Vol. 65/2

[9]  Gonçalves, R. M., Centeno, T. M., Candeias, A. L. B (2011), Autômatos celulares aplicados na modelagem de tendência em imagens multi-temporais. Revista Brasileira de Cartografia. Vol. 63/2, pp. 233-241

[10] Schiff, J. L. (2008), Cellular Automata: a discrete view of the world. A John Wiley & Sons, INC. USA

[11] Soares-Filho, B. S., Rodrigues, H., Costa, W. (2009) Modeling Environmental Dynamics with Dinamica EGO. Available at:
<http://www.csr.ufmg.br/dinamica/tutorial/Dinamica_EGO_guidebook.pdf>   Accessed: 27/04/2012

# Simulation platform by cellular automata based on spatial knowledge rules. Application to urban growth

## Edwige DUBOS-PAILLARD[1], Patrice LANGLOIS

[1]Université de Franche-Comté, Laboratoire ThéMA,
32, rue Mégevand, 25030 Besançon Cedex, France;
+33667013062;edwige.dubos-paillard@univ-fcomte.fr

## Abstract

Our reflections and the numerous works concerning the city, its planning and its transformations, showed all its complexity. The overall process of spatial development of the city system results from the interaction of social, political and economic factors, some being activators of its development and others inhibitors. In front of such a complexity and such a profusion of factors, it is difficult to produce a rigorous explanatory theory. Hence, in a parsimony perspective, we make the central hypothesis, that comes true rather widely through the simulations, that the great majority of the factors which pilot urban development are linked to processes that have spatial designs which reveal them. More exactly, urban processes (as sub-urbanization, large housing estates construction, business park development, etc,) are appearing from specific spatial configurations but are also producing characteristic spatial patterns.
Rather than producing a fine spatial analysis which tries to isolate the contributory factors, that is almost impossible because of their intricacy, we adopted a constructive approach by developing SpaCelle. This cellular automata platform obliges the modeller to a certain conceptual parsimony. It was developed on urban growth issues; nevertheless, it remains very general and can be used in other research fields concerned by spatial dynamics. SpaCelle is based on a classical cellular automata paradigm which means that each cell is only reactive. Indeed, contrarily to a more general agent based model, at each iteration a cell cannot do anything other than change its internal state from its previous state and that of its neighbours. Therefore, no flow can be modelled. This means that we can't modelize interactions since it requires a simultaneous exchange between two or more cells. In addition, the use of the platform requires no computer skills: a one click installation, graphical interface, no algorithmic programming. The dynamic model is defined by a list (unordered) of transition rules close to the natural language which permits to test explicit hypotheses of evolution of land use. The user must first build an initial spatial configuration by importing the different layers containing geographical data (grid for the land use or the topography, vector layer for networks, etc.). Then he has to build the base of knowledge of the cellular automata which defines the different states in each cellular layer and the dynamics of the model using two kind of

transition rules: environmental rules and life rules. These rules reflect the spatial aspects of processes in action. They are at every moment and in every place in competition with each other. It can thus handle the complexity of influences and constraints, often antagonistic that are overlapping in space. An important feature of this type of modelling comes from the verbal aspect of the formulation of the dynamic model, which provides by construction, an explanatory aspect by induction. Indeed most of the urban growth models are based either on deterministic dynamics that adjusts series of evolution curves or action curves according to the distance (as a potential), or on stochastic laws as Markov chains, methods that are not directly explanatory.

The cellular automata SpaCelle helped to enlarge and further improve our reflection on the city construction. The modelisation was applied to the Rouen area. The reflection was carried out from two directions.

The first, based on a retro-simulation approach, led to a model that improved the general understanding of urban dynamics during the second half of the twentieth century. We identified some ten processes, more or less old, that have animated urban spaces since the Second World War. It was validated using different methods.

The second, based on a prospective approach, aims at assist management of urban areas. It compares the simulations of different scenarios proposed by policy makers and local planners for 2025. Prospective scenarios were realized using the retro-simulation model, on which alternatives scenarios were constructed. The results of these scenarios were discussed with city planners who could appreciate visually some possible effects of the different political orientations.

Finally, the platform SpaCelle is not limited to the urban growth issues; it permits to simulate a wide variety of situations from the game of life to the spatial spread of epidemics, through ecological or climatic models.

# A chronological overview of cellular automata models for urban and spatial systems

## Nuno N. PINTO[1]; Jenni PARTANEN[2]

[1]Department of Civil Engineering, University of Coimbra
R. Luis Reis Santos Pólo II da Universidade, 3030-788 Coimbra, Portugal
+351 239 797 106, npinto@dec.uc.pt (correspondent author)
[2]Tampere University of Technology
School of Architecture
Urban Planning and Design
POB 600, 33101 Tampere, FINLAND
+358405184405, jenni.partanen@tut.fi

## Abstract

Literature reviews are key components for understanding the scientific progress of a research subject. They tend to be organized on a chronological way, but the large majority of them, if not all, focus on the features and details of the subjects, regardless of their chronological evolution. These perspectives may lose some important issues that had contributed for this evolution, in particular those regarding the technological and socioeconomic contexts, in which the subject was considered as valid and pertinent both for research and for practical application. This is increasingly more important when we are dealing with models of any sort. Models are intended to be controlled, affordable, understandable, and safe test beds for experimental research about more complex systems. For this reason, there is a very close connection between the needs and the context of societies and technology and the research made using models, a discussion somehow present in the famous papers of Douglass Lee [1, 2] and, more recently, in Helen Couclelis thoughts about the use of integrated models [3]. This presentation focus on an historical timeline for the research and application of cellular automata (CA) models in urban studies and geography, from their formulation by von Neumann and Ulam and the pioneer work of Tobler, to today's complex models that integrate a whole set of other modeling concepts in their formulation. We will relate CA models with the technological settings and with the planning practices that were the main trends at each moment during their already long existence, identifying how these tensions influenced the research on CA.

## References

[1]   Lee, D.B., Requiem for Large-Scale Models. *Journal of the American Institute of Planners*, 1973. **39**(3): p. 163-178.
[2]   Lee, D.B., Retrospective on Large-Scale Urban Models. *Journal of the American Planning Association*, 1994. **60**(1): p. 35-40.

[3]    Couclelis, H., "Where has the future gone?" Rethinking the role of integrated lad-use models in spatial planning. *Environment and Planning A*, 2005. **37**: p. 1353-1371.

# Are neighbourhood rules uniform across Europe?

**H. VAN DELDEN**

Research Institute for Knowledge Systems (RIKS)
P.O. Box 463, 6200 AL Maastricht, The Netherlands
+31 (043) 350 1750, hvdelden@riks.nl

**Keywords:** cellular automata, neighbourhood rules, scale issues, land use change, land use modelling

## Abstract

Over the past decade various authors have discussed to what extent the neighbourhood rules (also known as interaction rules) of CA-based land use change models are generic. Where some argue that local differences in behaviour are crucial for the accurate modelling of land use processes and need to be included in the neighbourhood rules, others advocate that their nature is more generic.

This research aims to investigate to what extent it is feasible to calibrate a CA-based land use model for Europe with one set of interaction rules and if a sub-division in large regions enhances the calibration results. The research is carried out with the Metronamica model that has been widely applied to cities, regions and countries worldwide (www.metronamica.nl). Main data sources used are Corine Land Cover maps, GISCO transport data, zoning information provided by EC DG Environment and the EC DG JRC and information on the bio-physical characteristics of the territory provided by EC DG JRC.

The research consisted of the following steps:

1. Analysis of historic land use changes in Europe to understand:
   a. how land use patterns have evolved over time.
   b. what land uses are over- or under-represented in the neighbourhood of cells that have changed over time, and why.

2. Calibration of the model to the whole of Europe as well as to the large regions in Europe, each time using the same underlying data and resolution (1x1 km$^2$). Calibration results are assessed for both the process and predictive accuracy and compared against a benchmark.

3. Comparison of the various calibration results to assess if it is possible to calibrate an application to Europe with one rule set, and if the calibration results will improve by sub-dividing Europe into large regions with similar behaviour and region-specific calibration parameters.

Analysis of land use change shows that both similarities and differences in land use change dynamics can be found across Europe. The continuation of the urbanization process and the development towards larger urban centres can be detected all over Europe. The exception to this is Western Europe, where the data shows that the

distribution of urban clusters remains largely constant over the analysis period. This may be because this area was already highly urbanized from the initial year of the analysis, compared to the rest of Europe and hence a development towards larger clusters is likely to have taken place before the analysis period. All over Europe urban sprawl can mainly be found in areas formerly occupied by agriculture, causing agricultural areas close to cities to be taken over by suburbanization. Differences are found in the way residential development is attracted by water bodies. Inland water bodies are important attractors for residential development in South-eastern Europe and Western Europe, while the coast is a main attractor for this development in the Mediterranean and Western Europe. Part of this behaviour can be explained by the desire of people to live near water bodies, but historical preference of cities to locate next to coasts or rivers for their transportation function are likely to contribute to these developments as well. The latter would indicate that including this behaviour in interaction rules should be done with caution, as the reason for current developments might be the proximity to the cities rather than to the water body.

Agriculture is the land use that shows the largest decline in surface area in the European territory. Strongest decreases are found in Western Europe, followed by the Mediterranean region. Conversion from agriculture to all other land uses can be detected throughout Europe, while new agricultural locations can mainly be found on land previously occupied by forest and natural vegetation. Contrary to what neo-classical economists expect as a result of transport costs to a central market, the data does not provide any indication of an attraction of agriculture to urban land uses.

Calibration results show that it is possible to calibrate a CA based land use model for Europe to the extent that it is able to outperform the chosen benchmark. However calibration results can be improved if the calibration rules are fine-tuned using the specific characteristics and behaviour observed in the large regions.

This research shows that neighbourhood rules for Europe are to a large extent similar, but that including information on regional characteristics regarding the behaviour enhances the calibration results.

# A comparison of three urban models of land use, transport and activity

Are different modeling traditions really worlds apart?

## Alex HAGEN-ZANKER

University of Surrey, Division of Civil, Chemical and Environmental Engineering
Guildford, Surrey GU2 7XH, United Kingdom
+44 (0)1483 300800, a.hagen-zanker@surrey.ac.uk

## Abstract

Urban modeling is inherently an interdisciplinary endeavor, with a broad societal relevance. It is not surprising that it brings together researchers from a wide range of backgrounds, carrying with them the paradigms, toolsets and terminology of their disciplines. These backgrounds include economists and econometricians, geographers, planners and architects, civil engineers, computer scientists and many more. This paper makes a systematic comparison between three models that are all concerned with the organization of land use and activities in space and that all see proximity and accessibility as major determinants of that organization. Despite these strong conceptual similarities, the models are conceived from fundamentally different starting points and assumptions, and it is often thought that there are irreconcilable differences.

The compared models are the MOLAND Cellular Automata model as introduced by White and Engelen [3]; the dynamic spatial interaction model UrbanSim [2]; and the MEPLAN regional economic land use and transport model as proposed by Echenique [1]. These models differ in their basic units: parcels of land in the cellular automata model and households and organizations in MEPLAN and UrbanSim. They also differ in their understanding of the predictability and regularity of the urban growth process: Central to the MOLAND model is the notion of complexity and self-organization, UrbanSim on the other hand assumes that rates of change follow continuous functions that may well be estimated using standard econometric techniques, and MEPLAN is based on a constant equilibrium in the demand and supply for land.

This paper compares the strengths and weaknesses of these models; it also shows how the models make concessions to their basic structure in order to overcome weaknesses. It then emerges that in practice the models are more similar than their theoretical roots suggest and the remaining differences are to a lesser extent fundamental conceptual differences, but rather differences in emphasis, terminology and computational methods.

The comparison of the models' strengths and weaknesses gives rise to the idea of a best-of-worlds hybrid solution. The paper concludes by setting out the basic

components of such a solution and presenting a number of suggestions to make it work computationally.

## References

[1] Echenique, M. (2004), Econometric models of land use and transportation. In Handbook of Transport Geography and Spatial ,Elsevier, Amsterdam, pp. 185-202

[2] Waddell P., (2002), UrbanSim: Modeling Urban Development for Land Use, Transportation and Environmental Planning. *Journal of the American Planning Association*, 68(3), pp. 297-314

[3] White, R., G. Engelen (1997), Cellular automata as the basis of integrated dynamic regional modelling. Environment and Planning B-Planning & Design, 24(2), pp. 235-246

# A multiscale cellular automata model for simulating land use change at regional/local scales

**Nuno N. PINTO[1]; António P. ANTUNES [2]; Josep ROCA[3]**

[1]Department of Civil Engineering, University of Coimbra
R. Luis Reis Santos Pólo II da Universidade, 3030-788 Coimbra, Portugal
+351 239 797 106, npinto@dec.uc.pt (correspondent author)
[2]Department of Civil Engineering, University of Coimbra
R. Luis Reis Santos Pólo II da Universidade, 3030-788 Coimbra, Portugal
+351 239 797 139, antunes@dec.uc.pt
[3]Center for Land Policy and Valuation, Technical University of Catalonia,
Av. Diagonal, 649, 4ª planta, 08028 Barcelona, Spain
+34 93 401 63 96, josep.roca@upc.edu

**Keywords:** cellular automata, multiscale, irregular cells, accessibility, Barcelona

## Abstract

Cellular Automata (CA) models are very popular models for simulating spatial change and they have been developed and applied intensively during the past two decades. Two main features made CA interesting for urban studies: first, their inherent spatiality which suits the simulation of a wide range of geographic phenomena; second, the possibility of simulating complex patterns of, for example, land use starting from a simple conceptual framework that includes the definition of a cell space (form), a neighborhood (interaction), and a finite set of transition rules (behaviors) applied to a finite set of cell states (land uses). This conjugation of form and function make CA models suitable for capturing the contribution of different phenomena to the complex processes of urban change. These models are commonly used to simulate land use change at a regional or metropolitan level considering land use dynamics at a local level. They consider increasingly smaller cells, making use of the high resolution of today's remote sense images to capture many interactions that occur at a very large scale. Regular cells are used at the local scale (pixels) and at a regional scale, as aggregations of smaller cells. This regularity does not match reality at both scales. We address these issues of scale and cell form by proposing a multiscale CA modeling platform that aims to capture land use dynamics at two different spatial and time scales: a macroscale CA that tries to simulate the aggregated land use change at a regional level; and a microscale CA that tries to simulate land use allocation at local scale. We use irregular cells at both scales – municipalities or similar units at the macrsocale and census blocks or derivatives at the microscale – as irregular cells to simulate land use change. The macroscale model generates aggregate values of land use demand as an input for the microscale model which will then try to allocate land use to best fit simulation to reality. We describe the main features of the models and of the calibration process. Finally, we present some modeling results for the Metropolitan Area of Barcelona.

## Acknowledgments

# AUTHOR INDEX